

Stony Brook University



OFFICIAL COPY

The official electronic file of this thesis or dissertation is maintained by the University Libraries on behalf of The Graduate School at Stony Brook University.

© All Rights Reserved by Author.

Preparation of the Organic Nanotubes

A Dissertation Presented

by

Te-Jung Hsu

to

The Graduate School

in Partial Fulfillment of the

Requirements

for the Degree of

Doctor of Philosophy

in

Chemistry

Stony Brook University

December 2013

Stony Brook University

The Graduate School

Te-Jung Hsu

We, the dissertation committee for the above candidate for the
Doctor of Philosophy degree, hereby recommend
acceptance of this dissertation.

Frank W. Fowler – Dissertation Advisor
Professor, Chemistry

Joseph W. Lauher – Dissertation Advisor
Professor, Chemistry

Nancy S. Goroff – Chairperson of Defense
Professor, Chemistry

Andreas Mayr – Third Member
Professor, Chemistry

Linwood L. Lee – Outside Member
Professor, Physics & Astronomy

This dissertation is accepted by the Graduate School

Charles Taber
Dean of the Graduate School

Abstract of the Dissertation

Preparation of Organic Nanotubes

by

Te-Jung Hsu

Doctor of Philosophy

in

Chemistry

Stony Brook University

2013

Carbon nanotubes have attracted a great deal of research interest because they have potential applications in many different areas, such as nanoprobes, molecular reinforcements in composites, displays, sensors, energy-storage media, and molecular electronic devices. Chemists have considered this a challenge as they have made many attempts to design and synthesize their own imaginative versions of tubular molecules. The first section is the investigation of a directed and controlled approach for the synthesis of nanotubes held together via covalent bonds. Numerous tubular molecules have been prepared by the self-assembly of a wide variety of substrates, via hydrogen bonds, π - π stacking or Van der waals contacts. Tubular structures held together by covalent bonds have also been studied for a long time. In our group we have been focusing upon designed topochemical polymerization reactions of diacetylenes. Based on this idea, the series of compounds were synthesized as the polymerizable diacetylene macrocycles that would self-assemble in accordance with the parameters needed for a topochemical polymerization.

The second section is the preparation of the non-covalent bonded organic nanotubes with guest accessible channels by utilizing the intermolecular oxalimide-oxalimide interactions. The ultimate goal of this work is to design artificial cavities that can direct diacetylene polymerization reactions with comparable levels of selectivity. The series of compounds were designed and synthesized to self-assemble at the desired distance of 4.9 Å, which is essential to align the diacetylene guest molecules at a distance required for the topochemical polymerization. As a result, the desired polymer will be obtained by heating or UV irradiation.

This dissertation is dedicated to my family

Table of Contents

List of Figures.....	vii
List of Schemes.....	xi
List of Tables.....	xii
List of Abbreviations.....	xiii

Chapter 1. Organic Nanotube

1.1. Introduction.....	2
1.2. Tubular design principle.....	2
1.3. Macrocycle synthesis techniques.....	4
1.4. Tubular structures from hollow coiled molecules.....	8
1.5. Tubular structure from macrocycles.....	11
1.6. Tubular structure from sector shaped subunits.....	19
1.7. Tubular structure from ring-rod molecules.....	21
1.8. Covalent crosslinking of organic assembled precursors.....	22
1.9. Potential applications of hollow tubular architectures.....	25
1.9.1. Membrane channels for ionic and neutral molecule transport.....	26
1.9.2. Hollow cylindrical materials for gas storage.....	27
1.9.3. Confined nanovessels for chemical reactions.....	29
1.10. Summary.....	30
1.11. References.....	31

Chapter 2. Design and Synthesis of Tubular Additional Polymer

2.1. Background.....	42
2.2. Preparation of polydiacetylenes.....	44
2.2.1. Homocrystal strategy.....	46
2.2.2. Cocrystal strategy.....	48
2.3. Research goal.....	52
2.4. Macrocycles based on host-guest approach.....	58
2.4.1. Synthesis of macrocycle M1.....	58
2.4.2. Crystal structure analysis of macrocycle M1.....	60
2.4.3. Synthesis of macrocycle M2.....	66
2.4.4. Crystal structure analysis of monomer M2(m).....	72
2.4.5. Synthesis of macrocycles M3 & M4.....	74
2.4.6. Synthesis of macrocycle M5.....	76
2.4.7. Crystal structure analysis of monomer M5(m).....	77
2.4.8. Conclusion.....	80

2.5. Macrocycles based on oxalamide moiety	84
2.5.1. Synthesis of oxalamide based macrocycle M6.....	84
2.5.2. Synthesis of oxalamide based macrocycle M7.....	87
2.5.3. Synthesis of oxalamide based macrocycle M8.....	92
2.5.4. Synthesis of oxalamide based macrocycle M9.....	95
2.5.5. Other characterizations of oxalamide based macrocycles.....	98
2.5.6. Conclusion.....	101
2.6. Macrocycles based on $\pi - \pi$ stacking.....	103
2.6.1. Synthesis of macrocycle M10	103
2.6.2. Crystal structure analysis of macrocycle M10	105
2.6.3. Synthesis of macrocycle M11	116
2.6.4. Conclusion.....	119
2.7. Summary	119
2.8. References	122

Chapter 3. Design and Synthesis of Self-assembled bis-Oxalamide Macrocycles used as Porous Reactor for Polydiacetylene

3.1. Introduction	126
3.2. Research Goal	126
3.3. Synthesis of First Generation Macrocycle M12.....	129
3.4. Synthesis of Second Generation Macrocycle M13	133
3.5. Conclusion Remarks	137
3.6. References	138

Chapter 4. Experimental Section

4.1. Experimental detail	141
4.2. Organic synthesis	143
4.3. References	176

Bibliography	177
---------------------------	------------

Appendix. Molecular Structure and Crystallography Data	191
---------------------------------------------------------------------	------------

List of Figures

Figure 1-1. Four possible approaches for the molecular assembly of tubular objects. a) Hollow, folded structures can be constructed by coiling the helical molecules. (b) Porous structures can be generated by assembly of rod-like molecules into barrel-stave fashion. (c) Tubular materials can be prepared by stacking the macrocycles. (d) Continuous cylinders can be obtained by assembly of sector or wedge-shaped molecules into discs.	3
Figure 1-2. Channels formed from hollow helical architectures; a) Pictures of a linear polymer folded into hollow helical tube. b) β -helical structure of gramicidin A. ⁴¹	9
Figure 1-3. (a) Representation of meta-Phenylene ethynylene oligomer family; (b) solvophobic folding from random coil to helix.	10
Figure 1-4. Water-soluble chiral polyisocyanides showing thermoresponsive	11
Figure 1-5. (a) Molecular structure of phenylacetylene macrocycle (PAM). (b) Hexagonal tubular structures formed by shaped-persistent PAM. ⁸⁴	13
Figure 1-6. Depending on the recrystallization solvent, Höger macrocycle x displayed two different stacking patterns: (left) growing crystals from pyridine. (right) growing crystals from THF (solvent molecules were removed in both cases). ⁸⁵	14
Figure 1-7. a. Molecular structure of the macrocycles. 1a-1c were designed to self-assemble into hydrogen-bonded tubular structure. 1d was designed for comparison since it cannot self-associate via hydrogen bonding. b. A snapshot of a helical stack of the macrocycles ⁸⁶	15
Figure 1-8. Bis-urea macrocycles reported by Shimizu and coworkers ^{81,89}	16
Figure 1-9. Cylindrical structures from stacking of the macrocycles; a) Schematic representation for the stacking of macrocycles on top of each other to form tubular structures. b) Cylindrical assembly of cyclic peptides as predicted by DeSantis and coworkers. ⁹⁰	17
Figure 1-10. Schematic representation of self-assembly of cyclic (<i>D,L</i>)- peptides into.....	17
Figure 1-11. a. Molecular structure of the macrocyclic diacetylenedicarboxamide compounds. b. Crystal structure of Macrocycle 4b. ⁹²	18
Figure 1-12. (a) Molecular structure of cyclodextrins. (b) Space filling model of cyclic oligosaccharide's self-assembly in solid-state. ⁶²	19
Figure 1-13. Tubular assembly from disc or sector shaped subunits; a) Representation of tobacco mosaic virus coat self-assembly. ⁹⁶ b) Self-assembly of wedge shape molecules into tubular frameworks. ¹⁰⁴	20
Figure 1-14. Schematic representation of proposed self-assembly for formation of hexameric macrocycle. ¹⁰⁶	20
Figure 1-15. a) The β -barrel pore structure naturally from α -hemolysin. ²¹ b) Schematic representation of self-assembly of <i>p</i> -octiphenylpeptide conjugates into cylindrical structures by β -sheet formation. ¹¹¹	21
Figure 1-16. A new approach to organic nanotubes from porphyrin-containing dendrimers. ¹¹⁶ Step a: The dendrimer x is polymerized (step a) to give x. step b: intramolecularly crosslinked by	

RCM of x to give the nanoarchitecture x . step c: cleaved of the central core region, in dark grey, to give the hollow tubular architecture x .	23
Figure 1-17. Synthesis and irradiation of amphiphilic poly(<i>m</i> -phenyleneethynylene) x (Tg=CH ₂ CH ₂ OCH ₂ CH ₂ OCH ₂ CH ₂ OCH ₃). Step a: trimethylsilylacetylene, [Pd(PPh ₃) ₄], CuI, DBU, MeCN, Δ. Step b: irradiation.	24
Figure 1-18. Strategy for the synthesis of uniform diameter carbon nanotubes.	25
Figure 1-19. a) <i>Cyclo</i> [-(<i>L</i> -Trp- <i>D</i> -Leu) ₃ - <i>L</i> -Gln- <i>D</i> -Leu-] ⁷¹ b) <i>Cyclo</i> [-(<i>L</i> Trp- <i>D</i> -Leu) ₄ - <i>L</i> -Gln- <i>D</i> -Leu-] ¹⁴⁹ c) Schematic representation of cyclic peptide tubular self-assembly in lipid bilayers.	27
Figure 1-20. Pore shape and structures of a) Zeolite A b) Zeolite Rho ¹⁵⁴ c) Channels of IRMOF 8 ^{139,155}	28
Figure 2-1. Representative structures of organic conjugated π -systems illustrating the most.....	43
Figure 2-2. Illustration of the necessary geometric orientation of individual diacetylene molecules for the production of polydiacetylene in a solid-state polymerization reaction. d = translation repeat distance, $R_{1,4}$ = the C1-C4 contact distance, and ϕ = the angle at with the diacetylenes are titled with respect to d	45
Scheme 2-1. Figure 2-3. Crystal structure of 1	47
Figure 2-4. a) The pale background drawing is the diacetylene monomers. The bold foreground drawing shows the polydiacetylene. ²⁶ b) Polymerization of triacetylenes induced by γ irradiation. ³¹ c) Polymerization of trienes induced by heat. ³²	50
Figure 2-5. A library of hydrogen bonding host molecules capable of self-assembling to give a predictable repeat distance.	51
Figure 2-6. One possible route to a tubular polymer is via a topochemical polymerization of a diacetylene-containing macrocycle. For the reaction to proceed, the macrocycles would need to be spaced near the 4.9 Å expected for polymers with neighboring diacetylene C1–C4' carbon atoms close to the van der Waals contact distance of 3.4 Å. The application of heat (or radiation) should bring about the polymerization.	53
Figure 2-7. The expected 1,4-polymerization of diacetylene macrocycle M1 under co-crystal with oxalamide of glycine.....	56
Figure 2-8. Schematic representation of cyclic oxalamide diyne that could self-assemble at the required 4.9 Å needed for a diacetylene polymerization	57
Figure 2-9. Color photograph of the crystals of (a) freshly prepared samples of macrocycle M1 (b) sample sitting at room temperature for 1 week.	59
Figure 2-10. Crystal structures of M1 : a) Single crystals grown from DCM/NMF (1/10). b) Single crystals grown from DCM/EtOAc (1/1). c) Single crystals grown from DCM/MeOH (1/1).	61
Figure 2-11. Color photograph of the crystals of monomeric M1	62
Figure 2-12. Crystal structures of monomeric M1 : a) view from top b) view from side	63
Figure 2-13. Color photograph of the crystals of M2	70
Figure 2-14. Color photograph of the crystals of monomer M2	72
Figure 2-15. Crystal structures of monomer M2 : a) view from top b) view from side	73
Figure 2-16. Color photograph of the crystals of monomer M5	78

Figure 2-17. Crystal structures of monomer M5 : a) view from top b) view from side	79
Figure 2-18. M6 gradually turns pink in color at temperatures above about 110 °C.	86
Figure 2-19. a) TLC plate used to screen the coupling reaction (with light exposure). b) TLC plate used to screen the coupling reaction (without light exposure). Eluent: EtOAc/MeOH/Hexanes: 4:2%:1.....	89
Figure 2-20. a) cyclomonomer M7 gradually turns pink in color at room temperature. b) cyclodimer M7 gradually turns pink in color at room temperature. c) cyclomonomer M7 gradually changes color under UV irradiation.d) cyclodimer M7 gradually changes color under UV irradiation.	90
Figure 2-21. cyclodimer M8 (left) and cyclomonomer M8 (right) gradually changes color under UV irradiation for 20 secs.....	94
Figure 2-22. cyclodimer M9 (left) and cyclomonomer M9 (right) gradually changes color under UV irradiation for 20 secs.....	97
Figure 2-23. The Raman spectrum of UV-treated macrocycle M6 (a) and M8 (b). The typical absorption of PDAs can be found around 1400 and 2000 cm^{-1} , respectively, referring to corresponding C=C and C≡C bonds in the backbone.....	98
Figure 2-24. The transmission electron microscopy (TEM) image of M6 , M7 and M8 , prepared by drop-casting ethanol onto a copper grid, reveals straight, rod-like assemblies.	99
Figure 2-25. Powder x-ray pattern of M7	100
Figure 2-26. (a) Freshly formed crystals of the monoclinic form of M10 grown at room temperature. (b) Freshly formed crystals of the triclinic polymorph of macrocycle M10 grown at 40 °C.	104
Figure 2-27. (a) The observed molecular stacking in the monoclinic form of macrocycle M10 . The repeat distance of 5.09 Å is longer than the ideal polymerization value of 4.9 Å	106
Figure 2-28. Observed molecular stacking in the triclinic form of macrocyclic monomer M10 . The observed repeat distance of 4.84 Å was much closer to the ideal value.....	108
Figure 2-29. Structure of polymer M10 obtained by slow annealing of the triclinic crystals at 40°.....	109
Figure 2-30. DSC plot of M10 (heating rate 10 °C/min). The black line shows the original heating curve with an exothermic transition at ~ 106 °C corresponding to the irreversible polymerization. The red line shows the cooling of the sample. The blue line shows that the re-heating of the fully polymerized sample is feature free.....	110
Figure 2-31. (a) The macrocycle monomers have a rectangular cross section of 7.5 Å × 9.5 Å. (b) The monomers stack at an angle such that the cross section of the tubular polymer is reduced with a 3.22 Å contact between opposite methylene groups.....	112
Figure 2-32. Molecular Conformations. In the monoclinic polymorph A three of the independent ether C-O bonds adopt a gauche configuration, while the fourth (O2-C18) adopts an anti configuration. In the triclinic polymorph B all four independent C-O bonds are gauche.	113
Figure 2-33. (a) Raman spectrum of the triclinic polymorph of M10 . The small amount of polymer that already exists prior to heat treatment dominates the spectrum giving the two distinct	

polymer absorptions at 2098 and 1491 cm^{-1} . (b) Raman spectrum of the polymer M10 . After full polymerization, the two distinct polymer absorptions occur at 2094 and 1484 cm^{-1}	114
Figure 2-34. Color photographs of the crystals of (a) freshly prepared samples of the triclinic polymorph of macrocyclic monomer M10 (b) the fully polymerized crystals after annealing. The crystals are 3-4 mm long, but as little as 0.10 mm in thickness. The tube axis is aligned along the length of crystals.	116
Figure 2-35. Needle like crystals of M11 obtained after crystallization.....	118
Figure 3-1. a. Molecular structure of M12. b. Molecular modeling of M12	128
Figure 3-2. molecular and crystal structure of the <i>L</i> -cystine-based bis-urea macrocycle.....	131
Figure 3-3. a. Molecular structure and b. X-ray crystal structure of the unsymmetrical bis-urea macrocycle	132
Figure 3-4. Molecular structures of M13 and M14.....	132
Figure 3-5. The transmission electron microscopy (TEM) image of M13 and M14 , prepared by drop-casting ethanol onto a copper grid, reveals no evidence of columnar structure formation.	136

List of Schemes

Scheme 1-1. Williamson ether synthesis of crown ether. The [2 + 2] cyclization product is made by the combination of 2 eq. of each reactant. On the other hand, the [1 + 1] cyclization product is the combination of 1 eq. of each component. ³¹	4
Scheme 1-2. A possible side-reaction that may lead to polymerization of 2 reactants.	5
Scheme 1-3. Potassium cation serves as a templates and the reactants are topologically fixed for a desired cyclization reaction. ³¹	6
Scheme 1-4. Höger and co-workers used a covalently bonded template to assist the formation of diacetylene linkage via homocoupling reaction. The template was then cleaved under basic conditions after the formation of the templated-macrocycle. ³⁶	7
Scheme 2-1.	
Figure 2-3. Crystal structure of 1	47
Scheme 2-2. Synthetic route for M1	58
Scheme 2-3. Synthetic route for M2	66
Scheme 2-4. A plausible copper-diether coordination complex 3 that may form during the Hay coupling reaction affect the formation of the product.	67
Scheme 2-5. An alternate synthetic route for M2	68
Scheme 2-6. A new synthetic approach to the desired macrocycle M2	69
Scheme 2-7. Synthetic route for M3 & M4	74
Scheme 2-8. Synthetic route for M5	76
Scheme 2-9. A plausible copper-diether coordination complex 11 that may alter the favorability during the Hay coupling condition on the original synthetic route.	77
Scheme 2-10. Synthetic pathway of M6	85
Scheme 2-11. Synthetic pathway of M7	88
Scheme 2-12. Synthetic pathway of M8	92
Scheme 2-13. Synthetic pathway of M9	95
Scheme 2-14. Original plan to generate the diether M9-3	96
Scheme 2-15. Synthesis of macrocycle M10 from readily available reagents.....	103
Scheme 2-16. Synthetic route for M11	117
Scheme 3-1. Synthetic route of macrocycle M12	129
Scheme 3-2. a. Original synthetic strategy of M13 . b. TLC plate used to monitor the reaction.	133
Scheme 3-3. Repeat the reaction in an even more dilute solution to testify the ring closure of M13	134
Scheme 3-4. New synthetic strategy of M13	135

List of Tables

Table 2-1. The unit cell data of macrocycle M1 obtained from material grown from the different solvent systems.....	60
Table 2-2. The unit cell data of monomer M1 obtained from material grown from DCM/hexanes (1/1).	62
Table 2-3. Co-crystal strategy for macrocycle M1	64
Table 2-4. The effect of concentration to the yields of macrocycles	71
Table 2-5. The unit cell data of monomer M2 obtained from material grown from DCM/hexanes (1/1).	72
Table 2-6. The unit cell data of monomer M5 obtained from material grown from DCM/hexanes (1/1).	78
Table 2-7. Chemical shifts of protons of the methylene groups in macrocycles (ppm).....	83
Table 2-8. The unit cell data of M10 obtained from material grown from the different solvent systems.	107

List of Abbreviations

Å	angstrom
AFM	Atomic Force Microscopy
d	repeat distance
DMAP	4-dimethylaminopyridine
DMSO	dimethyl sulfoxide
DSC	Differential Scanning Calorimetry
DCM	dichloromethane
DBU	1,8-diazabicyclo[5.4.0]undec-7-ene
EtOAc	Ethyl acetate
MS	Mass Spectrometry
NMR	Nuclear Magnetic Resonance
NMF	N-Methylformamide
PDA	polydiacetylene
PDI	polydispersity index
SEC	Size Exclusion Chromatography
SPM	shape-persistent macrocycle
TEA	triethylamine
TEM	Transmission electron microscopy
THF	tetrahydrofuran
TLC	Thin Layer Chromatography
TMEDA	<i>N,N'</i> -tetramethylethylenediamine
TMS	trimethylsilyl
XRD	X-ray diffraction
γ	declination angle

Acknowledgments

I would like to express my sincere gratitude to my supervisors, Prof. Bill Fowler and Joe Lauher, for supporting me during these past six years. Joe is someone you will never forget once you meet him. He is the funniest advisor and one of the smartest people I know. He always offers me a great amount of freedom to pursue various projects without objection. I cannot say thank you enough for his tremendous support and help. Bill is the most enthusiastic and energetic educator I have ever known. I hope someday I would be able to command an audience as well as he can. He always gives me many useful scientific advice and insightful discussions about my projects. I am really lucky to be a part of this group.

I would like to thank my thesis committees: Prof. Nancy S. Goroff, Prof. Andreas Mayr and Prof. Linwood L. Lee for their encouragement, and many scientific discussions and suggestions.

I also thank the great Ph.D. program at Stony Brook University. The fantastic staffs in this department are genuinely nice and always offer warm-hearted assistance and I am glad to have interacted with many. Moreover, I acknowledge financial support from National Sciences Foundation.

I am lucky to have had a wonderful group of friends who have provided hearty support and friendship that I needed through the last six years, in particular Yixiong Yang, David Tan and my lab mate, Bo Liu. My life would be so boring without them.

I cannot find words to express my profound gratitude from my deep heart to my beloved parents, and my siblings for their love and continuous support. They encouraged me so much in life and I am lucky to have been blessed with the family I have.

Finally, I would like to thank my dear son, Rhodey. He is so cute. Being a Mother is so tired but I am happy and satisfy.

Chapter 1

Organic Nanotubes

1.1. Introduction	2
1.2. Tubular design principle.....	2
1.3. Macrocycle synthesis techniques	4
1.4. Tubular structures from hollow coiled molecules.....	8
1.5. Tubular structure from macrocycles	11
1.6. Tubular structure from sector shaped subunits	19
1.7. Tubular structure from ring-rod molecules	21
1.8. Covalent crosslinking of organic assembled precursors	22
1.9. Potential applications of hollow tubular architectures	25
1.9.1. Membrane channels for ionic and neutral molecule transport	26
1.9.2. Hollow cylindrical materials for gas storage	27
1.9.3. Confined nanovessels for chemical reactions.....	29
1.10. Summary	30
1.11. References	31

1.1. Introduction

Organic tubular assemblies have attracted much attention due to their numerous potential applications in biology, chemistry, and material science.¹⁻¹² For example, the use of tubular molecules as conduits of chemical information has been demonstrated by protein-folding chaperonins^{13,14} and protein-degradation enzymes^{15,16} which formed transmembrane ion channels¹⁷ and provided confined reaction chambers. Furthermore, the inherent geometric features of the cylinder provide selectivity based on different substrate size. For instance, the membrane protein aquaporin has demonstrated the ability to transport only water via its central pipe and discriminates against other small molecules.¹⁸ Inspired by these important applications of tubular structures in biology, chemists have focused on the preparation of simpler synthetic tubes for functions as specific ion sensors, molecular sieves, nanoscale transport systems or molecular reaction vessels. The detail of the design and synthesis of various tubular molecules will be discussed in this chapter.

1.2. Tubular design principle

Basically, there are several possible approaches to construct open-ended hollow tubular objects. As shown in **Figure 1.1**, a tube-shaped molecule can be prepared either by rolling or sealing at opposing edges of the two-dimensional sheet-like precursor. Such strategies have been applied to the formation of carbon nanotubes from graphite.^{19,20}

Porous structures can also be constructed by assembly of rod-like subunits into bundle-shaped frameworks. For example, transmembrane pores can be made by β -barrel proteins such as α -hemolysin,²¹ porins,²²⁻²⁴ plus α -helical bundles of cholera toxin²⁵ and the potassium channel.²⁶ Moreover, hollow tubular structures can be prepared from linear starting materials that will self-organize into helical conformations. β -Helical structures formed by the natural antibiotic gramicidin A represented a successful example of this type of porous molecules.²⁷ Finally, stacking of disc or sector-shaped subunits can easily generate the tubular arrays. The best known biological example of this motif is the self-assembly of the tobacco mosaic virus (TMV) coat protein.²⁸⁻³⁰ Among all these strategies, the last three seems to offer the most flexibility and convergence in design and synthesis of tubular molecules. To further explore the synthesis of tubular structures, some examples from literatures will be introduced in the following sections.

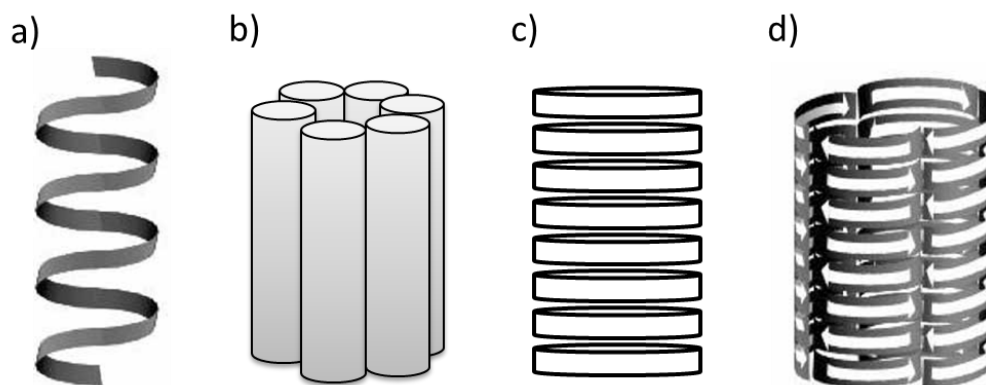
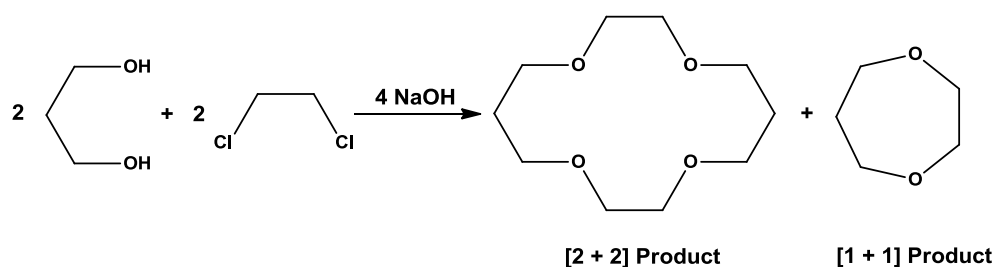


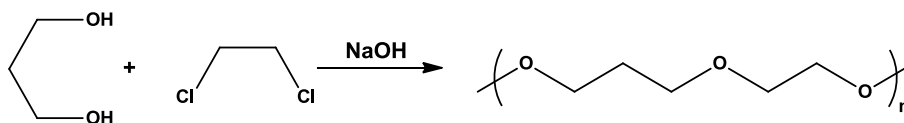
Figure 1-1. Four possible approaches for the molecular assembly of tubular objects. a) Hollow, folded structures can be constructed by coiling the helical molecules. (b) Porous structures can be generated by assembly of rod-like molecules into barrel-stave fashion. (c) Tubular materials can be prepared by stacking the macrocycles. (d) Continuous cylinders can be obtained by assembly of sector or wedge-shaped molecules into discs.³¹ (Reproduced with permission from reference 31. Copyright (2001) Wiley-VCH)

1.3. Macrocycle synthesis techniques

The development of synthetic techniques for the preparation of macrocycles is crucial and chemists have considered this being challenging as they have made many attempts to design and synthesize the desired macrocycles. There are several essential synthetic methods have been developed and are introduced as follows. Taking the preparation of crown ether as an example, through simple Williamson etherification, the crown ether can be synthesized as a [2 + 2] product by promoting a 2-component ring closure (**Scheme 1.1**).^{32,33} However, undesired side products will also form via the [1 + 1] cyclization or polymerization (**Scheme 1.2**). To avoid such complications, two efficient strategies have been proposed. The first one is introducing a template effect to facilitate cyclization^{32,34,35} and the second one is changing environmental conditions via carrying out the cyclization reaction in a highly diluted solution.^{32,35,36}

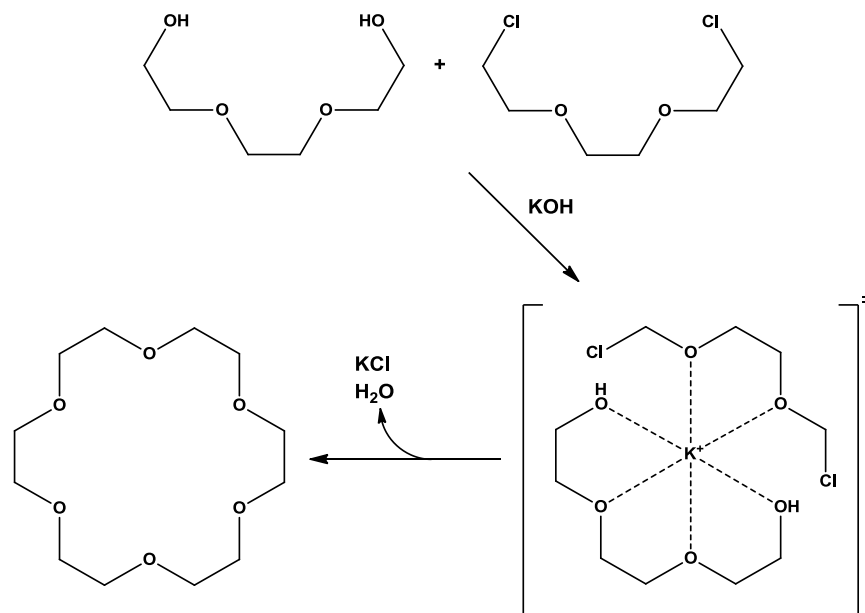


Scheme 1-1. Williamson ether synthesis of crown ether. The [2 + 2] cyclization product is made by the combination of 2 eq. of each reactant. On the other hand, the [1 + 1] cyclization product is the combination of 1 eq. of each component.³² (Reproduced with permission from reference 32. Copyright (2001) Wiley-VCH)



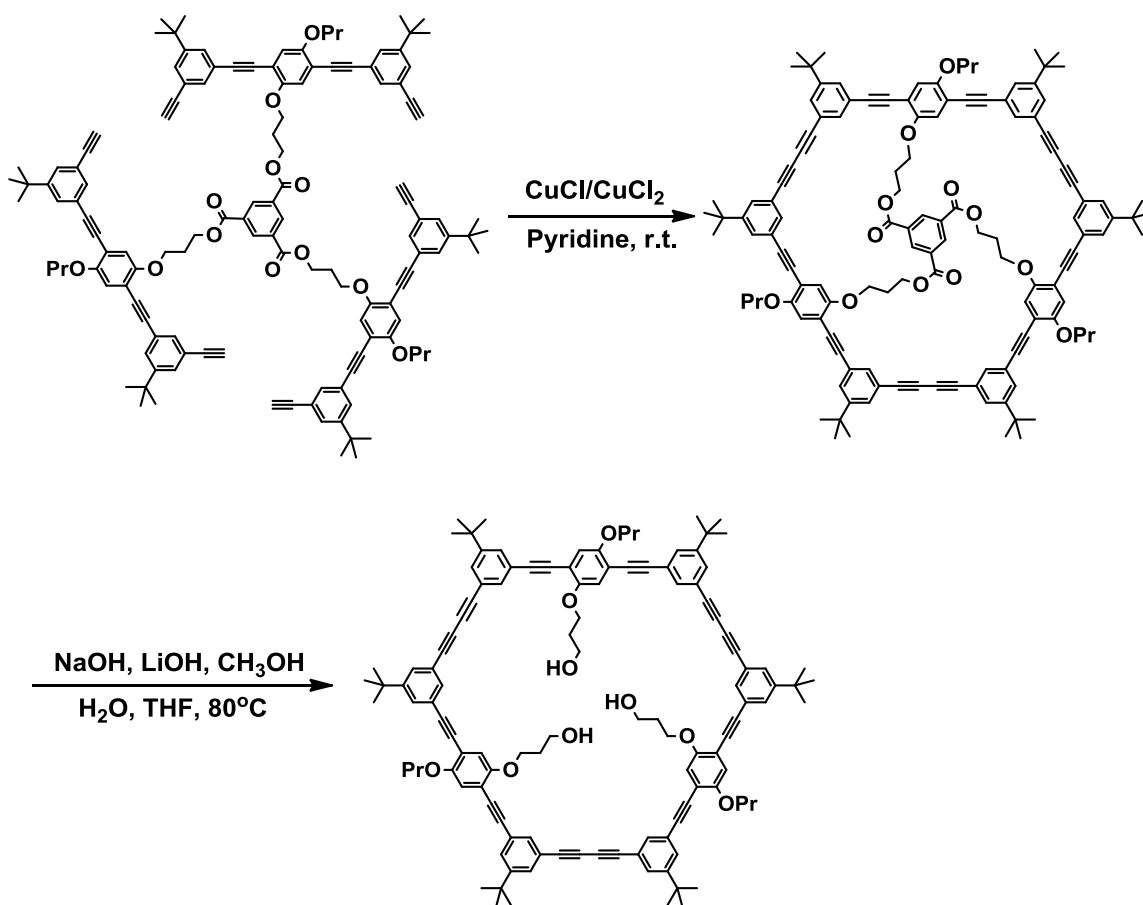
Scheme 1-2. A possible side-reaction that may lead to polymerization of 2 reactants.

The template effect: Introduction of templates will induce a variety of effects on the production of the desired compound. The principle of this method is using a template that functions as a blockage to facilitate cyclization: by separating and retaining the reactants in place prior to the reaction. As a result, these pre-organized fragments will be more favorable to give the desired cyclization product.³⁴ In this method, the template must be able to bind with the reactants either by covalent bonding³⁷ or non-covalent intermolecular attraction.³² Assisting by template molecule, we gain more geometric and topological control over the cyclization reaction and thereby reduce the production of the side products. An example of such is using the potassium cation as a template to coordinate with other reactants for the preparation of a crown ether (shown in **Scheme 1.3**),³² The template can be easily removed (via a washing procedure) after the completion of reaction to give the target molecule.



Scheme 1-3. Potassium cation serves as a template and the reactants are topologically fixed for a desired cyclization reaction.³² (Reproduced with permission from reference 32. Copyright (2001) Wiley-VCH)

The template effect can be demonstrated in two ways, the thermodynamic and the kinetic template effects.³² The thermodynamic template effect is based on the fact that in the absence of the template the desired cyclic products is indeed formed, but with one or more undesired compounds that are in equilibrium with target molecule. After template-reactant chelation, product equilibrium can be driven in the desired direction. On the other hand, when coordination between the template and reactants increases the cyclization rate, the reaction is under kinetic control.



Scheme 1-4. Höger and co-workers used a covalently bonded template to assist the formation of diacetylene linkage via homocoupling reaction. The template was then cleaved under basic conditions after the formation of the templated-macrocycle.³⁷ (Reproduced with permission from reference 37. Copyright (1997) American Chemical Society)

Several template cyclization reactions based on non-covalent interaction between the templates and the reactants are reported.^{32,34-36} In addition, templates that form covalent bond to the starting materials are also of interest. In these cases, the covalent bonded template should be easily cleaved after cyclization reactions. Höger and co-workers proposed the synthesis of acetylene linked macrocycle based on such covalent bonded template (**Scheme 1.4**).³⁷

Highly diluted solution: This method requires a large amount of solvent present during the reaction. The main purpose of using this highly diluted system is to avoid the polymerization of starting materials. Therefore, the [1 + 1] cyclization compound can be synthesized as the major product and the possibility of undesired polymers is greatly reduced. **Equation 1.1** reveals the correlation between reaction rate and reactant concentration. r_c is the cyclization rate and r_p is the polymerization rate.^{32,35,36}

$$\frac{r_c}{r_p} = \frac{k_c[\text{Reactant}]}{k_p[\text{Reactant}]^2} = \frac{k_c}{k_p[\text{Reactant}]} \quad (\text{Eq. 1.1})^{32}$$

Based on **Equation 1.1**, the ratio of the desired cyclic product will increase if the concentration of the reactants decreases. In order to raise the yield of the cyclized product, highly diluted environment has been utilized frequently for the preparation of macrocyclic compounds.

1.4. Tubular structures from hollow coiled molecules

As mentioned in previous section, open ended tubular structures can be prepared by several methods. One of them is through folding linear polymeric or oligomeric chains into stable hollow helical architectures to give tubular molecules with interior cavity (**Figure 1.2a**).¹ A good example to demonstrate this process is the formation of Gramicidin A. Gramicidin A is a hydrophobic linear polypeptide antibiotic consisting of

15 amino acids with alternating *D*- and *L*-configurations (HCO-*L*-Val-Gly-*L*-Ala-*D*-Leu-*L*-Ala-*D*-Val-*L*-Val-*D*-Val-*L*-Trp-*D*-Leu-*L*-Trp-*D*-Leu-*L*-Trp-NHCH₂CH₂OH). As shown in **Figure 1.2b**, the β -sheet type hydrogen bonds between amino acids help to stabilize the helical conformation formed by the polypeptide chain.³⁸⁻⁴¹

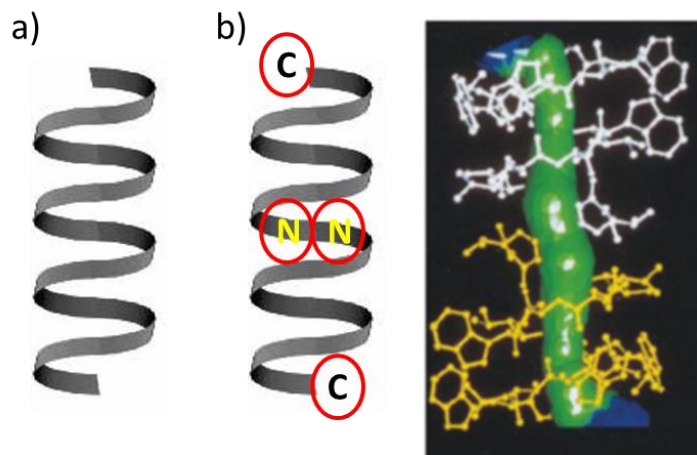


Figure 1-2. Channels formed from hollow helical architectures; a) Pictures of a linear polymer folded into hollow helical tube. b) β -helical structure of gramicidin A.⁴² (Reproduced with permission from reference 42. Copyright (1998) Elsevier)

In Gramicidin A, a channel-like pore is constructed by individual β -helices of two polypeptide chains associate in a head-to-head network through intermolecular backbone-backbone hydrogen bonds.^{27,43} This channel can be used for the transportation of the potassium ions to destroy the gradient across the cell membrane, resulting in the bacterial cell death.^{26,42}

Inspired by nature's exploitation of aromatic interactions and solvophobicity to generate and stabilize helical conformations among biomolecules,⁴⁴ Moore, Wolynes, and co-workers published a pioneering work on a series of amphiphilic *meta*-phenylene ethynylene (*m*PE) oligomers in 1997.⁴⁵⁻⁴⁸ The molecular structure is shown in **Figure 1.3**,

the aromatic non-polar scaffold (blue) bearing polar triethylene glycol side chains (red) are connected via acetylene bridges. These linear synthetic polymers or foldamers will pack into well-defined architectures through non-covalent interactions.⁴⁹⁻⁵¹

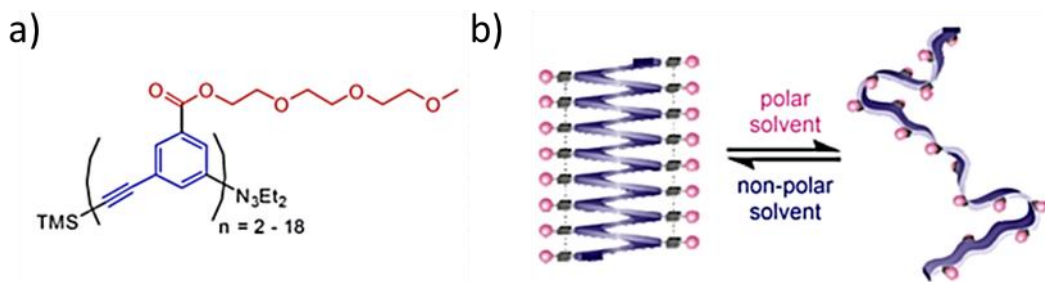


Figure 1-3. (a) Representation of meta-Phenylene ethynylene oligomer family; (b) solvophobic folding from random coil to helix.⁴⁶ (Reproduced with permission from reference 46. Copyright (1997) The American Association for the Advancement of Science.)

In polar solvents, the amphiphilic structure tends to segregate because the solvophobic regions hide from the solvent, while in non-polar solvent it forms a compact shape with the polar side chains pointing towards the solvent. The resulting adopted compact structure will be further stabilized by π - π interactions between aromatic rings of adjacent turns. Characterization of oligomers by ESR shows that each turn is composed of six repeat units.⁵² This result matches their expectation from the hexagonal symmetry and bond angle of 120° between *meta*-linked benzene ring. Moreover, the authors found that a tubular cavity of approximately 7 \AA in diameter is created upon folding of the molecule into a helix due to the structure's rigidity and shape-persistence.

Another example of synthetic helical polymers is the polyisocyanides. The structure of polyisocyanide consists of all-carbon backbone with a pendent group attach to each carbon atom. The helical structure results from restricted rotational freedom around the C-C single bonds connecting the main carbon atoms. This kind of polymer makes for

promising candidates for applications in optical and chiral materials.⁵³ Recently, a vast number of polyisocyanides carrying different pendent group has been developed by many groups.⁵⁴⁻⁶¹ In 2013, Zhang and co-workers published a series of novel oligoethylene glycol-based water-soluble chiral polyisocyanides (**Figure 1.4**).⁶² These helical polymers show thermoresponsive properties and might have potential application as stimuli-responsive materials, chiral recognition and separation materials.

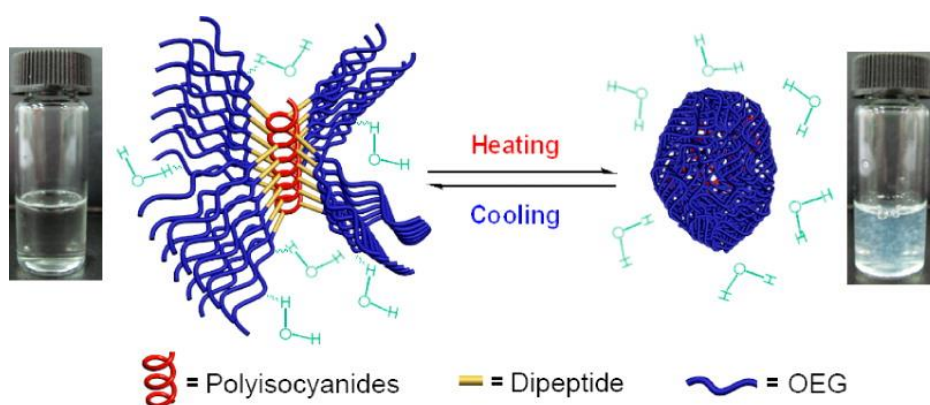


Figure 1-4. Water-soluble chiral polyisocyanides showing thermoresponsive behavior.⁶² (Reproduced with permission from reference 62. Copyright (2013) American Chemical Society).

1.5. Tubular structure from macrocycles

So far the most reliable method to construct a synthetic tubular structure is through self-assembly by stacking of macrocycles. In order to induce the cooperative action of weak bonds that leads to stable tubular molecules, ring-shaped molecules with flat

conformation and the right moieties arranged in a suitable way are required. Cyclic molecules can adopt or even intrinsically have a ring shape that generates a void space within them. Therefore macrocycles with not only rigid moieties such as multiple bonds or aromatic rings, but also functional groups capable of generating a directional non-covalent interaction like π - π stacking as well as hydrogen bond interactions are usually utilized to self-assemble into hollow cylindrical frameworks.⁶³⁻⁸² Other weak interactions, such as dipole-dipole and van der Waals interactions have been rarely used to build a nanotube. Only one report has described the formation of an organogel based on the self-assembling stacks of a boomerang-shaped molecule utilizing dipole-dipole interactions in combination with π - π interactions.⁸³

In 1985, Lehn *et al.* published the first attempts to construct columnar structure by using stacked macrocyclic liquid crystals.⁸⁴ At that time, a series of cyclic hexamines bearing long alkyl chains were synthesized. The columnar mesomorphic order was proved by XRD analysis. Modeling indicated that the formation of these parallel, hollow columns is based on supramolecular arrangement of the macrocyclic mesogens.

In 1994, Moore and co-workers investigated the solid-state structures of phenylacetylene macrocycles (PAM) decorated with hydrogen bonding functionalities (**Figure 1.5a**).⁸⁵ They found the phenolic derivative are connected to each other through hydrogen bonds, forming a layered structure (**Figure 1.5b**). The layers are aligned so that extended channels with diameters of ~ 9 Å are formed. The resulting nanotubular structures were stabilized by π - π interactions. By structural modification of PAM precursors, the pore size and solvophilicity can be manipulated. Moreover, X-ray

crystallographic analysis revealed that the resulting tubular structures are filled with solvent molecules.

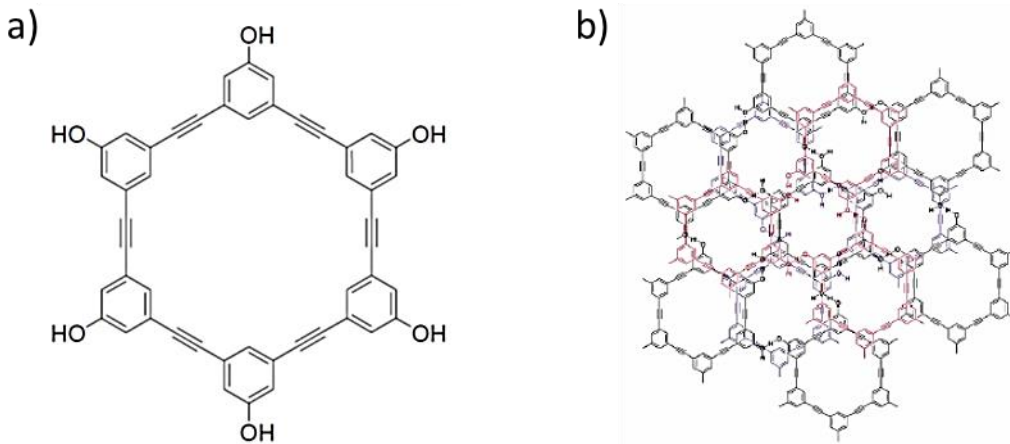


Figure 1-5. (a) Molecular structure of phenylacetylene macrocycle (PAM). (b) Hexagonal tubular structures formed by shaped-persistent PAM.⁸⁵ (Reproduced with permission from reference 85. Copyright (1994) Nature Publishing Group)

Later on Höger demonstrated how the nature of the solvent affects the stacking pattern of the macrocycle **1** in its single crystals (**Figure 1.6**).⁸⁶ Growing crystals of **x** from pyridine give the channel structures with a pore size of $\sim 4\text{-}5 \text{ \AA}$. X-ray measurement shows the two phenolic and two hexyloxy groups point inside the channel. However, crystallization from THF generates supramolecular tubes with large channels having pore sizes of $8 \times 12 \text{ \AA}$. Crystals from this solvent have the structure with all hexyloxy groups point outside of the macrocycle.

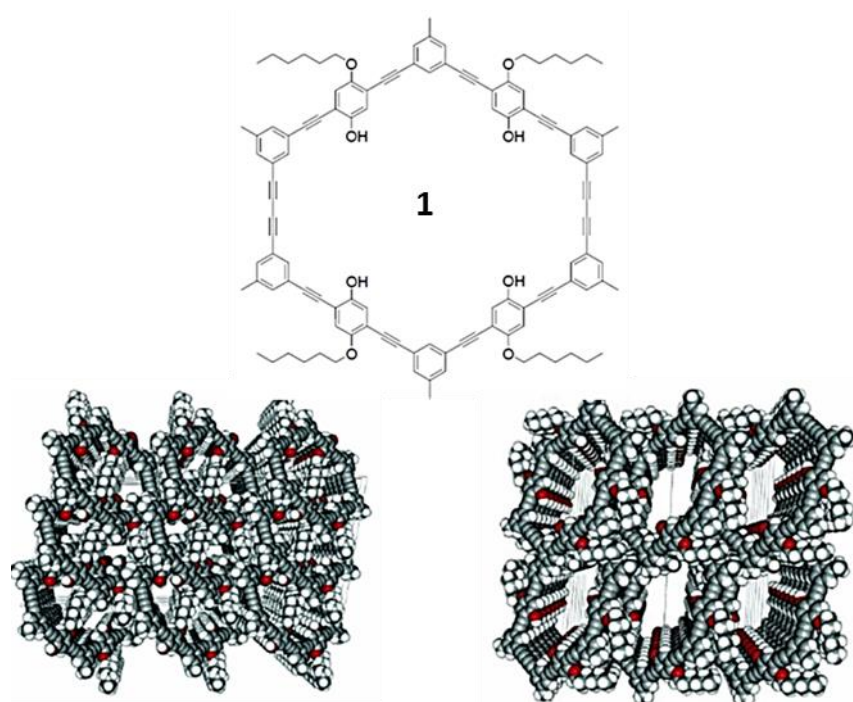


Figure 1-6. Depending on the recrystallization solvent, Höger macrocycle **1** displayed two different stacking patterns: (left) growing crystals from pyridine. (right) growing crystals from THF (solvent molecules were removed in both cases).⁸⁶ (Reproduced with permission from reference 86. Copyright (1999) Wiley-VCH)

In 2012, Gong and co-workers proposed a reliable strategy for controlling the formation of the hollow cylinder structure of shape-persistent macrocycles (**Figure 1.7a**).^{87,88} Naturally, these rigid macrocycles are reluctant to self-superpose. By introducing side-chain hydrogen bonding and the backbone π - π stacking interactions, the authors can force these rigid macrocycles to self-associate into well-defined nanotubes in both the solid state and solution (**Figure 1.7b**). The resulting nanotubes showed excellent ion selectivity and efficient water transport properties. Nanotubes constructed by this strategy might offer new opportunities in chemical and biological separation, sensing, and catalysis.⁸⁹

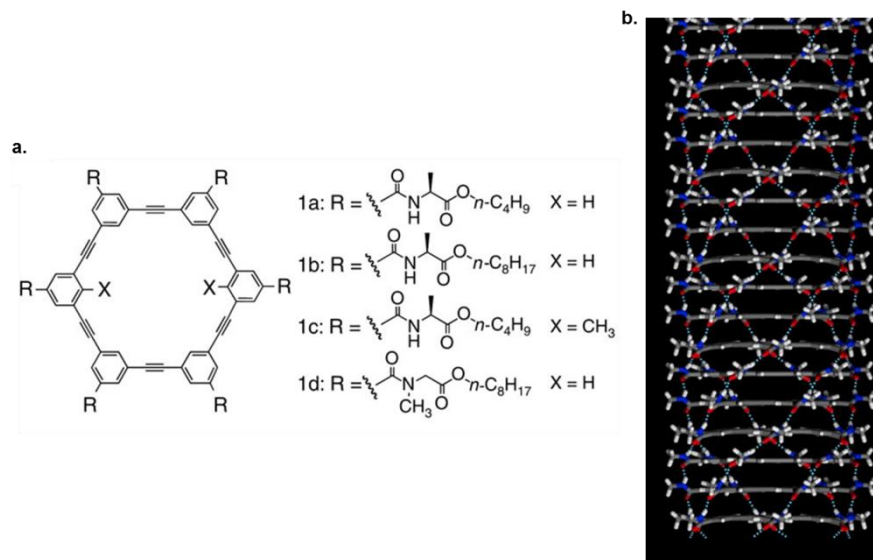


Figure 1-7. a. Molecular structure of the macrocycles. 1a-1c were designed to self-assemble into hydrogen-bonded tubular structure. 1d was designed for comparison since it cannot self-associate via hydrogen bonding. b. A snapshot of a helical stack of the macrocycles⁸⁶ (Reproduced with permission from reference 87. Copyright (2012) Nature Publishing Group)

In recent communications, the Shimizu group reported the self-assembly of bis-urea macrocycles which form columnar nanotubes through hydrogen bonding interactions.⁸² A schematic of structures of the macrocycles and the assembled tubes are presented in **Figure 1.8**. Single-crystal X-ray diffraction experiments revealed that the crystals formed upon slow cooling a solution of macrocycle in acetic acid were held together by intermolecular hydrogen bonding interactions to form tubular structures. In order to minimize the overall dipole moment, the urea functionalities are disposed in antiparallel fashion. In 2011, same group designed and synthesized a new macrocycle x.⁹⁰ This new macrocycle consists of two C-shaped phenylethyne units as spacers and two urea functionalities. The crystal structure shows that the nanotubes are not only stabilized by Hydrogen-bonding but also by π - π interactions of the phenylethyne linkers as well as by stacking interaction between the alkyne and phenyl on the neighboring macrocycle.

The resulting columnar nanotubes can be utilized as a confined environment for the selective photodimerization of coumarin.

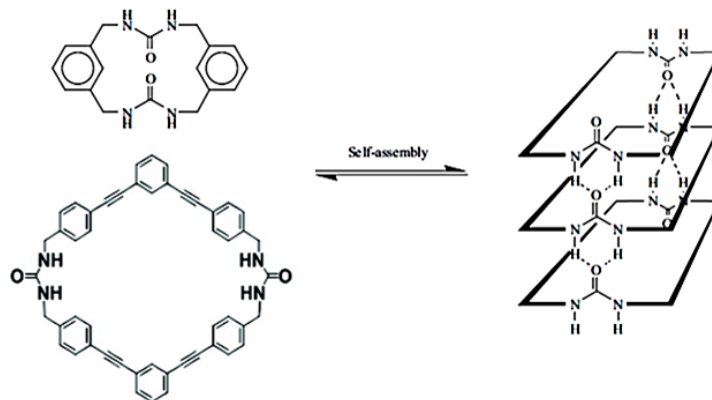


Figure 1-8. Bis-urea macrocycles reported by Shimizu and coworkers^{82,90} Reproduced by permission from reference 82. Copyright (2001) The Royal Society of Chemistry. (Reproduced with permission from reference 90. Copyright (2011) American Chemical Society).

The investigation of structure-function relationship of channels is of great interest as the channels play very important roles in sustaining biological systems as well as in nanotechnology. In 1974, DeSantis and co-workers discovered that peptides comprising an even number of alternating D- and L- amino acid could form closed rings.⁹¹ These peptide rings exhibit conformationally equivalent β -type dihedral angles and could self-assemble to nanotubes through hydrogen-bonding. **Figure 1.9** represents a typical working principle for the self-assembly of cyclic peptide rings.^{1,92} Peptide monomers are stacked via backbone-backbone hydrogen bonds between neighboring amide groups to a tubular structure.

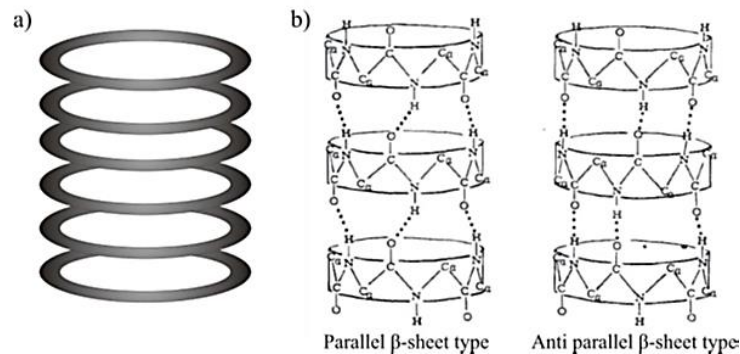


Figure 1-9. Cylindrical structures from stacking of the macrocycles; a) Schematic representation for the stacking of macrocycles on top of each other to form tubular structures. b) Cylindrical assembly of cyclic peptides as predicted by DeSantis and coworkers.⁹¹ (Reproduced with permission from reference 91. Copyright (1974) American Chemical Society).

In 1993, Ghadiri and co-workers published the first hollow structure assembly from cyclic peptides (cyclo $[-(\text{L-Gln-D-Ala-L-Glu-D-Ala})_2-]$) (**Figure 1.10**).⁷³ This type of porous molecule constructed by intermolecular interactions has been used in transmembrane ion channels.

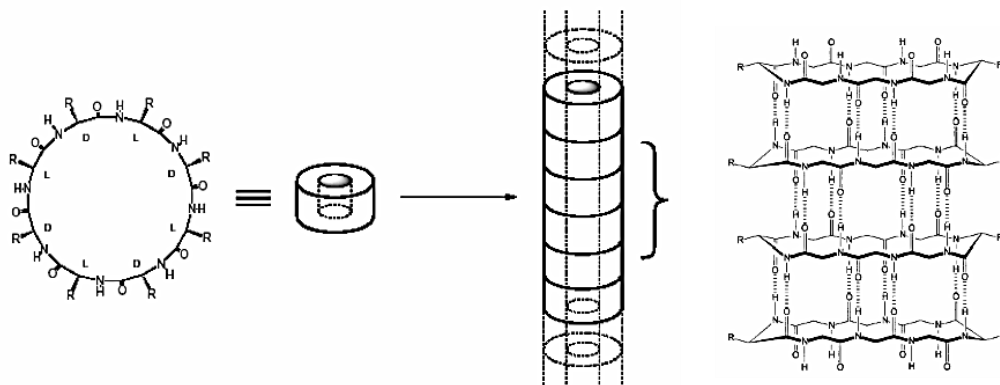


Figure 1-10. Schematic representation of self-assembly of cyclic (*D,L*)- peptides into hollow tubular structures.⁷³ (Reproduced with permission from reference 73. Copyright (1993) Nature Publishing Group)

In 2011, Tamaoki and co-workers published a series of novel macrocyclic compound constructed from L-glutamic acid and *trans*-1,4-cyclohexanediol (**Figure 1.11a**).⁹³ Due to

the strong hydrogen bonding between the amide groups, most of these macrocycles showed gelation properties in hydrophobic solvents. Irradiating these organogels with UV light led to a change in color to red or orange, suggesting that photopolymerization of diacetylene moieties was taking place. The crystal structure of one of the macrocycle demonstrated a tubular assembly based on intermolecular hydrogen-bonding (**Figure 1.11b**).

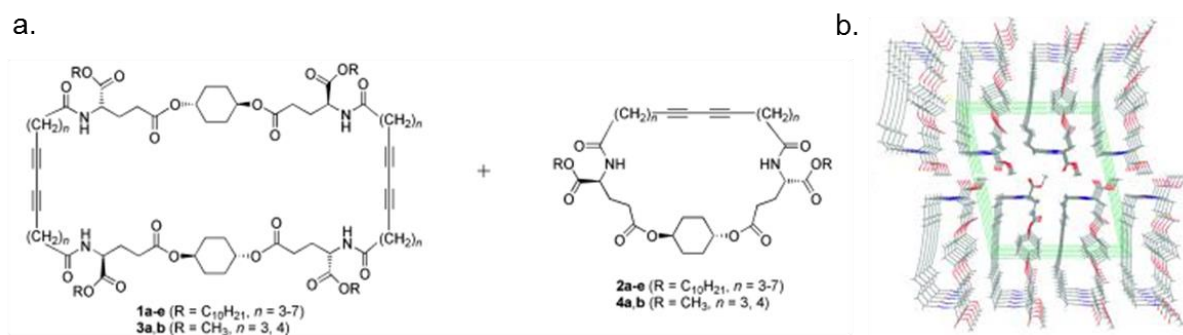


Figure 1-11. a. Molecular structure of the macrocyclic diacetylenedicarboxamide compounds.
 b. Crystal structure of Macrocycle 4b.⁹³ (Reproduced with permission from reference 93.
 Copyright (2011) Wiley-VCH)

Moreover, sugars have also been employed in the preparation of organic nanotubes (**Figure 1.12a**). In 1974, Stoddart and co-workers reported a tube-shaped molecule constructed from cyclic oligosaccharides (cyclodextrins). This nanotube shows inner diameters up to 13 Å (**Figure 1.12b**).^{63,70,94} Self-assembled nanotubes synthesized from *D*- and *L*-mannopyranose as well as *D*- and *L*-rhamnopyranose exhibited diameters ranging from 10 Å to 13 Å. Unlike cyclic peptides stacked via hydrogen-bonds, these tubular structures were held together by van der Waals contacts.⁷⁰

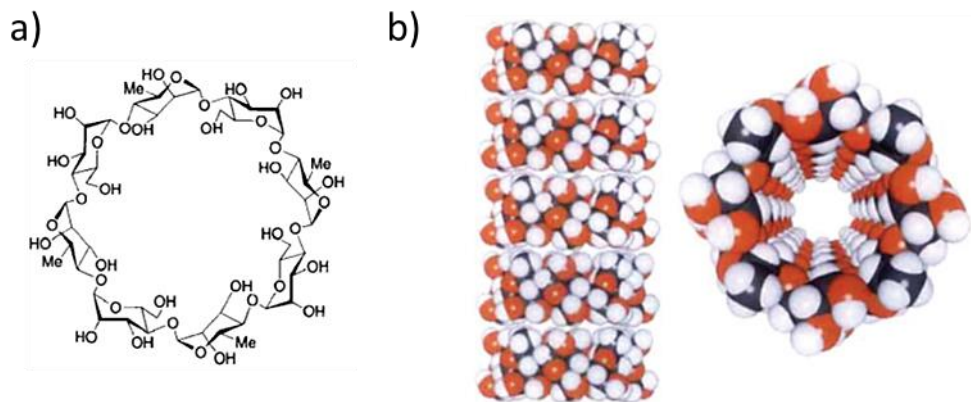


Figure 1-12. (a) Molecular structure of cyclodextrins. (b) Space filling model of cyclic oligosaccharide's self-assembly in solid-state.⁶³ (Reproduced with permission from reference 63. Copyright (1996) Wiley-VCH)

1.6. Tubular structure from sector shaped subunits

Discs or sector-shaped subunits can also be used to generate hollow cylindrical tubes.^{29,30,95-97} An impressive example of utilizing this pattern in biology is the preparation of the coat of the tobacco mosaic virus (TMV) from individual self-assembled proteins (**Figure 1.13a**).⁹⁷ Pioneering work by the Percec group demonstrated the application of taper-shaped monoesters and dendrimers for the construction of columnar mesophases.⁹⁸⁻¹⁰⁶ Wedge-shaped ester molecules such as 3,4,5-*tris*(*p*-dodecyloxy-benzyloxy) benzoic acid and ethylene glycol derivatives are used to self-assemble into a hexagonal columnar liquid crystalline tubular framework.^{101,103,104} The self-assembly process was driven by hydrophobic and hydrophilic interactions from the 3,4,5-*tris*(*p*-dodecyloxybenzyloxy) benzoate moiety as well as hydrogen-bonding from the oligo(oxyethylene) fragment (**Figure 1.13b**).^{98,105}

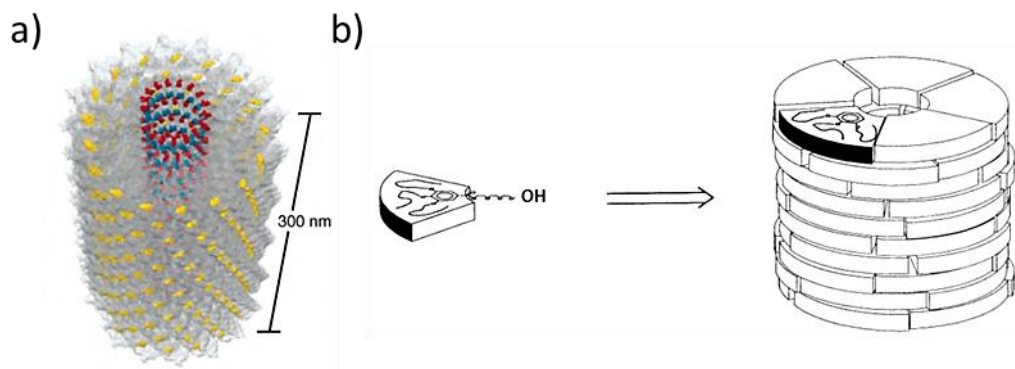


Figure 1-13. Tubular assembly from disc or sector shaped subunits; a) Representation of tobacco mosaic virus coat self-assembly.⁹⁷ (Reproduced with permission from reference 97. Copyright (2010) Royal Society Publishing) b) Self-assembly of wedge shape molecules into tubular frameworks.¹⁰⁵ (Reproduced from reference 105 by permission of The Royal Society of Chemistry)

In 2012, Lee and co-workers designed and synthesized the bent-shaped rigid-core molecules with flexible dendritic oligoether chain attached to the outer side of the backbone (**Figure 1.14**).^{107,108} In aqueous solution, they found these bent aromatic rods with nitrile groups at both ends can self-assemble into well-ordered supramolecular channels. In the solid state, these rod-coil block molecules self-assemble into a hexagonal columnar structure with weak long-range 3D correlations. The authors claimed that the driving force for the formation of the desired tubular architecture is the electrostatic interaction: the reaction between nitrile groups (electron withdrawing group) and phenoxy groups (electron donating group). This kind of materials might have potential application as novel ion transport channels and electro-optic nanomaterials.

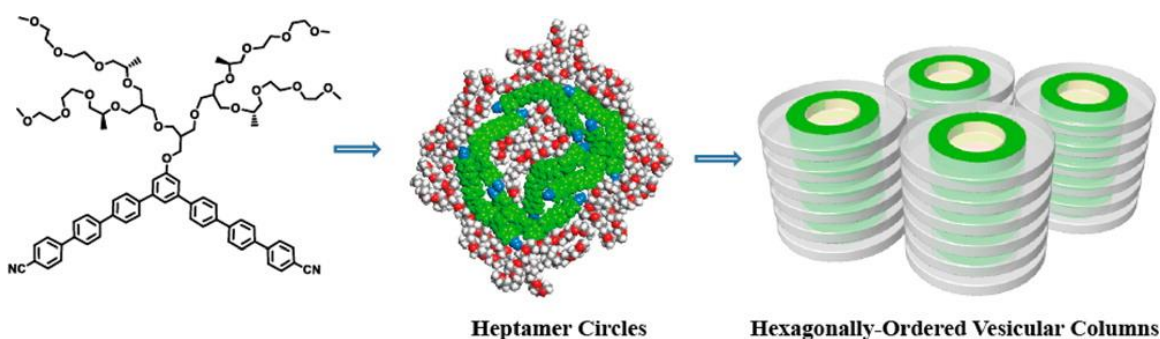


Figure 1-14. Schematic representation of proposed self-assembly for formation of hexameric macrocycle.¹⁰⁷ (Reproduced with permission from reference 107. Copyright (2012) Wiley-VCH)

1.7. Tubular structure from ring-rod molecules

Self-assembly of stave like subunits into tubular frameworks is an alternative method to make hollow cylindrical structures. As shown in **Figure 1.15a**,²¹⁻²³ *trans*-membrane pores form naturally from β -barrel proteins like porins or α -hemolysin. Matile and co-workers published the *p*-octiphenyl-peptide conjugates that can self-assemble to give cylindrical architectures with inner cavities.¹⁰⁹⁻¹¹⁵ In order to vertically align the carboxylic acid moieties along the axis of the *p*-octiphenyl backbones, the authors designed and synthesized the rigid rod staves, *p*-octiphenyl-peptide conjugates, to stack into nanotubes through intermolecular β -sheet formation (**Figure 1.15b**).¹¹⁶ The non-planar *p*-octiphenyl moieties hinder the linear aggregation of planar β -sheet into polymers.

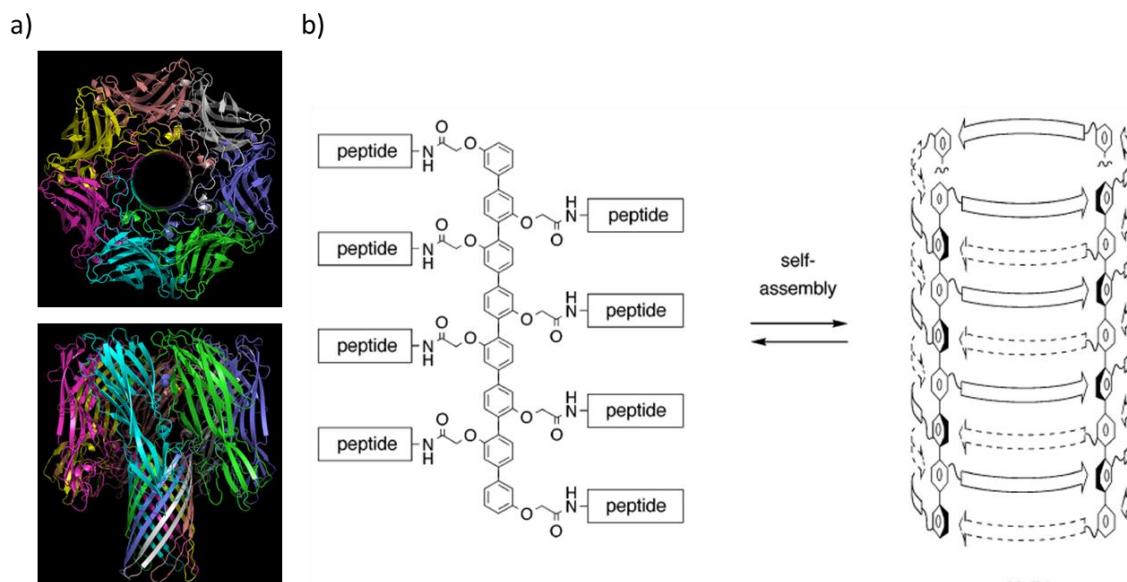


Figure 1-15. a) The β -barrel pore structure naturally from α -hemolysin.²¹ (Reproduced with permission from reference 21 American Association for the Advancement of Science) b) Schematic representation of self-assembly of *p*-octiphenylpeptide conjugates into cylindrical structures by β -sheet formation.¹¹² (Reproduced with permission from reference 112. Copyright (2005) American Chemical Society)

1.8. Covalent crosslinking of organic assembled precursors

The nanotubes introduced so far are all held together through non-covalent interactions. Covalent synthesis of the cylindrical nano-objects is also an interesting approach for chemists to design and synthesis their own imaginative version of tubular molecules. In 2003 Zimmermann *et al.* first reported a core-shell approach by molding dendritic frameworks around an oligoporphyrin core.¹¹⁷ The authors extend the traditional approaches for the preparation of molecularly imprinted polymers,¹¹⁸⁻¹²⁰ their design is based on a general strategy to synthesize cored dendrimers and the materials can be easily tailored with affinity and selectivity for a target guest molecule. The overall synthetic route includes three steps (**Figure 1.16**): first, covalent attachment of the dendrons to a porphyrin core. In this case, the Sn(IV) porphyrin core with multiple alkene end groups were oligomerized with succinic acid to give dendritic polymer **3**. Follow by cross-linking of the end groups of the dendrons through a ring-closing metathesis (RCM) reaction under high dilution conditions. The final step regards the removal of the oligoporphyrin core through a transesterfication reaction, to give the tubular architecture **5**. The thickness of the wall as well as the inner diameter depend on the dendron generation and the choice of the core.

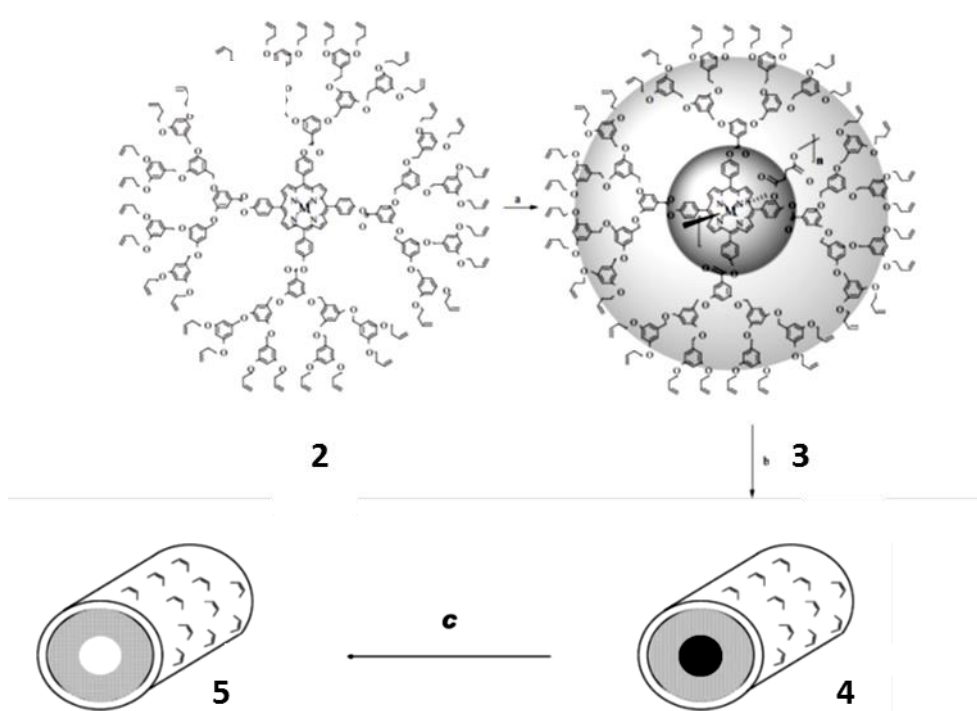


Figure 1-16. A new approach to organic nanotubes from porphyrin-containing dendrimers.¹¹⁷ (Reproduced with permission from reference 117. Copyright (2003) Wiley-VCH) Step a: The dendrimer 2 is polymerized (step a) to give 3. step b: intramolecularly crosslinked by RCM of 3 to give the nanoarchitecture 4. step c: cleaved of the central core region, in dark grey, to give the hollow tubular architecture 5.

Another example, investigated by Hecht and co-workers, represents a covalently stabilized organic nanotube based on intramolecular cross-linking of helically folded polymer backbones.¹²¹ The choice of the monomer is critical in their design: monomers with folding-promoting features and crossing-linking units are required to give the desired hollow tubular structures. Because the conformational behavior can easily be monitored by UV-Vis and fluorescence, and π - π stacking can help to properly pre-organize the reactive moieties for the cross-linking process, poly(*m*-phenyleneethynylene)s were chosen as the backbone. As shown in **Figure 1.17**, polymer 7 was prepared from monomer 6. Cinnamate groups play an important role since they can

undergo [2+2] photodimerization reaction to yield stable covalent-bonded helical structures. The resulting nanotube was obtained by irradiation under high-dilution conditions in acetonitrile.

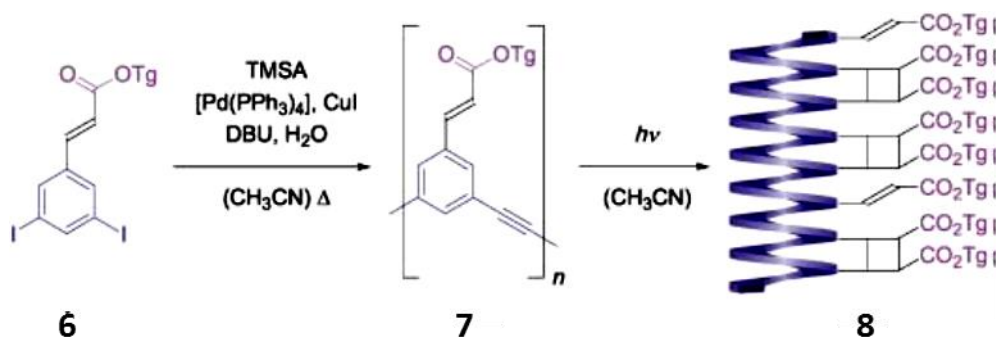


Figure 1-17. Synthesis and irradiation of amphiphilic poly(*m*-phenyleneethynylene) x (Tg=CH₂CH₂OCH₂CH₂OCH₂CH₂OCH₃). Step a: trimethylsilylacetylene, [Pd(PPh₃)₄], CuI, DBU, MeCN, Δ. Step b: irradiation.¹²¹ (Reproduced with permission from reference 121. Copyright (2003) American Chemical Society).

In 2012, Scott and co-workers developed a practical strategy for synthesizing [5,5] nanotube (**9**, **Figure 1.18**).¹²² These short, rigid and bowl shaped molecules can be prepared in just three steps. The crystal structure of the [5,5] nanotube showed that the bowl depth is 5.16 Å. The shortest distance between 5-fold axis of the hydrocarbon and its nearest neighbor is 9.4 Å, which corresponds to a carbon nanotube diameter (10 Å). Although the elongation of [5,5] nanotube **9** remains a large challenge, this work has the potential to a reliable method for constructing of single-wall carbon nanotubes.

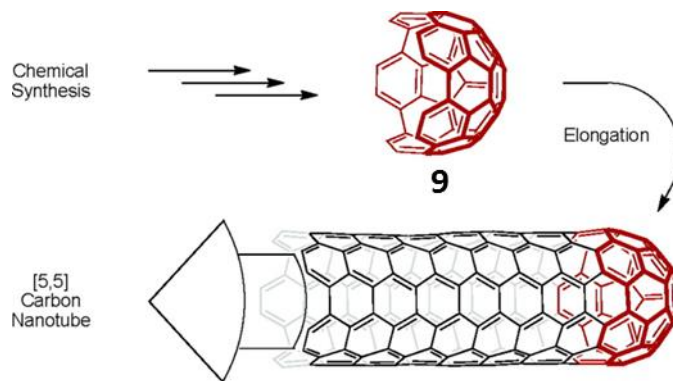


Figure 1-18. Strategy for the synthesis of uniform diameter carbon nanotubes.¹²² (Reproduced with permission from reference 122. Copyright (2012) American Chemical Society).

1.9. Potential applications of hollow tubular architectures

We have described several motifs for the construction of organic nanotubes in the above sections. Next, we will briefly introduce some potential applications of these tubular assemblies. So far, various organic, inorganic as well as a combination of both organic and inorganic based cylindrical molecules have been utilized in chemistry, biology and material science.¹²³⁻¹²⁷ Those include peptide based nanotubes,¹²⁸ graphite nanotubes,^{19,20} zeolites,^{129,130} porous metal organic scaffolds,^{131,132} cyclodextrins,^{70,75} tubular mesophases,^{133,134} microporous organic frameworks^{135,136} and bis-urea nanotubes.^{81,82,137,138} The major application of these tubular molecules is the ability to selectively encapsulate neutral and charged substrates to form host-guest complexes. This molecular recognition process can be controlled through weak non-covalent interactions. Because of these recognition properties, such nanotubes have been investigated as gas

storage materials,¹³⁹⁻¹⁴¹ chemical separation materials,^{121,122} sensors,^{78,142-144} transmembrane channels,^{145,146} and confined reaction vessels.¹⁴⁷⁻¹⁴⁹

1.9.1. Membrane channels for ionic and neutral molecule transport

Cylindrical structures have applications as transmembrane channels. In order to form transmembrane channels, the surface properties of the nanotubes are essential: substrate insertion into the membrane will not proceed unless they match the physical properties of the surrounding membrane. In 1994 Ghadiri *et al.* proposed that by separating the nonpolar lipid bilayers of the membrane, the cyclic D, L-peptides with hydrophobic side chains can self-organize into cylindrical structures (**Figure 1.19c**).⁷² **Figure 1.19a** represents the structure of the synthetic membrane channel named *cyclo[-(L-Trp-D-Leu)₃-L-Gln-D-Leu-]*. The pore diameter of this macrocycle is around 7.5 Å. The authors investigated the ions transport activity of these compounds and found these transmembrane channels show high transport activities for K⁺ and Na⁺ (10⁷ ions/sec). This result is three times faster than the natural membrane channel gramicidin A. By varying the number of amino acid moieties the ring size can be easily altered. Based on this idea, Ghadiri and co-workers designed and synthesized a decapeptide based macrocycle, *cyclo[-(L-Trp-D-Leu)₄-L-Gln-D-Leu-]* with an internal diameter of 10 Å (**Figure 1.19b**). The resulting larger macrocyclic assembly proved useful in the delivery of glucose across the lipid bilayers.¹⁵⁰ These findings suggest that an even larger cyclic peptide is required for the transportation of pharmacologically active agents. Many other synthetic channels for efficient delivery of ions and neutral molecules have attracted attention in recent research.^{88,111,112,151-154}

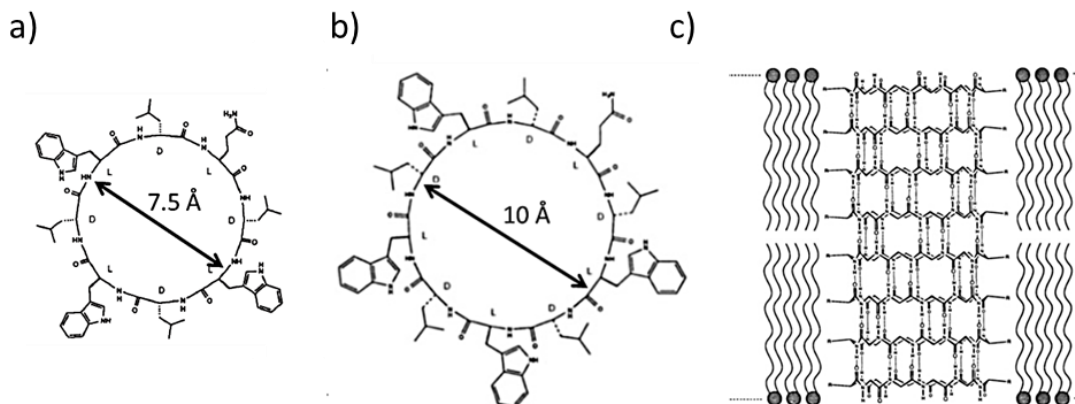


Figure 1-19. a) $Cyclo[-(L-Trp-D-Leu)_3-L-Gln-D-Leu-]$ ⁷² (Reproduced with permission from reference 72. Copyright (1994) Nature Publishing Group) b) $Cyclo[-(L-Trp-D-Leu)_4-L-Gln-D-Leu-]$ ¹⁵⁰ c) Schematic representation of cyclic peptide tubular self-assembly in lipid bilayers.¹⁵⁰ (Reproduced with permission from reference 150. Copyright (1994) American Chemical Society).

1.9.2. Hollow cylindrical materials for gas storage

Tubular pores play important roles in material science since they have applications as containers for gases or reactive reagents. One such substrate is hydrogen, which is a colorless, odorless and highly flammable gas. Hydrogen has been touted as an environmentally friendly wonder fuel that can be used in vehicles and burns to produce only water as a byproduct. To date the biggest challenge is to find efficient ways to safely store and transport hydrogen for use as an alternative fuel. Porous materials provide potential applications for storing hydrogen gas at ambient temperature.^{155,156} Fraenkel and Weitkamp found that up to 65 mL/g hydrogen gas can be stored utilizing zeolites.^{157,158} In this case, the hydrogen storage can take place at elevated temperature (200-400 °C) and pressures (20-900 bar) (**Figure 1.20a** and **1.20b**). After cooling the gas can be captured in the channels of the zeolites. In 2004, the Yaghi group explored the first use of metal-organic frameworks (MOF-5, IRMOF-6, IRMOF-8) for hydrogen gas uptake (1.0 to 2.0

wt %) at 10 bar pressure and room temperature (**Figure 1.20c**).¹⁴⁰ These metal organic scaffolds can be easily prepared by heating a mixture of $Zn(NO_3)_2 \cdot 4H_2O$ and 2,6-naphthalenedicarboxylate (2,6-NDC) in N,N' -diethylformamide. After this work, many efforts have been made to develop new types of metal-organic frameworks for hydrogen gas storage.¹⁴¹

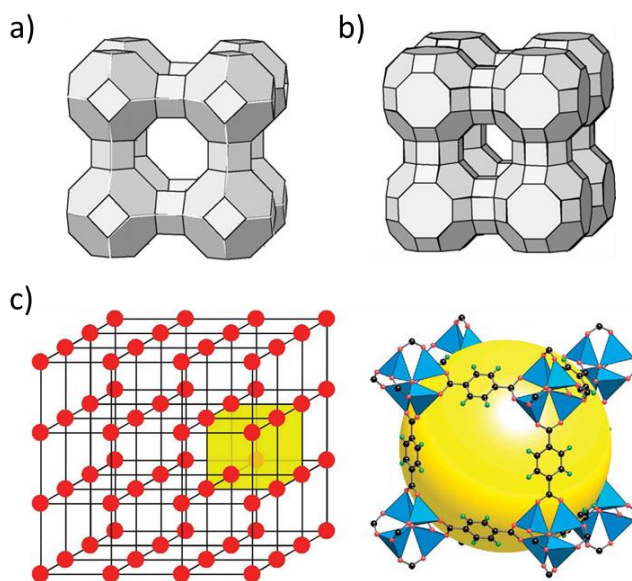


Figure 1-20. Pore shape and structures of a) Zeolite A b) Zeolite Rho¹⁵⁵ (Reproduced with permission from reference 155. Copyright (2007) Elsevier). c) Channels of IRMOF-8^{140,156} (Reproduced with permission from [references 140 and 156] American Association for the Advancement of Science).

1.9.3. Confined nanovessels for chemical reactions

Due to the important application as bio-based feedstock for industrial chemistry, a great deal of attention has been directed towards the oxidation of small-molecule alkenes.¹⁵⁹⁻¹⁶¹ Traditionally, the oxidants used have been potassium permanganate, selenium dioxide and strong acids like chromic as well as nitric acid. However, these oxidants are toxic and highly reactive. The use of these reagents always results in the production of unwanted chemical hazard. Oxidation using molecular oxygen is an alternative and more environment friendly method. With the assistance of triplet sensitizers such as Rose Bengal or benzophenone, singlet oxygen can be generated by irradiation of ground-state triplet oxygen with light. Unfortunately, oxidation reactions via this method often give poor product selectivity. Many scientists have been working to improve selectivity and regiochemistry of the oxidation reaction.^{162,163} In 2013, Shimizu reported the use of benzophenone bis-urea macrocycles as confined porous reactors for selective oxidation of 2-methyl-2-butene into the allylic alcohol, 3-methyl-2-buten-1-ol, at 90% selectivity as well as the selective reaction of cumene to the tertiary alcohol, α,α' -dimethyl benzyl alcohol, at 63% selectivity.¹³⁸ The authors found that the macrocycle they designed can produce a stable radical when exposed to UV-irradiation. They attribute the generation of the stable radical to the supramolecular assembly of the benzophenone bis-urea macrocycles. Although the mechanism of this transformation is still unclear, this work is a successful example to show the power of tubular material as confined environment for organic reactions.

1.10. Summary

Due to nanotubes' remarkable functions in material, electrical, and medical applications, the tubular structure has become a very important architecture in chemistry. A vast research effort in synthetic organic nanotubes is carried out. Relatively weak, non-covalent intermolecular interactions like ion-ion interactions, ion-dipole interactions, dipole-dipole interactions, π - π interactions and van der Waals forces can be used to direct the formation of complicated supermolecules. Indeed, supramolecular chemistry has become one of the most preferred strategies to accomplish a synthetic hollow cylindrical structure. However, the preparation of organic nanotubes held together by covalent bonds has recently attracted considerable attention because a continuous network of covalent bonds throughout the tubular network would make the tube more robust. The following chapters will discuss the design, synthesis and crystal structures of synthetic organic nanotubes developed from tubular addition polymers.

1.11. References

- (1) Bong, D. T.; Clark, T. D.; Granja, J. R.; Ghadiri, M. R.: Self-Assembling Organic Nanotubes. *Angewandte Chemie-International Edition* **2001**, *40*, 988-1011.
- (2) Bradley, K.; Gabriel, J. C. P.; Gruner, G.: Flexible Nanotube Electronics. *Nano Lett.* **2003**, *3*, 1353-1355.
- (3) Dalton, A. B.; Collins, S.; Munoz, E.; Razal, J. M.; Ebron, V. H.; Ferraris, J. P.; Coleman, J. N.; Kim, B. G.; Baughman, R. H.: Super-Tough Carbon-Nanotube Fibres - These Extraordinary Composite Fibres Can Be Woven into Electronic Textiles. *Nature* **2003**, *423*, 703-703.
- (4) Gannon, C. J.; Cherukuri, P.; Yakobson, B. I.; Cognet, L.; Kanzius, J. S.; Kittrell, C.; Weisman, R. B.; Pasquali, M.; Schmidt, H. K.; Smalley, R. E.; Curley, S. A.: Carbon Nanotube-Enhanced Thermal Destruction of Cancer Cells in a Noninvasive Radiofrequency Field. *Cancer* **2007**, *110*, 2654-2665.
- (5) Moore, J. S.: Shape-Persistent Molecular Architectures of Nanoscale Dimension. *Acc. Chem. Res.* **1997**, *30*, 402-413.
- (6) Postma, H. W. C.; Teepen, T.; Yao, Z.; Grifoni, M.; Dekker, C.: Carbon Nanotube Single-Electron Transistors at Room Temperature. *Science* **2001**, *293*, 76-79.
- (7) Shu, L.; Mayor, M.: Shape-Persistent Macrocyclic with a Self-Complementary Recognition Pattern Based on Diacetylene-Linked Alternating Hexylbenzene and Perfluorobenzene Rings. *Chem. Commun.* **2006**, 4134-4136.
- (8) Simmons, T. J.; Hashim, D.; Vajtai, R.; Ajayan, P. M.: Large Area-Aligned Arrays from Direct Deposition of Single-Wall Carbon Nanotube Inks. *J. Am. Chem. Soc.* **2007**, *129*, 10088-10089.
- (9) Singh, R.; Pantarotto, D.; McCarthy, D.; Chaloin, O.; Hoebeke, J.; Partidos, C. D.; Briand, J. P.; Prato, M.; Bianco, A.; Kostarelos, K.: Binding and Condensation of Plasmid DNA onto Functionalized Carbon Nanotubes: Toward the Construction of Nanotube-Based Gene Delivery Vectors. *J. Am. Chem. Soc.* **2005**, *127*, 4388-4396.
- (10) Tseng, Y. C.; Xuan, P. Q.; Javey, A.; Malloy, R.; Wang, Q.; Bokor, J.; Dai, H. J.: Monolithic Integration of Carbon Nanotube Devices with Silicon Mos Technology. *Nano Lett.* **2004**, *4*, 123-127.
- (11) Zhang, M.; Fang, S. L.; Zakhidov, A. A.; Lee, S. B.; Aliev, A. E.; Williams, C. D.; Atkinson, K. R.; Baughman, R. H.: Strong, Transparent, Multifunctional, Carbon Nanotube Sheets. *Science* **2005**, *309*, 1215-1219.
- (12) Zhao, D. H.; Moore, J. S.: Shape-Persistent Arylene Ethynylene Macrocyclics: Syntheses and Supramolecular Chemistry. *Chem. Commun.* **2003**, 807-818.
- (13) Horwich, A. L.; Weber-Ban, E. U.; Finley, D.: Chaperone Rings in Protein Folding and Degradation. *Proc. Natl. Acad. Sci. U. S. A.* **1999**, *96*, 11033-11040.
- (14) Sigler, P. B.; Xu, Z. H.; Rye, H. S.; Burston, S. G.; Fenton, W. A.; Horwich, A. L.: Structure and Function in Groel-Mediated Protein Folding. *Annu. Rev. Biochem.* **1998**, *67*, 581-608.
- (15) Voges, D.; Zwickl, P.; Baumeister, W.: The 26s Proteasome: A Molecular Machine Designed for Controlled Proteolysis. *Annu. Rev. Biochem.* **1999**, *68*, 1015-1068.
- (16) Zwickl, P.; Voges, D.; Baumeister, W.: The Proteasome: A Macromolecular Assembly Designed for Controlled Proteolysis. *Philosophical Transactions of the Royal Society of London Series B-Biological Sciences* **1999**, *354*, 1501-1511.
- (17) Eisenberg, B.: Ionic Channels in Biological Membranes: Natural Nanotubes. *Acc. Chem. Res.* **1998**, *31*, 117-123.

- (18) Borgnia, M.; Nielsen, S.; Engel, A.; Agre, P.: Cellular and Molecular Biology of the Aquaporin Water Channels. *Annu. Rev. Biochem.* **1999**, *68*, 425-458.
- (19) Ajayan, P. M.; Ebbesen, T. W.: Nanometre-Size Tubes of Carbon. *Reports on Progress in Physics* **1997**, *60*, 1025-1062.
- (20) Iijima, S.: Helical Microtubules of Graphitic Carbon. *Nature* **1991**, *354*, 56-58.
- (21) Song, L. Z.; Hobough, M. R.; Shustak, C.; Cheley, S.; Bayley, H.; Gouaux, J. E.: Structure of Staphylococcal Alpha-Hemolysin, a Heptameric Transmembrane Pore. *Science* **1996**, *274*, 1859-1866.
- (22) Cowan, S. W.; Schirmer, T.; Rummel, G.; Steiert, M.; Ghosh, R.; Pauptit, R. A.; Jansonius, J. N.; Rosenbusch, J. P.: Crystal-Structures Explain Functional-Properties of 2 Escherichia-Coli Porins. *Nature* **1992**, *358*, 727-733.
- (23) Schirmer, T.; Keller, T. A.; Wang, Y. F.; Rosenbusch, J. P.: Structural Basis for Sugar Translocation through Maltoporin Channels at 3.1-Angstrom Resolution. *Science* **1995**, *267*, 512-514.
- (24) Weiss, M. S.; Schulz, G. E.: Structure of Porin Refined at 1.8 Angstrom Resolution. *J. Mol. Biol.* **1992**, *227*, 493-509.
- (25) Merritt, E. A.; Sarfaty, S.; Vandenaeker, F.; Lhoir, C.; Martial, J. A.; Hol, W. G. J.: Crystal-Structure of Cholera-Toxin B-Pentamer Bound to Receptor G(M1) Pentasaccharide. *Protein Sci.* **1994**, *3*, 166-175.
- (26) Doyle, D. A.; Cabral, J. M.; Pfuetzner, R. A.; Kuo, A. L.; Gulbis, J. M.; Cohen, S. L.; Chait, B. T.; MacKinnon, R.: The Structure of the Potassium Channel: Molecular Basis of K⁺ Conduction and Selectivity. *Science* **1998**, *280*, 69-77.
- (27) Ketchum, R. R.; Hu, W.; Cross, T. A.: High-Resolution Conformation of Gramicidin-a in a Lipid Bilayer by Solid-State Nmr. *Science* **1993**, *261*, 1457-1460.
- (28) Caspar, D. L.; Namba, K.: Switching in the Self-Assembly of Tobacco Mosaic Virus. *Advances in biophysics* **1990**, *26*, 157-185.
- (29) Klug, A.: From Macromolecules to Biological Assemblies (Nobel Lecture). *Angewandte Chemie-International Edition in English* **1983**, *22*, 565-582.
- (30) Namba, K.; Stubbs, G.: Structure of Tobacco Mosaic-Virus at 3.6-a Resolution - Implications for Assembly. *Science* **1986**, *231*, 1401-1406.
- (31) Bong, D. T.; Clark, T. D.; Granja, J. R.; Ghadiri, M. R.: Self-Assembling Organic Nanotubes. *Angew. Chem., Int. Ed.* **2001**, *40*, 988-1011.
- (32) Parkin, I. P.: Supramolecular Chemistry. J.W. Steed and J.L. Atwood. John Wiley & Sons Ltd, Chichester, 2000. Xxvii + 745 Pages. £29.95 (Paperback). Isbn 0-471-98791-3. *Appl. Organomet. Chem.* **2001**, *15*, 236-236.
- (33) Pedersen, C. J.: Cyclic Polyethers and Their Complexes with Metal Salts. *J. Am. Chem. Soc.* **1967**, *89*, 7017.
- (34) Busch, D. H.; Stephenson, N. A.: Molecular-Organization, Portal to Supramolecular Chemistry - Structural-Analysis of the Factors Associated with Molecular-Organization in Coordination and Inclusion Chemistry, Including the Coordination Template Effect. *Coord. Chem. Rev.* **1990**, *100*, 119-154.
- (35) Zhang, W.; Moore, J. S.: Shape-Persistent Macrocycles: Structures and Synthetic Approaches from Arylene and Ethynylene Building Blocks. *Angewandte Chemie-International Edition* **2006**, *45*, 4416-4439.
- (36) Illuminati, G.; Mandolini, L.: Ring-Closure Reactions of Bifunctional Chain Molecules. *Acc. Chem. Res.* **1981**, *14*, 95-102.
- (37) Hoger, S.; Meckenstock, A. D.; Pellen, H.: High-Yield Macrocyclization Via Glaser Coupling of Temporary Covalent Templated Bisacetylenes. *J. Org. Chem.* **1997**, *62*, 4556-4557.
- (38) Ishii, S. I.; Witkop, B.: Gramicidin A .1. Determination of Composition and Amino Acid Configuration by Enzymatic and Gas Chromatographic Methods. *J. Am. Chem. Soc.* **1963**, *85*, 1832.

- (39) Sarges, R.; Witkop, B.: Formyl Novel Nh₂-Terminal Blocking Group in Naturally Occurring Peptide - Identity of Seco-Gramicidin with Desformylgramicidin. *J. Am. Chem. Soc.* **1964**, *86*, 1861.
- (40) Sarges, R.; Witkop, B.: Gramicidin A .4. Primary Sequence of Valine + Isoleucine Gramicidin A. *J. Am. Chem. Soc.* **1964**, *86*, 1862.
- (41) Syngé, R. L. M.: Gramicidin-S - over-All Chemical Characteristics and Amino-Acid Composition. *Biochem. J.* **1945**, *39*, 363-367.
- (42) Wallace, B. A.: Recent Advances in the High Resolution Structures of Bacterial Channels: Gramicidin A. *Journal of Structural Biology* **1998**, *121*, 123-141.
- (43) Urry, D. W.: Gramicidin-a Transmembrane Channel - Proposed Pi(L,D) Helix. *Proc. Natl. Acad. Sci. U. S. A.* **1971**, *68*, 672.
- (44) Bishop, R.; Dance, I. G.: New Types of Helical Canal Inclusion Networks. *Top. Curr. Chem.* **1988**, *149*, 137-188.
- (45) Gin, M. S.; Yokozawa, T.; Prince, R. B.; Moore, J. S.: Helical Bias in Solvophobiclly Folded Oligo(Phenylene Ethynylene)S. *J. Am. Chem. Soc.* **1999**, *121*, 2643-2644.
- (46) Nelson, J. C.; Saven, J. G.; Moore, J. S.; Wolynes, P. G.: Solvophobiclly Driven Folding of Nonbiological Oligomers. *Science* **1997**, *277*, 1793-1796.
- (47) Prince, R. B.; Brunsveld, L.; Meijer, E. W.; Moore, J. S.: Twist Sense Bias Induced by Chiral Side Chains in Helicallly Folded Oligomers. *Angewandte Chemie-International Edition* **2000**, *39*, 228.
- (48) Prince, R. B.; Okada, T.; Moore, J. S.: Controlling the Secondary Structure of Nonbiological Oligomers with Solvophobic and Coordination Interactions. *Angewandte Chemie-International Edition* **1999**, *38*, 233-236.
- (49) Appella, D. H.; Christianson, L. A.; Klein, D. A.; Powell, D. R.; Huang, X. L.; Barchi, J. J.; Gellman, S. H.: Residue-Based Control of Helix Shape in Beta-Peptide Oligomers. *Nature* **1997**, *387*, 381-384.
- (50) Gellman, S. H.: Foldamers: A Manifesto. *Acc. Chem. Res.* **1998**, *31*, 173-180.
- (51) Stoncius, S.; Orentas, E.; Butkus, E.; Ohrstrom, L.; Wendt, O. F.; Warnmark, K.: An Approach to Helical Tubular Self-Aggregation Using C-2-Symmetric Self-Complementary Hydrogen-Bonding Cavity Molecules. *J. Am. Chem. Soc.* **2006**, *128*, 8272-8285.
- (52) Matsuda, K.; Stone, M. T.; Moore, J. S.: Helical Pitch of M-Phenylene Ethynylene Foldamers by Double Spin Labeling. *J. Am. Chem. Soc.* **2002**, *124*, 11836-11837.
- (53) Yashima, E.; Maeda, K.; Iida, H.; Furusho, Y.; Nagai, K.: Helical Polymers: Synthesis, Structures, and Functions. *Chem. Rev.* **2009**, *109*, 6102-6211.
- (54) Cornelissen, J. J. L. M.; Donners, J. J. J. M.; de Gelder, R.; Graswinckel, W. S.; Metselaar, G. A.; Rowan, A. E.; Sommerdijk, N. A. J. M.; Nolte, R. J. M.: B-Helical Polymers from Isocyanopeptides. *Science* **2001**, *293*, 676-680.
- (55) Amabilino, D. B.; Ramos, E.; Serrano, J.-L.; Sierra, T.; Veciana, J.: Chiral Teleinduction in the Polymerization of Isocyanides. *Polymer* **2005**, *46*, 1507-1521.
- (56) Amabilino, D. B.; Serrano, J.-L.; Veciana, J.: Reversible and Irreversible Conformational Changes in Poly(Isocyanide)S: A Remote Stereoelectronic Effect. *Chem. Commun.* **2005**, 322-324.
- (57) Takei, F.; Onitsuka, K.; Takahashi, S.: Thermally Induced Helical Conformational Change in Poly(Aryl Isocyanide)S with Optically Active Ester Groups. *Macromolecules* **2005**, *38*, 1513-1516.
- (58) Onitsuka, K.; Mori, T.; Yamamoto, M.; Takei, F.; Takahashi, S.: Helical Sense Selective Polymerization of Bulky Aryl Isocyanide Possessing Chiral Ester or Amide Groups Initiated by Arylrhodium Complexes. *Macromolecules* **2006**, *39*, 7224-7231.
- (59) Kajitani, T.; Okoshi, K.; Yashima, E.: Helix-Sense-Controlled Polymerization of Optically Active Phenyl Isocyanides. *Macromolecules* **2008**, *41*, 1601-1611.

- (60) Yashima, E.; Maeda, K.; Furusho, Y.: Single- and Double-Stranded Helical Polymers: Synthesis, Structures, and Functions. *Acc. Chem. Res.* **2008**, *41*, 1166-1180.
- (61) Schwartz, E.; Koepf, M.; Kitto, H. J.; Nolte, R. J. M.; Rowan, A. E.: Helical Poly(Isocyanides): Past, Present and Future. *Polymer Chemistry* **2011**, *2*, 33-47.
- (62) Hu, G.; Li, W.; Hu, Y.; Xu, A.; Yan, J.; Liu, L.; Zhang, X.; Liu, K.; Zhang, A.: Water-Soluble Chiral Polyisocyanides Showing Thermoresponsive Behavior. *Macromolecules* **2013**, *46*, 1124-1132.
- (63) Ashton, P. R.; Brown, C. L.; Menzer, S.; Nepogodiev, S. A.; Stoddart, J. F.; Williams, D. J.: Synthetic Cyclic Oligosaccharides - Syntheses and Structural Properties of a Cyclo (1->4)-Alpha-L-Rhamnopyranosyl-(1->4)-Alpha-D-Mannopyranosyl Trios Ide and -Tetraoside. *Chemistry-a European Journal* **1996**, *2*, 580-591.
- (64) Ashton, P. R.; Cantrill, S. J.; Gattuso, G.; Menzer, S.; Nepogodiev, S. A.; Shipway, A. N.; Stoddart, J. F.; Williams, D. J.: Achiral Cyclodextrin Analogues. *Chemistry-a European Journal* **1997**, *3*, 1299-1314.
- (65) Baldini, L.; Sansone, F.; Casnati, A.; Ugozzoli, F.; Ungaro, R.: Peptidocalix[4]Arene Self-Assembled Nanotubes. *J. Supramol. Chem.* **2002**, *2*, 219-226.
- (66) Casnati, A.; Liantonio, R.; Metrangolo, P.; Resnati, G.; Ungaro, R.; Ugozzoli, F.: Molecular and Supramolecular Homochirality: Enantiopure Perfluorocarbon Rotamers and Halogen-Bonded Fluorous Double Helices. *Angewandte Chemie-International Edition* **2006**, *45*, 1915-1918.
- (67) Dalgarno, S. J.; Cave, G. W. V.; Atwood, J. L.: Toward the Isolation of Functional Organic Nanotubes. *Angewandte Chemie-International Edition* **2006**, *45*, 570-574.
- (68) Dawson, C.; Horton, P. N.; Hursthouse, M. B.; James, S. L.: Channelled Crystals Formed by Tubular Stacking of a 4+4 Phenylene-Piperazine Macrocyclic. *CrystEngComm* **2010**, *12*, 1048-1050.
- (69) Fromm, K. M.; Bergougnant, R. D.: Transport Properties of Solid State Crown Ether Channel Systems. *Solid State Sci.* **2007**, *9*, 580-587.
- (70) Gattuso, G.; Menzer, S.; Nepogodiev, S. A.; Stoddart, J. F.; Williams, D. J.: Carbohydrate Nanotubes. *Angewandte Chemie-International Edition in English* **1997**, *36*, 1451-1454.
- (71) Gauthier, D.; Baillargeon, P.; Drouin, M.; Dory, Y. L.: Self-Assembly of Cyclic Peptides into Nanotubes and Then into Highly Anisotropic Crystalline Materials. *Angewandte Chemie-International Edition* **2001**, *40*, 4635.
- (72) Ghadiri, M. R.; Granja, J. R.; Buehler, L. K.: Artificial Transmembrane Ion Channels from Self-Assembling Peptide Nanotubes. *Nature* **1994**, *369*, 301-304.
- (73) Ghadiri, M. R.; Granja, J. R.; Milligan, R. A.; McRee, D. E.; Khazanovich, N.: Self-Assembling Organic Nanotubes Based on a Cyclic Peptide Architecture. *Nature* **1993**, *366*, 324-327.
- (74) Harada, A.; Li, J.; Kamachi, M.: The Molecular Necklace - a Rotaxane Containing Many Threaded Alpha-Cyclodextrins. *Nature* **1992**, *356*, 325-327.
- (75) Harada, A.; Li, J.; Kamachi, M.: Synthesis of a Tubular Polymer from Threaded Cyclodextrins. *Nature* **1993**, *364*, 516-518.
- (76) Kloo, L.; Svensson, P. H.; Taylor, M. J.: Investigations of the Polyiodides H₃O Center Dot I-X (X=3, 5 or 7) as Dibenzo-18-Crown-6 Complexes. *Journal of the Chemical Society-Dalton Transactions* **2000**, 1061-1065.
- (77) Lazar, A. N.; Dupont, N.; Navaza, A.; Coleman, A. W.: Helical Aquatubes of Calix 4 Arene Di-Methoxycarboxylic Acid. *Chem. Commun.* **2006**, 1076-1078.
- (78) Motesharei, K.; Ghadiri, M. R.: Diffusion-Limited Size-Selective Ion Sensing Based on Sam-Supported Peptide Nanotubes. *J. Am. Chem. Soc.* **1997**, *119*, 11306-11312.

- (79) Organo, V. G.; Leontiev, A. V.; Sgarlata, V.; Dias, H. V. R.; Rudkevich, D. M.: Supramolecular Features of Calixarene-Based Synthetic Nanotubes. *Angewandte Chemie-International Edition* **2005**, *44*, 3043-3047.
- (80) Semetey, V.; Didierjean, C.; Briand, J. P.; Aubry, A.; Guichard, G.: Self-Assembling Organic Nanotubes from Enantiopure Cyclo-N,N '-Linked Oligoureas: Design, Synthesis, and Crystal Structure. *Angewandte Chemie-International Edition* **2002**, *41*, 1895.
- (81) Shimizu, L. S.; Hughes, A. D.; Smith, M. D.; Davis, M. J.; Zhang, B. P.; zur Loye, H. C.; Shimizu, K. D.: Self-Assembled Nanotubes That Reversibly Bind Acetic Acid Guests. *J. Am. Chem. Soc.* **2003**, *125*, 14972-14973.
- (82) Shimizu, L. S.; Smith, M. D.; Hughes, A. D.; Shimizu, K. D.: Self-Assembly of a Bis-Urea Macrocyclic into a Columnar Nanotube. *Chem. Commun.* **2001**, 1592-1593.
- (83) Hisaki, I.; Shigemitsu, H.; Sakamoto, Y.; Hasegawa, Y.; Okajima, Y.; Nakano, K.; Tohnai, N.; Miyata, M.: Octadecahydrodibenzo 12 Annulene-Based Organogels: Two Methyl Ester Groups Prevent Crystallization and Promote Gelation. *Angewandte Chemie-International Edition* **2009**, *48*, 5465-5469.
- (84) Cuccia, L. A.; Lehn, J. M.; Homo, J. C.; Schmutz, M.: Encoded Helical Self-Organization and Self-Assembly into Helical Fibers of an Oligoheterocyclic Pyridine-Pyridazine Molecular Strand. *Angewandte Chemie-International Edition* **2000**, *39*, 233.
- (85) Venkataraman, D.; Lee, S.; Zhang, J. S.; Moore, J. S.: An Organic-Solid with Wide Channels Based on Hydrogen-Bonding between Macrocyclics. *Nature* **1994**, *371*, 591-593.
- (86) Höger, S.: Highly Efficient Methods for the Preparation of Shape-Persistent Macrocyclics. *Journal of Polymer Science Part A: Polymer Chemistry* **1999**, *37*, 2685-2698.
- (87) Zhou, X.; Liu, G.; Yamato, K.; Shen, Y.; Cheng, R.; Wei, X.; Bai, W.; Gao, Y.; Li, H.; Liu, Y.; Liu, F.; Czajkowsky, D. M.; Wang, J.; Dabney, M. J.; Cai, Z.; Hu, J.; Bright, F. V.; He, L.; Zeng, X. C.; Shao, Z.; Gong, B.: Self-Assembling Subnanometer Pores with Unusual Mass-Transport Properties. *Nature Communications* **2012**, *3*.
- (88) Gong, B.; Shao, Z.: Self-Assembling Organic Nanotubes with Precisely Defined, Sub-Nanometer Pores: Formation and Mass Transport Characteristics. *Acc. Chem. Res.* **2013**.
- (89) Gin, D. L.; Noble, R. D.: Designing the Next Generation of Chemical Separation Membranes. *Science* **2011**, *332*, 674-676.
- (90) Dawn, S.; Dewal, M. B.; Sobransingh, D.; Paderes, M. C.; Wibowo, A. C.; Smith, M. D.; Krause, J. A.; Pellechia, P. J.; Shimizu, L. S.: Self-Assembled Phenylethynylene Bis-Urea Macrocyclics Facilitate the Selective Photodimerization of Coumarin. *J. Am. Chem. Soc.* **2011**, *133*, 7025-7032.
- (91) Desantis, P.; Morosett, S.; Rizzo, R.: Conformational-Analysis of Regular Enantiomeric Sequences. *Macromolecules* **1974**, *7*, 52-58.
- (92) Pasini, D.; Ricci, M.: Macrocyclics as Precursors for Organic Nanotubes. *Curr. Org. Synth.* **2007**, *4*, 59-80.
- (93) Nagasawa, J. i.; Yoshida, M.; Tamaoki, N.: Synthesis, Gelation Properties and Photopolymerization of Macrocyclic Diacetylenedicarboxamides Derived from L-Glutamic Acid and Trans-1,4-Cyclohexanediol. *Eur. J. Org. Chem.* **2011**, *2011*, 2247-2255.
- (94) Gattuso, G.; Nepogodiev, S. A.; Stoddart, J. F.: Synthetic Cyclic Oligosaccharides. *Chem. Rev.* **1998**, *98*, 1919-1958.
- (95) Butler, P. J. G.: Self-Assembly of Tobacco Mosaic Virus: The Role of an Intermediate Aggregate in Generating Both Specificity and Speed. *Philosophical Transactions of the Royal Society of London Series B-Biological Sciences* **1999**, *354*, 537-550.
- (96) Lebeurier, G.; Nicolaieff, A.; Richards, K. E.: Inside-out Model for Self-Assembly of Tobacco Mosaic-Virus. *Proc. Natl. Acad. Sci. U. S. A.* **1977**, *74*, 149-153.
- (97) Soto, C. M.; Ratna, B. R.: Virus Hybrids as Nanomaterials for Biotechnology. *Curr. Opin. Biotechnol.* **2010**, *21*, 426-438.

- (98) Hudson, S. D.; Jung, H. T.; Percec, V.; Cho, W. D.; Johansson, G.; Ungar, G.; Balagurusamy, V. S. K.: Direct Visualization of Individual Cylindrical and Spherical Supramolecular Dendrimers. *Science* **1997**, 278, 449-452.
- (99) Johansson, G.; Percec, V.; Ungar, G.; Zhou, J. P.: Fluorophobic Effect in the Self-Assembly of Polymers and Model Compounds Containing Tapered Groups into Supramolecular Columns. *Macromolecules* **1996**, 29, 646-660.
- (100) Percec, V.; Bera, T. K.: Cell Membrane as a Model for the Design of Ion-Active Nanostructured Supramolecular Systems. *Biomacromolecules* **2002**, 3, 167-181.
- (101) Percec, V.; Heck, J.; Tomazos, D.; Falkenberg, F.; Blackwell, H.; Ungar, G.: Self-Assembly of Taper-Shaped Monoesters of Oligo(Ethylene Oxide) with 3,4,5-Tris(P-Dodecyloxybenzyloxy)Benzoic Acid and of Their Polymethacrylates into Tubular Supramolecular Architectures Displaying a Columnar Mesophase. *Journal of the Chemical Society-Perkin Transactions 1* **1993**, 2799-2811.
- (102) Percec, V.; Heck, J. A.; Tomazos, D.; Ungar, G.: The Influence of the Complexation of Sodium and Lithium Triflate on the Self-Assembly of Tubular-Supramolecular Architectures Displaying a Columnar Mesophase Based on Taper-Shaped Monoesters of Oligoethylene Oxide with 3,4,5-Tris P-(N-Dodecan-1-Yloxy)Benzyloxy Benzoic Acid and of Their Polymethacrylates. *Journal of the Chemical Society-Perkin Transactions 2* **1993**, 2381-2388.
- (103) Percec, V.; Johansson, G.; Heck, J.; Ungar, G.; Batty, S. V.: Molecular Recognition Directed Self-Assembly of Supramolecular Cylindrical Channel-Like Architectures from 6,7,9,10,12,13,15,16-Octahydro-1,4,7,10,13-Pentaoxabenzocyclopentadecen- 2-Ylmethyl 3,4,5-Tris(P-Dodecyloxybenzyl-Oxy)Benzoate. *Journal of the Chemical Society-Perkin Transactions 1* **1993**, 1411-1420.
- (104) Percec, V.; Johansson, G.; Ungar, G.; Zhou, J. P.: Fluorophobic Effect Induces the Self-Assembly of Semifluorinated Tapered Monodendrons Containing Crown Ethers into Supramolecular Columnar Dendrimers Which Exhibit a Homeotropic Hexagonal Columnar Liquid Crystalline Phase. *J. Am. Chem. Soc.* **1996**, 118, 9855-9866.
- (105) Percec, V.; Tomazos, D.; Heck, J.; Blackwell, H.; Ungar, G.: Self-Assembly of Taper-Shaped Monoesters of Oligo(Ethylene Oxide) with 3,4,5-Tris(N-Dodecan-1-Yloxy)Benzoic Acid and of Their Polymethacrylates into Tubular Supramolecular Architectures Displaying a Columnar Hexagonal Mesophase. *Journal of the Chemical Society-Perkin Transactions 2* **1994**, 31-44.
- (106) Ungar, G.; Abramic, D.; Percec, V.; Heck, J. A.: Self-Assembly of Twin Tapered Bisamides into Supramolecular Columns Exhibiting Hexagonal Columnar Mesophases. Structural Evidence for a Microsegregated Model of the Supramolecular Column. *Liq. Cryst.* **1996**, 21, 73-86.
- (107) Kim, H.-J.; Liu, F.; Ryu, J.-H.; Kang, S.-K.; Zeng, X.; Ungar, G.; Lee, J.-K.; Zin, W.-C.; Lee, M.: Self-Organization of Bent Rod Molecules into Hexagonally Ordered Vesicular Columns. *J. Am. Chem. Soc.* **2012**, 134, 13871-13880.
- (108) Kim, Y.; Li, W.; Shin, S.; Lee, M.: Development of Toroidal Nanostructures by Self-Assembly: Rational Designs and Applications. *Acc. Chem. Res.* **2013**.
- (109) Baumeister, B.; Matile, S.: Programmed Assembly of Expanded Rigid-Rod Beta-Barrels by Supramolecular Preorganization. *Chem. Commun.* **2000**, 913-914.
- (110) Baumeister, B.; Sakai, N.; Matile, S.: Giant Artificial Ion Channels Formed by Self-Assembled, Cationic Rigid-Rod Beta-Barrels. *Angewandte Chemie-International Edition* **2000**, 39, 1955.
- (111) Das, G.; Matile, S.: Transmembrane Pores Formed by Synthetic P-Octiphenyl Beta-Barrels with Internal Carboxylate Clusters: Regulation of Ion Transport by Ph and Mg²⁺ Complexed 8-Aminonaphthalene-1,3,6-Trisulfonate. *Proc. Natl. Acad. Sci. U. S. A.* **2002**, 99, 5183-5188.

- (112) Sakai, N.; Mareda, J.; Matile, S.: Rigid-Rod Molecules in Biomembrane Models: From Hydrogen-Bonded Chains to Synthetic Multifunctional Pores. *Acc. Chem. Res.* **2005**, *38*, 79-87.
- (113) Sakai, N.; Matile, S.: Synthetic Multifunctional Pores: Lessons from Rigid-Rod Beta-Barrels. *Chem. Commun.* **2003**, 2514-2523.
- (114) Sorde, N.; Das, G.; Matile, S.: Enzyme Screening with Synthetic Multifunctional Pores: Focus on Biopolymers. *Proc. Natl. Acad. Sci. U. S. A.* **2003**, *100*, 11964-11969.
- (115) Matile, S.: En Route to Supramolecular Functional Plasticity: Artificial Beta-Barrels, the Barrel-Stave Motif, and Related Approaches. *Chem. Soc. Rev.* **2001**, *30*, 158-167.
- (116) Sakai, N.; Majumdar, N.; Matile, S.: Self-Assembled Rigid-Rod Ionophores. *J. Am. Chem. Soc.* **1999**, *121*, 4294-4295.
- (117) Kim, Y.; Mayer, M. F.; Zimmerman, S. C.: A New Route to Organic Nanotubes from Porphyrin Dendrimers. *Angewandte Chemie-International Edition* **2003**, *42*, 1121-1126.
- (118) Takeuchi, T.; Mukawa, T.; Matsui, J.; Higashi, M.; Shimizu, K. D.: Molecularly Imprinted Polymers with Metalloporphyrin-Based Molecular Recognition Sites Coassembled with Methacrylic Acid. *Anal. Chem.* **2001**, *73*, 3869-3874.
- (119) Umpleby, R. J.; Baxter, S. C.; Rampey, A. M.; Rushton, G. T.; Chen, Y. Z.; Shimizu, K. D.: Characterization of the Heterogeneous Binding Site Affinity Distributions in Molecularly Imprinted Polymers. *Journal of Chromatography B-Analytical Technologies in the Biomedical and Life Sciences* **2004**, *804*, 141-149.
- (120) Zimmerman, S. C.; Wendland, M. S.; Rakow, N. A.; Zharov, I.; Suslick, K. S.: Synthetic Hosts by Monomolecular Imprinting inside Dendrimers. *Nature* **2002**, *418*, 399-403.
- (121) Hecht, S.; Khan, A.: Intramolecular Cross-Linking of Helical Folds: An Approach to Organic Nanotubes. *Angewandte Chemie-International Edition* **2003**, *42*, 6021-6024.
- (122) Scott, L. T.; Jackson, E. A.; Zhang, Q.; Steinberg, B. D.; Bancu, M.; Li, B.: A Short, Rigid, Structurally Pure Carbon Nanotube by Stepwise Chemical Synthesis. *J. Am. Chem. Soc.* **2011**, *134*, 107-110.
- (123) Colombo, G.; Soto, P.; Gazit, E.: Peptide Self-Assembly at the Nanoscale: A Challenging Target for Computational and Experimental Biotechnology. *Trends Biotechnol.* **2007**, *25*, 211-218.
- (124) Huang, K.; Tang, W.; Tang, R.; Xu, Z.; He, Z.; Li, Z.; Xu, Y.; Li, X.; He, G.; Feng, G.; He, L.; Shi, Y.: Positive Association between Olig2 and Schizophrenia in the Chinese Han Population. *Hum. Genet.* **2008**, *122*, 659-660.
- (125) Li, D.; Huang, J.; Kaner, R. B.: Polyaniline Nanofibers: A Unique Polymer Nanostructure for Versatile Applications. *Acc. Chem. Res.* **2009**, *42*, 135-145.
- (126) Brea, R. J.; Reiriz, C.; Granja, J. R.: Towards Functional Bionanomaterials Based on Self-Assembling Cyclic Peptide Nanotubes. *Chem. Soc. Rev.* **2010**, *39*, 1448-1456.
- (127) Feng, C.; Khulbe, K. C.; Matsuura, T.: Recent Progress in the Preparation, Characterization, and Applications of Nanofibers and Nanofiber Membranes Via Electrospinning/Interfacial Polymerization. *J. Appl. Polym. Sci.* **2010**, *115*, 756-776.
- (128) Anzini, P.; Xu, C.; Hughes, S.; Magnotti, E.; Jiang, T.; Hemmingsen, L.; Demeler, B.; Conticello, V. P.: Controlling Self-Assembly of a Peptide-Based Material Via Metal-Ion Induced Registry Shift. *J. Am. Chem. Soc.* **2013**, *135*, 10278-10281.
- (129) Tung, C.-H.; Wu, L.-Z.; Zhang, L.-P.; Chen, B.: Supramolecular Systems as Microreactors: Control of Product Selectivity in Organic Phototransformation. *Acc. Chem. Res.* **2002**, *36*, 39-47.
- (130) Yang, Q.; Han, D.; Yang, H.; Li, C.: Asymmetric Catalysis with Metal Complexes in Nanoreactors. *Chemistry – An Asian Journal* **2008**, *3*, 1214-1229.
- (131) Eddaoudi, M.; Moler, D. B.; Li, H. L.; Chen, B. L.; Reineke, T. M.; O'Keeffe, M.; Yaghi, O. M.: Modular Chemistry: Secondary Building Units as a Basis for the Design of Highly Porous and Robust Metal-Organic Carboxylate Frameworks. *Acc. Chem. Res.* **2001**, *34*, 319-330.

- (132) Rowsell, J. L. C.; Yaghi, O. M.: Metal-Organic Frameworks: A New Class of Porous Materials. *Microporous Mesoporous Mater.* **2004**, *73*, 3-14.
- (133) Malthete, J.; Levelut, A. M.; Lehn, J. M.: Tubular Mesophases - a Structural-Analysis. *Journal of the Chemical Society-Chemical Communications* **1992**, 1434-1436.
- (134) Zhang, J. S.; Moore, J. S.: Nanoarchitectures .6. Liquid-Crystals Based on Shape-Persistent Macrocyclic Mesogens. *J. Am. Chem. Soc.* **1994**, *116*, 2655-2656.
- (135) Cote, A. P.; Benin, A. I.; Ockwig, N. W.; O'Keeffe, M.; Matzger, A. J.; Yaghi, O. M.: Porous, Crystalline, Covalent Organic Frameworks. *Science* **2005**, *310*, 1166-1170.
- (136) Gorbitz, C. H.: Microporous Organic Materials from Hydrophobic Dipeptides. *Chemistry-a European Journal* **2007**, *13*, 1022-1031.
- (137) Shimizu, L. S.; Hughes, A. D.; Smith, M. D.; Samuel, S. A.; Ciurtin-Smith, D.: Assembled Columnar Structures from Bis-Urea Macrocycles. *Supramol. Chem.* **2005**, *17*, 27-30.
- (138) Geer, M. F.; Walla, M. D.; Solntsev, K. M.; Strassert, C. A.; Shimizu, L. S.: Self-Assembled Benzophenone Bis-Urea Macrocycles Facilitate Selective Oxidations by Singlet Oxygen. *The Journal of Organic Chemistry* **2013**, *78*, 5568-5578.
- (139) Eddaoudi, M.; Kim, J.; Rosi, N.; Vodak, D.; Wachter, J.; O'Keeffe, M.; Yaghi, O. M.: Systematic Design of Pore Size and Functionality in Isorecticular Mofs and Their Application in Methane Storage. *Science* **2002**, *295*, 469-472.
- (140) Rosi, N. L.; Eckert, J.; Eddaoudi, M.; Vodak, D. T.; Kim, J.; O'Keeffe, M.; Yaghi, O. M.: Hydrogen Storage in Microporous Metal-Organic Frameworks. *Science* **2003**, *300*, 1127-1129.
- (141) Sun, Y.; Wang, L.; Amer, W.; Yu, H.; Ji, J.; Huang, L.; Shan, J.; Tong, R.: Hydrogen Storage in Metal-Organic Frameworks. *J. Inorg. Organomet. Polym. Mater.* **2013**, *23*, 270-285.
- (142) Halder, G. J.; Kepert, C. J.; Moubaraki, B.; Murray, K. S.; Cashion, J. D.: Guest-Dependent Spin Crossover in a Nanoporous Molecular Framework Material. *Science* **2002**, *298*, 1762-1765.
- (143) Uemura, K.; Kitagawa, S.; Kondo, M.; Fukui, K.; Kitaura, R.; Chang, H. C.; Mizutani, T.: Novel Flexible Frameworks of Porous Cobalt(III) Coordination Polymers That Show Selective Guest Adsorption Based on the Switching of Hydrogen-Bond Pairs of Amide Groups. *Chemistry-a European Journal* **2002**, *8*, 3586-3600.
- (144) Lerner, M. B.; Kybert, N.; Mendoza, R.; Villechenon, R.; Bonilla Lopez, M. A.; Charlie Johnson, A. T.: Scalable, Non-Invasive Glucose Sensor Based on Boronic Acid Functionalized Carbon Nanotube Transistors. *Appl. Phys. Lett.* **2013**, *102*, -.
- (145) Kim, H. S.; Hartgerink, J. D.; Ghadiri, M. R.: Oriented Self-Assembly of Cyclic Peptide Nanotubes in Lipid Membranes. *J. Am. Chem. Soc.* **1998**, *120*, 4417-4424.
- (146) Helsel, A. J.; Brown, A. L.; Yamato, K.; Feng, W.; Yuan, L.; Clements, A. J.; Harding, S. V.; Szabo, G.; Shao, Z.; Gong, B.: Highly Conducting Transmembrane Pores Formed by Aromatic Oligoamide Macrocycles. *J. Am. Chem. Soc.* **2008**, *130*, 15784-15785.
- (147) Corma, A.; Garcia, H.: Zeolite-Based Photocatalysts. *Chem. Commun.* **2004**, 1443-1459.
- (148) Fiedler, D.; Leung, D. H.; Bergman, R. G.; Raymond, K. N.: Selective Molecular Recognition, C-H Bond Activation, and Catalysis in Nanoscale Reaction Vessels. *Acc. Chem. Res.* **2005**, *38*, 349-358.
- (149) Vriezema, D. M.; Aragonés, M. C.; Elemans, J.; Cornelissen, J.; Rowan, A. E.; Nolte, R. J. M.: Self-Assembled Nanoreactors. *Chem. Rev.* **2005**, *105*, 1445-1489.
- (150) Granja, J. R.; Ghadiri, M. R.: Channel-Mediated Transport of Glucose across Lipid Bilayers. *J. Am. Chem. Soc.* **1994**, *116*, 10785-10786.
- (151) Clark, T. D.; Buehler, L. K.; Ghadiri, M. R.: Self-Assembling Cyclic Beta(3)-Peptide Nanotubes as Artificial Transmembrane Ion Channels. *J. Am. Chem. Soc.* **1998**, *120*, 651-656.
- (152) Gokel, G. W.; Mukhopadhyay, A.: Synthetic Models of Cation-Conducting Channels. *Chem. Soc. Rev.* **2001**, *30*, 274-286.
- (153) Montenegro, J.; Ghadiri, M. R.; Granja, J. R.: Ion Channel Models Based on Self-Assembling Cyclic Peptide Nanotubes. *Acc. Chem. Res.* **2013**.

- (154) Otis, F.; Auger, M.; Voyer, N.: Exploiting Peptide Nanostructures to Construct Functional Artificial Ion Channels. *Acc. Chem. Res.* **2013**.
- (155) Langmi, H. W.; McGrady, G. S.: Non-Hydride Systems of the Main Group Elements as Hydrogen Storage Materials. *Coord. Chem. Rev.* **2007**, *251*, 925-935.
- (156) Ward, M. D.: Molecular Fuel Tanks. *Science* **2003**, *300*, 1104-1105.
- (157) Fraenkel, D.; Shabtai, J.: Encapsulation of Hydrogen in Molecular-Sieve Zeolites. *J. Am. Chem. Soc.* **1977**, *99*, 7074-7076.
- (158) Weitkamp, J.; Fritz, M.; Ernst, S.: Zeolites as Media for Hydrogen Storage. *Int. J. Hydrogen Energy* **1995**, *20*, 967-970.
- (159) Kessel, D.; Reiners, J.: Light-Activated Pharmaceuticals: Mechanisms and Detection. *Isr. J. Chem.* **2012**, *52*, 674-680.
- (160) Ogilby, P. R.: Singlet Oxygen: There Is Indeed Something New under the Sun. *Chem. Soc. Rev.* **2010**, *39*, 3181-3209.
- (161) Cuquerella, M. C.; Lhiaubet-Vallet, V.; Cadet, J.; Miranda, M. A.: Benzophenone Photosensitized DNA Damage. *Acc. Chem. Res.* **2012**, *45*, 1558-1570.
- (162) Arumugam, S.: Alkali Metal Cation Exchanged Nafion as an Efficient Micro-Environment for Oxidation of Olefins by Singlet Oxygen. *Journal of Photochemistry and Photobiology A: Chemistry* **2008**, *199*, 242-249.
- (163) Griesbeck, A. G.; Cho, M.: Singlet Oxygen Addition to Homoallylic Substrates in Solution and Microemulsion: Novel Secondary Reactions. *Tetrahedron Lett.* **2009**, *50*, 121-123.

Chapter 2

Design and Synthesis of Tubular Addition Polymers

2.1. Background	42
2.2. Preparation of polydiacetylenes	44
2.2.1. Homocrystal strategy	46
2.2.2. Cocrystal strategy	48
2.3. Research goal	52
2.4. Macrocycles based on host-guest approach	58
2.4.1 Synthesis of macrocycle M1.....	58
2.4.2. Crystal structure analysis of macrocycle M1	60
2.4.3. Synthesis of macrocycle M2.....	66
2.4.4. Crystal structure analysis of monomer M2(m).....	72
2.4.5. Synthesis of macrocycles M3 & M4	74
2.4.6. Synthesis of macrocycle M5.....	76
2.4.7. Crystal structure analysis of monomer M5(m).....	77
2.4.8. Conclusion	80
2.5. Macrocycles based on oxalamide moiety	84
2.5.1. Synthesis of oxalamide based macrocycle M6.....	84
2.5.2. Synthesis of oxalamide based macrocycle M7.....	87
2.5.3. Synthesis of oxalamide based macrocycle M8.....	92
2.5.4. Synthesis of oxalamide based macrocycle M9.....	95
2.5.5. Other characterizations of oxalamide based macrocycles	98
2.5.6. Conclusion	101
2.6. Macrocycles based on $\pi - \pi$ stacking	103
2.6.1. Synthesis of macrocycle M10.....	103

2.6.2.	Crystal structure analysis of macrocycle M10	105
2.6.3.	Synthesis of macrocycle M11.....	116
2.6.4.	Conclusion.....	119
2.7.	Summary	119
2.8.	References	122

2.1. Background

In the early 1970's, a graduate student from Japan discovered the metal-like polyacetylene by inadvertently adding excess amount of catalyst to cause the acetylene molecules to link each other. The resulting polyacetylene exhibited surprisingly high electrical conductivity. This important discovery led to the 2000 Nobel Prize in Chemistry for the pioneering development of electrically conductive polymers.¹ Since then, the study of conjugated polymers (also called conducting or semiconducting polymers) has attracted much attention in many different fields such as synthetic chemistry, physics of condensed matter and materials sciences. Conjugated polymers are, typically, organic molecules constructed from alternating single and multiple bonds in the polymer chain. They are known as the simplest model of “molecular wire” because π electrons can delocalize along their highly conjugated backbone. Such a unique molecular structure results in numerous fascinating chemical and physical properties like semiconducting properties,^{2,3} electro-conductivity,² non-linear optical behaviors,⁴ electroluminescence^{5,6} and exceptional mechanical properties.⁷ However, the applications of conjugated polymers are limited by the poor solubility towards ambient conditions (H_2O and O_2) as well as the lack of processability to characterize these materials. Therefore, the development of well-defined conjugated polymers with improved solubility and processability characteristics is in high demand. Over the decades, much effort has been put into the construction of various polyconjugated molecules and their derivatives with enhanced properties. Several common examples of conjugated polymers are listed in **Figure 2.1**. Our group has focused upon the preparation of polydiacetylene by topochemical polymerization. Based on this idea, we design and synthesize a series of

diacetylene based tubular addition polymers. In this section, we will introduce the fundamental principles and prior research which are directly relevant to this thesis.

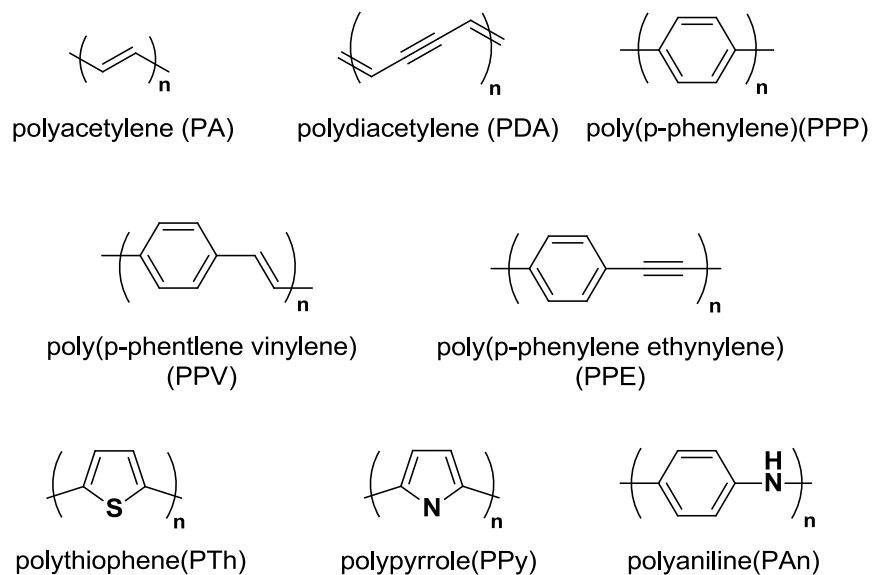


Figure 2-1. Representative structures of organic conjugated π -systems illustrating the most commonly studied building blocks

2.2. Preparation of polydiacetylenes

The preparation of PDAs is a very challenging process due to the multifunctionalities of diacetylene moiety; there are 4 reactive sp-hybridized carbons in diacetylene which complicate the polymerization process. In 1969, Wegner first reported the using of topochemical polymerization of diacetylene derivatives in the condensed phase via 1,4-addition reaction.⁸ Throughout the time, this remains to be the most successful technique to yield the desired conjugated polydiacetylenes. Topochemical reactions were investigated by Schmidt and co-workers and were described as “*a reaction in the solid state occurs within a minimum amount of atomic or molecular movement*”.⁹ According to this idea, the product formation is determined by the molecular geometry and orientation of the neighboring monomers in the crystalline lattice in topochemical polymerization. In the case of diacetylenes, it has been known that an efficient polymerization will only occur when the monomers are preorganized in molecular assemblies with an intermolecular identity period of about 5.0 Å, the same distance as the resulting polymer repeat, and an inclination angle of 45° with respect to the translation axis. Another limitation is that the distance R between C1 of one monomer and C4 of the neighboring monomer has to be within the van der Waals radius of C1 and C4 (~3.5 Å). The necessary geometric orientation of diacetylenes for topochemical polymerization is schematized in **Figure 2.2**.¹⁰

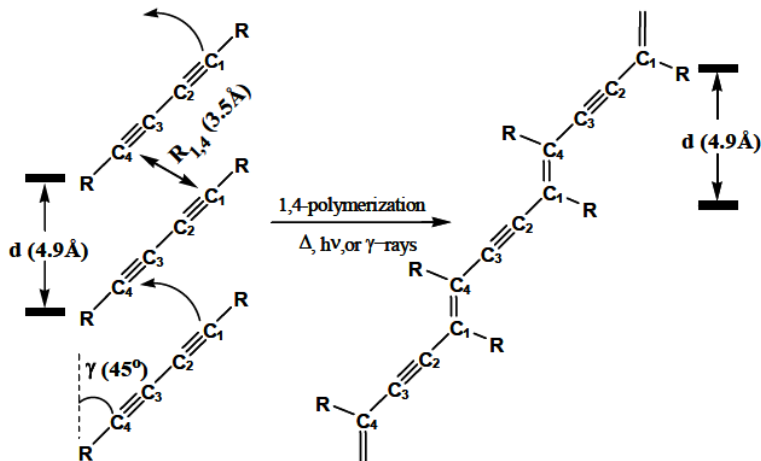
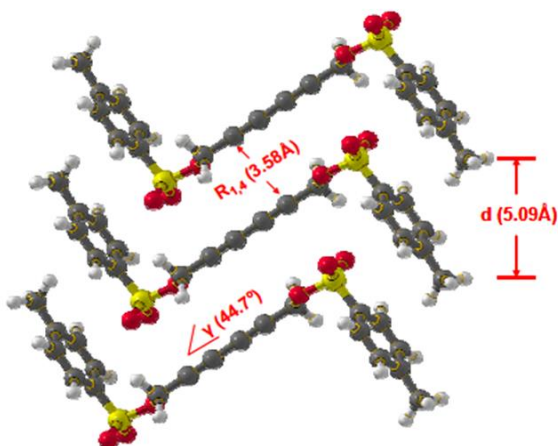
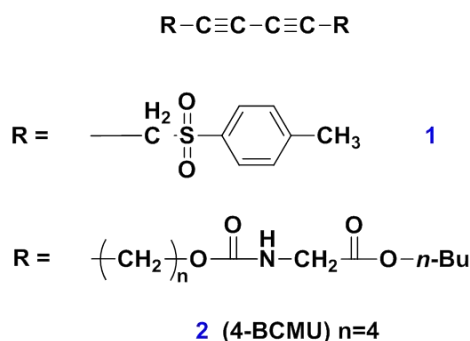


Figure 2-2. Illustration of the necessary geometric orientation of individual diacetylene molecules for the production of polydiacetylene in a solid-state polymerization reaction. d = translation repeat distance, $R_{1,4}$ = the C1-C4 contact distance, and ϕ = the angle at which the diacetylenes are tilted with respect to d

By lining up the monomer atoms at the same distance as found in the corresponding polymer, the polymerization may proceed with only minimal packing rearrangements. In order to obtain high quality and defect-free polydiacetylenes, usage of well-designed diacetylene monomers basing on these requirements is critical. Any large motion during the polymerization propagation may destroy the crystal lattice and thus terminate the further polymerization resulting in a disordered polymer. Many sophisticated supramolecular architectures have been designed to satisfy the requirements for topochemical polymerization. Most of them focus on 1,4-polymerization in solid-state. Recently, there are several different approaches to the topochemical reactions, such as applying polymerization in liquid-crystalline state, in diacetylene based lipids as well as in many other unique supramolecular assemblies. The study described here focuses on single-crystal-to-single-crystal polymerization of macrocyclic diacetylene. The detail of solid-state diacetylene polymerization will be discussed in the following section.

2.2.1. Homocrystal strategy

As mentioned above, the orientation of the diacetylene monomers plays an important role in preparing high quality polydiacetylene materials. However, how to properly preorganize the PDA monomer is still remains as a great challenge. In general, there are two strategies to generate supramolecular chemistry: One is the use of single molecules; the other is the application of a host-guest/co-crystal approach. Due to the fact that the interactions between the end groups attached to the diacetylene unit will greatly affect the molecular packing in the monomer crystals, these groups are critical in molecular design. It is generally believed that solid-state diacetylene monomers with large end groups are more reactive than those with small end groups. In addition, the flexibility of the end groups is also important and needs to be taken into consideration when constructing the polymerizable diacetylene molecule. A great number of research groups have worked on the solid-state polymerization of various diacetylene monomers. However, only a few of them have successfully obtained precisely aligned monomers with the parameters that were required for the topochemical polymerization which can yield nearly perfect polymers via heating or irradiation. One of the most successful cases for solid-state topochemical polymerization using the homocrystal strategy is hexa-2,4-diyne-1,6-diyl bis(*p*-toluene sulfonate) **1** (Scheme 2.1). The crystal structure of **1** is shown in Figure 2.3.



Scheme 2-1.

Figure 2-3. Crystal structure of **1**

As shown, the molecular packing is nearly perfect for 1,4-polymerization. Indeed, heating the single crystals brought about a clean polymerization producing the poly(PTS) which were in the form of macroscopic crystals. The polymerization process was investigated by the occurrence of an induction period, the time when the polymerization rate increased by a factor up to 200.¹¹ Bloor et al.¹² found that the mismatch of the polymer and monomer lattices will generate some degree of lattice strain thus result in ~10% contraction of the crystal along the chain axis after polymerization. Baughman¹³ then proposed that a strain-dependent rate of chain initiation as well as propagation can be used to quantitatively elucidate the autocatalytic effects observed during polymerization. Based on this idea, the extent of the polymerization was probably affected by the crystal strain field. However, the exact molecular weight of poly(PTS) was difficult to determined due to the poor solubility of the polymer in a wide range of standard solvents.

Another impressive class of polydiacetylenes, *n*-butoxycarbonylmethyl urethane (*n*-BCMU), is shown in **Scheme 2.1**. It has been reported that when there were 4 methylene

groups between the diacetylene unit and the head group ($n = 4$), the topochemical polymerization by γ -irradiation will work very efficiently.¹⁴ Currently, this is the most well-studied example among all reported diacetylenes. The resulting polymer, poly(4-BCMU), can be fully characterized to investigate the structure and physical properties since the excellent solubility in most organic solvents. By optimizing the γ -irradiation, the size of polymer can reach up to $M_n \sim 2.6 \times 10^6$ g/mol which corresponds to ~ 5100 repeat units. The measurement of the molecular weight distribution using Size Exclusion Chromatography (SEC) gives a very narrow range of value (For the best case: Polydispersity index or PDI = 1.01; for the average: PDI < 1.5).¹⁵

2.2.2. Cocrystal strategy

Over the past two decades, there has been a great interest in design and synthesis diacetylene compounds with the possibility to provide the corresponding PDAs in solid state. However, preparation of high quality polydiacetylenes via single molecules is not a promising method due to the lack of controlled manner for diacetylene monomers to self-assemble at the distance commensurate with the desired polymer.

The Fowler/Lauher group has successfully developed a cocrystal strategy that can properly pre-organize the diacetylene monomers in the solid state for the topochemical polymerization.¹⁶⁻²⁹ This reliable method is based on both supramolecular chemistry and crystal engineering and is so far the most promising way for synthesizing ordered polydiacetylenes. The principle of this approach is to create a host-guest cocrystal system

for semi-predictable molecular packing. Our group has built up a library of host candidates to study their hydrogen bonding behavior as well as the molecular packing information. As shown in **Figure 2.5**, the ureas and oxalamides seem to be the best functionalities for serving as the host molecules for the topochemical diacetylene polymerization due to their near to 4.9 Å repeat distance. Based on this finding, the most important geometric parameter **d** can be controlled by the host molecules that can form reliable H-bonding network with diacetylene monomers, the guest molecules, to place the reaction component at the desired distance, 4.9 Å, for 1,4-polymerization. Clearly, both the host and guest molecules play important roles in the cocrystal systems. Controlling the proper intermolecular arrangement by hosts plus providing the reactive functionalities by guests make the host-guest approach extremely useful in preparing PDAs. One advantage of the host-guest strategy is that this method is based on supramolecular chemistry, the totally synthetic work needed for developing new polymerizable diacetylene individuals will be greatly simplified, allowing for more variations among diacetylenes. Another advantage is that the host can easily be removed after the polymerization to give neat PDAs since the interactions between the hosts and guests are hydrogen bonds, which are weaker than covalent bonds. No doubt the host-guest method does exhibit great intelligence in the sense of molecular design and construction.

Based on this strategy, we have succeeded in preparing various polydiacetylenes.^{18,19,21,30} More importantly, some long-standing challenges such as the polymerization of triacetylenes³¹ and trienes,³² have been solved using this method as well (**Figure 2.4**).

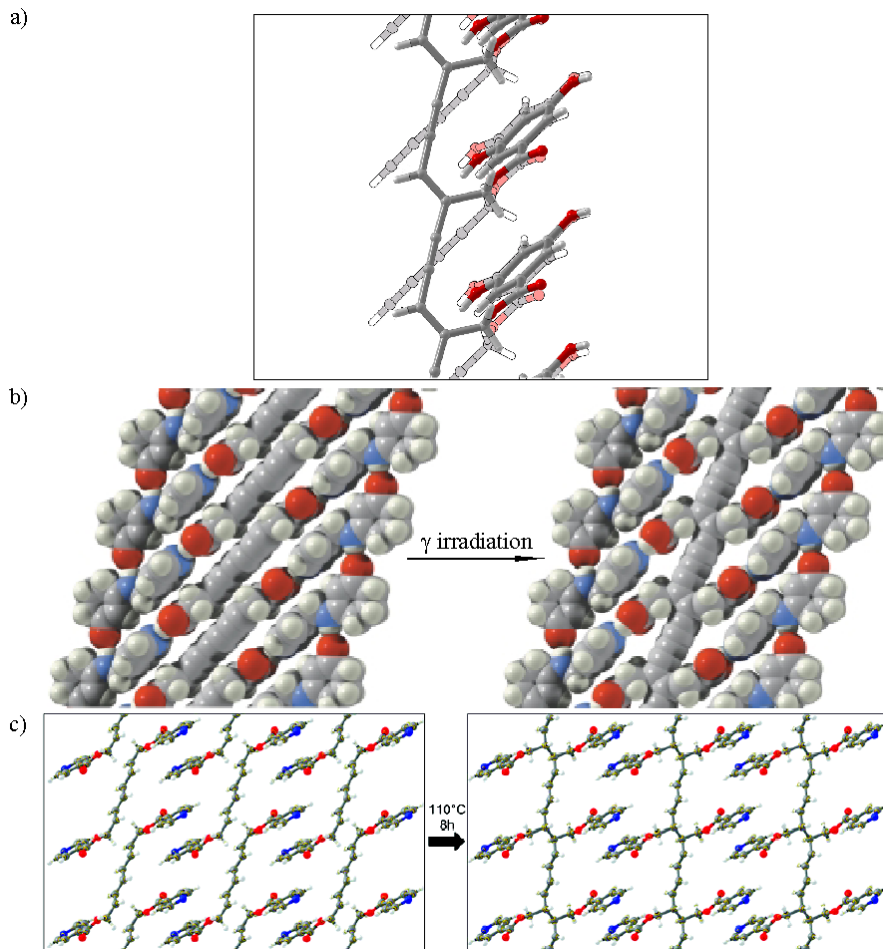


Figure 2-4. a) The pale background drawing is the diacetylene monomers. The bold foreground drawing shows the polydiacetylene.²⁶ b) Polymerization of triacetylenes induced by γ irradiation.³¹ c) Polymerization of trienes induced by heat.³²

Although the repeat distance can be well controlled through host-guest strategy, the orientation angle γ , another important factor required for diacetylene polymerization, cannot be easily achieved by this method. In most cases, we found that the control of **d** is fairly reliable by choosing the most optimized host molecules. However, the deviation of γ from the idea 45° often results in the incomplete or failed in the polymerization processes. Nevertheless, this method based on supramolecular chemistry still shows great potential in molecular design and synthesis.

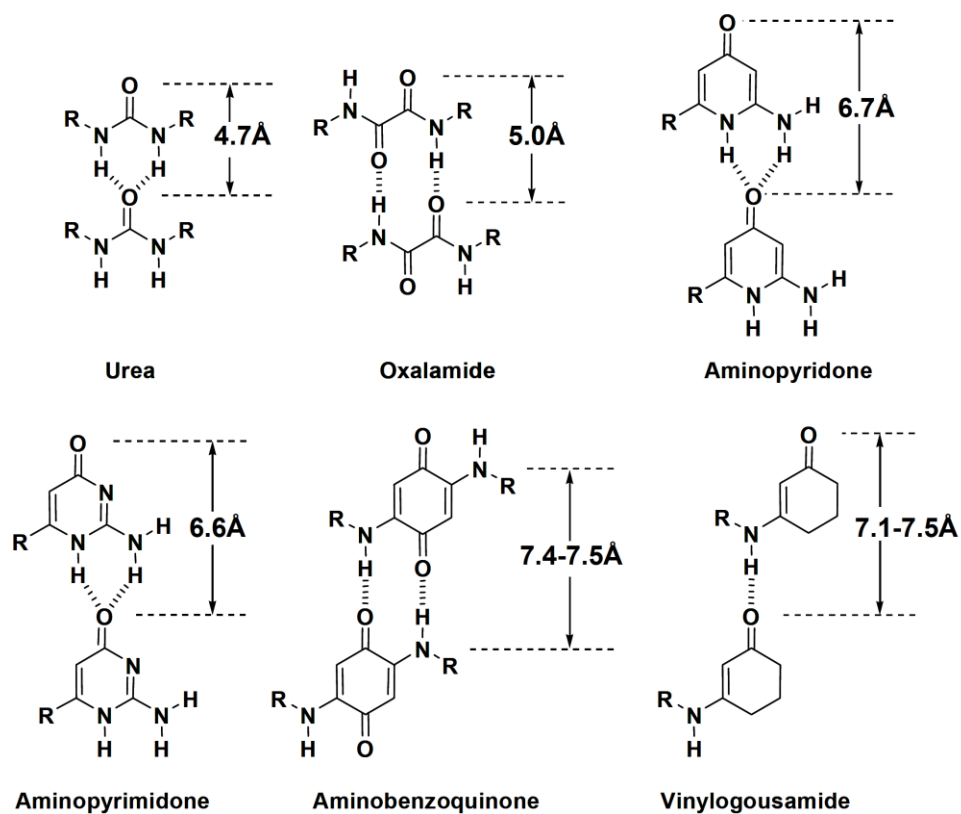


Figure 2-5. A library of hydrogen bonding host molecules capable of self-assembling to give a predictable repeat distance.

2.3. Research goal

Carbon nanotubes have attracted a great deal of research interest because they have potential applications in many different areas, such as nanoprobe, molecular reinforcements in composites, displays, sensors, energy-storage media, and molecular electronic devices.^{33,34} Single walled carbon nanotubes have a diameter of essentially one nanometer, but can have lengths in the millimeter range. From a structural point of view it is difficult to imagine a better molecular tube.

Chemists from around the world have made numerous attempts to design and synthesize their own imaginative versions of tubular molecules, yet the task still remains challenging. In the nanoworld, the structures have often been based upon the ideas of molecular self-assembly and supramolecular chemistry. Numerous tubular structures have been prepared by the self-assembly of a wide variety of substrates. Macrocyclic peptides, carbohydrates, and many purely synthetic monomers form tubular structures via hydrogen bonds.³⁵⁻³⁷ Various molecules and polymers have been found to coil naturally into helical structures with a tubular core.^{38,39} Aromatic macrocycles have been designed to selfassemble via π - π stacking to give tubes.^{40,41} Tubular structures held together by covalent bonds have been formed from cyclodextrins threaded on to a polyethyleneglycol chain.⁴² Ghadiri used olefin metathesis to dimerize peptide macrocycles, yielding short tubular structures.⁴³

One promising approach is the preparation of a tubular addition polymer (**Figure 2.6**).⁴⁴ An advantage of tubular addition polymers is that they would be robust due to a continuous network of covalent bonds throughout the tubular network. This is a property

that they would share with carbon nanotubes. However, a potential advantage of tubular addition polymers, not shared with conventional carbon nanotubes, is that they would be prepared by organic synthesis which allows continuous structural variation for different application. The implementation of such a strategy presents two primary challenges. First, a general synthetic strategy for the preparation of tubular addition polymers must be developed and second, the molecular structure of such a polymer must be proven.

A key element in the development of a strategy for the preparation of a tubular addition polymer is the pre-organization of the monomers into a tubular array for polymerization. This pre-organization of monomers could be accomplished using anisotropic environments such as organic crystals, layered materials, surface or membrane environments.

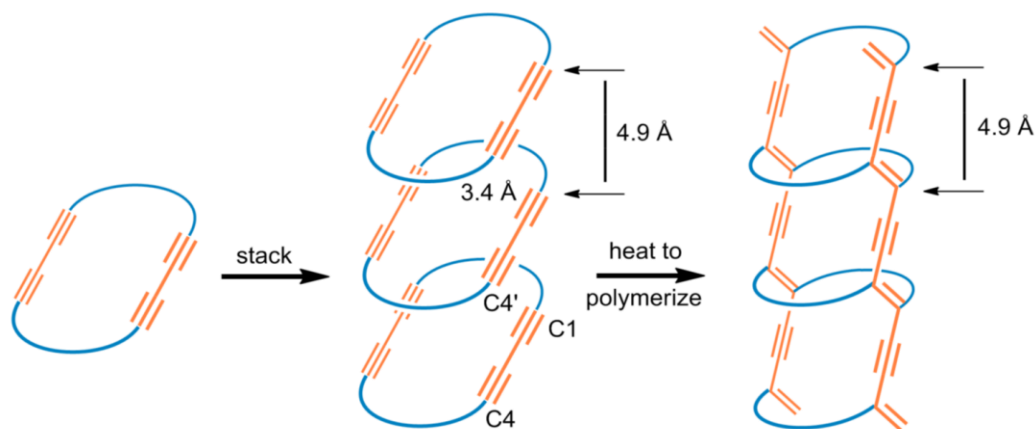


Figure 2-6. One possible route to a tubular polymer is via a topochemical polymerization of a diacetylene-containing macrocycle. For the reaction to proceed, the macrocycles would need to be spaced near the 4.9 Å expected for polymers with neighboring diacetylene C1–C4' carbon atoms close to the van der Waals contact distance of 3.4 Å. The application of heat (or radiation) should bring about the polymerization.

In our previous work we have focused upon designed topochemical polymerization reactions of diacetylenes.⁴⁵ These are polymerizations that take place in a condensed phase,^{8,46} most often in a single crystal. The polymerization occurs only if the monomers are properly aligned for the polymerization reaction and only if they are spaced at a distance commensurate with the desired polymer. Using a host guest methodology we have designed and prepared various new polydiacetylenes, including the first terminal polydiacetylene,²⁶ the first well characterized aryl substituted diacetylene,⁴⁷ and the recently reported polydiiododiacetylene.⁴⁸ In this previous work a host molecule, designed to self assemble at 4.9 Å via hydrogen bonds, was used to align the diacetylene containing guest molecule at the required spacing. Subsequent heat or radiation treatments brought about the desired polymerization. Extensions of this work beyond the diacetylenes led us to the first known 1-6-triacetylenepolymerization³¹ and the first 1-6-polytriene polymerization.³² These studies demonstrate the value of the solid state for controlling the polymerization process. The polymeric products are produced as single crystals. This allows straight forward structural characterization via X-ray crystallography and gives the polymers unique properties due to their highly ordered structures.

What kind of monomer would be needed to give a tubular addition polymer? The obvious candidate would be a macrocycle, one that would self-assemble into a polymerizable stack. Since our own work has been focused on diacetylenes, we considered a macrocycle with a pair of diacetylene functionalities (**Figure 2.6**). The difficulty is controlling the spacing. For polymerization to take place, the monomers need to be spaced at a distance near 4.9 Å.

This approach is not new. All sorts of diacetylene macrocycles are known in the literature.^{44,49-51} The first reported attempt at macrocycle polymerization was by Vollhardt and Youngs,⁴⁹ but their system had a long repeat distance of over 6 Å. More recently, Shimizu⁴⁴ reported the polymerization of a diacetylene macrocycle that self-assembled via amide hydrogen bonds. Their spacing was 4.98 Å, very close to the ideal, but a loss of crystallinity prevented the determination of the polymer structure. Nagasawa⁵² just reported the polymerization of various gels also formed from amide diacetylene macrocycles. Previously we used a host molecule designed to self assemble at 4.9 Å via hydrogen bonds to align a diacetylene containing guest molecule.⁴⁵ We believe that such a host guest approach should work for a macrocyclic system as well.

Over the past few years, our group has been investigating a directed and controlled approach for the synthesis of single walled nano-tubes of exact dimensions by topochemical polymerization of cyclic systems that contain diacetylenes using a host-guest strategy. Based on our idea, a series of compounds (**M1** to **M5**) with hydrogen bond accepting group have been designed and synthesized. The host compound, either a urea of glycine or an oxalamide of glycine, may properly organize the guest compound, macrocyclic diacetylene monomer, via hydrogen bonds to give the ideal spacing for a topochemical polymerization to form a covalently bonded organic tube (**Figure 2.7**).

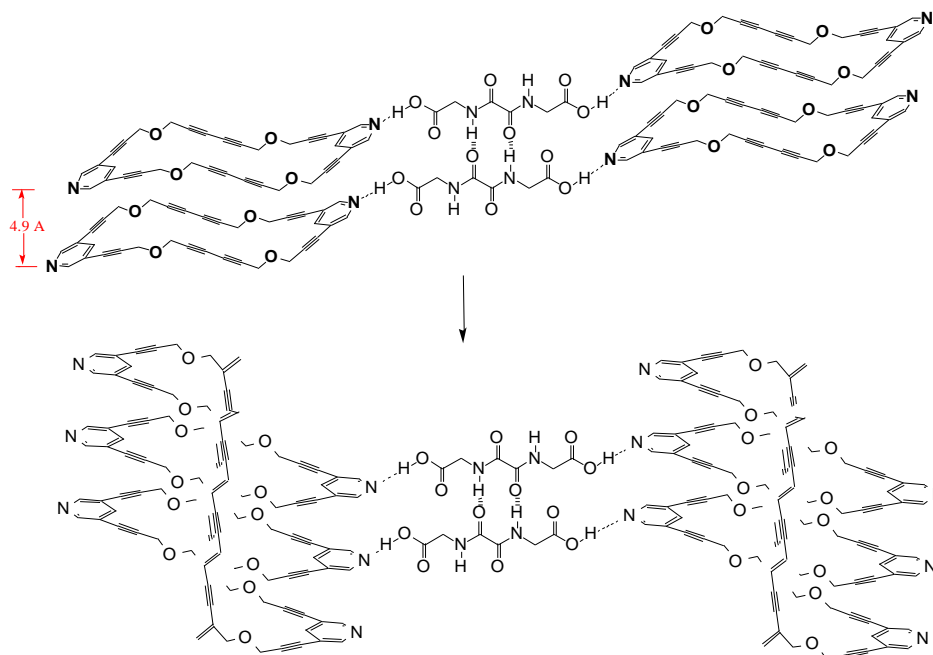


Figure 2-7. The expected 1,4-polymerization of diacetylene macrocycle **M1** under co-crystal with oxalamide of glycine.

Another possible strategy that could align the macrocyclic diacetylene monomer for topochemical polymerization to give the desired tubular structures is to utilize π - π stacking of an aromatic system. A simple π - π stack aligned directly in a direction perpendicular to an aromatic ring would give a van der Waals spacing comparable to graphite, 3.4 Å. But a slipped π - π stack is much more common and distances in excess of 4 Å are found. A number of aromatic derivatives of hexa-2,4-diyne-1,6-diol are known to stack at distances commensurate with the desired 4.9 Å spacing.⁸ We reasoned that a macrocycle built from aromatic rings and hexa-2,4-diyne-1,6-diol might give such a stacking. This led us to design compounds **M10** and **M11**. Synthesis and crystal structure analysis will be detailed in the following sections.

In addition to the host-guest approach, we are also interested in design the macrocycles that would self-assemble at the desired distance of 4.9 Å (**Figure 2.8**). Based on our design, the control of molecular spacing and orientation can be achieved by incorporating the host functional group into the macrocycle itself. One would expect that a well-designed macrocyclic system should be able to stack in columns with the idea intermolecular spacing.

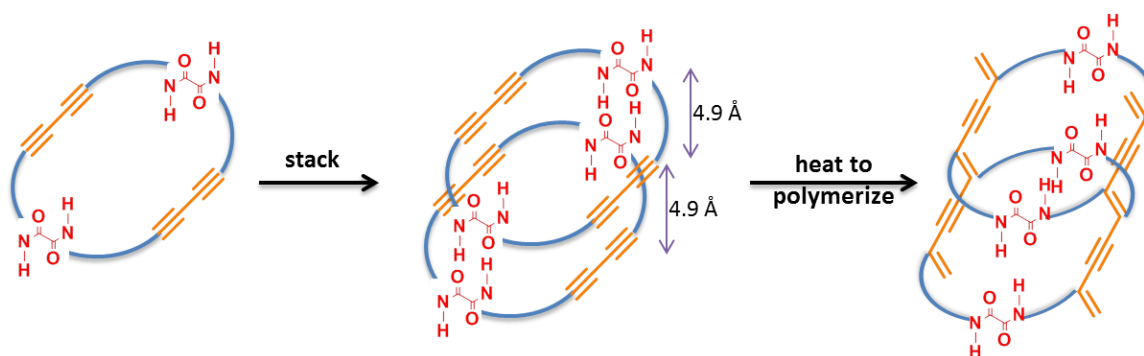
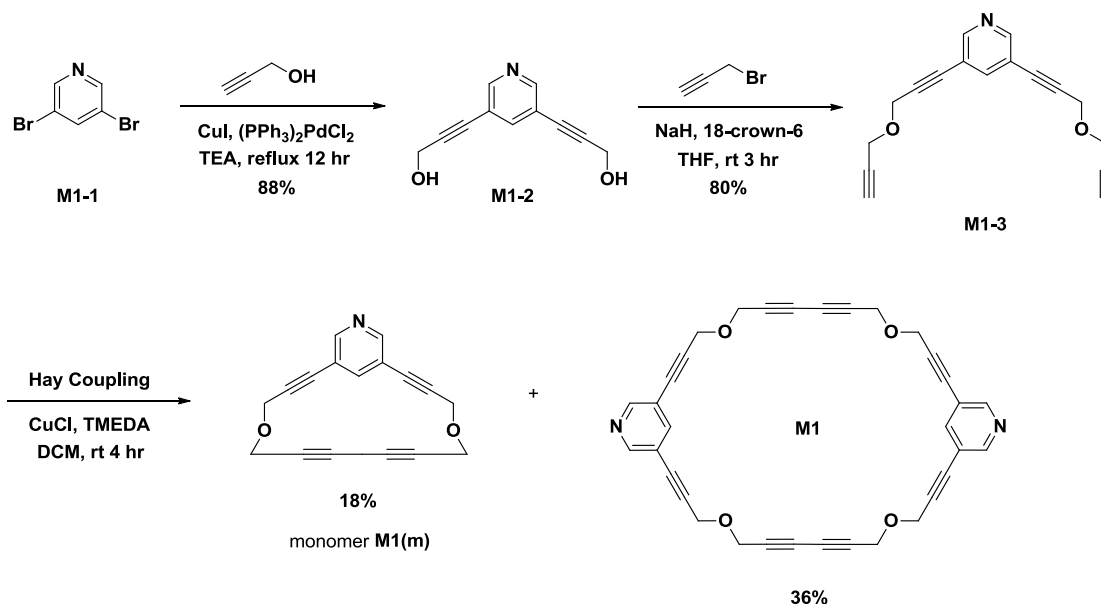


Figure 2-8. Schematic representation of cyclic oxalamide diene that could self-assemble at the required 4.9 Å needed for a diacetylene polymerization

2.4. Macrocycles based on host-guest approach

2.4.1 Synthesis of macrocycle M1

The first attempt to synthesize the 3,5-pyridine-based macrocycle **M1**, was carried out by Ti Wang. The synthetic route for macrocycle **M1** is outlined in **Scheme 2.2**:



Scheme 2-2. Synthetic route for **M1**

Coupling of propargyl alcohol with 3,5-dibromopyridine **M1-1**, a Sonogashira coupling reaction, was successfully carried out by using a palladium catalyst, a copper(I) cocatalyst, and an amine base (TEA). Ti Wang tried to optimize the coupling conditions by adding pyridine as a co-solvent, which can increase the solubility of the reactants. However, in our work, TEA was used as only solvent because pyridine will cause a trouble during purification. The diethers **M1-3** were produced by condensing diols with propargyl bromide in the presence of sodium hydride and 18-crown-6 ether. By using the

crown ether, the sodium cation which may surround the oxygen anion was trapped and the yield of this reaction was very good.

The synthesis of macrocycle **M1** was accomplished via Hay coupling as a key step.²⁰ In addition to the target molecule, intramolecular self-cyclization monomer **M1(m)** was obtained as minor product. The problem with this reaction is that the yield was very low. More than 5 spots were observed on TLC plate. This may result from the flexibility of two methylene groups increase the possibilities to other isomers (for example, monomer, trimer, tetramer). We have tried to lower the concentration of the reactant; however, we still could not avoid the formation of other side products.

We have found that macrocycle **M1** is relatively unstable once the solvent is removed. The color changes from white to yellow then to deep orange (**Figure 2.9b**) when the sample sitting at room temperature for one week. When the deep orange compound has formed, it is hard to dissolve in common organic solvents. The dark orange compound may be a polymer or a mixture of oligomer. Therefore, it is important to store **M1** in the refrigerator as soon as we have purified it.

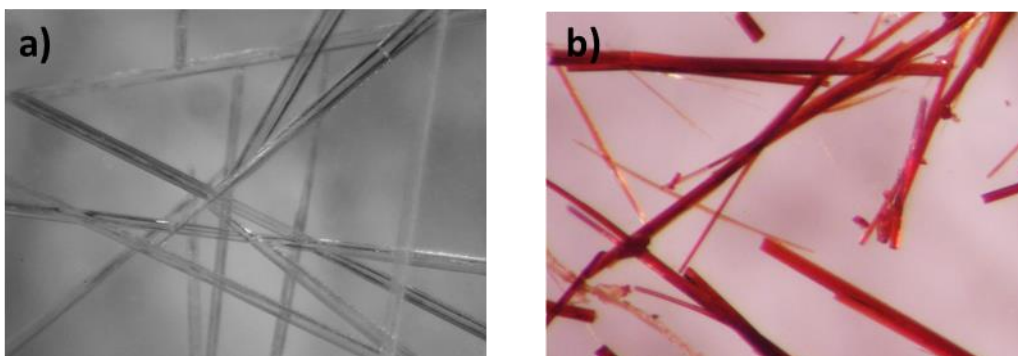


Figure 2-9. Color photograph of the crystals of (a) freshly prepared samples of macrocycle **M1** (b) sample sitting at room temperature for 1 week.

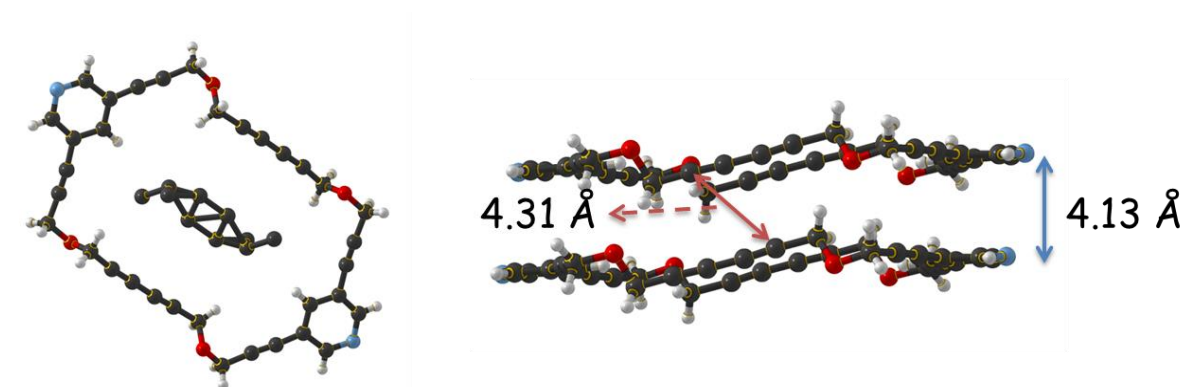
2.4.2. Crystal structure analysis of macrocycle M1

The crystals of **M1** are colorless and needle-like (**Figure 2.9a**). They gradually turn black and start to polymerize when the temperature is over 150°C. Single crystals have been grown by slow evaporation of three different binary solvent systems: DCM/NMF (1/10), DCM/EtOAc (1/1), and DCM/MeOH (1/1), respectively. The crystal structures are shown in **Figure 2.10**. Compared with the crystal structure which was obtained from material grown with a different solvent system (DCM/EtOAc/hexanes mixture) by Ti Wang, it turns out that they all have the same space group (P2₁/n) and similar unit cell dimension (**Table 2.1**). In **Figure 2.10**, the intermolecular repeating period (**d**) in each case is much shorter than the ideal value, 4.9 Å. The distance **R** between C1 of one monomer and C4' of the neighboring monomer is longer than the requirement for polymerization (3.5 Å). The data indicated that it will be difficult to obtain 1,4-polymerization of **M1** without introducing a host molecule that can provide suitable distance for topochemical polymerization.

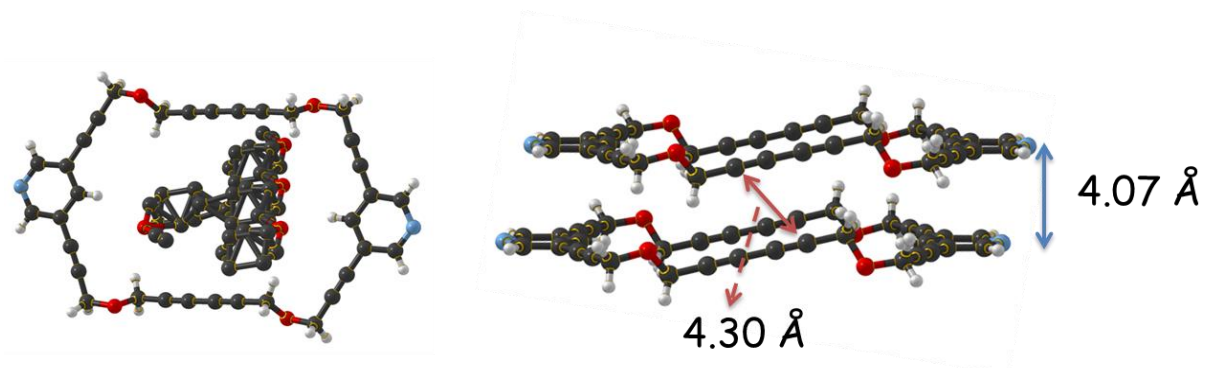
Solvent systems	a (Å)	b (Å)	c (Å)	α (°)	β (°)	γ (°)	Volume	Space group
DCM/NMF (1/10)	4.13	16.91	23.44	90.00	92.54	90.00	1636.06	P2 ₁ /n
DCM/EtOAc (1/1)	4.07	16.85	23.18	90.00	91.60	90.00	1588.75	P2 ₁ /n
DCM/MeOH (1/1)	4.11	16.79	23.25	90.00	92.48	90.00	1604.21	P2 ₁ /n
DCM/ EtOAc/ hexanes	4.13	16.92	23.50	90.00	92.70	90.00	1641.4	P2 ₁ /n

Table 2-1. The unit cell data of macrocycle **M1** obtained from material grown from the different solvent systems.

a)



b)



c)

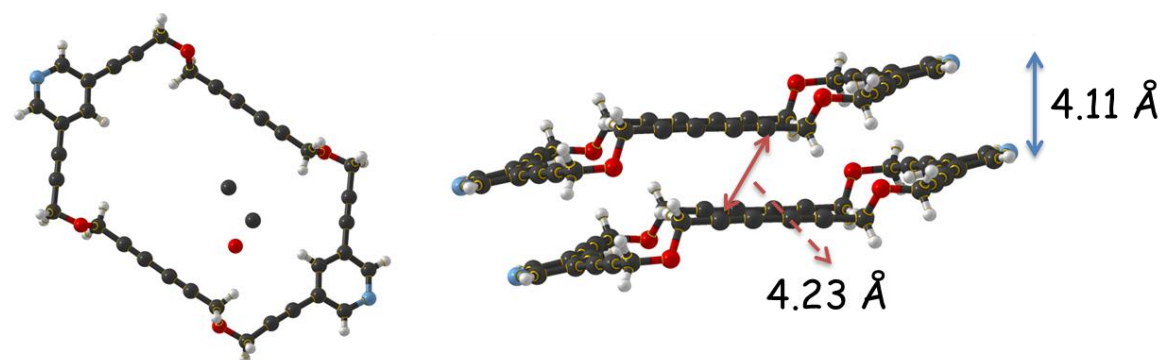


Figure 2-10. Crystal structures of M1: a) Single crystals grown from DCM/NMF (1/10). b) Single crystals grown from DCM/EtOAc (1/1). c) Single crystals grown from DCM/MeOH (1/1).

As we can see, the crystal structures of **M1** in **Figure 2.10** showed evidences that the solvent molecules were trapped in this ring shaped organic nanotubes (Residual peaks of electron density map can be assigned as solvent). This means the designed macrocycle is capable of the small molecules uptake and this might be a useful character for further study.

The crystals of monomer **M1(m)** are colorless and needle-like (**Figure 2.11**). Single crystals were grown from DCM/hexanes (1/1). **Figure 2.12** represents the crystal structure of monomer **M1(m)**. No solvent molecules were trapped inside the macrocycle. The intermolecular interaction that organizes these macrocycles is mainly by π - π stacking interaction. The data shown that monomer **M1(m)** has the same crystal system and space group as dimer **M1**. Since the translation repeating distance between two monomers and the contact distance between C1 and C4' are 4.13 Å and 4.17 Å respectively, the monomer **M1(m)** is not a good candidate for 1, 4-polymerization either.

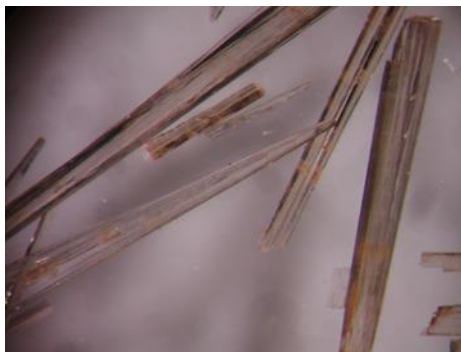
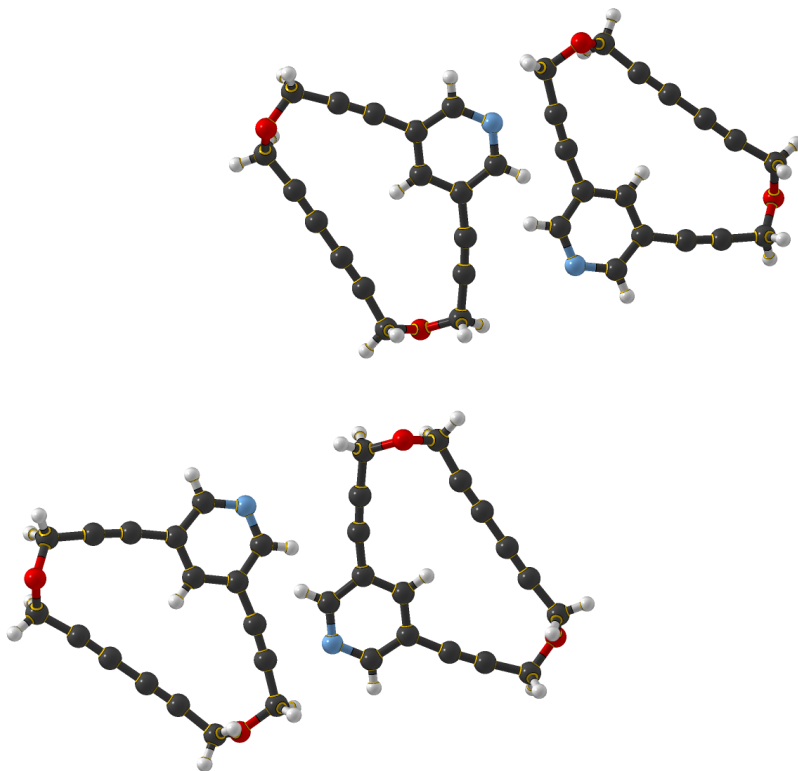


Figure 2-11. Color photograph of the crystals of monomeric **M1**

Solvent systems	a (Å)	b (Å)	c (Å)	α (°)	β (°)	γ (°)	Volume	Space group
DCM/hexanes (1/1)	4.10	27.90	11.67	90.00	90.22	90.00	1335.7	P2 ₁ /n

Table 2-2. The unit cell data of monomer **M1** obtained from material grown from DCM/hexanes (1/1).

a)



b)

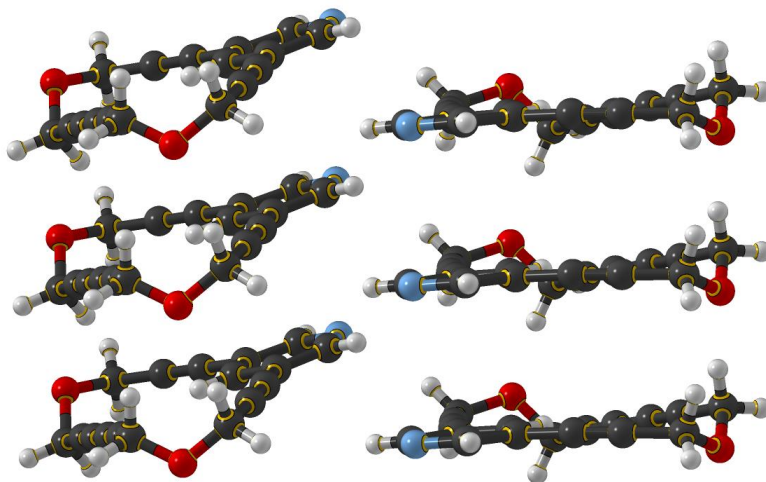


Figure 2-12. Crystal structures of monomeric **M1(m)**: a) view from top b) view from side

Co-crystal strategy

With the dimer **M1** in hand, the next step is to co-crystallize the macrocycle with a suitable oxalamide host. We have already synthesized many such molecules with acidic side groups capable of hydrogen bonding to the outward pointing pyridine nitrogen atoms of the macrocycle. The oxalamide hydrogen bonds, should establish the requisite 4.9 Å intermolecular spacing. As seen in **Table 2.3**, oxalamide hosts, A, B and C, were chosen to co-crystallize with the macrocycle guest due to their reasonable solubility in common organic solvent. However, the result was not promising: Macrocyclic guest and oxalamide host always crystallized separately. One possible reason for that is due to the different solubility of the hosts and guests in organic solvent: the hosts only dissolve in very polar solvent like methanol, while guest molecules usually dissolve in relative non-polar solvent such as chloroform and methylene chloride.

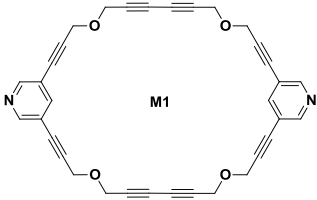
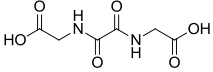
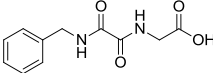
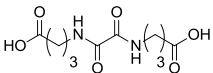
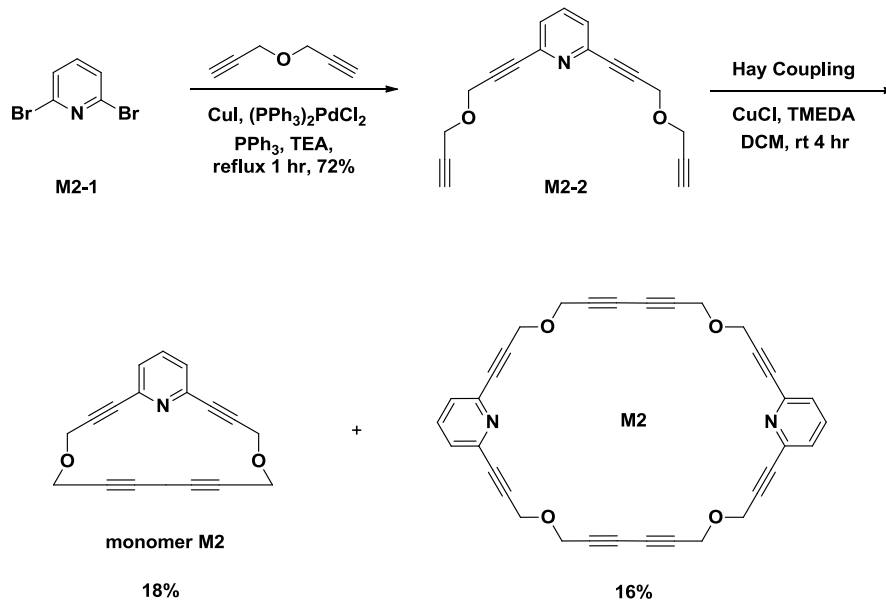
Guest	Host	Ratio	Solvent	XRD
	 A	1:1	MeOH/THF	No co-crystal
	 B	1:2	MeOH/THF	No co-crystal
	 C	1:1	MeOH/THF/EtOAc	No co-crystal

Table 2-3. Co-crystal strategy for macrocycle **M1**

Since the attempt to use host guest methodology for **M1** has not worked, a design of a more compatible guest is necessary and other new host compounds should be tried to grow co-crystals.

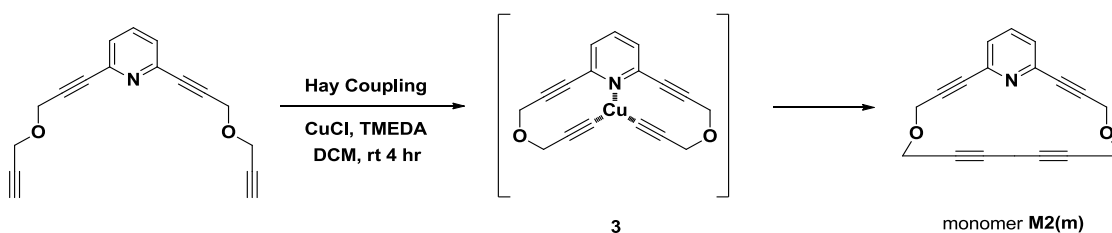
2.4.3. Synthesis of macrocycle M2

2,6-pyridine-based macrocycle **M2** is another candidate good for host-guest strategy. The calculated distance across the ring between the in-pointing nitrogen atoms is around 12-13 Å depending upon molecular conformation. This is enough room for the oxalamide of glycine or some other small hydrogen bonding molecules. The preparation of 2,6-pyridine-based macrocycle **M2** was first tried by our group member, Steven Chow. In the first trial, he followed the method identical to making the macrocycle **M1**. However, the purification process of the first step was very difficult as well as the yield of the propargyl group addition that forms **M2-2** was very low. Therefore, a modified synthetic route for macrocycle **M2** was proposed to solve these problems. As we can see in **Scheme 2.3**, the new method only needs two steps to prepare the desired macrocycle **M2**:



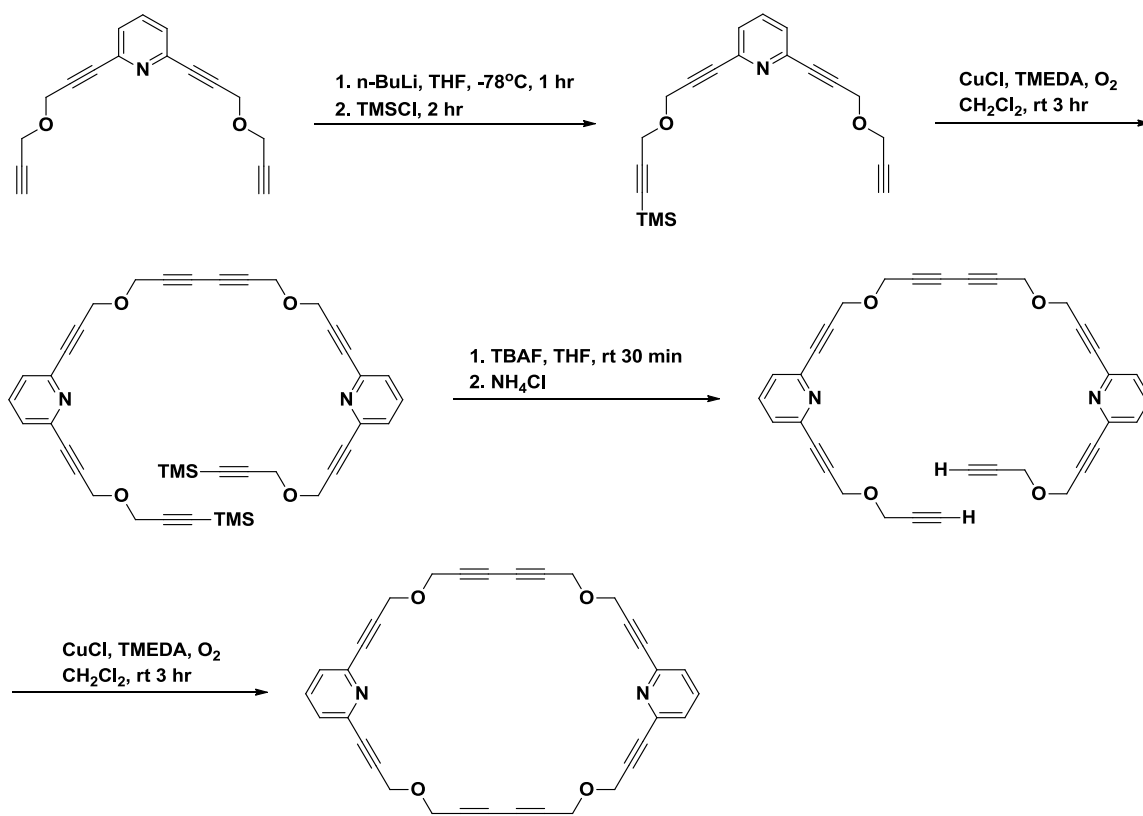
Scheme 2-3. Synthetic route for **M2**

A direct Sonogashira coupling of 2,6-dibromopyridine **M2-1** with propargyl ether as the first step was followed by Hay coupling to afford the macrocycle **M2**. At that time, the only isolatable compound was an intermolecular cyclization monomer **M2(m)**. The desired dimer **M2** was obtained in a trace amount and was insufficient to obtain a meaningful $^1\text{H-NMR}$ spectrum. The reason is probably the coordination of the copper metal with the pyridine of diether **3**, thus favoring formation of macrocycle monomer **M2(m)** (**Scheme 2.4**).



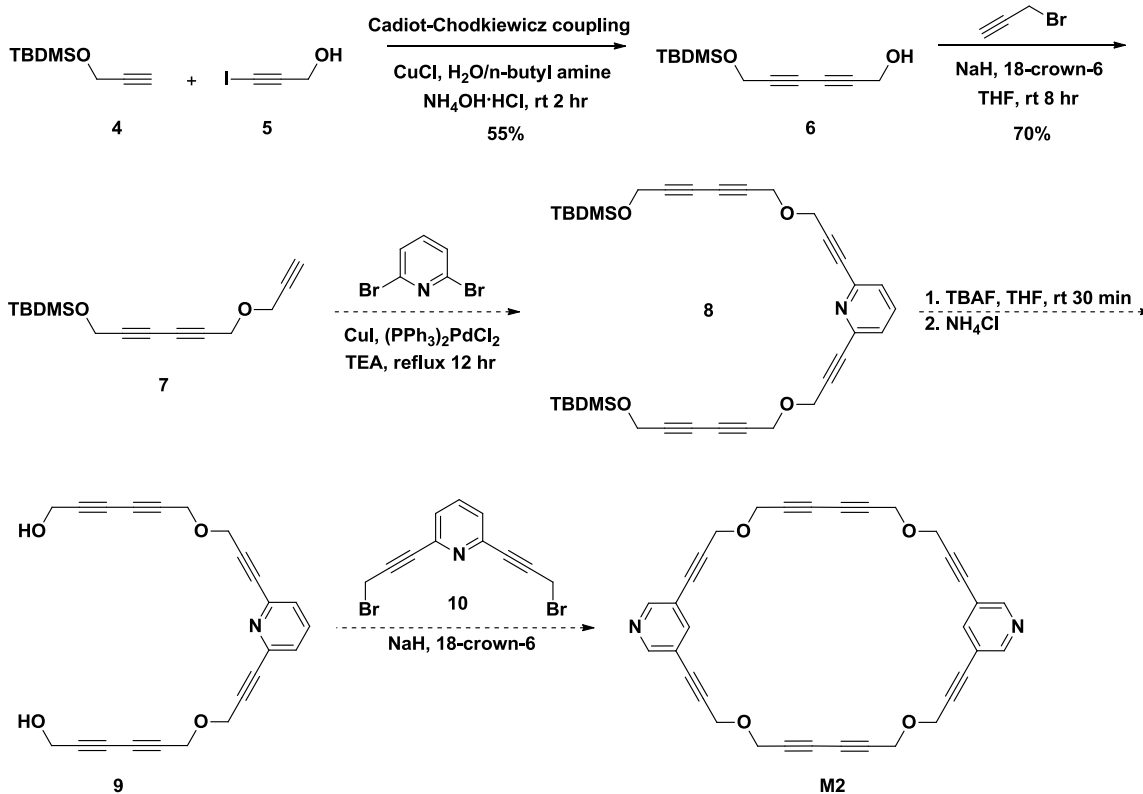
Scheme 2-4. A plausible copper-diether coordination complex **3** that may form during the Hay coupling reaction affect the formation of the product.

Furthermore, Chow also tried an alternate pathway (**Scheme 2.5**) which was designed in order to prevent the mono-cyclization by protecting one side of the terminal alkyne to prepare the target macrocycle **M2**.



Scheme 2-5. An alternate synthetic route for **M2**

Unfortunately, the crude product from the reaction was not soluble in most organic solvents, thus there was no way to identify it. Since the synthesis of macrocycle **M2** was still a mystery, one of the goal of this project is to figure out a reliable way to make this target macrocycle. A new synthetic approach to the desired ring is shown in **Scheme 2.6**.



Scheme 2-6. A new synthetic approach to the desired macrocycle **M2**

In order to prevent the formation of the copper-pyridine diether complex, the diacetylene moiety will be introduced at the very beginning. The first two steps moved smoothly: Starting with Cadiot-Chodkiewicz coupling of compound **5** with TBDMS protected hydroxyl compound **4**, followed by Williamson etherification with the propargyl bromide, compound **7** can be prepared in good yields. However the third step, Sonogashira coupling, was facing difficulties: The TLC plate shown at least 6 compounds after the reaction and none of them were the desired product. This may result from the polymerization of the existing triple bonds. Without the compound **8** in hand, the following procedure cannot be achieved.

As mentioned in chapter 1, the concentration plays an important role in the macrocycle preparation. In very concentrated condition, polymer or oligomer will be the major products. While in a very dilute condition, the formation of the monomer will be more favorable. Based on this idea, compound **M2-2** was synthesized for a series of tests with different concentrations. **Table 2.4** represents the relationship between the concentration and the products formed. An attempt to increase the dimerization probability by using 1/5 of the original amount (50 mL) of DCM was finally successful. We also found that once the macrocycle **M2** was isolated from the solution, it became very difficult to redissolve in most organic solvents. Moreover, even if the macrocycle **M2** was stored in solution as well as in the fridge, the color of the solution changed from transparent to brown (**Figure 2.13**). This result indicated that the 2,6-pyridine based macrocycle **M2** is very unstable. Due to the solubility problem, further investigation of macrocycle **M2** was limited.



Figure 2-13. Color photograph of the crystals of **M2**

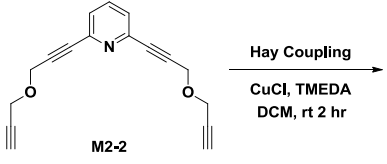
			Monomer	Dimer	Trimer
Entry	Reaction Conditions	Conc.	Yield	Yield	Yield
1	Hay coupling CuCl, TMEDA, DCM, 2h	0.003M	Major	None obtained	Trace amount
2	Hay coupling CuCl, TMEDA, DCM, 2h	0.004M	Major	None obtained	Trace amount
3	Hay coupling CuCl, TMEDA, DCM, 2h	0.005M	Major	Trace amount	Minor
4	Hay coupling CuCl, TMEDA, DCM, 2h	0.01M	Minor	Minor	Major
5	Hay coupling CuCl, TMEDA, DCM, 2h	0.02M	Trace amount	Major	Major
6	Hay coupling CuCl, TMEDA, DCM, 2h	0.04M	Trace amount	Minor	Major

Table 2-4. The effect of concentration to the yields of macrocycles

2.4.4. Crystal structure analysis of monomer M2(m)

Single crystals of macrocyclic monomer **M2(m)** suitable for X-ray diffraction were obtained from slow evaporation of EtOAc/hexanes (1/1). These crystals are needle-like and colorless (**Figure 2.14**). they gradually turns brown, even when stored in the refrigerator. Studying the structure by X-ray crystallography, the data show that the crystal system is monoclinic and the space group is C_2/c (**Table 2.5**). The single-crystal structure of monomer **M2(m)** is shown in **Figure 2.15**. As we can see, there are no solvent molecules were trapped in the ring. Moreover, macrocyclic monomer **M2(m)** tends to stack in an alternating pattern: the monomers do no stack on top of each other. Thus there was no proper diacetylene alignment, and no desired nano tubular framework was formed. The repeat distance between macrocyclic monomers is 3.66 Å .

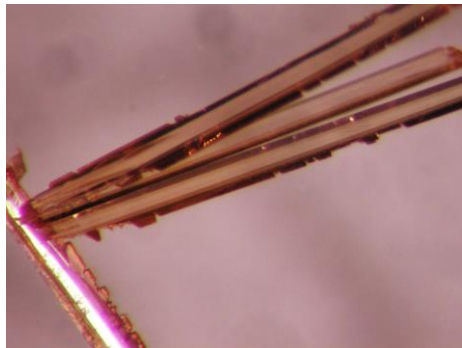
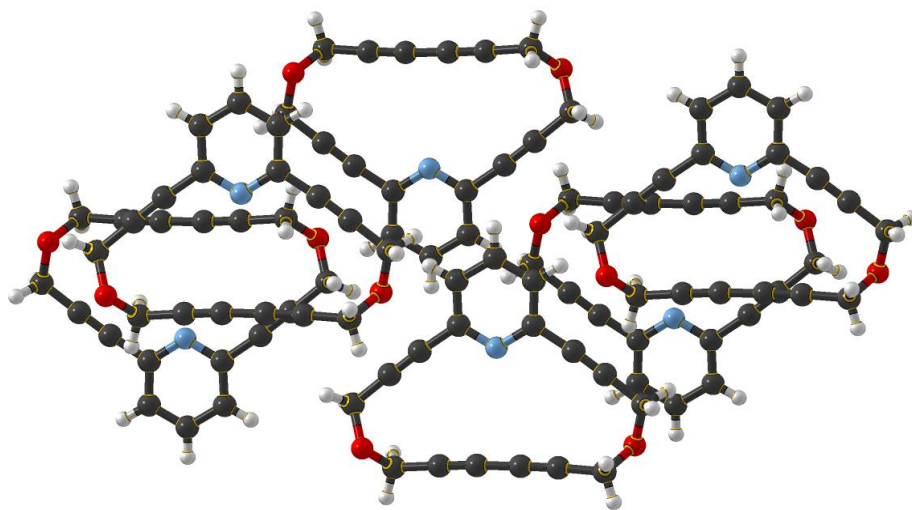


Figure 2-14. Color photograph of the crystals of monomer **M2(m)**

Solvent systems	a (Å)	b (Å)	c (Å)	α (°)	β (°)	γ (°)	Volume	Space group
EtOAc/hexanes (1/1)	15.53	10.04	8.81	90.00	102.17	90.00	1341.5	C_2/c

Table 2-5. The unit cell data of monomer **M2(m)** obtained from material grown from DCM/hexanes (1/1).

a)



b)

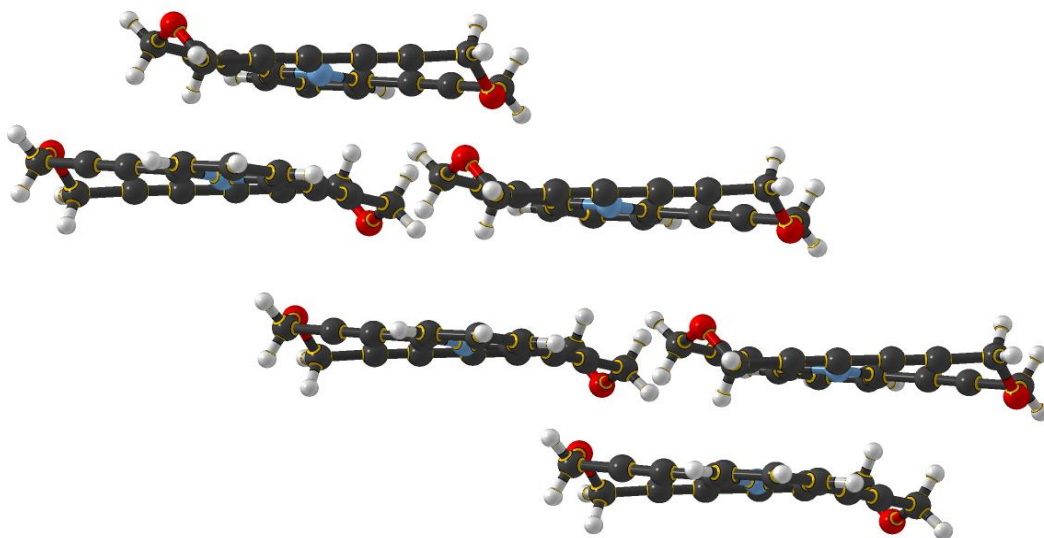
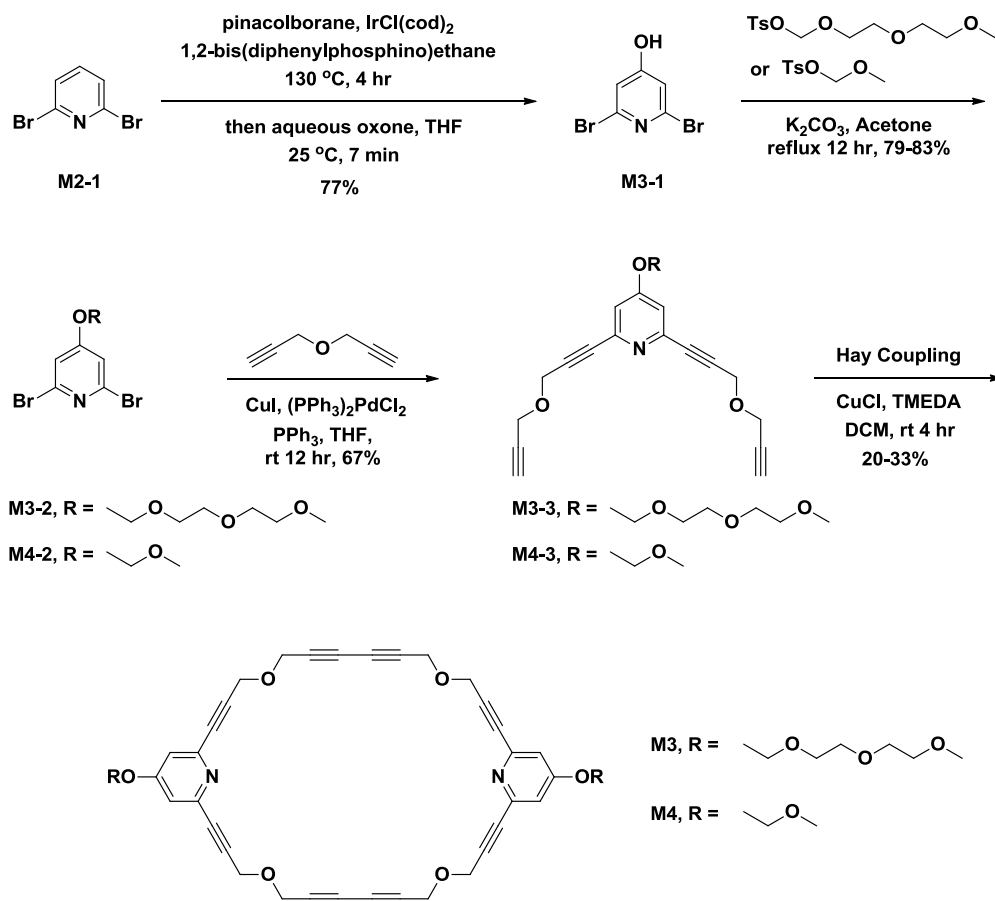


Figure 2-15. Crystal structures of monomer **M2(m)**: a) view from top b) view from side

2.4.5. Synthesis of macrocycles **M3** & **M4**

Macrocycle **M3** and **M4** were designed and synthesized to overcome the solubility problem. As shown in **Scheme 2.7**, the aliphatic mono- and triethylene glycol side chains at the 4-positions of the pyridine rings were introduced to improve solubility.



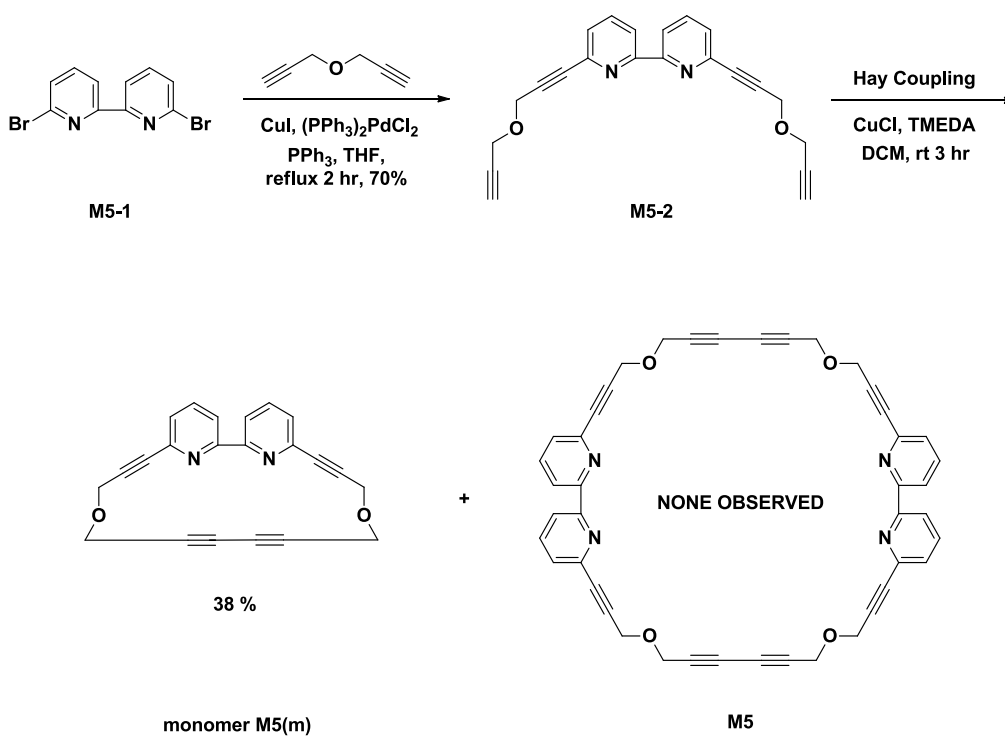
Scheme 2-7. Synthetic route for **M3** & **M4**

Commercially available 2,6-dibromopyridine **M2-1** was converted into 2,6-dibromopyridin-4-ol **M3-1** through iridium-catalyzed direct boration and subsequent oxidative cleavage of the C-B bond. The mono- and triethylene glycolic derivatives,

M3-2 and **M4-2**, were obtained by Williamson reaction and were further converted into diethers (**M3-3**, **M4-3**) by Sonogashira couplings with propargyl ether. Finally, Hay coupling of diethers furnished the target macrocycles **M3** and **M4**. These two rings did exhibit a reasonable solubility in organic solvents. Growing the single crystals of macrocycles for structural study was performed by several different methods such as cooling, evaporation, and liquid-liquid diffusion. The results shown that macrocycle **M3**, the ring with tri-(ethylene glycol) monomethyl ether as side chains is much too “soft” and lacks crystallinity; while in **M4**, the ring bearing ethylene glycol monomethyl ether as side chains provide more crystallinity than **M3**. Unfortunately, single crystals of sufficient size for X-ray study cannot be obtained so far. Only tinny crystals can be obtained from layering a 1 to 1 ratio of methylene chloride and methanol. The color of freshly prepared crystals is light yellow. When the crystal is heated up to ~120 °C, it turns brown gradually; indicating that polymerization or decomposition is taking place. The compound does not melt up to 300 °C.

2.4.6. Synthesis of macrocycle **M5**

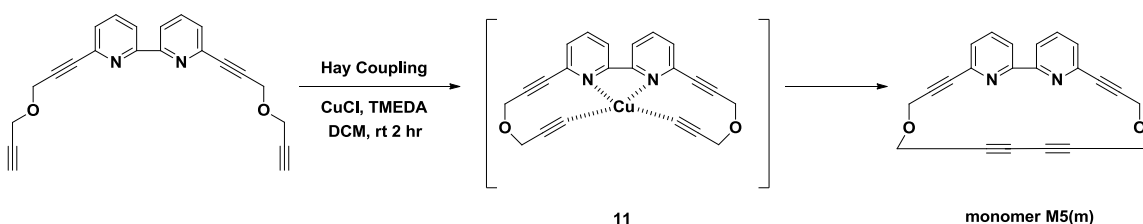
The last ring interested this project is the bipyridine-containing macrocycle **M5**. The bipyridine moieties were introduced in order to bind many different chemical species, from inorganic or organic cations to anionic species. The planned synthesis of the macrocycle **M5** is shown in **Scheme 2.8**.



Scheme 2-8. Synthetic route for **M5**

Starting with the Sonogashira coupling of 6,6'-dibromo-2,2'-dipyridine **M5-1** with the propargyl ether, compound **M5-2** was obtained in 70% yield. With diether **M5-2** in hand, we would expect the macrocyclic dimer can be prepared by a simple Hay coupling reaction. However, the result shown that the only product formed was the macrocyclic monomer **M5(m)**. Several different reaction conditions were tried; none of them gave

the target macrocyclic dimer **M5**. One possible explanation is that due to the great binding ability between the metal ions and the dipyridine moieties, the copper-dipyridine coordination complexes would be formed in the solution rapidly (**Scheme 2.9**). As a result, the conformation of this coordination complex will favor the formation of the monomer **M5(m)** and inhibited the production of the desired dimer **M5**.



Scheme 2-9. A plausible copper-diether coordination complex **11** that may alter the favorability during the Hay coupling condition on the original synthetic route.

2.4.7. Crystal structure analysis of monomer **M5(m)**

Single crystals of macrocyclic monomer **M5(m)** have been grown from DCM/hexanes (1/1) by slow evaporation. These crystals are rod-like and light yellow (**Figure 2.16**). **Figure 2.17** represents the crystal structure of monomer **M5(m)**. Like monomer **M1** and **M2**, monomer **M5(m)** has no solvent molecules inside the ring either. Moreover, there was no desired nano-cylinder architecture observed, because these macrocyclic monomers do not stack on top of each other. Studying the structure by X-ray crystallography, the data show that the crystal system is triclinic and the space group is P-1 (**Table 2.6**).

We also found it is quite stable, the color does not show any changes after a long period of time sitting at room temperature. When the crystal is heated up to ~180 °C, turns brown gradually, suggesting that the occurrences of polymerization or decomposition of diacetylene functionalities. The compound does not melt up to 300 °C.

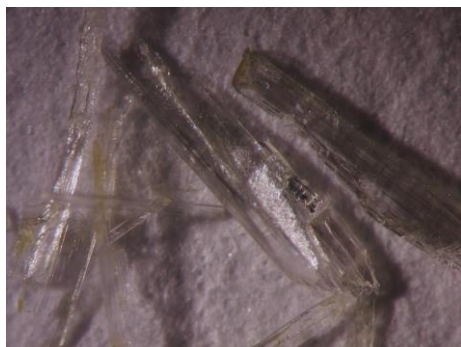
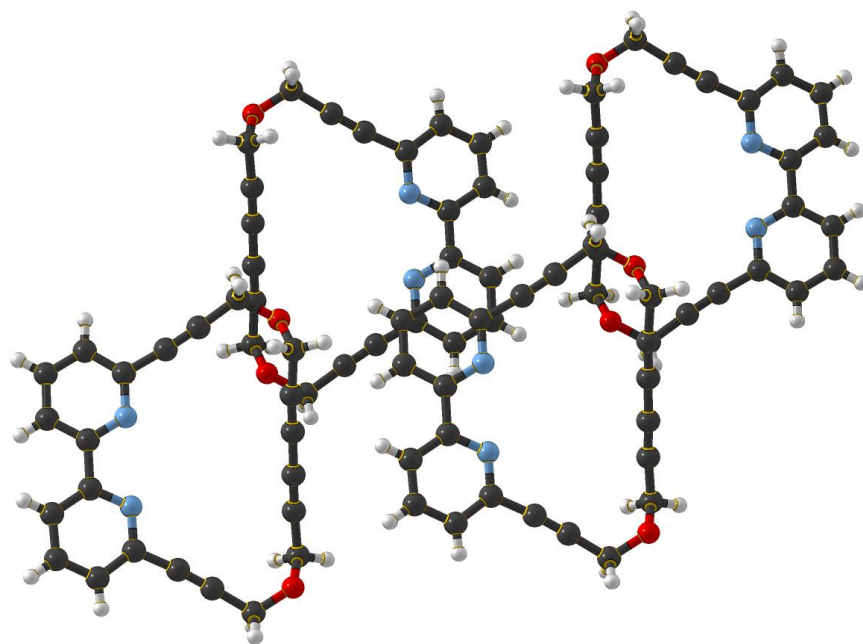


Figure 2-16. Color photograph of the crystals of monomer **M5(m)**

Solvent systems	a (Å)	b (Å)	c (Å)	α (°)	β (°)	γ (°)	Volume	Space group
DCM/hexanes (1/1)	8.65	10.14	10.86	70.96	84.87	70.51	848.37	P-1

Table 2-6. The unit cell data of monomer **M5(m)** obtained from material grown from DCM/hexanes (1/1).

a)



b)

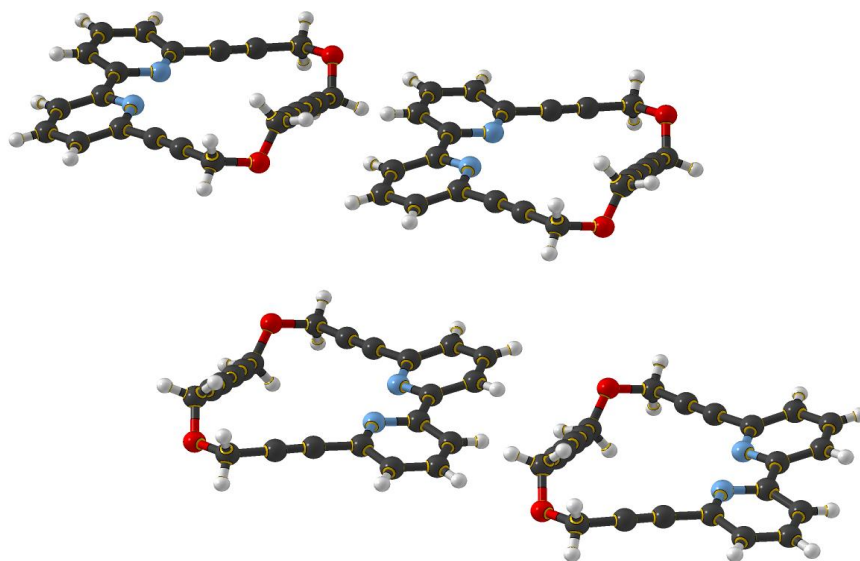


Figure 2-17. Crystal structures of monomer **M5(m)**: a) view from top b) view from side

2.4.8. Conclusion

In order to utilize host-guest approach to achieve single-crystal-to-single-crystal polymerization of tubular molecular networks, a series of macrocyclic diacetylene compounds (**M1** to **M5**) incorporating hydrogen bond accepting group have been synthesized and tested their possibilities of co-crystallizing with the host molecules for topochemical polymerization. Unfortunately, because of solubility problems, the co-crystal strategies were not successful.

In fact, poor solubility of the prepared macrocycles remains the biggest issue in our macrocycle design and synthesis. Poor solubility not only makes the purification process very difficult but also limits the chances for crystal growth and possible applications for macrocycles. Designing a macrocycle with better solubility in organic solvent is one of the key goals in this project. In order to increase the solubility, we tried to introduce the glycolic moieties in our macrocyclic systems. These glycol-based macrocycles (**M3**, **M4**) did show reasonable solubility. Although single crystals of these two rings suitable for x-ray study have not been obtained, we believe that by utilizing this approach, more soluble macrocycles can be synthesized in the future. In our future work, a new macrocyclic system with the incorporation of the functional groups which show large polarity or hydrogen bonding ability should be considered. We believe that it may enhance the solubility of the macrocycles in polar protic solvents.

Macrocycles **M1**, **M3**, **M4** and **M5** exhibited relatively good stability in solution while some of them changed color gradually when sitting in the atmosphere or in solid state, indicating partial polymerization process happened. The properties of macrocycle **M2** were very different from the other rings we mentioned above. **M2** appears unstable,

as it changes color quickly even when it is stored in solution and in the refrigerator. Moreover, **M2** showed the worst solubility among these desired macrocycles. It cannot redissolve in most of the organic solvents once it is isolated from the solution which limited characterization of the pure products. This is the reason why Steven Chow did not succeed in preparing this compound. Due to the poor stability as well as solubility of **M2**, special attention has to be paid to handle this compound. Keeping **M2** in a suitable solution at low temperature after the solution was degassed might help to keep it fresh.

The synthetic routes we proposed for the preparation of these macrocycles are very straightforward. The only difficult step was the final step: Hay coupling reaction. Some competition reactions may occur (formation of the monomers, trimmers, oligomers) the yield for this step is always low. Among these side reactions, the formation of intramolecular self-cyclization products (cyclic monomers) seems to be the biggest competition reaction. By adjusting the concentration of the macrocycle precursors, we have successfully reduced the possibility of macrocyclic monomer formation. It is worth to mention that when the macrocyclic dimer and monomer have been prepared, one way to identify them is through mass spectroscopy and the other is using x-ray crystallography to study the molecular structure. The structure of the macrocycle is symmetric and the chemical environments for dimer and monomer are very similar, it is not surprising that they have almost identical chemical shifts in ^1H NMR spectra. Therefore, one would not expect the ^1H NMR be a proper method to distinguish the dimer from the monomer. However, in our case, after a series of macrocyclic dimers and monomers have been synthesized, we did find an empirical rule in ^1H NMR spectrum which can be applied to the macrocycle characterization.

Table 2.7 lists the chemical shifts as well as the peak splitting for the two sets of methylene hydrogens in macrocycles. There are two different types of protons from the methylene moieties with different chemical environment in the macrocyclic dimers (Shown in blue and red, respectively). Consequently, two singlet peaks with chemical shifts ~4.4 and ~4.5 ppm respectively will be detected for the dimer. On the other hand, though there are two different types of protons in the macrocyclic monomer as well, the ^1H NMR data indicate only one singlet peak will be observed representing these two methylene groups in the macrocyclic monomer. So far, this rule works for most of the macrocyclic systems we have made.

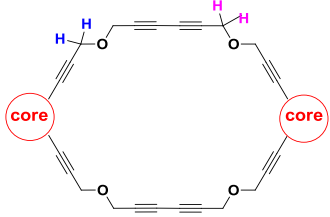
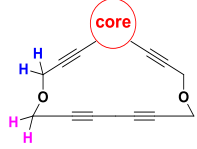
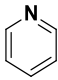
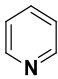
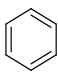
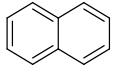
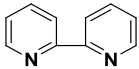
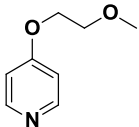
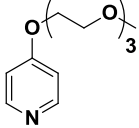
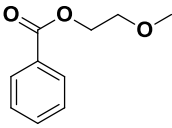
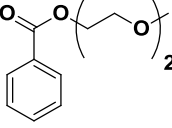
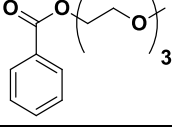
Products					
	Core	# of peaks for CH ₂	Chemical shift	# of peaks for CH ₂	Chemical shift
		2	4.41, 4.50	1	4.42
		2	4.43, 4.48	1	4.41
		2	4.41, 4.49	1	4.41
		2	4.45, 4.54	None obtained	
		None obtained		2	4.50, 4.56
		2	4.40, 4.48	None obtained	
		2	4.41, 4.49	None obtained	
		2	4.41, 4.49	1	4.41
		2	4.41, 4.50	1	4.42
		2	4.42, 4.50	1	4.41

Table 2-7. Chemical shifts of protons of the methylene groups in macrocycles (ppm)

2.5. Macrocycles based on oxalamide moiety

2.5.1. Synthesis of oxalamide based macrocycle M6

As we mentioned in the previous section, during the attempt of growing co-crystal of **M1** with host candidates we met a considerable amount of problems due to solubility difference. The host-guest approach we have applied for our other topochemical polymerization did not produce any promising results for our macrocyclic system. Hence, we have employed an alternative method, a single molecule approach, to resolve the problem. In this project, our primary goal was to design a polymerizable macrocyclic system that would self-assemble, held together by hydrogen bonds, in accordance with the parameters needed for a topochemical polymerization. Our initial design was inspired by the cyclic peptides of Ghardari and considered how we could add a pair of 1,3-butadiyne subunits to the ring. Here we proposed a cyclic oxalamide diyne that could self-assemble at the required 4.9 Å needed for a diacetylene polymerization (**Figure 2.8**).

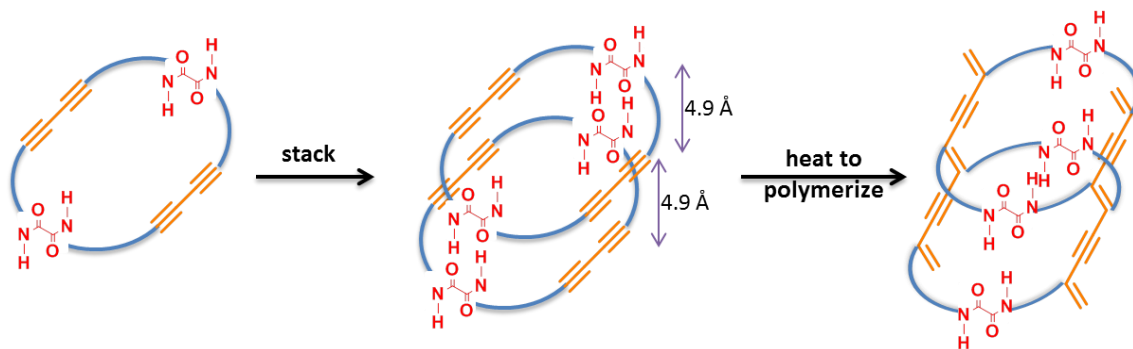
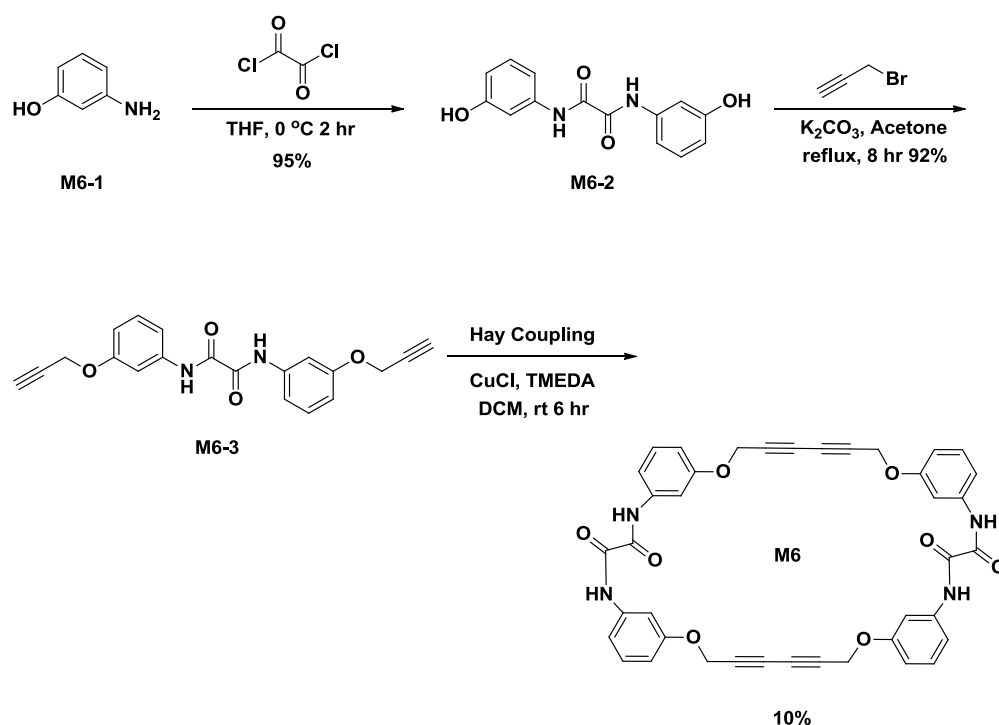


Figure 2.8. Schematic representation of cyclic oxalamide diyne that could self-assemble at the required 4.9 Å needed for a diacetylene polymerization

Macrocyclic **M6** has been designed and prepared for the single molecule approach. The oxalamide group was used to control the packing distance between each ring. Since the host functionality has been incorporated into the macrocyclic system, we would expect to simultaneously overcome the solubility problem which we encountered during the host-guest approach.



Scheme 2-10. Synthetic pathway of **M6**

The synthetic pathway to the macrocycle **M6** is shown below (**Scheme 2.10**). **M6** has been synthesized in three steps. Due to the stronger nucleophilicity of nitrogen atom, the sequence of the first and the second steps cannot be reversed. In the first step, the oxalamide group is formed by attaching oxalyl chloride to two 3-aminophenol moieties.

Since oxalyl chloride is very sensitive to water, reacting with water to liberate HCl gas, the reaction has to be carried out under an anhydrous condition. The yield of this step is very good.

The diether compound **M6-2** was synthesized via Williamson alkylation. Acetone was used as the solvent because it can be removed easily after the reaction. Consequently, it affords an excellent yield. When carried out the Hay coupling is carried out in the final step, similar problem apropos to low yield occurred. Several different sets of reaction conditions were tested to improve the yield of the macrocycle **M6**.

As shown in **Figure 2.18**, **M6** gradually turns pink in color at temperatures above about 110 °C and it turns to a deep brown color when the temperature is over 160 °C, which is a sign of thermal polymerization. However, due to a strong intermolecular hydrogen bonding of **M6**, significant solubility problems were encountered; attempts to grow single crystals of **M6** did not show promising results.

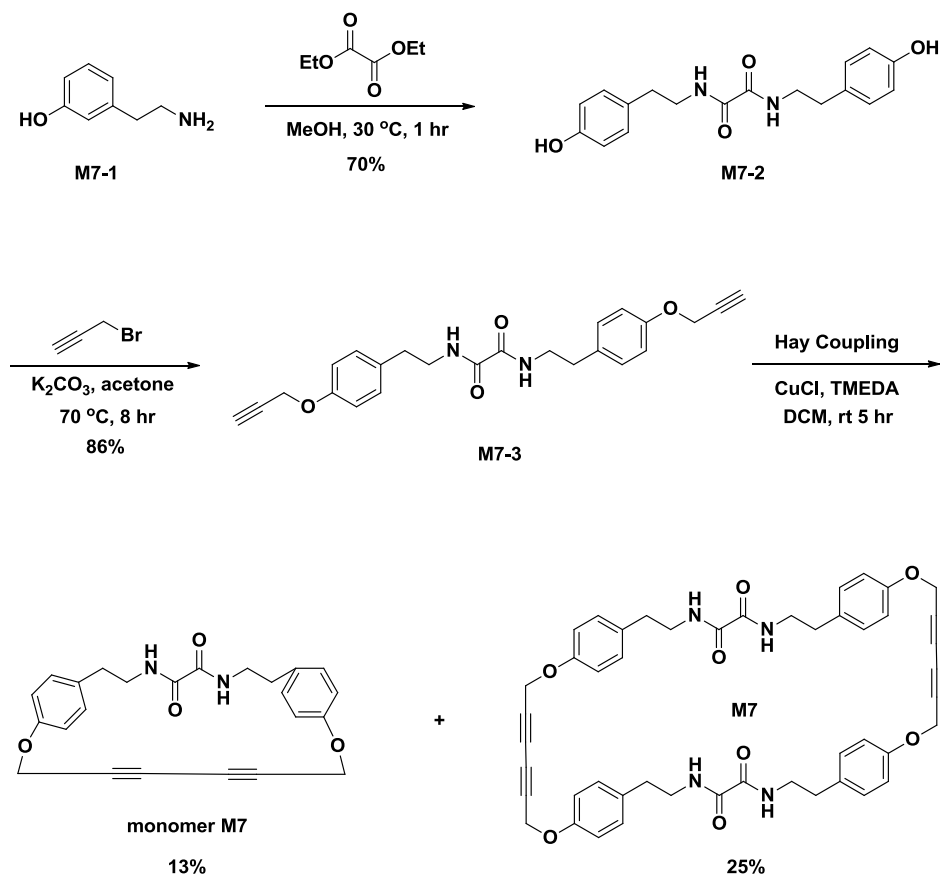


Figure 2-18. **M6** gradually turns pink in color at temperatures above about 110 °C.

2.5.2. Synthesis of oxalamide based macrocycle M7

Based on our prior studies, the solubility of the molecules can be increased by introducing an alkyl group next to the oxalimide moieties. In order to make the target macrocycles more soluble, the following molecules (**M7**, **M8**, and **M9**) were designed and synthesized.

Synthetic route for **M7** is shown in **Scheme 2.11**. Compound **M7-2** can be prepared in a good yield by reacting tyramine **M7-1** with diethyl oxalylate in methanol for 1 hour. Further alkylation of **M7-2** with propargyl bromide, diether **M7-3** can be obtained. Since diphenol **M7-2** shown poor solubility in most of the organic solvents, DMF was used as substitute for acetone in the second step. DMF is a very polar and high-boiling solvent; thus it is difficult to remove. The typical way to remove DMF from a reaction mixture is by ether/water extractions; in that case, a large quantity of ether and water is required. This process is not only time-consuming, but also very environment unfriendly. In order to minimize the utilization of hazardous substances used in chemical processes, we tried to optimize the workup procedures. We found that by adding a small amount of water to the reaction mixtures, the desired product will precipitate. Therefore, only a simple filtration was needed to collect the pure compound **M7-3**. With the diether **M7-3** in hand, the final step is the Hay coupling reaction of two terminal alkynes to give the designed macrocycle **M7**.



Scheme 2-11. Synthetic pathway of **M7**

It is worth mentioning that during the coupling reaction, TLC plate was used to monitor the progress of this reaction. Interestingly, an unusual phenomenon was observed, that is, no product spot was visible on the TLC plate. Several different eluents were tested to get a better analysis but none of them worked. The only thing observable on the TLC plate was a pink spot stuck at the bottom line. As time goes by, the color of that spot became deeper and deeper (**Figure 2.19**). Without any promising information from TLC plate, we can barely do any purification to get the pure product. In order to solve the problem, we decide to run a flash column with high polarity eluent, EtOAc/MeOH, to

collect the crude product first. Then, ^1H NMR spectrum or other instrument can be performed to analyze the component of the mixture. Once some crude products were obtained, we noticed that they are very sensitive to light. The freshly collected samples were white color but turned pink color in a short period of time. This reminded us what we have observed on TLC plate. The pink spot could be the polymerized product resulting from light exposure. It turns out that how to prevent the formation of the polymer was the key point in this reaction. The modified reaction procedures which require the coverage of the reaction flask with aluminum foil as well as handling the reaction in the dark room were proposed. By following this new strategy, compound **M7** has been successfully prepared in a total of 33% yield.

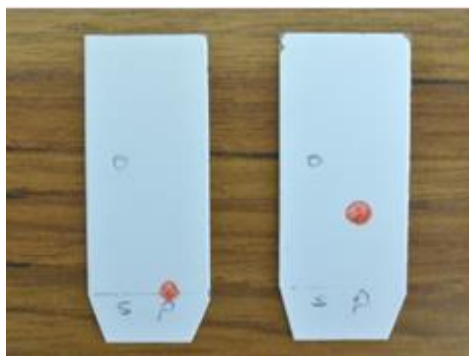


Figure 2-19. a) TLC plate used to screen the coupling reaction (with light exposure). b) TLC plate used to screen the coupling reaction (without light exposure). Eluent: EtOAc/MeOH/Hexanes: 4:2%:1

As we can see in **Figure 2.20a** and **2.20b**, cyclomonomer **M7(m)** and cyclodimer **M7** gradually turned pink in color at room temperature. Also, a very impressive property was observed, that is, they changed color under UV irradiation (**Figure 2.20c** and **2.20d**)

indicating the occurrence of polymerization of the diacetylene groups. This phenomenon was exactly as what we would expect. With the oxalamide moieties based framework, these macrocycles should form hydrogen bonds and stack at a distance of about 5.0 angstroms, which is the distance need to polymerize the diacetylenes.

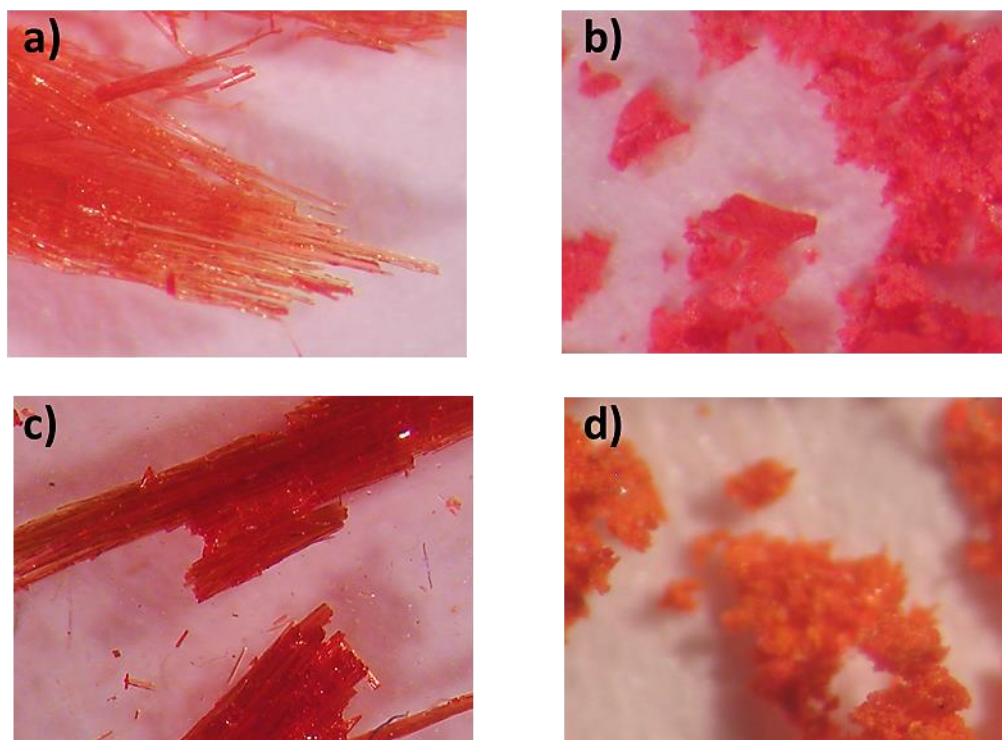
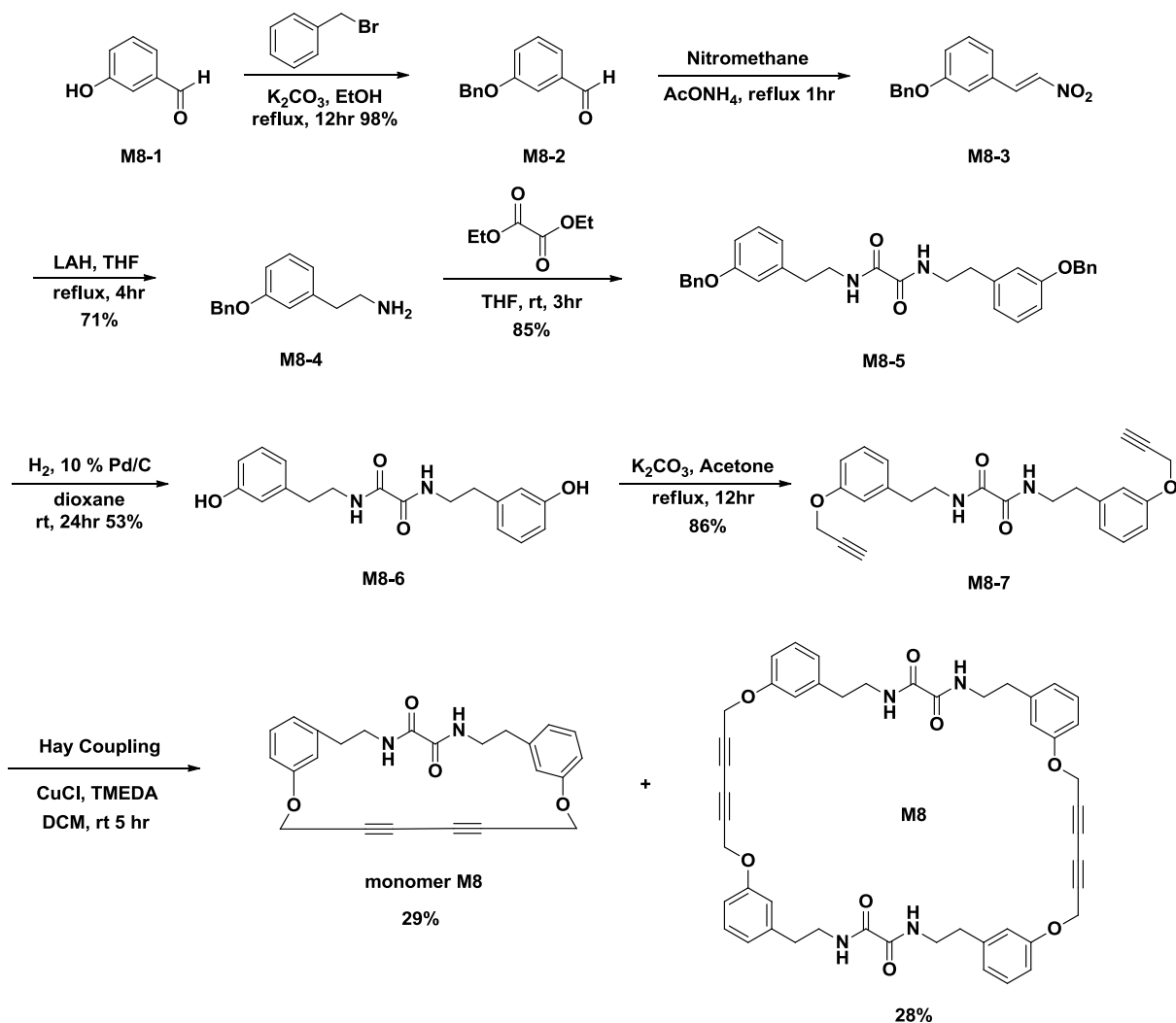


Figure 2-20. a) cyclomonomer **M7(m)** gradually turns pink in color at room temperature. b) cyclodimer **M7** gradually turns pink in color at room temperature. c) cyclomonomer **M7(m)** gradually changes color under UV irradiation. d) cyclodimer **M7** gradually changes color under UV irradiation.

Unfortunately, we did not succeed in growing single crystals for cyclomonomer **M7(m)** and cyclodimer **M7**. Even with the solubility-enhancing functionalities, ethylene groups, they still had poor solubility due to the strong intermolecular hydrogen bonding. In fact, the cotton-like precipitation always forms after it came off the column. Once the solid appears, it is almost impossible to dissolve them in any organic solvent again.

In an attempt to dissolve the insoluble product, acetic acid and trifluoroacetic acid were used as co-solvent. The reason for using these acids as co-solvent is to break the intermolecular hydrogen bonds. The result turned out to be unsuccessful while the insoluble residue remains and was not soluble in either case.

2.5.3. Synthesis of oxalamide based macrocycle M8



Scheme 2-12. Synthetic pathway of **M8**

The synthesis of **M8** is more complicated than **M7** (Scheme 2.12). Since compound **M8-4** is not commercially available, we decide to start from 3-hydroxybenzaldehyde **M8-1**. Benzylation reaction was applied to **M8-1** to protect hydroxyl phenol moiety. Then, condensation of aldehydes with nitromethane under base catalysis was performed to obtain the nitroalkene **M8-3** in 70% yield. Alkylamine **M8-4** was accessible via

reduction of nitroalkenes **M8-3** with lithium aluminum hydride. Usually the alkylamines are relatively unstable, thus they are not isolated and need to be used immediately after preparation in further reactions. Without further purification of the alkylamines **M8-4**, the next step is the introduction of the oxalamide moieties. Compound **M8-5** can be prepared in 55% yield for two steps. Deprotection of benzyl ethers under hydrogenolysis conditions with 10% palladium catalyst was carried out to generate the hydroxyl group of oxalamide-phenol moieties **M8-6**. Etherification of propargyl bromide with phenols proceeds smoothly in the presence of excess amount of potassium carbonate to afford the di-terminal alkyne compound **M8-7** in 90% yield. Based on our previous experience with macrocycle **M7**, the final step, Hay coupling, was carried out without light exposure. Coupling of two terminal alkynes **M8-7** catalyzed by TMEDA complex of copper(I) chloride produced the desired macrocycle **M8**.

Like **M7**, freshly prepared cyclomonomer **M8(m)** and cyclodimer **M8** were white in color with a cotton-like appearance. Once they were removed from the solvent and exposed to UV irradiation for 20 seconds, it started to change color suggesting that the polymerization is taking place (**Figure 2.21**).

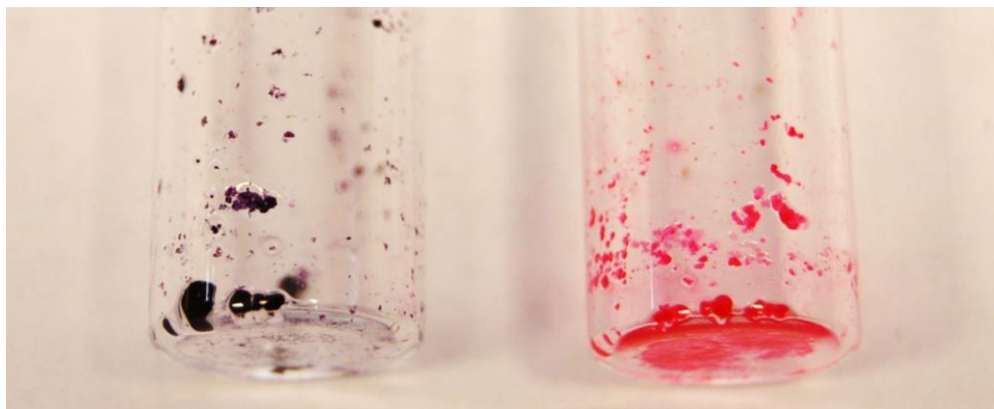
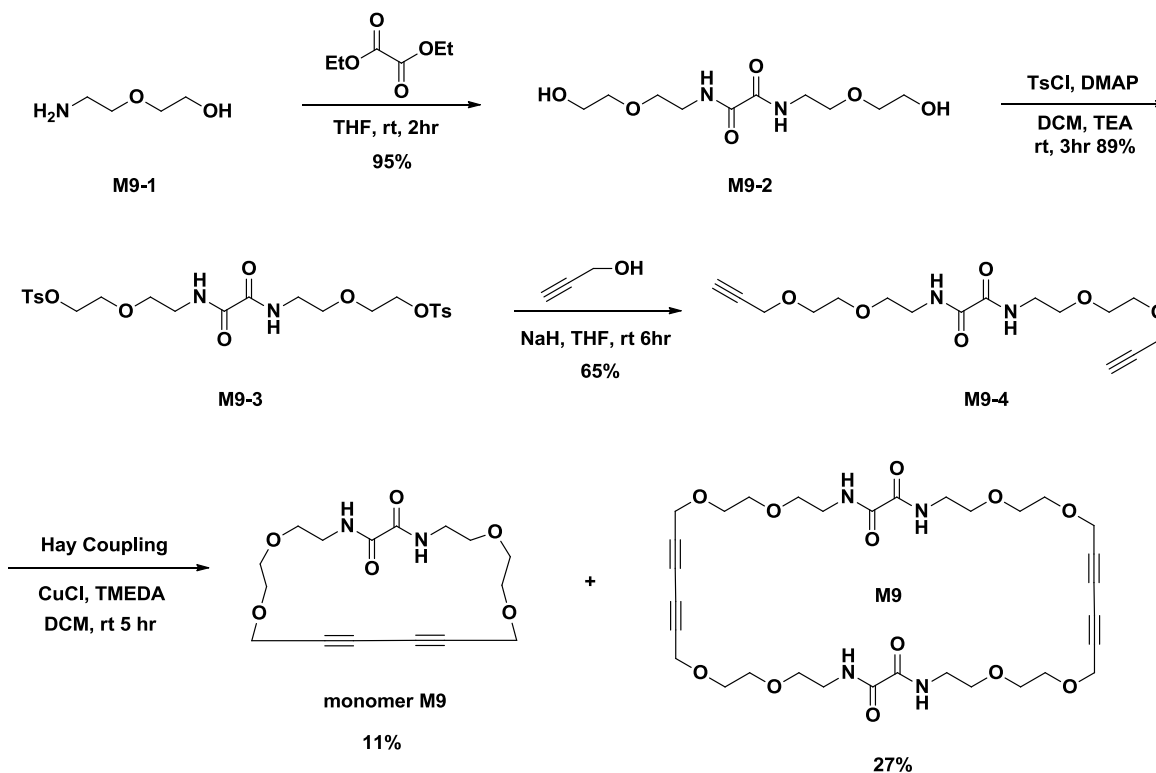


Figure 2-21. cyclodimer **M8** (left) and cyclomonomer **M8(m)** (right) gradually changes color under UV irradiation for 20 secs.

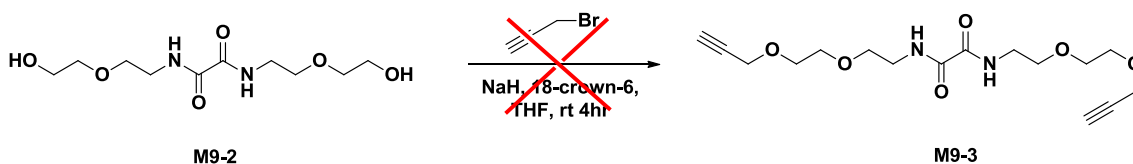
2.5.4. Synthesis of oxalamide based macrocycle M9



Scheme 2-13. Synthetic pathway of M9

As mentioned in the first section, the ethylene glycol moiety was always used to increase the solubility. Therefore, a new macrocyclic system with the incorporation of the diethylene glycol functionalities in the backbone was designed (Scheme 2.13). M9 was prepared in a total of 4 steps. Oxalamide diol M9-2 was synthesized in a good yield by reacting two equivalents of 2-(2-aminoethoxy)ethanol M9-1 with one equivalent of diethyl oxalate in THF. With the diol M9-2 in hand, we proceeded with the original plan:

deprotonation the diols in order to attack the propargyl bromide to give the diether **M9-3** (Scheme 2.14).



Scheme 2-14. Original plan to generate the diether **M9-3**.

However, the result indicates that the base we used for the deprotonation will also destroy the oxalamide moiety. The TLC plate shown many other side products formed after the reaction and the yield for this step was very low (< 10%). An alternative way to obtain the diether product was to first convert the hydroxyl group into a good leaving group, then utilizing propargyl alcohol as a nucleophile to accomplish the reaction. The new methods did work very well. Conversion of the hydroxyl unit into the tosyl group was carried out in methylene chloride with the help of catalytic amount of DMAP. Etherification of propargyl alcohol with the tosyl compound was performed under basic condition to generate the desired product **M9-4**. The final step was the oxidative coupling of the terminal alkynes. The purification process of this step was difficult. Since there are six oxygens inside the structure, the polarity of the macrocycle tends to be high. Column chromatography with methylene chloride as an eluent was running to generate the macrocyclic product. The result showed that the compound moved very slowly and nothing can be collected. Small amount of methanol was added to increase the polarity of

the eluent. Finally, purification via column chromatography with EtOAc and DCM (4 to 1) plus 10% MeOH as eluent furnished macrocyclic monomer **M9(m)** and dimer **M9**.

Compared with other macrocycles we prepared above, this glycol based macrocycle **M9** did show better solubility in organic solvents such as DCM and EtOAc. The tinny needle-like white crystals can be obtained from mixed solvents methylene chloride and ethyl acetate (1/1). However, the small size of the crystals prohibits a full X-ray diffraction study. Macrocycle **M9** does not melt even the temperature is over 300 °C.

Figure 2.22 represented color change of macrocyclic monomer **M9(m)** and dimer **M9** when exposed to UV irradiation for 20 seconds. Like **M7** and **M8**, macrocycle **M9** exhibited self-assembly behaviors via hydrogen bonding from oxalamide functional group.

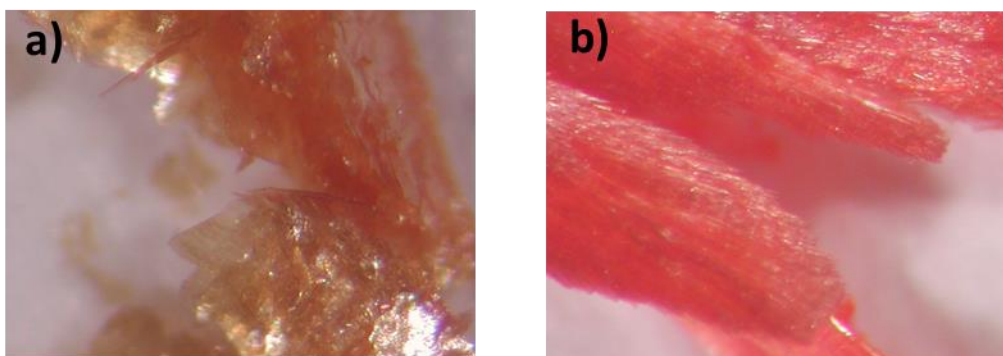
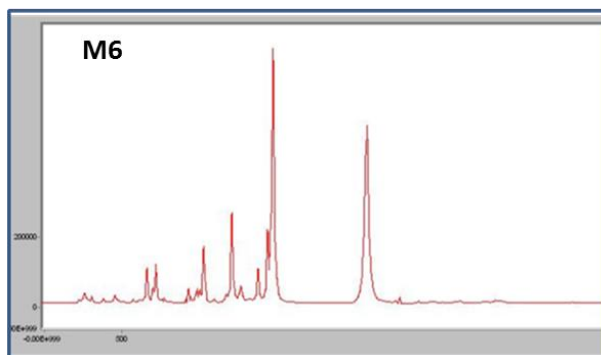


Figure 2-22. cyclodimer **M9** (left) and cyclomonomer **M9(m)** (right) gradually changes color under UV irradiation for 20 secs.

2.5.5. Other characterizations of oxalamide based macrocycles

Aside from color changing, the polymerization is also confirmed by other characterizations. Raman spectroscopy is recognized as a reliable tool for the study of the structure and properties of conjugated polymers like polydiacetylenes. **Figure 2.23a** and **b** represents the Raman spectra of macrocycles **M6** and **M8**. As we can see, there are two major bands appears at 1473 cm^{-1} and 2076 cm^{-1} , corresponding to the carbon-carbon double ($\nu(\text{C}=\text{C})$), and triple bond ($\nu(\text{C}\equiv\text{C})$) stretches, respectively. The Raman spectra provide strong evidence for the formation of polydiacetylenes.

a)



b)

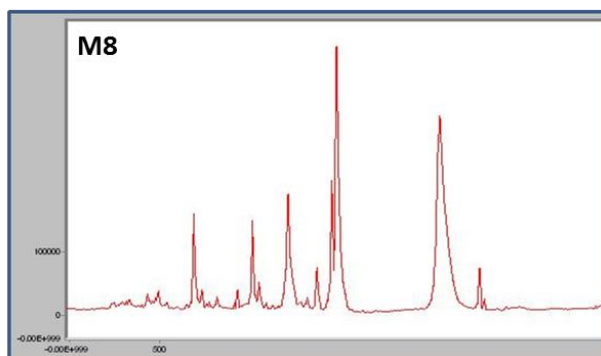


Figure 2-23. The Raman spectrum of UV-treated macrocycle **M6** (a) and **M8** (b). The typical absorption of PDAs can be found around 1400 and 2000 cm^{-1} , respectively, referring to corresponding $\text{C}=\text{C}$ and $\text{C}\equiv\text{C}$ bonds in the backbone.

Based on our design, the hydrogen bonding between the oxalamide groups should hold the macrocycles together to give the tubular structure. This hypothesis was confirmed by examining the assembly of **M6**, **M7** and **M8** in the solid state. The sample for transmission electron microscopy (TEM) were prepared by well dispersing these three samples in EtOH and dripping them onto copper/carbon mash grid, followed by gradual evaporating of the solvent. TEM images of these materials reveal long, rod-like assemblies. (**Figure 2.24**)

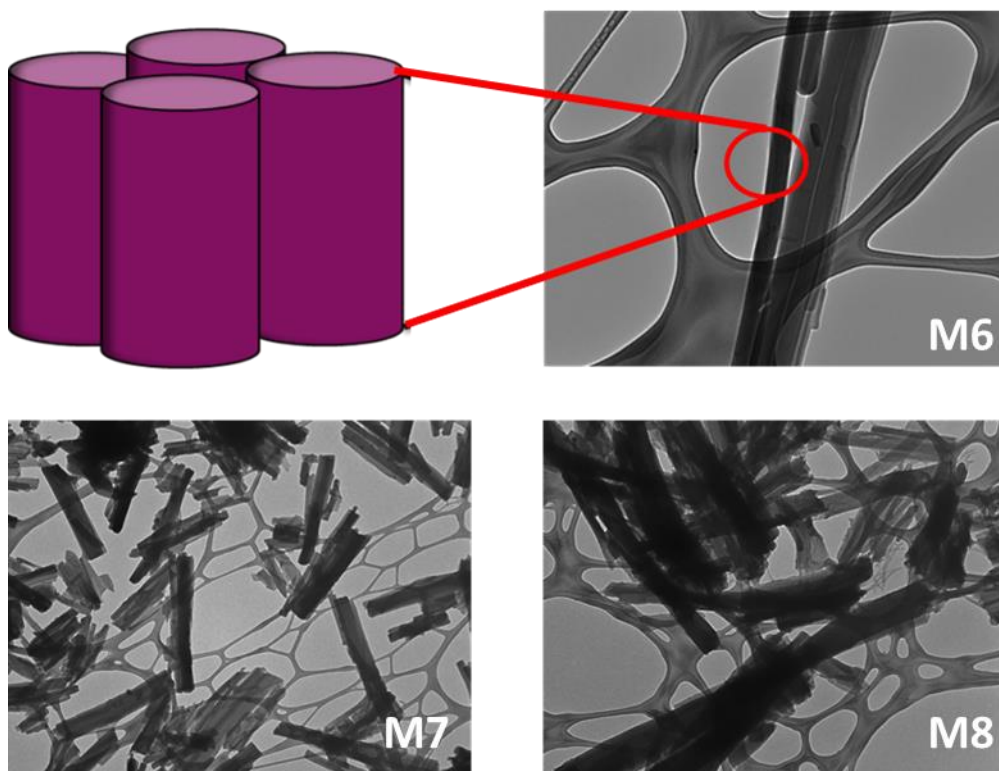


Figure 2-24. The transmission electron microscopy (TEM) image of **M6**, **M7** and **M8**, prepared by drop-casting ethanol solutions onto a copper grid, reveals straight, rod-like assemblies.

Furthermore, X-ray diffraction (XRD) was performed in order to study the details on the assembly of **M7**. As shown in **Figure 2.25**, the peak at 4.8 Å was detected. Due to the presence of the oxalamide moieties, each macrocycle should stack at a distance suitable for a 1, 4-polymerization, which is 4.9 Å. The result turns out to be consistent with our molecular design.

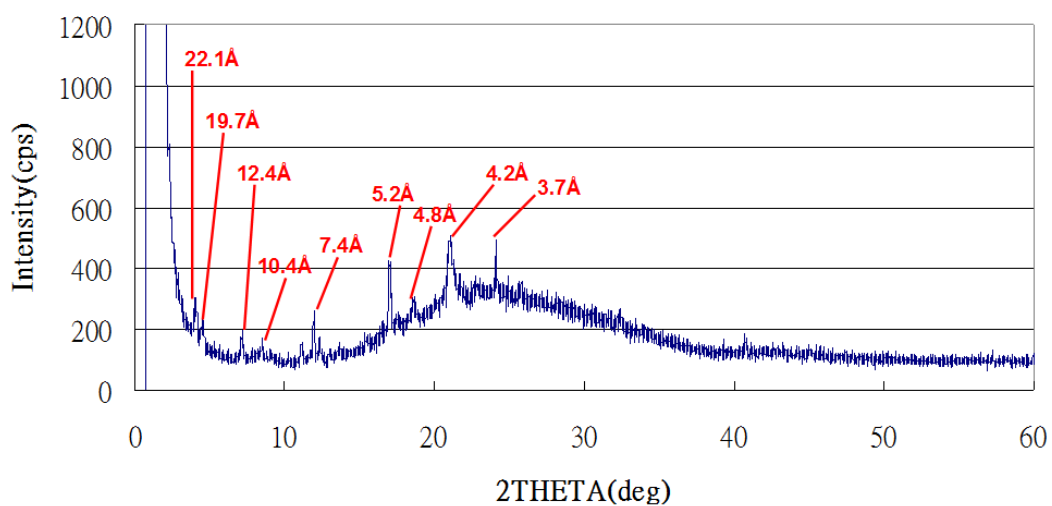


Figure 2-25. Powder x-ray pattern of **M7**.

2.5.6. Conclusion

A series of interesting diacetylene macrocyclic molecules which might have potential to self-polymerize to give the synthetic nanotubes (**M6-M9**) were successfully prepared. By incorporating the oxalamide moiety into the framework, these macrocycles should form inter-molecular hydrogen bonds and stack at a distance of about 5.0 angstroms which is the distance need for the 1,4-polymerization of the diacetylenes.

The results showed that they have poor solubility due to the strong inter-molecular hydrogen bonding between the oxalamide groups, but they crystallize with a one-dimensional morphology and change color when exposed to the atmosphere as well as under UV irradiation implies the occurrence of polymerization of diacetylenes. Since the prepared macrocycles polymerized rapidly when exposed to the atmosphere, a modified reaction procedures which require the coverage of the reaction flask with aluminum foil and handling the reaction in the dark room were proposed.

Because of poor solubility of the synthesized macrocycles, the crystals we obtained were not of X-ray quality. We could not confirm the formation of the tubular structures via single crystal X-ray diffraction. In order to study the properties and packing detail of these macrocycles, other instrumental analysis (ex. Powder XRD, Raman and TEM) were performed. Strong evidence for the formation of polydiacetylenes was provided by Raman spectroscopy: two major peaks around 1400 and 2100 cm^{-1} corresponding to the carbon-carbon double ($\nu(\text{C}=\text{C})$) and triple bond ($\nu(\text{C}\equiv\text{C})$) stretches, respectively. Moreover, the assembly of the macrocycles was investigated by TEM. According to TEM images, these materials exhibit long, cylinder-like assemblies. This result was

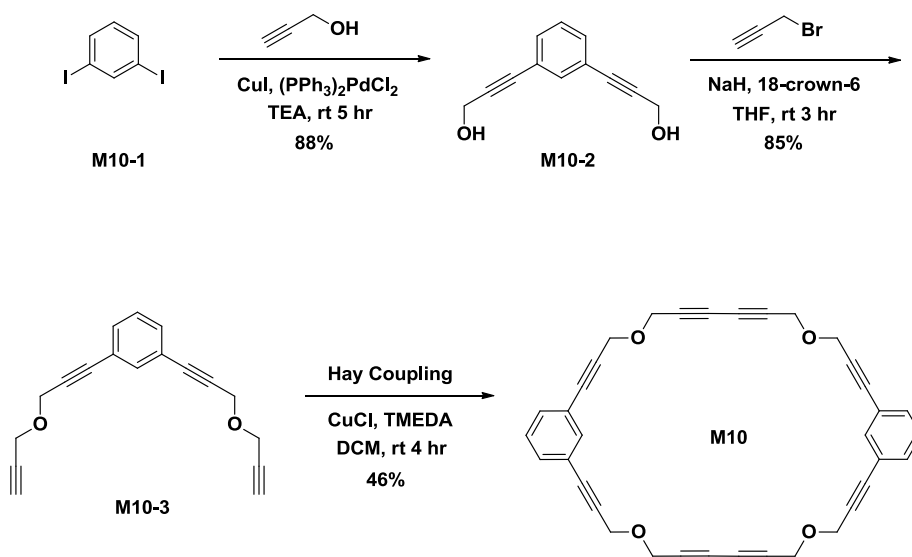
consistent with our molecular design. Finally, powder XRD was performed on macrocycle **M7** to get more molecular packing information. Based on our design, the hydrogen bonding between the oxalamide moieties should be able to hold the macrocycles at a distance suitable for a 1, 4-polymerization, which is 4.9 Å. This hypothesis has been proven due to the appearance of the peak at 4.8 Å.

It would be nice if single crystals of sufficient size can be obtained for the structural study. Therefore, in our future work, growing crystal in different conditions, such as at gradually increasing temperatures or using acid as co-solvent will be the major task. Also, modification of the macrocyclic architectures should be considered to get better solubility.

2.6. Macrocycles based on $\pi - \pi$ stacking

2.6.1. Synthesis of macrocycle **M10**

In addition to the previous two series of macrocyclic systems, we are also interested in design a new system based upon $\pi - \pi$ stacking of an aromatic system. As we know, a simple $\pi - \pi$ stack would give a van der Waals spacing comparable to graphite, 3.4 Å. But a slipped $\pi - \pi$ stack is very common and it has been reported that some of the $\pi - \pi$ interstack distance can be longer than 4 Å. A lot of aromatic derivatives of hexa-2,4-diyne-1,6-diol are known to stack at a distance commensurate with the desired 4.9 Å spacing. This is the reason why compound **M10**, a 34 atom macrocyclic ether with two potentially polymerizable functionalities (**Scheme 2.15**) has been designed. We believe that a macrocycle built from aromatic rings and hexa-2,4-diyne-1,6-diol might give such a stacking.



Scheme 2-15. Synthesis of macrocycle **M10** from readily available reagents.

Compound **M10** was prepared in three steps from relatively common starting materials. The first step, Pd-Catalyzed Sonogashira cross-coupling of propargyl alcohol with 1,3-diiodobenzene **M10-1**, was carried out at room temperature to give the diol moiety **M10-2**. Follow by Williamson alkylation with propargyl bromide, diether derivative was obtained in a decent yield. The difficult step was the last step where the terminal diacetyene **M10-3** was subjected to a cyclic dimerization using a copper catalyzed oxidative Hay coupling to give the desired macrocycle **M10** in 46 percent yield. A smaller 10 percent yield of the cyclomonomer was isolated, a small amount of the cyclic trimer was characterized and the rest of the yield was likely polymeric material. As we mentioned in the first section, the possible reason for that is the flexibility of two methylene groups increase the chance to these isomers. The overall yield of compound **M10** starting from 1,3-diiodobenzene was 34%.

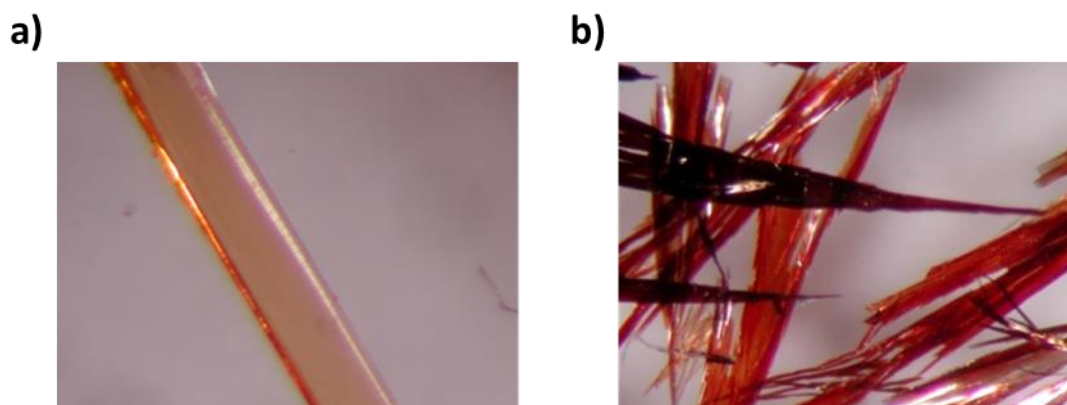


Figure 2-26. (a) Freshly formed crystals of the monoclinic form of **M10** grown at room temperature. (b) Freshly formed crystals of the triclinic polymorph of macrocycle **M10** grown at 40 °C.

2.6.2. Crystal structure analysis of macrocycle **M10**

The next step in the project required the preparation of single crystals of sufficient size and quality for a single-crystal X-ray diffraction study. A number of solvent systems were investigated, the best turning out to be 1:1 methylene chloride/ hexane. Slow evaporation of a solution of **M10** in this mixed solvent at room temperature gave pale-orange needles (**Figure 2.26(a)**). When the evaporation was carried out at an elevated temperature of 40°, some of the crystals had an initial orange-red color (**Figure 2.26(b)**) but in a short time developed a darker color with a blue cast. Subsequent experiments showed that these two different crystalline forms were two different polymorphs of macrocycle **M10**.

Single-crystal X-ray diffraction experiments revealed that the crystals formed at room temperature were monoclinic (**Figure 2.27**), with the molecules of macrocycle **M10** stacked in accordance with the design. The repeat distance of 5.09 Å was longer than the ideal repeat distance of 4.9 Å but within the range reported for other successful polymerizations.⁴⁵ When the crystals were kept at room temperature, they became completely amorphous in about 30 days. These transformations were accompanied by a color change to a deep-red, nearly black color.

Based on the crystallographic data of **M10**, we believe that it has great potential for 1,4-polymerization on its own. Since **M10** is quite unstable at room temperature, we assume that heating the crystals at low temperature might be able to induce the desired polymeration. In order to keep track of the changes of the crystal structure, we start to heat it from 30 °C. A single crystal was chosen and heated from 30 °C to 50 °C. We

studied the change in crystal structure after each run of heating using single-crystal X-ray diffraction. The whole crystal lattice data change procedure was listed in **Table 2.8**. Crystal was examined on the X-ray diffractometer at various stages as the crystallinity was lost, but no structural change could be detected before the crystals became amorphous.

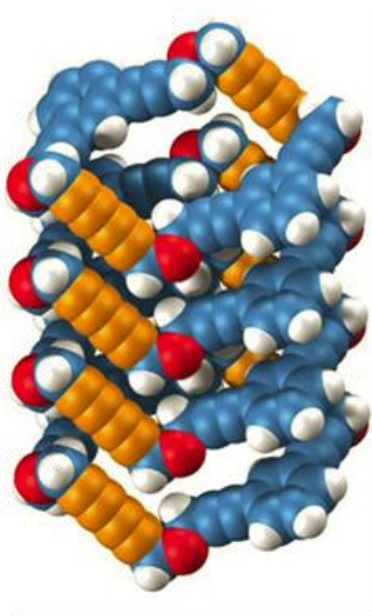


Figure 2-27. (a) The observed molecular stacking in the monoclinic form of macrocycle **M10**. The repeat distance of 5.09 Å is longer than the ideal polymerization value of 4.9 Å .

Time(h)	Temp.	Color	a (Å)	b (Å)	c (Å)	α (°)	β (°)	γ (°)
0	r.t.	Pale-orange	33.769	5.081	17.982	90.00	117.56	90.00
16	30	Pale-orange	33.798	5.083	17.997	90.00	117.54	90.00
24	35	Pale-orange	33.797	5.084	18.007	90.00	117.49	90.00
24	35	Deep-Orange	33.741	5.076	17.997	90.00	117.45	90.00
24	40	Deep-Orange	33.739	5.070	18.001	90.00	117.22	90.00
5	45	Deep-red	33.842	5.079	18.054	90.00	117.08	90.00
8	50	Black	No spots can be collected by X-ray.					

Table 2-8. The unit cell data of **M10** obtained from material grown from the different solvent systems.

From **Table 2.8**, we found that the crystal structure started to show some changes as temperature has gradually increased. We continue the heating process by increasing the temperature to 45 °C. However, this continual heating did not afford the result we were expecting. Nonetheless a sign of partial polymerization was observed and the crystal structure appeared to be more disordered. It is surmised that partial polymerization may give rise to disorderness because the overall intermolecular interaction is disrupted. However, as more polymers are being formed, more orderness is expected because the rigid structure reinforces its structural integrity. Unfortunately, heating the crystal at 50 °C for 8 hours rapidly converted the crystals to an amorphous (and nondiffracting) state. As a consequence, the crystal failed to polymerized in 1,4-fashion.

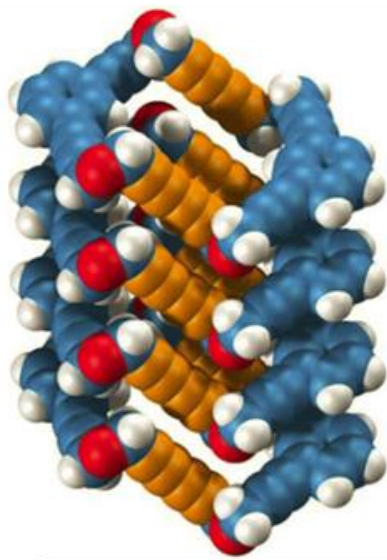


Figure 2-28. Observed molecular stacking in the triclinic form of macrocyclic monomer **M10**. The observed repeat distance of 4.84 Å was much closer to the ideal value.

The crystals of **M10** grown at 40 °C, the second polymorph, belong to the triclinic space group $P\bar{1}$. The molecules of the triclinic form had a different molecular conformation than the molecules of the original monoclinic form, but they had a similar stacked structure (**Figure 2.28**). The molecular repeat distance in the triclinic form was 4.84 Å, quite close to the ideal value of 4.9 Å. Even though the repeat distance within the triclinic polymorph was a bit closer to the ideal value, the triclinic crystals were somewhat more robust than the monoclinic crystals. Initial experiments showed that the triclinic crystals were stable at room temperature but rapidly became amorphous upon heating to 50 °C

In previous work with noncyclic diacetylenes, we found that slow annealing of a diacetylene monomer crystal at a relatively low temperature can bring about a single-crystal-to-single-crystal polymerization that is otherwise unobservable. Following this

idea, one particularly well formed crystal of the triclinic polymorph of **M10** was chosen, and the molecular structure was verified using single-crystal X-ray diffraction. The crystal was then subjected to slow annealing at 40° in a temperature-controlled oven. At various intervals the crystal was removed from the oven and returned to the diffractometer, and the structure was redetermined. Signs of polymerization could be seen after 3 days of heating, as additional peaks appeared in the diffraction-determined electron density maps.

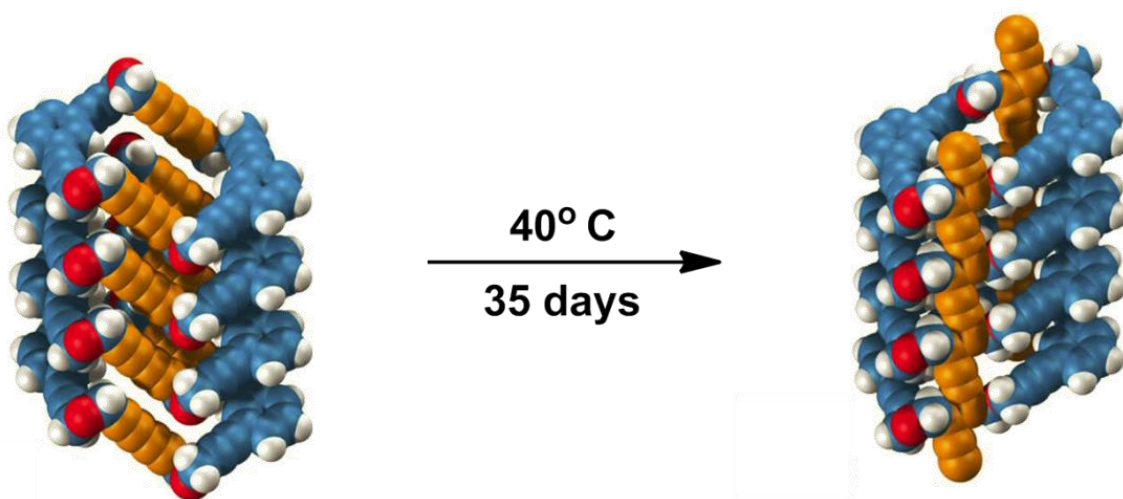


Figure 2-29. Structure of polymer **M10** obtained by slow annealing of the triclinic crystals at 40°.

As the heating continued day by day, the percentage of polymer could be seen to increase, accompanied by a decrease in monomer content as well as a decrease in crystal quality. After 35 days of annealing at 40 °C, the crystal was returned to the diffractometer for the 20th and last successful crystal structure determination. This final structural analysis of the annealed crystal showed only the desired polymer structure (**Figure 2.29**). Because of a lack of data, the structure of polymer **M10** was not of high quality, but the

polymerization appeared to be substantially complete. Further heating of the crystal gave only a scattering of diffraction data so the annealing experiment was brought to an end.

Differential scanning calorimetry (DSC) studies of **M10** showed a single exothermic event at 106 °C consistent with a solid-state polymerization reaction. The cooling and reheating curves of the polymerized material were featureless, indicating a nonreversible solid- state change (**Figure 2.30**).

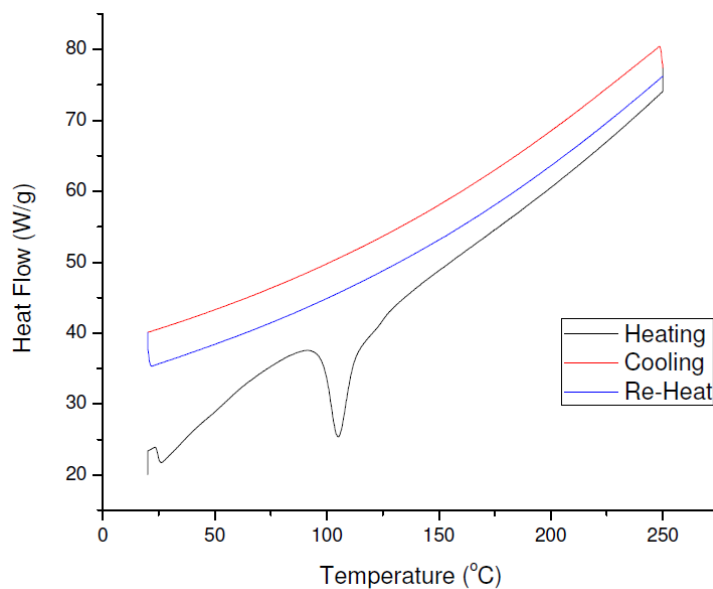


Figure 2-30. DSC plot of **M10** (heating rate 10 °C/min). The black line shows the original heating curve with an exothermic transition at ~ 106 °C corresponding to the irreversible polymerization. The red line shows the cooling of the sample. The blue line shows that the re-heating of the fully polymerized sample is feature free.

The molecular structure of polymer **M10** (**Figure 2.28**) is in complete accordance with the design shown in **Figure 2.6**. The macrocyclic monomers have undergone a double addition polymerization reaction to give a tubular polymer.

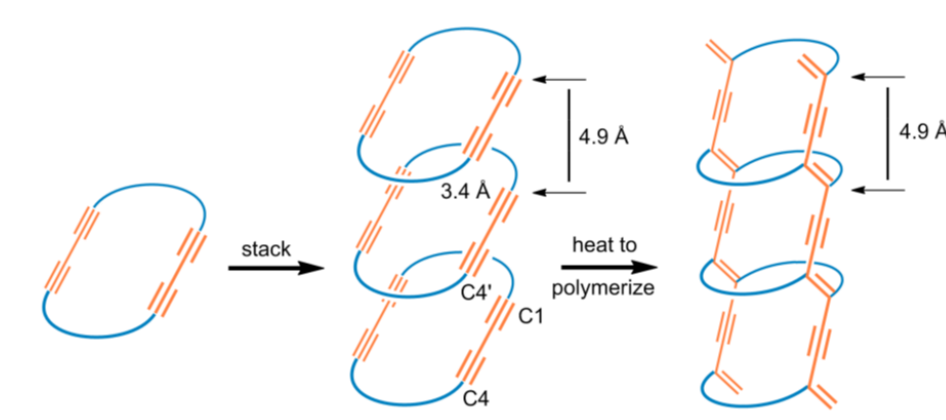


Figure 2.6. One possible route to a tubular polymer is via a topochemical polymerization of a diacetylene containing macrocycle. For the reaction to proceed, the macrocycles would need to be spaced near the 4.9 Å expected for polymers with neighboring diacetylene C1–C4' carbon atoms close to the van der Waals contact distance of 3.4 Å. The application of heat (or radiation) should bring about the polymerization.

The inner cross section of an idealized macrocyclic monomer is an oval roughly 11 Å x 12 Å or roughly a circular nanometer, large enough to hold a guest molecule within its interior. However, the molecules crystallize to form a tube with an empty interior with the macrocycle adopting a conformation with a smaller 7.5 Å x 11.5 Å cross (**Figure 2.31a**). Furthermore the rings tilt when they stack closing down the tube interior bringing opposing methylene groups into contact (**Figure 2.31b**). This is in keeping with the well known principle, “*Natura abhorret vacuum*”, one simply does not expect to find empty space within condensed matter. The molecular tilting is expected from a packing perspective, because a direct stacking of flat molecules would bring atoms into direct

“bump to bump” contact. Tilting removes these unfavorable contacts and also brings the neighboring C1-C4' atoms into the close contact needed for the polymerization step.

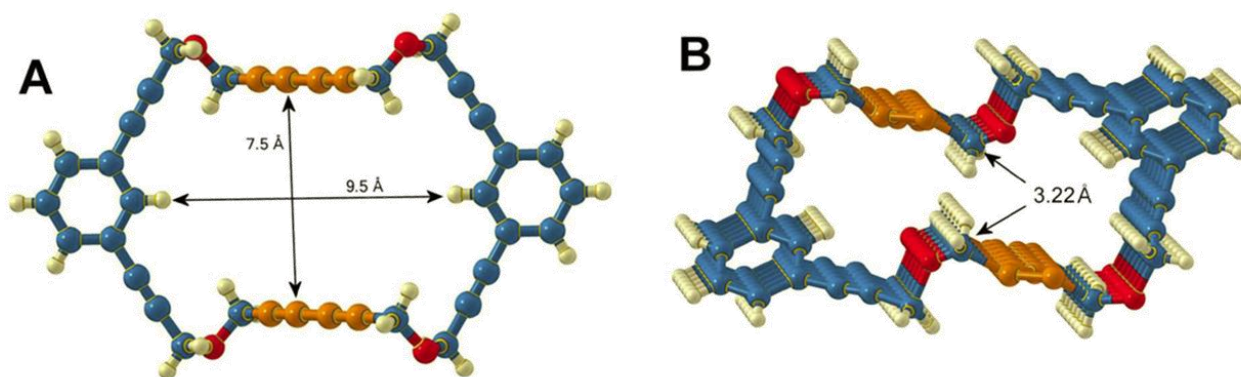


Figure 2-31. (a) The macrocycle monomers have a rectangular cross section of $7.5 \text{ \AA} \times 9.5 \text{ \AA}$. (b) The monomers stack at an angle such that the cross section of the tubular polymer is reduced with a 3.22 \AA contact between opposite methylene groups.

It is interesting that two polymorphs of macrocycle **M10** were isolated. As shown in **Figure 2.32**, the conformations of the molecules in the two polymorphs are different. Each has inversion symmetry with four independent ether C–O bonds. In the monoclinic polymorph, three of these bonds are gauche and one is anti. In the triclinic polymorph, all four independent C–O bonds are gauche. Despite this major conformation difference, both polymorphs have the molecules stacked in accordance with the parameters needed for the polymerization. The monoclinic form has a longer repeat distance of 5.09 \AA versus a distance of 4.84 \AA in the triclinic form. The important neighboring C1–C4' contact between potential reacting atoms (3.7 \AA) is shorter in the monoclinic structure than in the triclinic structure (3.9 \AA). The “ideal” distances are 4.9 \AA for the repeat and

3.4 Å for the contact. Both the monoclinic and triclinic forms appear to undergo the polymerization reaction, but only for the triclinic form is a crystal-to-crystal process. The repeat distance appears to be the most important parameter. An incommensurate monomer-polymer repeat distance would naturally lead to more crystal motion and presumably be more likely to yield an amorphous solid.¹⁸

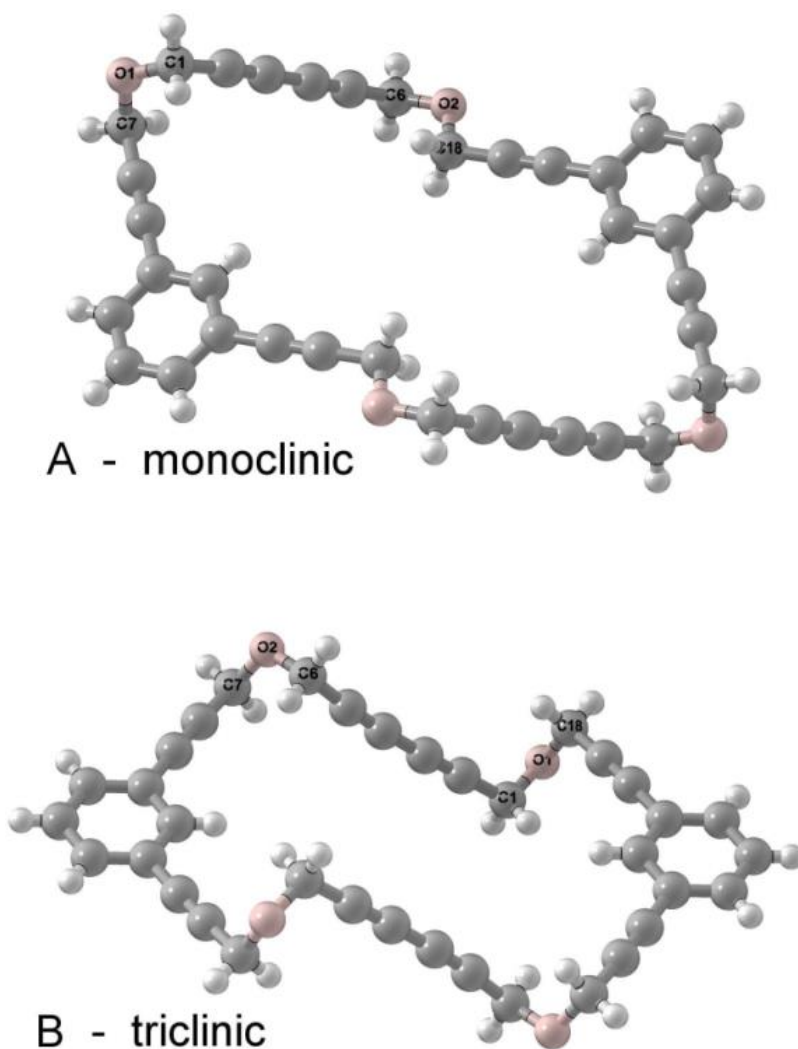
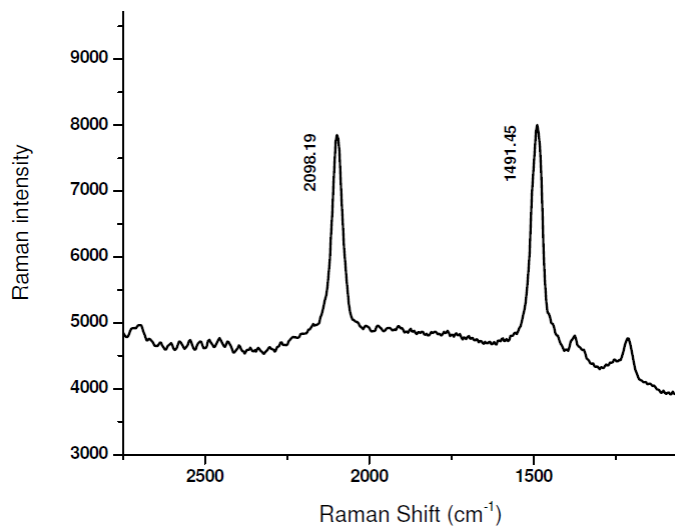


Figure 2-32. Molecular Conformations. In the monoclinic polymorph **A** three of the independent ether C-O bonds adopt a gauche configuration, while the fourth (O2-C18) adopts an anti configuration. In the triclinic polymorph **B** all four independent C-O bonds are gauche.

a)



b)

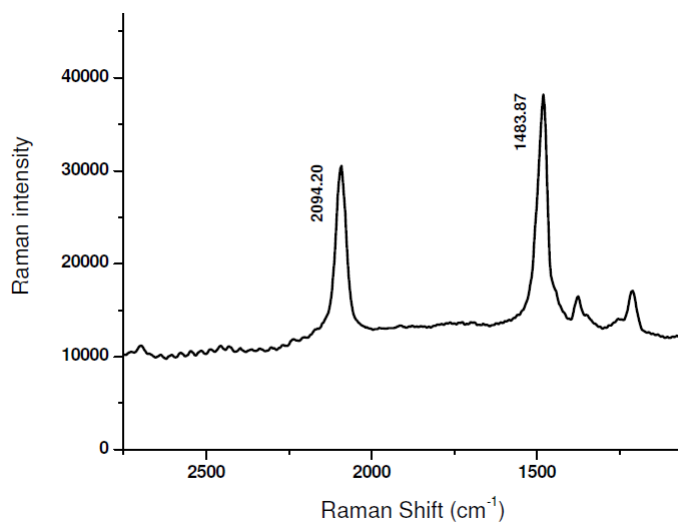


Figure 2-33. (a) Raman spectrum of the triclinic polymorph of **M10**. The small amount of polymer that already exists prior to heat treatment dominates the spectrum giving the two distinct polymer absorptions at 2098 and 1491 cm⁻¹. (b) Raman spectrum of the polymer **M10**. After full polymerization, the two distinct polymer absorptions occur at 2094 and 1484 cm⁻¹.

Freshly made samples of **M10** rapidly acquired color indicative of the polymerization even though the amount of polymer was at a level not detected by the single-crystal X-ray studies. However, evidence of this initial polymerization could be seen in a Raman spectrum of a fresh sample, which showed the two strong resonance-enhanced bands characteristic of polydiacetylenes (**Figure 2.33a**). The Raman spectrum of the fully polymerized crystals of **M10** showed these two bands, at 1484 and 2095 cm^{-1} , at a much greater intensity (**Figure 2.33b**).

Figure 2.34 displayed the color images of the crystals of compounds macrocyclic monomer **M10** and polymer **M10**. Freshly prepared samples of the triclinic polymorph of macrocyclic monomer **M10** already show significant color due to a small amount of polymerization. After annealing the fully polymerized crystals have a darker color and tend to curl. Once the polymerization occurred, we found the crystals to be totally insoluble in a wide range of standard solvents. One would expect an isolated tube to be a flexible molecule able to incorporate solvent or other small molecules within the interior. Because of the complete lack of solubility, we have not yet been able to verify this hypothesis. The synthesis of **M10** is straightforward from readily available starting materials, and more soluble analogues should be possible using similar synthetic methodology. Soluble analogues should have the open void space that would increase the potential applicability of molecular tubes.⁵³

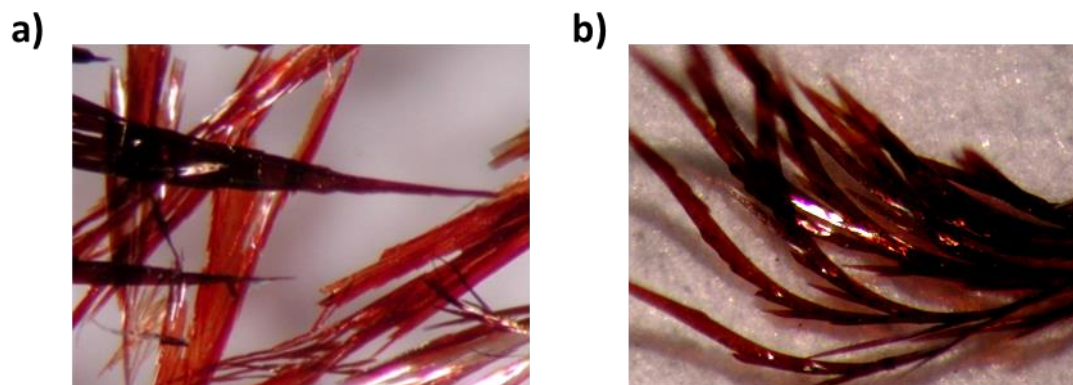


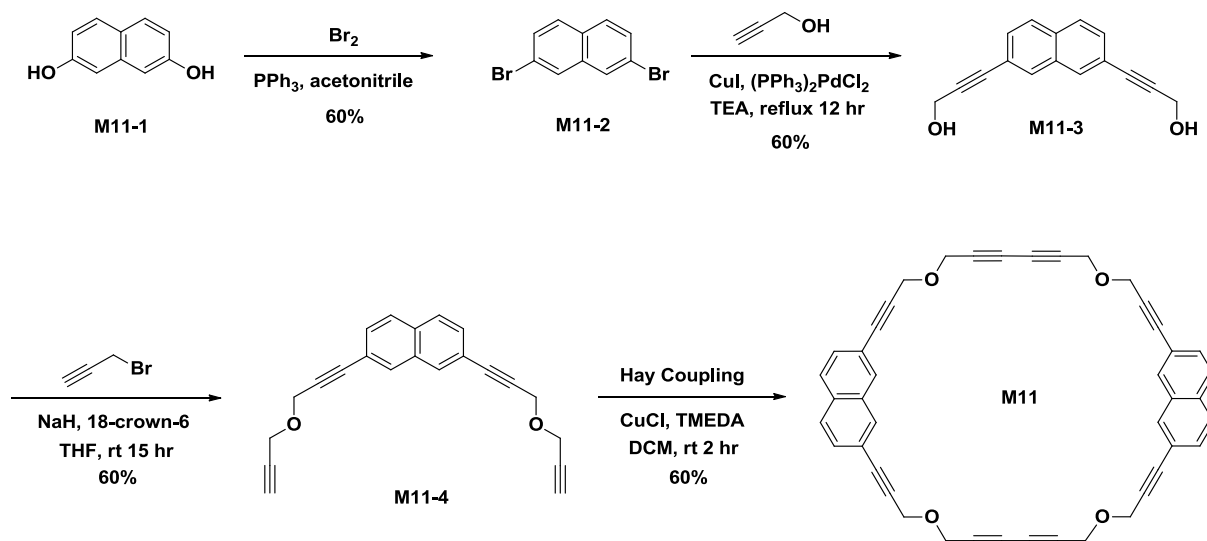
Figure 2-34. Color photographs of the crystals of (a) freshly prepared samples of the triclinic polymorph of macrocyclic monomer **M10** (b) the fully polymerized crystals after annealing. The crystals are 3-4 mm long, but as little as 0.10 mm in thickness. The tube axis is aligned along the length of crystals.

2.6.3. Synthesis of macrocycle M11

The ultimate goal of this project is to design and prepare a covalently bonded nanotube able to show potential application for sensors, templates for directed reactions, or small molecule transport systems. As we mentioned in the previous section, **M10** molecules crystallize to form a tube with a smaller empty interior than we expected. Therefore, how to expand the size of the synthetic tube is our next topic. In order to

achieve our goal, the naphthalene moiety was used to replace the original benzene core.

The synthetic route for **M11** is represented in **Scheme 2.16**.



Scheme 2-16. Synthetic route for **M11**

As outlined in **Scheme 2-16**, the conversion of the -OH functional group of 2,7-dihydroxy-naphthalene **M11-1** into Br group was accomplished by treating the diol compound with the mixture of bromine and triphenylphosphine following the literature know procedure. The yield of this step was decent. However, as the reaction proceeded, a lot of HBr were produced. Thus, the use of cold NaOH solution to trap the HBr was necessary. With the dibromo compound in hand, we followed the standard procedure for preparing other macrocycles. **M11** was successfully synthesized in total 41% yield.

Freshly prepared macrocycle **M11** reveals white color. Sitting at the room temperature for one day, it gradually turned to light brown color. Keeping the compound in the refrigerator can prevent future changes in color. Although the only dissimilarity

between **M10** and **M11** was the rigid core of the ring, the solubility of these two compounds did show great difference. **M10** had no difficulty to dissolve in most common organic solvent such as methylene chloride, ethyl acetate, or chloroform. However, **M11** can only dissolve in chloroform when warmed. In order to study the molecular structure and packing patterns of **M11**, several different solvent systems and methods were tried to grow the single crystals. Unfortunately, none of them gave us good quality crystals with large enough size suitable for X-ray diffraction analysis. Tiny needle-like crystals were obtained after each run of crystallization (**Figure 2.35**). As we mentioned before, heating is necessary to completely dissolve our compound in chloroform. However, an unwanted problem might be caused by heating as well, that is, polymerization. After each attempt of crystallization, some of the compound was no longer able to dissolve. Since the crystallization of **M11** was not successful, its structure is still a mystery. More crystal growth conditions should be tried in this project.



Figure 2-35. Needle like crystals of **M11** obtained after crystallization

2.6.4. Conclusion

Should one call polymer **M10** a synthetic nanotube? We believe so. The interior is 1 nm across in the long direction, and the outer dimensions are about 1 nm × 2 nm; the length is indeterminately long. In an idealized conformation, the tubes would have a roughly circular cross section of about 1 nm, very similar to that of a single-walled carbon nanotube. The significance of this new polymer is that it is the first example of a structurally characterized tubular addition polymer and that a general strategy for synthesizing any tubular polymer has been confirmed. One can imagine that the power of organic synthesis may lead to similar polymers that can be tailor designed for a wide range of applications.

2.7. Summary

In this project, we successfully developed a reliable and straightforward method for the preparation of the macrocycles containing diacetylene functionalities. Although the final step, Hay coupling reaction, always gives relatively low yields, we believe our strategy is by far the simplest and most efficient way to synthesizing diacetylene based macrocycles.

In order to properly align the macrocycles, three different approaches have been applied: Host-guest approach, Hydrogen bonding from oxalamide moieties approach, and $\pi - \pi$ stacking approach, respectively.

Generally speaking, host-guest approach should be the most powerful method to control the distance between the diacetylene functionalities since it is convergent at the final step and has efficient combinatorial aspects. Due to poor solubility of the synthesized macrocycles, we did not succeed in co-crystallizing the macrocycle guest molecules with the oxalamide host molecules. We demonstrated that the installation of glycol moieties could greatly enhance the solubility. Based on this, new macrocyclic system with improved solubility can be achieved in the future. Moreover, macrocycles with polar substituents should be considered because they might show good solubility in polar protic solvents.

The second approach was to use hydrogen bonding between the oxalamide moieties to give the desired molecular packing of the macrocycles. In this work, a series macrocycles containing oxalamide groups were prepared. The result showed that our design was very successful: The synthesized macrocycles changed color rapidly when exposed to atmosphere or under UV irradiation indicating the polymerization of the diacetylenes did happen. However, poor solubility resulted from strong inter-molecular hydrogen bonding made the crystal growing process become very challenging. Without high quality single crystals in hand, the formation of the desired tubular structures could not be confirmed via X-ray diffraction. Other instrumental analysis (ex. XRD, Raman and TEM) were performed in order to study the properties and packing detail of these macrocycles. In the future work, we will try more different conditions for crystal growing. Also based on our firsthand experience, design a new oxalamide based macrocycle by introducing the glycolic side chain might help to solve the solubility problem.

The third approach we utilized π - π stacking among the aromatic rings to form the desired molecular packing. The distance for π - π stacking has been reported in the range of 3.5 Å to 6.3 Å. Therefore, it does show potential to give the desired packing distance which is 4.9 Å. By using the π - π stacking approach, we successfully obtained the first structure of a synthetic nanotube prepared by the solid-state polymerization of a stacked column of diacetylene-based macrocycles **M10**. **M10** crystallize to form a tube with a smaller empty interior than we expected. Also, we found that once the nanotube was formed, the crystals became totally insoluble in a wide range of standard solvents. This is not a perfect situation because we always want the synthesized nanotube to be a flexible molecule which is big enough to incorporate solvent or other small molecules within the interior. Therefore, our future work will focus on design more soluble analogues with expanded size.

2.8. References

- (1) Shirakawa, H.; Ikeda, S.: Infrared Spectra of Poly(Acetylene). *Polymer Journal* **1971**, *2*, 231.
- (2) Burroughes, J. H.; Jones, C. A.; Friend, R. H.: New Semiconductor-Device Physics in Polymer Diodes and Transistors. *Nature* **1988**, *335*, 137-141.
- (3) Sirringhaus, H.; Tessler, N.; Friend, R. H.: Integrated Optoelectronic Devices Based on Conjugated Polymers. *Science* **1998**, *280*, 1741-1744.
- (4) Sauteret, C.; Hermann, J. P.; Frey, R.; Pradere, F.; Ducuing, J.; Baughman, R. H.; Chance, R. R.: Optical Nonlinearities in One-Dimensional-Conjugated Polymer Crystals. *Phys. Rev. Lett.* **1976**, *36*, 956-959.
- (5) Burroughes, J. H.; Bradley, D. D. C.; Brown, A. R.; Marks, R. N.; Mackay, K.; Friend, R. H.; Burns, P. L.; Holmes, A. B.: Light-Emitting-Diodes Based on Conjugated Polymers. *Nature* **1990**, *347*, 539-541.
- (6) Friend, R. H.; Gymer, R. W.; Holmes, A. B.; Burroughes, J. H.; Marks, R. N.; Taliani, C.; Bradley, D. D. C.; Dos Santos, D. A.; Bredas, J. L.; Logdlund, M.; Salaneck, W. R.: Electroluminescence in Conjugated Polymers. *Nature* **1999**, *397*, 121-128.
- (7) Wang, C. S.; Burkett, J.; Lee, C. Y. C.; Arnold, F. E.: Structure and Electrical-Conductivity of Ion-Implanted Rigid-Rod and Ladder Polymers. *Journal of Polymer Science Part B-Polymer Physics* **1993**, *31*, 1799-1807.
- (8) Wegner, G.: Topochemical Reactions of Monomers with Conjugated Triple Bonds .I. Polymerization of 2,4-Hexadiyne-1,6-Diols Derivatives in Crystalline State. *Zeitschrift Fur Naturforschung Part B-Chemie Biochemie Biophysik Biologie Und Verwandten Gebiete* **1969**, *B 24*, 824.
- (9) Cohen, M. D.; Schmidt, G. M. J.: Topochemistry .1. Survey. *Journal of the Chemical Society* **1964**, 1996.
- (10) Enkelmann, V.: Solid-State Reactivity of Triacetylenes. *Chem. Mater.* **1994**, *6*, 1337-1340.
- (11) McGhie, A. R.; Kalyanaraman, P. S.; Garito, A. F.: Kinetics of Thermal Polymerization in Solid-State - 2,4-Hexadiyne-1,6 Diol Bis (Para-Toluenesulfonate). *Journal of Polymer Science Part C-Polymer Letters* **1978**, *16*, 335-338.
- (12) Bloor, D.; Koski, L.; Stevens, G. C.; Preston, F. H.; Ando, D. J.: Solid-State Polymerization of Bis-(Para-Toluene Sulfonate) of 2,4-Hexadiyne-1,6-Diol .1. X-Ray-Diffraction and Spectroscopic Observations. *J. Mater. Sci.* **1975**, *10*, 1678-1688.
- (13) Baughman, R. H.: Solid-State Reaction-Kinetics in Single-Phase Polymerizations. *J. Chem. Phys.* **1978**, *68*, 3110-3121.
- (14) Chance, R. R.; Eckhardt, H.; Swerdloff, M.; Federici, R. R.; Szobota, J. S.; Turi, E. A.; Boudreaux, D. S.; Schott, M.: Urethane-Substituted Polydiacetylenes - Solid-State Polymerization, Crystal Optics, and Conformational Transitions. *ACS Symp. Ser.* **1987**, *337*, 140-151.
- (15) Spagnoli, S.; Berrehar, J.; LapersonneMeyer, C.; Schott, M.; Rameau, A.; Rawiso, M.: Gamma-Ray Polymerization of Urethane-Substituted Diacetylenes: Reactivity and Chain Lengths. *Macromolecules* **1996**, *29*, 5615-5620.
- (16) Chang, Y. L.; West, M. A.; Fowler, F. W.; Lauher, J. W.: An Approach to the Design of Molecular-Solids - Strategies for Controlling the Assembly of Molecules into 2-Dimensional Layered Structures. *J. Am. Chem. Soc.* **1993**, *115*, 5991-6000.
- (17) Coe, S.; Kane, J. J.; Nguyen, T. L.; Toledo, L. M.; Wininger, E.; Fowler, F. W.; Lauher, J. W.: Molecular Symmetry and the Design of Molecular Solids: The Oxalamide Functionality as a Persistent Hydrogen Bonding Unit. *J. Am. Chem. Soc.* **1997**, *119*, 86-93.

- (18) Curtis, S. M.; Le, N.; Fowler, F. W.; Lauher, J. W.: A Rational Approach to the Preparation of Polydipyridyldiacetylenes: An Exercise in Crystal Design. *Cryst. Growth Des.* **2005**, *5*, 2313-2321.
- (19) Curtis, S. M.; Le, N.; Nguyen, T.; Xi, O. Y.; Tran, T.; Fowler, F. W.; Lauher, J. W.: What Have We Learned About Topochemical Diacetylene Polymerizations? *Supramol. Chem.* **2005**, *17*, 31-36.
- (20) Fowler, F. W.; Lauher, J. W.: A Rational Design of Molecular Materials. *J. Phys. Org. Chem.* **2000**, *13*, 850-857.
- (21) Kane, J. J.; Liao, R. F.; Lauher, J. W.; Fowler, F. W.: Preparation of Layered Diacetylenes as a Demonstration of Strategies for Supramolecular Synthesis. *J. Am. Chem. Soc.* **1995**, *117*, 12003-12004.
- (22) Kane, J. J.; Nguyen, T.; Xiao, J.; Fowler, F. W.; Lauher, J. W.: The Host Guest Co-Crystal Approach to Supramolecular Structure. *Mol. Cryst. Liq. Cryst.* **2001**, *356*, 449-458.
- (23) Liao, R. F.; Lauher, J. W.; Fowler, F. W.: The Application of the 2-Amino-4-Pyrimidones to Supramolecular Synthesis. *Tetrahedron* **1996**, *52*, 3153-3162.
- (24) Nguyen, T. L.; Fowler, F. W.; Lauher, J. W.: Commensurate and Incommensurate Hydrogen Bonds. An Exercise in Crystal Engineering. *J. Am. Chem. Soc.* **2001**, *123*, 11057-11064.
- (25) Nguyen, T. L.; Scott, A.; Dinkelmeyer, B.; Fowler, F. W.; Lauher, J. W.: Design of Molecular Solids: Utility of the Hydroxyl Functionality as a Predictable Design Element. *New J. Chem.* **1998**, *22*, 129-135.
- (26) Ouyang, X.; Fowler, F. W.; Lauher, J. W.: Single-Crystal-to-Single-Crystal Topochemical Polymerizations of a Terminal Diacetylene: Two Remarkable Transformations Give the Same Conjugated Polymer. *J. Am. Chem. Soc.* **2003**, *125*, 12400-12401.
- (27) Toledo, L. M.; Lauher, J. W.; Fowler, F. W.: Design of Molecular-Solids - Application of 2-Amino-4(1h)-Pyridones to the Preparation of Hydrogen-Bonded Alpha-Networks and Beta-Networks. *Chem. Mater.* **1994**, *6*, 1222-1226.
- (28) Toledo, L. M.; Musa, K. M.; Lauher, J. W.; Fowler, F. W.: Development of Strategies for the Preparation of Designed Solids - an Investigation of the 2-Amino-4(1h)-Pyrimidone Ring-System for the Molecular Self-Assembly of Hydrogen-Bonded Alpha-Networks and Beta-Networks. *Chem. Mater.* **1995**, *7*, 1639-1647.
- (29) Zhao, X. Q.; Chang, Y. L.; Fowler, F. W.; Lauher, J. W.: An Approach to the Design of Molecular-Solids - the Ureylenedicarboxylic Acids. *J. Am. Chem. Soc.* **1990**, *112*, 6627-6634.
- (30) Okuno, T.; Izuoka, A.; Ito, T.; Kubo, S.; Sugawara, T.; Sato, N.; Sugawara, Y.: Reactivity of Mesogenic Diacetylenes Coupled with Phase Transitions between Crystal and Liquid Crystal Phases. *Journal of the Chemical Society-Perkin Transactions 2* **1998**, 889-895.
- (31) Xiao, J.; Yang, M.; Lauher, J. W.; Fowler, F. W.: A Supramolecular Solution to a Long-Standing Problem: The 1,6-Polymerization of a Triacetylene. *Angewandte Chemie-International Edition* **2000**, *39*, 2132.
- (32) Hoang, T.; Lauher, J. W.; Fowler, F. W.: The Topochemical 1,16-Polymerization of a Triene. *J. Am. Chem. Soc.* **2002**, *124*, 10656-10657.
- (33) Ajayan, P. M.: Nanotubes from Carbon. *Chem. Rev.* **1999**, *99*, 1787-1799.
- (34) Baughman, R. H.; Zakhidov, A. A.; de Heer, W. A.: Carbon Nanotubes - the Route toward Applications. *Science* **2002**, *297*, 787-792.
- (35) Bong, D. T.; Clark, T. D.; Granja, J. R.; Ghadiri, M. R.: Self-Assembling Organic Nanotubes. *Angewandte Chemie-International Edition* **2001**, *40*, 988-1011.
- (36) Gattuso, G.; Menzer, S.; Nepogodiev, S. A.; Stoddart, J. F.; Williams, D. J.: Carbohydrate Nanotubes. *Angewandte Chemie-International Edition in English* **1997**, *36*, 1451-1454.
- (37) Pasini, D.; Ricci, M.: Macrocycles as Precursors for Organic Nanotubes. *Curr. Org. Synth.* **2007**, *4*, 59-80.

- (38) Hecht, S.; Khan, A.: Intramolecular Cross-Linking of Helical Folds: An Approach to Organic Nanotubes. *Angewandte Chemie-International Edition* **2003**, *42*, 6021-6024.
- (39) Yashima, E.; Maeda, K.; Furusho, Y.: Single- and Double-Stranded Helical Polymers: Synthesis, Structures, and Functions. *Acc. Chem. Res.* **2008**, *41*, 1166-1180.
- (40) Hill, J. P.; Jin, W. S.; Kosaka, A.; Fukushima, T.; Ichihara, H.; Shimomura, T.; Ito, K.; Hashizume, T.; Ishii, N.; Aida, T.: Self-Assembled Hexa-Peri-Hexabenzocoronene Graphitic Nanotube. *Science* **2004**, *304*, 1481-1483.
- (41) Moore, J. S.: Shape-Persistent Molecular Architectures of Nanoscale Dimension. *Acc. Chem. Res.* **1997**, *30*, 402-413.
- (42) Harada, A.; Hashizume, A.; Yamaguchi, H.; Takashima, Y.: Polymeric Rotaxanes. *Chem. Rev.* **2009**, *109*, 5974-6023.
- (43) Hartgerink, J. D.; Clark, T. D.; Ghadiri, M. R.: Peptide Nanotubes and Beyond. *Chemistry-a European Journal* **1998**, *4*, 1367-1372.
- (44) Xu, Y.; Smith, M. D.; Geer, M. F.; Pellechia, P. J.; Brown, J. C.; Wibowo, A. C.; Shimizu, L. S.: Thermal Reaction of a Columnar Assembled Diacetylene Macrocycle. *J. Am. Chem. Soc.* **2010**, *132*, 5334.
- (45) Lauher, J. W.; Fowler, F. W.; Goroff, N. S.: Single-Crystal-to-Single-Crystal Topochemical Polymerizations by Design. *Acc. Chem. Res.* **2008**, *41*, 1215-1229.
- (46) Baughman, R. H.: Solid-State Synthesis of Large Polymer Single-Crystals. *Journal of Polymer Science Part B-Polymer Physics* **1974**, *12*, 1511-1535.
- (47) Li, Z.; Fowler, F. W.; Lauher, J. W.: Weak Interactions Dominating the Supramolecular Self-Assembly in a Salt: A Designed Single-Crystal-to-Single-Crystal Topochemical Polymerization of a Terminal Aryldiacetylene. *J. Am. Chem. Soc.* **2009**, *131*, 634-643.
- (48) Sun, A. W.; Lauher, J. W.; Goroff, N. S.: Preparation of Poly(Diododiacetylene), an Ordered Conjugated Polymer of Carbon and Iodine. *Science* **2006**, *312*, 1030-1034.
- (49) Baldwin, K. P.; Matzger, A. J.; Scheiman, D. A.; Tessier, C. A.; Vollhardt, K. P. C.; Youngs, W. J.: Synthesis, Crystal-Structure, and Polymerization of 1,2/5,6/9,10-Tribenzo-3,7,11,13-Tetrahydro 14 Annulene. *Synlett* **1995**, 1215.
- (50) Haley, M. M.; Brand, S. C.; Pak, J. J.: Carbon Networks Based on Dehydrobenzoannulenes: Synthesis of Graphdiyne Substructures. *Angewandte Chemie-International Edition in English* **1997**, *36*, 836-838.
- (51) Suzuki, M.; Comito, A.; Khan, S. I.; Rubin, Y.: Nanochannel Array within a Multilayered Network of a Planarized Dehydro 24 Annulene. *Org. Lett.* **2010**, *12*, 2346-2349.
- (52) Nagasawa, J. i.; Yoshida, M.; Tamaoki, N.: Synthesis, Gelation Properties and Photopolymerization of Macrocyclic Diacetylenedicarboxamides Derived from L-Glutamic Acid and Trans-1,4-Cyclohexanediol. *Eur. J. Org. Chem.* **2011**, 2247-2255.
- (53) Dalgarno, S. J.; Thallapally, P. K.; Barbour, L. J.; Atwood, J. L.: Engineering Void Space in Organic Van Der Waals Crystals: Calixarenes Lead the Way. *Chem. Soc. Rev.* **2007**, *36*, 236-245.

Chapter 3

Design and Synthesis of Self-assembled bis-Oxalamide Macrocycles Used as Porous Reactor for Polydiacetylene

3.1. Introduction	126
3.2. Research goal	126
3.3. Synthesis of first generation macrocycle M12	129
3.4. Synthesis of second generation macrocycle M13	133
3.5. Conclusion.....	137
3.6. References	138

3.1. Introduction

The potential applications of tubular structures as sensors, templates for directed reactions, and ion-ion or small molecule transport systems have attracted great attention.¹⁻
⁴ Many strategies have been adapted from nature to create porous materials. For example, one may design macrocycles that can self-assemble into hollow cylindrical frameworks.⁵⁻
⁷ Design and synthesis of networks with capability of selectively bind to specific guest molecules is one of the great challenges in the field of hollow material. In 2008, Shimizu reported the use of phenylether bis-urea macrocycle as a confined reaction chamber for a highly selective photodimerization of 2-cyclohexenone.⁸ Recently Inouye investigated the selective binding ability of acetylene-linked pyridine macrocycle to disaccharide, β -Maltoside.⁹ Well-designed and well-organized porous materials such as cyclodextrins, clays, nanocapsules, and nanocages have been proved that they can be used to control the stereo- or regiochemistry of a reaction.^{10,11}

3.2. Research goal

As stated in Chapter 2, previous work by our group has successfully developed methods to align diacetylenes in the solid-state through topochemically-controlled polymerization by using the host-guest strategy and crystal engineering.¹² Theoretically, in order to investigate the detailed and properties of PDAs, the non-polymer components (including the host molecules, unreacted monomers and short oligomers) have to be removed after the polymerization. So far, the most common method to get rid of the non-

polymer parts was extraction. This process relies on the efficient diffusion of solvent molecules into the crystal lattice, and impurities can be completely removed only if the solvent thoroughly diffuse into the host-guest PDA assemblies. Nevertheless, in most cases the resulting host-guest PDA assemblies form highly packed crystalline, thus makes them inaccessible to the solvent molecule. As a result, full removal of impurities was unachievable in most of the host-guest PDA system. In order to obtain the pure PDAs, we plan to design a new generation of host system which can: (1) properly control the particular arrangement of diacetylenes to provide the desired spacing in a crystal. (2) Maintain the ordered, unaggregated PDA crystalline to avoid interactions between PDA strands, therefore keep the PDA chains extended during extraction.

Base on this demand, one can image that if we can design a hallow tubular framework which has enough room to accommodate the diacetylene guest molecules as well as can self-assemble at the required distance of 4.9 Å to align these diacetylene guest molecules, 1,4-polymerization may has a good chance to occur in this well designed nanotube. Since individual PDA strands will be protected in the closed framework, the possibility of unwanted interaction will be greatly reduced.

In this Chapter, we discuss the preparation of the non-covalent bonded organic nanotubes with guest accessible cannels by utilizing the intermolecular oxalimide-oxalimide interactions (**Figure 2**). The ultimate goal of this work is to design artificial cavities that can direct diacetylene polymerization reactions with comparable levels of selectivity. The series of compounds were designed and synthesized to self-assemble at the desired distance of 4.9 Å, which is essential to align the diacetylene guest molecules

at a distance required for the topochemical polymerization. Subsequently, the desired polymer will be obtained by heating or UV irradiation.



Figure 2. Bisoxalimide macrocycle self-assembles into tubular structures that can be a confined environment for organic reactions.

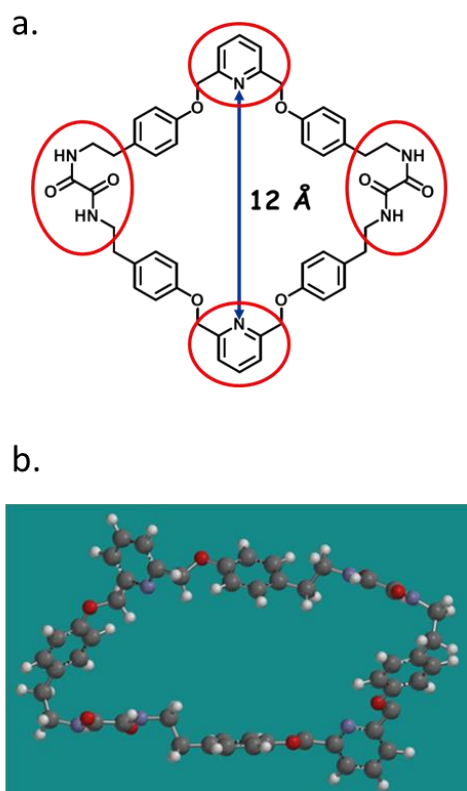
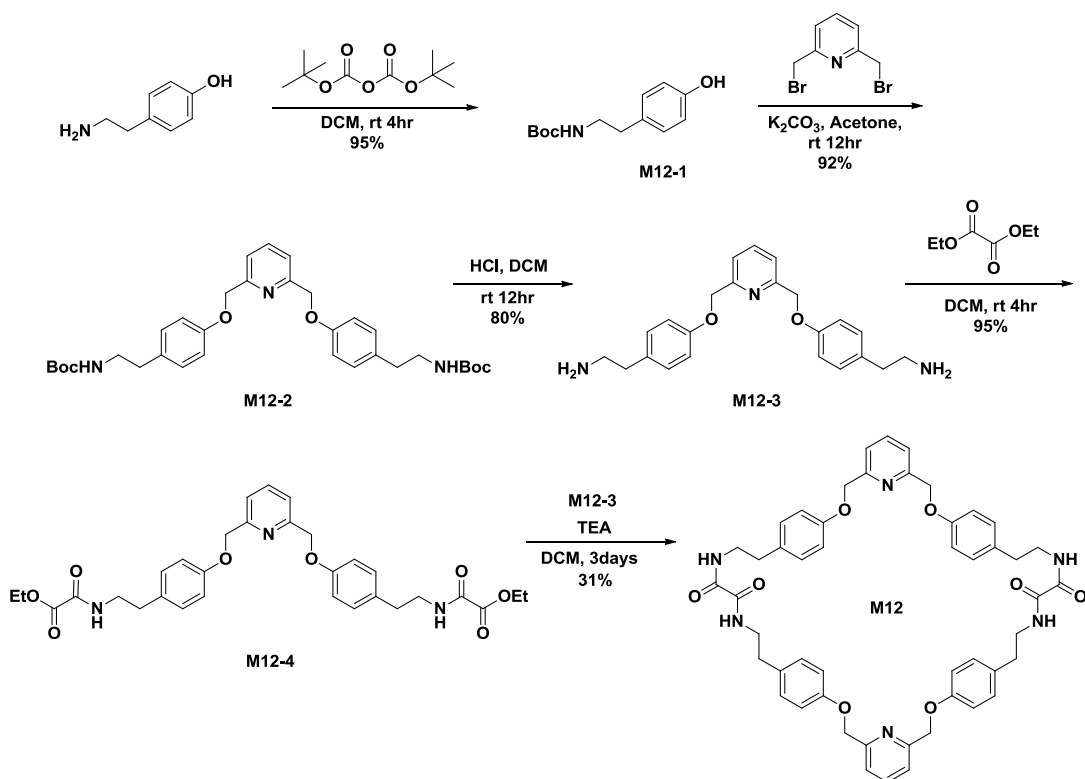


Figure 3-1. a. Molecular structure of M12. b. Molecular modeling of M12

3.3. Synthesis of first generation macrocycle M12

Figure 3-1a represents the molecular structure of our first generation macrocyclic host, **M12**. In order to make sure the inner space of our ring is big enough for diacetylene guest molecules, molecular modeling was performed to analyze the size of the ring (Figure 3-1b). The result showed that the calculated distance between two opposite pyridyl nitrogens is approximately 12Å, which is spacious enough for a simple diacetylene molecule. The oxalamide functional group was installed as the distance control element to preorganize the guest molecules; pyridyl moieties were incorporated as the recognition sites which can bind to the diacetylene guest molecules to implement the host-guest strategy.



Scheme 3-1. Synthetic route of macrocycle **M12**

Macrocycle **M12** was synthesized using the sequence shown in **Scheme 3-1**. Starting from tyramine, the amino group was first protected by a Boc group. Followed by Williamson etherification of Boc-protected tyramine **M12-1** and 2,6-bis(bromomethyl) - pyridine, compound **M12-2** was prepared in a good yield. After the Boc protecting group was removed under acidic conditions, the terminal diamine compound **M12-3** reacted with diethyl oxalate to give **M12-4** in a decent yield. With terminal diamine compound **M12-3** and **M12-4** in hand the following step was the construction of the target macrocycle. Several different reaction conditions (temperature, solvent and concentration) were tried to accomplish the final step. The best turned out to be carry out the reaction in a highly dilute dichloromethane solution with TEA as the base stirred at room temperature for 72 hours.

After **M12** was successfully prepared we continued to examine the particle, check if the oxalamide-oxalamide interaction can properly align the macrocycle to self-assemble into columnar structures with guest accessible channels. To study the assembly process carefully, we attempted to grow single crystals from various solvents by slow evaporation. Unfortunately, due to the poor solubility of **M12**, no crystals with sufficient size can be obtained for X-ray diffraction study. We attribute this poor solubility to the number of the rigid segments in the backbone. Based on our design, **M12** was constructed with six aromatic spacers and two oxalamide groups. According to our first-hand experiences as well as literature reports¹³, a decrease in flexibility of the backbone due to the introduction of the rigid aromatic group is responsible for the lower solubility of the molecule. Therefore, finding out how to modify the ring structure of the first generation of bis-oxalamide macrocycle is our next task in this project.

Ranganathan and others reported that the columnar assemblies could also be constructed by more flexible bis-ureas.¹⁴⁻¹⁸ In their case the *L*-cystine-based bis-urea macrocycle could self assemble into cylindrical structures from CHCl₃/MeOH. **Figure 3-2** represents the crystal structure of the flexible macrocyclic bis-urea. As we can see, the macrocycles pack into columnar structures with the disulfide-containing spacer stacked on one side and the alkyl group aligned on the opposite side. The authors claim that the intermolecular hydrogen-bonding between urea and urea functional group is strong enough to direct the assembly of the flexible and asymmetric macrocycle.

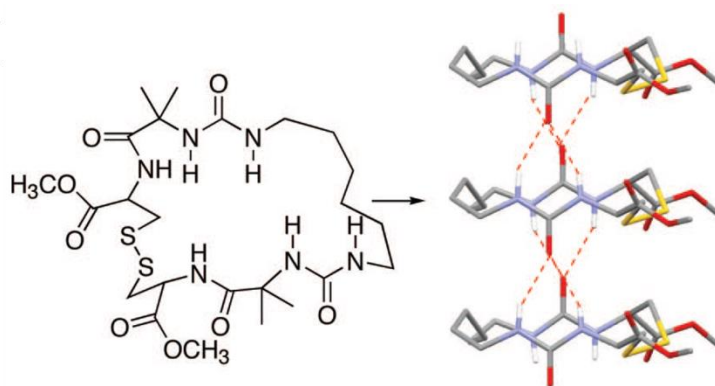


Figure 3-2. Molecular and crystal structure of the *L*-cystine-based bis-urea macrocycle.^{14, 19} (Reproduced with permission from reference 19. Copyright (2008) American Chemical Society)

More recently, Shimizu group published another successful example of the columnar self-assembly of an unsymmetrical bis-urea macrocycle.¹⁹ **Figure 3-3** shows the molecular and X-ray crystal structure of the unsymmetrical bis-urea macrocycle. The macrocycles stack into column from AcOH solution. The authors also found that by introducing the greater flexibility their macrocyclic system not only shows better solubility but also higher synthetic yield.

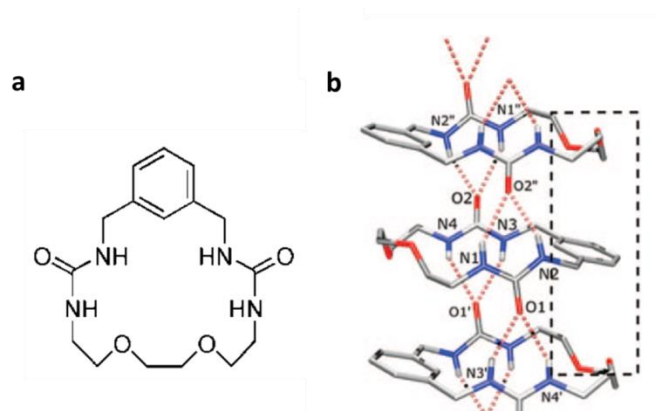


Figure 3-3. a. Molecular structure and b. X-ray crystal structure of the unsymmetrical bis-urea macrocycle¹⁹ (Reproduced with permission from reference 19. Copyright (2008) American Chemical Society)

Inspired by these successful examples, we considered installing a more flexible, functionalized unit in our own bis-oxalamide systems. A series of second-generation bis-oxalamide macrocycles, **M13** and **M14**, that are unsymmetrical and incorporate additional heteroatoms were designed in order to study their self-assembly (**Figure 3-4**). These heteroatoms might provide additional recognition sites, which can help to line the columnar channel. The introduction of a flexible moiety into the macrocycles should increase their solubility. The yields of the cyclization step should also be improved due to these new features.

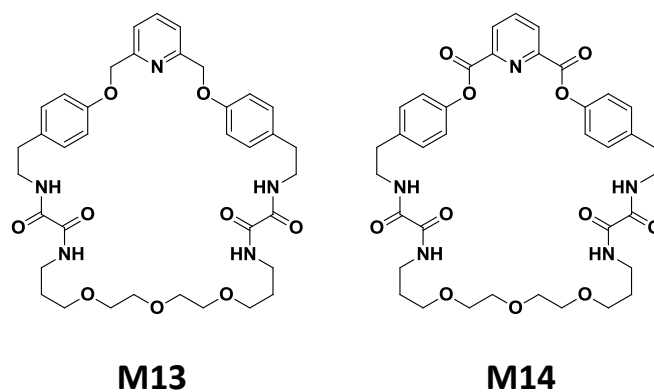
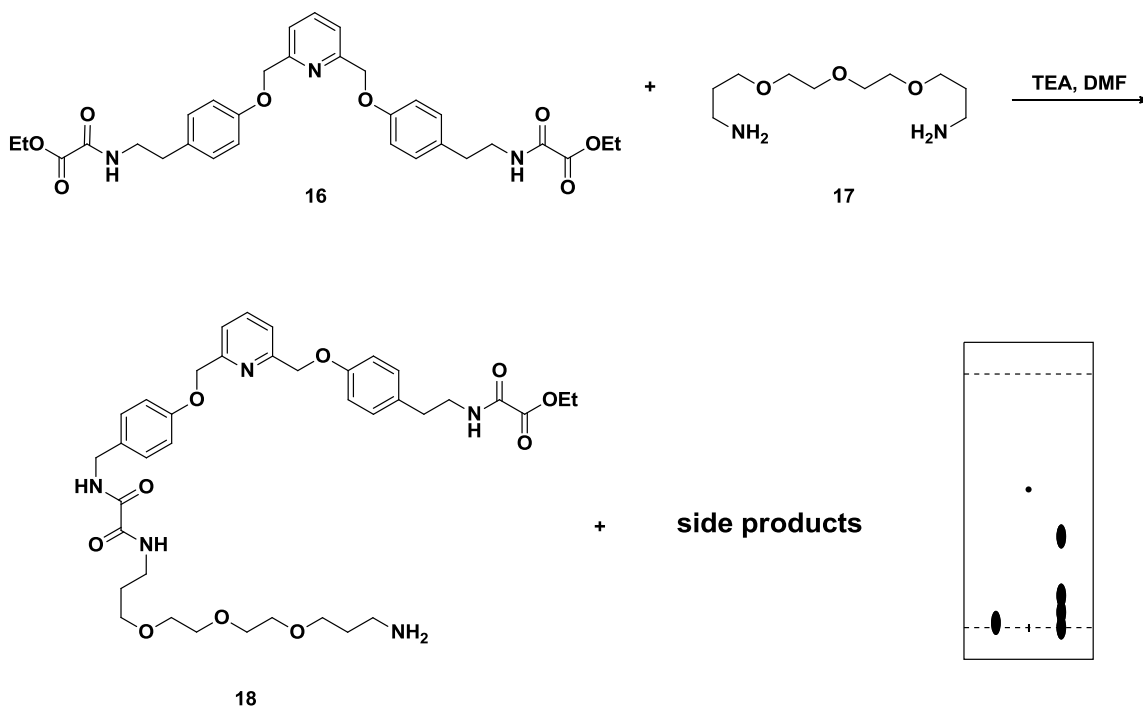


Figure 3-4. Molecular structures of M13 and M14

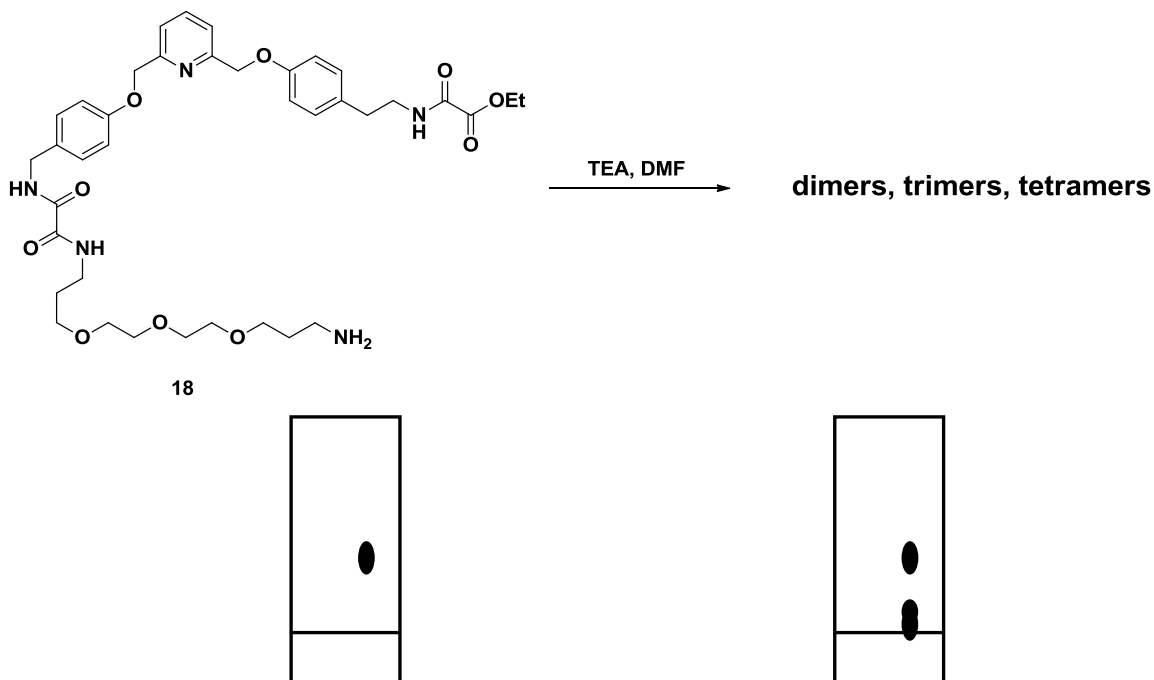
3.4. Synthesis of second generation macrocycle **M13**



Scheme 3-2. a. Original synthetic strategy of **M13**. b. TLC plate used to monitor the reaction.

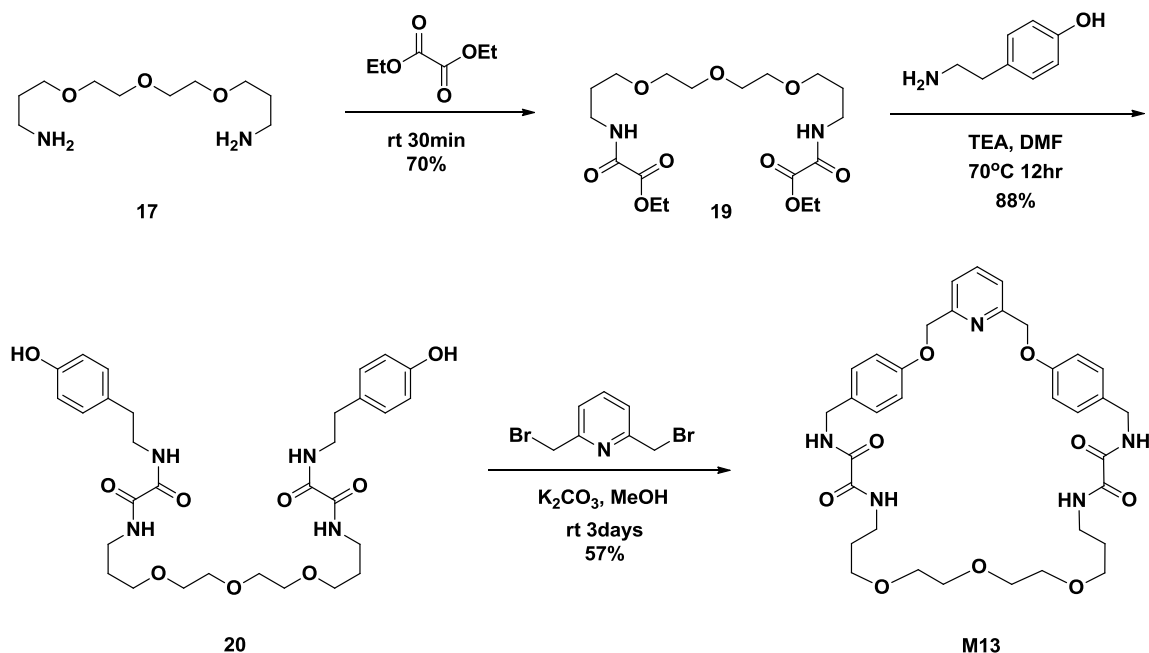
As **Scheme 3-2a** shows, the original synthetic strategy of **M13** started from reacting compound **16** with the commercially available diamine **17**. In the presence of triethylamine, **M13** should be prepared successfully in one step. Unfortunately, a complication occurred: **M13** was not the major product of the reaction. In fact, more than four spots were observed on the TLC plate (**Scheme 3-2b**). After separation by column chromatography, the major product which was also the highest spot on the TLC was collected. Analyzing by NMR, we found that instead of the target ring, **M13**, the major

product was a mono-substituted derivative **18**. We tried to repeat the reaction in an even more dilute solution to test the ring closure (**Scheme 3-3**).



Scheme 3-3. Repeat the reaction in an even more dilute solution to testify the ring closure of **M13**

However, the result turned out not to be promising. Since the mono-substituted compound has one free amino group, its polarity should be higher than our desired molecule **M13**. Based on the result of the TLC plate, there was no other visible spot above the mono-substituted compound. The spots below the mono-substituted product could be the dimers, trimers or tetramers. Therefore, we predicted that **M13** was not formed following our synthetic route.



Scheme 3-4. New synthetic strategy of **M13**

After closely analyzing our unsuccessful attempts, we proposed an alternative route to prepare the target molecule. **Scheme 3-4** represents a new pathway for the synthesis of **M13**. Commercially available diamine compound **17** reacted with diethyl oxalate under neat conditions at room temperature to give compound **19**. This reaction is very fast and only some excess diethyl oxalate had to be removed by flash column chromatography after the reaction is completed. Then the oxalamide moiety was installed by reacting the tyramine with **19**. With diphenol **20** prepared, we subsequently introduce the “core” into the framework to accomplish the synthesis. To avoid the formation of other side products such as dimers and trimers, several different concentrations were investigated. The best reaction conditions turned out to be reacting the diphenol **20** with 2,6-bis(bromomethyl)pyridine in 0.006 M methanol using potassium carbonate as base. The reaction mixture was stirred at room temperature for 72 hours to give macrocycle **M13** in

decent yield. Following the same procedure, macrocycles **M14**, have been synthesized successfully.

To study the assembly process of these new macrocycles, we tried to grow single crystals from various solvent systems. Unfortunately, the second generation bis-oxalamide macrocycles did not crystallize. Only white powder can be observed under microscope. We attribute the poor stack ability of these unsymmetrical macrocycles to the greater flexibility of the ethylene glycol spacer. Introduction of the flexible spacer might disrupt the self-assembly process. Transmission electron microscopy (TEM) was performed to investigate the self-assembly process more carefully. As shown in **Figure 3-5**, TEM images revealed no evidence of columnar structure formation.

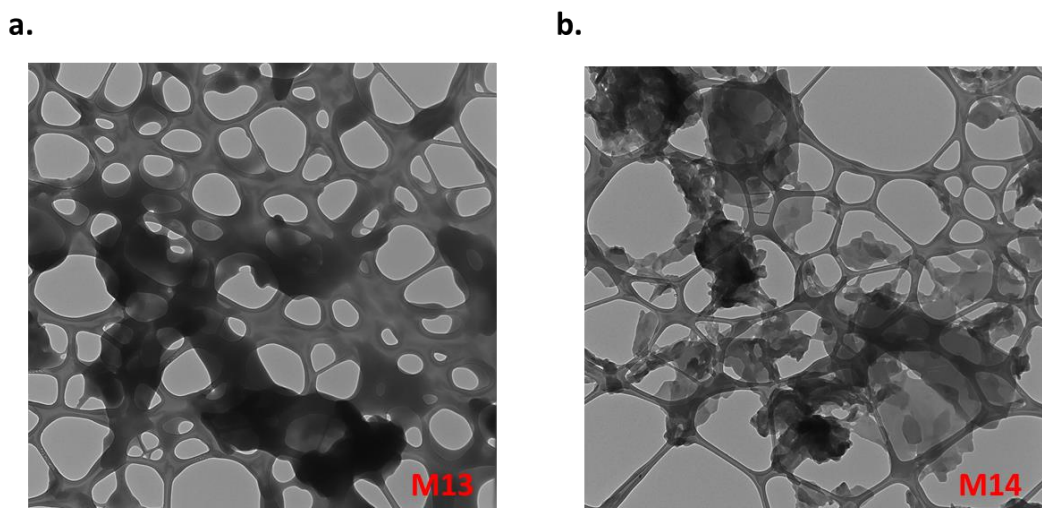


Figure 3-5. The transmission electron microscopy (TEM) image of **M13** and **M14**, prepared by drop-casting ethanol solution onto a copper grid, reveals no evidence of columnar structure formation.

3.5. Conclusion

The first generation macrocycle **M12** as well as second generation macrocycles **M13** and **M14** have been synthesized successfully. The solubility of macrocycle **M12** is very poor, which limited its accessibility to further studies and applications. Although incorporation of flexible spacer into the second generation macrocycles did improve their solubility and increase the synthetic yield, it also destroyed the self-assembly process. Crystallization of **M13** and **M14** only gave powder-like product. TEM images showed random patterns, indicating no columnar architecture formation. Since these macrocycles do not contain diacetylene moieties in their structure, they are very stable both in solution as well as in the solid state. No special treatment was required for these compounds. In the future, we will try to grow single crystals under different conditions.

Considering the disadvantages of previously obtained macrocycles, design a new macrocyclic system with better solubility is necessary in the future. In our first project, we demonstrated that the incorporation of glycolic segments could increase the solubility of the macrocycles. Based on this, we could add the glycolic side chain to the next generation of macrocycle. Moreover, one possible reason for the poor solubility of **M12** is that it contains too many rigid aromatic groups. Therefore, decreasing the number of the rigid spacer should be taken into consideration in the design of the new macrocycles.

3.6. References

- (1) Chui, J. K. W.; Fyles, T. M.: Ionic Conductance of Synthetic Channels: Analysis, Lessons, and Recommendations. *Chem. Soc. Rev.* **2012**, *41*, 148-175.
- (2) Matile, S.; Vargas Jentsch, A.; Montenegro, J.; Fin, A.: Recent Synthetic Transport Systems. *Chem. Soc. Rev.* **2011**, *40*, 2453-2474.
- (3) Carlson, L. J.; Krauss, T. D.: Photophysics of Individual Single-Walled Carbon Nanotubes. *Acc. Chem. Res.* **2008**, *41*, 235-243.
- (4) Xu, Y.; Smith, M. D.; Krause, J. A.; Shimizu, L. S.: Control of the Intramolecular [2+2] Photocycloaddition in a Bis-Stilbene Macrocyclic Host. *The Journal of Organic Chemistry* **2009**, *74*, 4874-4877.
- (5) Roy, K.; Wibowo, A. C.; Pellechia, P. J.; Ma, S.; Geer, M. F.; Shimizu, L. S.: Absorption of Hydrogen Bond Donors by Pyridyl Bis-Urea Crystals. *Chem. Mater.* **2012**, *24*, 4773-4781.
- (6) Lim, Y.-b.; Moon, K.-S.; Lee, M.: Stabilization of an α Helix by β -Sheet-Mediated Self-Assembly of a Macrocyclic Peptide. *Angew. Chem., Int. Ed.* **2009**, *48*, 1601-1605.
- (7) Roy, K.; Wang, C.; Smith, M. D.; Pellechia, P. J.; Shimizu, L. S.: Alkali Metal Ions as Probes of Structure and Recognition Properties of Macrocyclic Pyridyl Urea Hosts. *The Journal of Organic Chemistry* **2010**, *75*, 5453-5460.
- (8) Yang, J.; Dewal, M. B.; Profeta, S.; Smith, M. D.; Li, Y.; Shimizu, L. S.: Origins of Selectivity for the [2+2] Cycloaddition of α,β -Unsaturated Ketones within a Porous Self-Assembled Organic Framework. *J. Am. Chem. Soc.* **2007**, *130*, 612-621.
- (9) Abe, H.; Chida, Y.; Kurokawa, H.; Inouye, M.: Selective Binding of D_{2h}-Symmetrical, Acetylene-Linked Pyridine/Pyridone Macrocycles to Maltoside. *The Journal of Organic Chemistry* **2011**, *76*, 3366-3371.
- (10) Shimizu, L. S.; Hughes, A. D.; Smith, M. D.; Samuel, S. A.; Ciurtin-Smith, D.: Assembled Columnar Structures from Bis-Urea Macrocycles. *Supramol. Chem.* **2005**, *17*, 27-30.
- (11) Shimizu, L. S.; Hughes, A. D.; Smith, M. D.; Davis, M. J.; Zhang, B. P.; zur Loye, H.-C.; Shimizu, K. D.: Self-Assembled Nanotubes That Reversibly Bind Acetic Acid Guests. *J. Am. Chem. Soc.* **2003**, *125*, 14972-14973.
- (12) Ouyang, X.; Fowler, F. W.; Lauher, J. W.: Single-Crystal-to-Single-Crystal Topochemical Polymerizations of a Terminal Diacetylene: Two Remarkable Transformations Give the Same Conjugated Polymer. *J. Am. Chem. Soc.* **2003**, *125*, 12400-12401.
- (13) Kim, W. H.; Kodali, N. B.; Kumar, J.; Tripathy, S. K.: A Novel, Soluble Poly(Diacetylene) Containing an Aromatic Substituent. *Macromolecules* **1994**, *27*, 1819-1824.
- (14) Semetey, V.; Didierjean, C.; Briand, J.-P.; Aubry, A.; Guichard, G.: Self-Assembling Organic Nanotubes from Enantiopure Cyclo-N,N'-Linked Oligoureas: Design, Synthesis, and Crystal Structure. *Angew. Chem., Int. Ed.* **2002**, *41*, 1895-1898.
- (15) Ranganathan, D.; Lakshmi, C.; Karle, I. L.: Hydrogen-Bonded Self-Assembled Peptide Nanotubes from Cystine-Based Macrocyclic Bisureas. *J. Am. Chem. Soc.* **1999**, *121*, 6103-6107.
- (16) Hemmerlin, C.; Marraud, M.; Rognan, D.; Graff, R.; Semetey, V.; Briand, J.-P.; Guichard, G.: Helix-Forming Oligoureas: Temperature-Dependent Nmr, Structure Determination, and Circular Dichroism of a Nonamer with Functionalized Side Chains. *Helv. Chim. Acta* **2002**, *85*, 3692-3711.
- (17) Harris, K. D. M.: Fundamental and Applied Aspects of Urea and Thiourea Inclusion Compounds. *Supramol. Chem.* **2007**, *19*, 47-53.
- (18) Harris, K. D. M.: Meldola Lecture: Understanding the Properties of Urea and Thiourea Inclusion Compounds. *Chem. Soc. Rev.* **1997**, *26*, 279-289.

(19) Yang, J.; Dewal, M. B.; Sobransingh, D.; Smith, M. D.; Xu, Y.; Shimizu, L. S.: Examination of the Structural Features That Favor the Columnar Self-Assembly of Bis-Urea Macrocycles. *The Journal of Organic Chemistry* **2008**, *74*, 102-110.

Chapter 4

Experimental section

4.1. Experimental detail	141
4.2. Organic synthesis	143
4.3. References	176

4.1. Experimental detail

General Information: Thin layer chromatography was performed on Whatman AL SIL G/UV254, and visualization was accomplished with UV light. ^1H NMR spectra were recorded with a Varian Gemini-300 MHz, Inova-400 MHz, or Inova-500 MHz spectrometer in deuterated solvents using residual protons as an internal reference. (CDCl_3 at 7.26 ppm for ^1H and 77.00 ppm for ^{13}C). All chemical shifts are reported in parts per million (ppm). Coupling constants are reported in hertz (Hz) and are described as being either singlet (s), doublet (d), doublet of doublet (dd), triplet (t), quartet (q), quintet (qt) or multiplet (m). Proton decoupled ^{13}C NMR spectra were recorded on an Inova-400 (100 MHz) or Inova-500 (125 MHz) spectrometer and are reported in ppm using solvent as internal standard. Flash Column chromatography was performed using Merk silica gel 60, 230-400 mesh. Chemicals were purchased from Aldrich Chemical Company, Fisher Scientific Company or GFS Chemical Company. CuCl was purified by according to the literature procedure.¹

Melting Points: Melting points were measured on a Thomas Hoover Capillary melting point apparatus and are uncorrected.

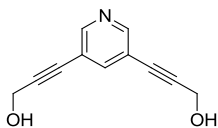
MS: Mass Spectrometry was carried out on an Agilent LC-MSD that consists of an 1100 HPLC and a G1956A mass spectrometer. The 1100 HPLC provides liquid solvent delivery to the electrospray ionization (ESI) source of the mass spectrometer. The mass analyzer is a single quadrupole providing MS capabilities with unit resolution over the m/z range 50-1500Da.

Raman: Raman spectroscopy was performed using a WiTec Alpha 500 dispersive Raman spectrometer coupled with an infinity corrected, confocal design microscope. The spectrometer uses a 532-nm class I laser, and the data were collected in the reflection mode of the microscope at a slit width of 25 μm . The data were collected and analyzed using the Omnic software suite (Nicolet, USA).

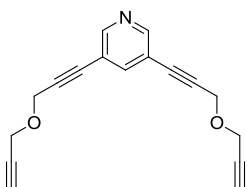
Differential scanning calorimetry: DSC data were collected on Perkin Elmer DSC-7 using a heating rate of 10 $^{\circ}\text{C}/\text{min}$ from 20 to 250 $^{\circ}\text{C}$ under nitrogen.

X-ray diffraction studies: Crystals were obtained as described below, selected and mounted on glass fibers using epoxy glue. The crystals were optically centered and data was collected on an Oxford Gemini A diffractometer and X-ray data were collected at 100 K using monochromated Cu radiation. The structures were solved and refined with standard SHELX procedures. The graphics of crystals were drawn in Chem-Ray program.

4.2. Organic synthesis

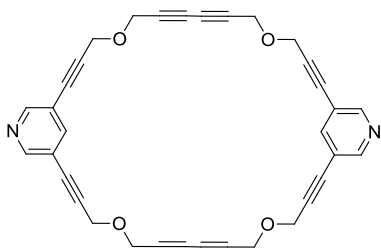


3,5-bis(3-hydroxy-1-propynyl) pyridine (M1-2)²: To a stirred solution of 1,3-diiodobenzene **M1-1** (3.28 g, 10 mmol) in 75 mL of triethylamine (TEA) was added (Ph₃P)₂PdCl₂ (0.75 g, 1.1 mmol), CuI (0.06 g, 0.32 mmol) and propargyl alcohol (4.0 mL, 68.4 mmol). This reaction mixture was stirred under room temperature. After 5 hours, TEA was removed in *vacuo*. The crude product was purified by column chromatography (eluent: EtOAc/hexane = 2:1) to give 1.63 g (88%) of diol **M1-2** as yellow oil. ¹H NMR (300MHz, DMSO-*d*₆): δ 4.32 (d, J = 6 Hz, 4H), 5.44 (t, J = 6 Hz, 2H), 7.87 (t, J = 2.1 Hz, 1H), 8.58 (d, J = 2.1 Hz, 2H). ¹³C NMR (400 MHz, DMSO-*d*₆): δ 50.2, 80.3, 94.7, 120.0, 140.8, 151.3



3,5-bis(3-(prop-2-yn-1-yloxy)prop-1-yn-1-yl)pyridine (M1-3)³: A solution of **M1-2** (0.94 g, 5 mmol) in 20 mL of freshly distilled THF was added slowly to a solution of sodium hydride (1.16 g, 48.3 mmol) in 30 mL of THF under nitrogen in ice bath. The mixture was stirred for an additional 20 min. Then, 18-crown-6 (2.8 g, 10.6 mmol) was added and stirred for another 20 min. 3.2 mL of propargyl bromide (30 mmol) was added dropwise, and the ice bath was removed. The reaction mixture was allowed to warm to room temperature and stirred for 3 hours before it was quenched by cold water. The THF was removed in *vacuo* and then the mixture was extracted with diethyl ether. The combined organic phases were dried with MgSO₄ and concentrated. The pure yellow oil was obtained by column chromatography (eluent: EtOAc/hexane = 1:4) (1.05 g, 80%). ¹H NMR (400MHz, CDCl₃): δ 2.49 (t, J = 2.1 Hz, 2H), 4.32 (d, J = 2.1 Hz, 4H), 4.50 (s, 4H), 7.77 (t, J = 1.8

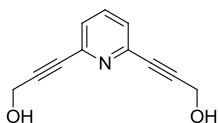
Hz, 1H), 8.59 (d, J = 1.8 Hz, 2H). ¹³C NMR (400 MHz, CDCl₃): δ 56.8, 57.1, 75.3, 78.6, 82.5, 88.4, 119.1, 140.1, 151.2.



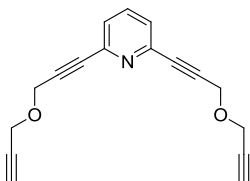
5,12,24,31-tetraoxa-18,37-diazatricyclo[33.3.1.116,20]tetraconta-1(39),16,18,20(40),35,37-hexaene-2,7,9,14,21,26,28,33-octayne (M1)³: To a stirred solution

of diether **M1-3** (0.26 g, 0.99 mmol) in 250 mL of dry methylene chloride (DCM) was added CuCl (0.733g, 7.3 mmol) and 1.6 mL (18.2 mmol) of tetramethylethylenediamine (TMEDA). O₂ was bubbled into this solution. The reaction was monitored by TLC. After 4 hours DCM was removed in *vacuo*. The crude product was purified by column chromatography (eluent: DCM/hexane = 5:1) to yield 0.18 g (36%) of the desired macrocycle **M1** as white solid. Single crystals were grown by dissolving **M1** in DCM followed by the addition of an equal amount of hexanes slowly along the wall of the sample vial. The vial was covered by an aluminum foil, the cover punctured with 5-10 needle holes, and the solution was allowed to evaporate at room temperature yielding crystals of **M1**. ¹H NMR (400MHz, CDCl₃): δ 4.41 (s, 8H), 4.50 (s, 8H), 7.84 (t, 2H, J = 1.8 Hz), 8.60 (d, 4H, J = 1.8 Hz). ¹³C-NMR (300 MHz, CDCl₃): δ 57.4, 57.6, 71.4, 75.0, 83.3, 88.4, 141.8, 151.6.

Monomer M1: ¹H NMR (400MHz, CDCl₃): δ 4.42 (s, 8H), 8.43 (s, 1H), 8.50 (s, 2H). ¹³C NMR (300 MHz, CDCl₃): δ 59.8, 61.0, 70.6, 77.3, 84.4, 90.5, 119.7, 141.4, 148.1.

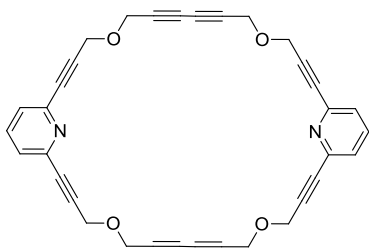


2,6-bis(3-hydroxy-1-propynyl) pyridine (M2-2)⁴: To a stirred solution of 2,6-dibromopyridine **M2-1** (2.34 g, 10 mmol) in 75 mL of triethylamine (TEA) was added (Ph₃P)₂PdCl₂ (0.75 g, 1.1 mmol), CuI (0.06 g, 0.32 mmol) and propargyl alcohol (4.0 mL, 68.4 mmol). This reaction mixture was stirred under room temperature. After 5 hours, TEA was removed in vacuo. The crude product was purified by column chromatography (eluent: EtOAc/hexane = 2:1) to give 1.43 g (76%) of diol as yellow oil. ¹H NMR (300MHz, DMSO-*d*₆): δ 4.37 (d, J = 6 Hz, 4H), 5.50 (t, J = 6 Hz, 2H), 7.51 (d, J = 7.8 Hz, 2H), 7.85 (t, J = 7.8 Hz, 1H). ¹³C NMR (400MHz, DMSO-*d*₆): δ 49.2, 82.8, 89.7, 126.1, 137.4, 142.4.



2,6-bis(3-(prop-2-yn-1-yloxy)prop-1-yn-1-yl)pyridine (M2-3)⁴: A solution of **M2-2** (0.94 g, 5 mmol) in 20 mL of freshly distilled THF was added slowly to a solution of sodium hydride (1.16 g, 48.3 mmol) in 30 mL of THF under nitrogen in ice bath. The mixture was stirred for an additional 20 min. Then, 18-crown-6 (2.8 g, 10.6 mmol) was added and stirred for another 20 min. 3.2 mL of propargyl bromide (30 mmol) was added dropwise, and the ice bath was removed. The reaction mixture was allowed to warm to room temperature and stirred for 3 hours before it was quenched by cold water. The THF was removed in *vacuo* and then the mixture was extracted with diethyl ether. The combined organic phases were dried with MgSO₄ and concentrated. The pure yellow oil was obtained by column chromatography (eluent: EtOAc/hexane = 1:4) (0.95 g, 72%). ¹H NMR (300MHz, CDCl₃): δ 2.47 (t, J = 2.4 Hz, 2H), 4.31 (d, J = 2.4 Hz, 4H), 4.49 (s, 4H), 7.37 (d, J = 8.1

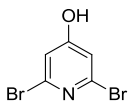
Hz, 2H), 7.62 (t, $J = 7.5$ Hz, 1H). ^{13}C NMR (400MHz, CDCl_3): δ 56.6, 56.8, 75.3, 78.7, 84.7, 85.3, 126.5, 136.5, 142.7.



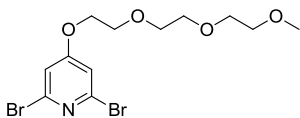
M2⁴: To a stirred solution of diether **M2-3** (0.26 g, 0.99 mmol) in 250 mL of anhydrous methylene chloride (DCM) was added CuCl (0.733g, 7.3 mmol) and 1.6 mL (18.2 mmol) of tetramethylethylenediamine (TMEDA). O₂ was bubbled into this solution. The reaction was monitored by TLC. After 4 hours DCM was removed in *vacuo*. The crude product was purified by column chromatography (eluent; DCM/hexane = 5:1) to yield 0.042 g (16%) of the desired macrocycle **M2** as white solid. ^1H NMR (300MHz, CDCl_3): δ 4.43 (s, 8H), 4.48 (s, 8H), 7.55 (d, $J = 7.8$ Hz, 2H), 7.85 (t, $J = 7.5$ Hz, 1H).

Monomer M2: Single crystals were grown by dissolving monomer **M2** in DCM followed by the addition of an equal amount of hexanes slowly along the wall of the sample vial. The vial was covered by an aluminum foil, the cover punctured with 5-10 needle holes, and the solution was allowed to evaporate at room temperature yielding crystals of monoclinic polymorph of monomer **M2**. ^1H NMR (400MHz, CDCl_3): δ 4.41 (s, 8H), 7.23 (d, $J = 7.5$ Hz, 2H), 7.58 (t, $J = 7.8$ Hz, 1H) ^{13}C NMR (300 MHz, CDCl_3): δ 56.6, 56.8, 75.3, 78.7, 84.7, 85.3, 126.5, 136.5, 142.7.

Trimer M2: ^1H NMR (400MHz, CDCl_3): δ 4.40 (s, 12H), 4.50 (s, 12H), 7.40 (d, $J = 7.8$ Hz, 6H), 7.65 (t, $J = 7.5$ Hz, 3H)

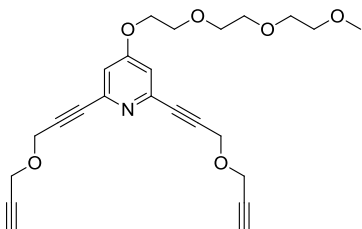


2,6-dibromopyridin-4-ol (M3-1)⁵: 2,6-dibromopyridin-4-ol was prepared by Ir-catalyzed direct boration^x of 2,6-dibromopyridine (**M2-1**) and subsequent oxidation. A mixture of **M2-1** (12.17 g, 52.0 mmol), pinacolborane (33.03 g, 250.0 mmol), [$\text{IrCl}(\text{cod})\text{]}_2$ (cod=1,5-cyclooctadiene; 0.68 g, 1.0 mmol), and 1,2-bis(diphenylphosphino) ethane (0.85 g, 2.1 mmol) was stirred under N_2 for 4 hours at 130 °C. The resulting mixture was allowed to cool to room temperature and evaporated *in vacuo*. The concentrated residue was diluted with THF (190 mL). Oxone (34.6 g, 57.0 mmol in 170 mL) was added slowly to the THF solution over 5 min. After stirring for 7 min at room temperature, the mixture was quenched with aqueous NaHSO_3 and extracted with diethyl ether. The separated ethereal layer was washed with water and brine, dried with MgSO_4 , evaporated, and purified by column chromatography (eluent: EtOAc/hexane = 1:5) to afford **M3-1** (10 g, 77%) as a white solid. ^1H NMR (400 MHz, CDCl_3): δ 7.03 (s, 2 H), 11.78 (br s, 1 H); ^{13}C NMR (400 MHz, CDCl_3): δ 115.06, 140.43, 167.19.



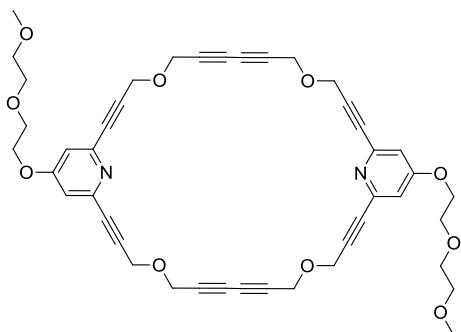
2,6-dibromo-4-(2-(2-(2-methoxyethoxy)ethoxy)ethoxy)pyridine (M3-2)⁵: To a suspension of **M3-1** (0.88 g, 3.4 mmol) and potassium carbonate (2.46 g, 17.8 mmol) in acetone (15 mL) was added triethylene glycol monomethyl ether monotosylate (1.10 g, 3.5 mmol), and then the mixture was refluxed for 12 hours. The mixture was filtered and evaporated, and the resulting residue was purified by column chromatography (eluent: EtOAc/hexane = 2:3) to afford **M3-2** (1.42 g, 83%) as a colorless oil. ^1H NMR (400 MHz, CDCl_3): δ 3.33 (s, 3H), 3.48 (m, 2H), 3.65-3.53 (m, 6H), 3.80 (m, 2H), 4.13 (t, J = 5.9 Hz, 2H), 6.97 (s, 2H). ^{13}C NMR

(400 MHz, CDCl₃): δ 58.06, 67.52, 68.09, 69.61, 69.64, 69.97, 70.91, 112.97, 140.02, 165.95.



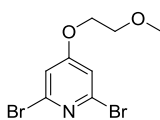
4-(2-(2-(2-methoxyethoxy)ethoxy)ethoxy)-2,6-bis(3-(prop-2-yn-1-yloxy)prop-1-yn-1-yl)pyridine (M3-3): A mixture of dibromide **M3-2** (3.37 g, 8.5 mmol), i-Pr₂NH (20 mL), and THF (20 mL) was bubbled with nitrogen for

30 min, and then PdCl₂(PPh₃)₂ (240 mg, 0.32 mmol), propargyl ether (2.1 mL, 20 mmol), and CuI (13.2 mg, 0.066 mmol) were added to the mixture subsequently. The reaction mixture was stirred for 12 hours at room temperature. The insoluble materials were filtered off. The filtrate was concentrated with a rotary evaporator and the resulting residue was subjected to column chromatography (eluent: EtOAc/hexane = 2:3) to afford **M3-3** (2.4 g, 67%) as a yellow oil. ¹H NMR (400 MHz, CDCl₃): δ 2.45 (t, J = 2.4 Hz, 2H), 3.34 (s, 3H), 3.49-3.70 (m, 8H), 3.81-3.84 (m, 2H), 4.12-4.15 (m, 2H), 4.28 (d, J = 2.7 Hz, 4H), 4.45 (s, 4H), 6.92 (s, 2H). ¹³C NMR (400 MHz, CDCl₃): δ 56.77, 56.93, 59.02, 67.84, 69.14, 70.59, 70.63, 70.94, 71.90, 75.26, 78.77, 84.31, 85.51, 113.58, 143.86, 165.10.

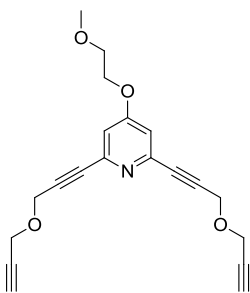


M3: To a stirred solution of diether **M3-3** (0.417 g, 0.98 mmol) in 100 ml of dry methylene chloride (DCM) was added CuCl (0.733 g, 7.3 mmol) and 1.6 mL (18.2 mmol) of TMEDA. O₂ was bubbled

into this solution. The reaction was monitored by TLC. After 4 hours DCM was removed in *vacuo*. The crude product was purified by column chromatography (eluent: EtOAc/hexane = 3:2) to yield 0.14 g (33%) of the desired macrocycle **M3**. ¹H NMR (400 MHz, CDCl₃): δ 3.71 (s, 6H), 3.52-3.71 (m, 16H), 3.83-3.86 (m, 4H), 4.14-4.17 (m, 4H), 4.41 (s, 8H), 4.49 (s, 8H), 6.94 (s, 4H). ¹³C NMR (400 MHz, CDCl₃): δ 56.96, 57.04, 59.06, 67.85, 69.17, 70.63, 70.66, 70.96, 71.15, 71.93, 74.59, 84.03, 85.87, 113.59, 143.85, 165.18. MS *m/z* [M + H]⁺ calculated for [C₄₄H₄₂N₂O₁₀ + H]⁺ 759.3, found: 759.3.

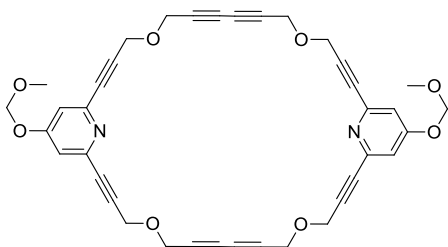


2,6-dibromo-4-(2-methoxyethoxy)pyridine (M4-2)⁵: 2-methoxyethyl-4-methylbenzenesulfonate **M18-1** (0.81 g, 3.5 mmol) was added to a suspension of 2,6-dibromopyridin-4-ol **M3-1** (0.88 g, 3.4 mmol) and potassium carbonate (2.46 g, 17.8 mmol) in acetone (15 mL), and then the mixture was refluxed for 12 hours. The mixture was filtered and evaporated, and the resulting residue was purified by silica-gel column chromatography (eluent: EtOAc/hexane 2:3) to afford **M4-2** (0.83 g, 79%) as a colorless oil. ¹H NMR (400 MHz, CDCl₃): δ 3.30 (s, 3H), 3.79 (t, J = 5.9 Hz, 2H), 4.31 (t, J = 5.9 Hz, 2H), 7.43 (s, 2H). ¹³C NMR (400 MHz, CDCl₃): δ 59.30, 69.01, 72.22, 114.17, 145.23, 164.95.

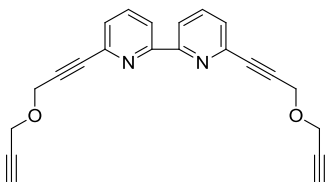


4-(2-(2-(2-methoxyethoxy)ethoxy)ethoxy)-2,6-bis(3-(prop-2-yn-1-yloxy)prop-1-yn-1-yl)pyridine (M4-3): A mixture of dibromide **M4-2** (2.54 g, 8.2 mmol), *i*-Pr₂NH (20 mL), and THF (20 mL) was bubbled with nitrogen for 30 min, and then PdCl₂(PPh₃)₂ (240 mg,

0.32 mmol), propargyl ether (2.1 mL, 20.0 mmol), and CuI (13.2 mg, 0.066 mmol) were added to the mixture subsequently. The reaction mixture was stirred for 12 hours at room temperature, and was diluted with ether (25 mL). The insoluble materials were filtered off. The filtrate was concentrated with a rotary evaporator and the resulting residue was subjected to column chromatography (eluent: EtOAc /hexane = 3:2) to afford **M4-3** (1.82 g, 66%) as a yellow oil. ^1H NMR (400 MHz, CDCl_3): δ 2.42 (t, $J = 2.4$ Hz, 2H), 3.35 (s, 3H), 3.65-3.68 (m, 2H), 4.07-4.09 (m, 2H), 4.24 (d, $J =$ Hz, 4H), 4.40 (d, $J = 3.4$ Hz, 4H), 6.89 (s, 2H). ^{13}C NMR (100 MHz, CDCl_3): δ 56.73, 56.89, 59.19, 67.69, 70.29, 75.30, 78.76, 84.32, 85.46, 113.52, 143.84, 165.03.

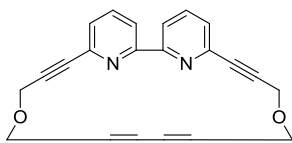


M4: To a stirred solution of diether **M4-3** (0.34 g, 1.0 mmol) in 250 ml of anhydrous methylene chloride was added CuCl (0.733 g, 7.3 mmol) and 1.6 mL (18.2 mmol) of TMEDA. O₂ was bubbled into this solution. The reaction was monitored by TLC. After 5 hours DCM was removed *in vacuo*. The crude product was purified by column chromatography (eluent: EtOAc /hexane = 3:1) to yield 0.07 g (20%) of the desired macrocycle **M4**. ^1H NMR (400 MHz, CDCl_3): δ 3.41 (s, 6H), 3.72 (t, $J = 4.4$ Hz, 4H), 4.13 (t, $J = 4.4$ Hz, 4H), 4.40 (s, 8H), 4.48 (s, 8H), 6.94 (s, 4H). ^{13}C NMR (400 MHz, CDCl_3): δ 165.12, 143.85, 113.54, 85.84, 84.06, 74.59, 71.14, 70.34, 67.72, 59.27, 57.05, 56.96. MS m/z $[\text{M} + \text{NH}_4]^+$ calculated for $[\text{C}_{38}\text{H}_{30}\text{N}_2\text{O}_8 + \text{NH}_4]^+$ 660.2, found: 660.2.



6,6'-bis(3-(prop-2-yn-1-yloxy)prop-1-yn-1-yl)-2,2'-bipyridine (M5-2): To a solution of 6,6'-dibromo-2,2'-bipyridine **M5-1** (3.14 g, 10 mmol), Ph₃P (0.42 g, 1.6 mmol),

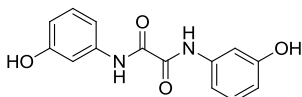
and CuI (0.08 g, 0.4 mmol) in 100 mL triethylamine and 50 mL THF was slowly added the mixture of PdCl₂(PPh₃)₂ (0.23 mg, 0.3 mmol) and propargyl ether (5.6 mL, 55.0 mmol). The reaction mixture was stirred for 2 hour at 80 °C under nitrogen. After cooling down to the room temperature, the insoluble materials were filtered off. The filtrate was concentrated with a rotary evaporator and the resulting residue was subjected to column chromatography (eluent: EtOAc/hexane = 4:1) to afford **M5-2** (2.4 g, 71%) as a yellow oil. ¹H NMR (400 MHz, CDCl₃): δ 2.48 (t, J = 2.4 Hz, 2H), 4.36 (d, J = 2.4 Hz, 4H), 4.55 (s, 4H), 7.48 (d, J = 7.6 Hz, 2H), 7.78 (t, J = 7.8 Hz, 2H), 8.42 (d, J = 8 Hz, 2H). ¹³C NMR (400 MHz, CDCl₃): δ 56.85, 57.20, 75.23, 78.85, 84.05, 86.25, 121.12, 127.61, 137.15, 141.94, 155.74.



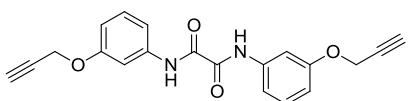
Monomer M5: To a stirred solution of diether **M5-2** (0.33 g, 0.98 mmol) in 125 mL of dry methylene chloride was added CuCl (0.733 g, 7.3 mmol) and 1.6 mL (18.2 mmol) of TMEDA.

O₂ was bubbled into this solution. The reaction was monitored by TLC. After 3 hours DCM was removed in *vacuo*. The crude product was purified by column chromatography (eluent: EtOAc /hexane = 2:3) to yield 0.22 g (64%) of the desired macrocyclic monomer **M5**. Single crystals were grown by dissolving 1 in DCM followed by the addition of an equal amount of hexanes slowly along the wall of the sample vial. The vial was covered by an aluminum foil, the cover punctured with 5-10 needle holes, and the solution was

allowed to evaporate at room temperature yielding crystals of monoclinic polymorph of 1. ^1H NMR (400 MHz, CDCl_3): δ 4.50 (s, 8H), 4.56 (s, 8H), 7.43 (dd, $J = 2.4$ and 6.6 Hz, 4H), 7.74-7.78 (m, 8H).

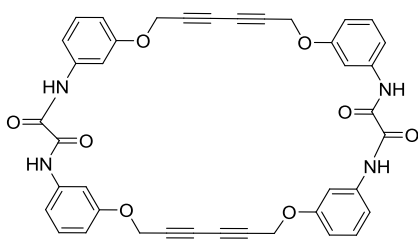


Bis-(3-hydroxyphenyl)oxamide (M6-2)⁶: A 100 mL flask containing a solution of oxalyl chloride, 0.8 g (6.3 mmol) in 10 THF, was equipped with dropping funnel. The flask was connected to a flask containing a saturated NaOH solution and cooled in an ice bath. With vigorous stirring, 3-aminophenol (1.4 g, 12.9 mmol) was added dropwise to the solution of oxalyl chloride through dropping funnel. After the addition, the mixture was stirred for an additional one hour until heat release ceased before it was quenched by cold water (25 mL). THF was removed in *vacuo*. The precipitated white solid was collected by filtration, wash with water, and dried overnight in air and in *vacuo*. Yield: 1.7 g (95%). The pure product is a white solid. m.p.: $>280^\circ\text{C}$. ^1H (400 MHz, CDCl_3): δ 6.57 (m, 2H), 7.14 (m, 2H), 7.24 (m, 2H), 7.40 (m, 2H), 9.49 (s, 2H), 10.61 (s, 2H). ^{13}C (400 MHz, CDCl_3): δ 107.25, 111.21, 111.70, 129.29, 138.53, 157.50, 158.49.



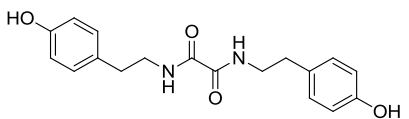
***N,N'*-bis(3-(prop-2-ynoxy)phenyl)oxamide (M6-3)**: Anhydrous acetone (50 mL), 2.8 g of K_2CO_3 (20 mmol), 1.4 g of **M6-2** (5 mmol) and 1.4 g of propargyl bromide (12 mmol) were successively introduced into a 100 three-necked round-bottomed flask. The reaction mixture was stirred and heated to reflux for 8 hours. The mixture was then quenched with water (20 mL). Acetone was removed in *vacuo*. The precipitated white solid was

collected by filtration, wash with water, and dried overnight in air and in *vacuo*. The pure product is a white solid. Yield: 1.65 g (92%). ^1H NMR (300 MHz, $\text{DMSO-}d_6$): δ 3.57 (t, 2H, $J = 2.4$ Hz), 4.77 (d, 4H, $J = 2.1$ Hz), 6.77 (d, 2H, $J = 8.1$ Hz), 7.28 (t, 2H, $J = 7.8$ Hz), 7.48 (d, 2H, $J = 8.1$ Hz), 7.60 (s, 2H). ^{13}C (400 MHz, CDCl_3): δ 55.94, 75.83, 78.24, 106.56, 112.29, 112.97, 130.12, 137.33, 157.41, 158.22.



M6: To a stirred solution of 0.35 g of **M6-3** (1.0 mmol) in 250 mL of anhydrous methylene chloride (DCM) was added 0.73 g of CuCl and 1.6 mL of *N,N'*-tetramethylethylene-diamine (TMEDA). O_2 was

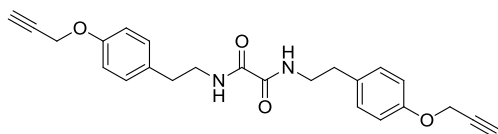
bubbled into this solution. The reaction was monitored by TLC. After 6 hours DCM was removed in *vacuo*. The crude product was added 50 mL of 10% $\text{HCl}_{(\text{aq})}$. The precipitates were collected by filtration, wash with water and ether, and dried overnight in air and in *vacuo*. The pure product is a white solid. Yield: 0.03 g (10%). ^1H NMR (300 MHz, $\text{DMSO-}d_6$): δ 4.93 (d, $J = 2.1$ Hz, 8H), 6.76 (d, $J = 7.8$ Hz, 4H), 7.28 (t, $J = 8.7$ Hz, 4H), 7.51 (d, $J = 7.8$ Hz, 4H), 7.57 (s, 4H), 10.84 (s, 2H). MS m/z $[\text{M} + \text{H}]^+$ calculated for $[\text{C}_{40}\text{H}_{28}\text{N}_4\text{O}_8 + \text{H}]^+$ 693.2, found: 693.2.



***N,N'*-Bis(4-hydroxyphenylethyl)oxalamide (M7-2)**⁷:

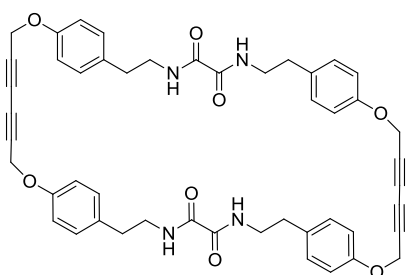
Tyramine **M7-1** (520 mg, 3.8 mmol) and diethyl oxalate (280 mg, 1.9 mmol) were dissolved in methanol (30 mL) at 30 °C and stirred for 1 hour. Evaporation of the methanol produced a colorless solid which was isolated by filtration.

Recrystallization from methanol afforded **3** as a colorless crystalline solid (0.44 g, 70%). m.p. 245-248 °C. ^1H (400 MHz, $\text{DMSO}-d_6$): δ 2.63 (t, $J = 7.2$ Hz, 2H), 3.26 (q, $J = 7.0$ Hz, 2H), 6.64 (d, $J = 7.5$ Hz, 2H), 6.95 (d, $J = 7.5$ Hz, 2H), 8.68 (t, 1H), 9.19 (s, 1H).



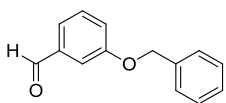
***N,N'*-bis(4-(prop-2-yn-1-yloxy)-phenethyl)-oxalamide (M7-3):** Propargyl bromide (0.87 g,

7.5 mmol) was added to a suspension of **M7-2** (1.2 g, 3.4 mmol) and potassium carbonate (2.4 g, 17.4 mmol) in acetone (25 mL), and then the mixture was refluxed for 8 hours. The mixture was filtered and evaporated, and the resulting residue was purified by silica-gel column chromatography (eluent: EtOAc/hexane = 2:3) to afford **M7-3** (1.11 g, 86%). ^1H NMR (400 MHz, CDCl_3): δ 2.51 (t, $J = 2.4$ Hz, 2H), 2.79 (t, $J = 7.2$ Hz, 4H), 3.52 (q, $J = 7$ Hz, 4H), 4.67 (d, $J = 2.3$ Hz, 4H), 6.92 (d, $J = 8.6$ Hz, 4H), 7.12 (d, $J = 8.5$ Hz, 4H), 7.50 (s, 2H). ^{13}C (400 MHz, CDCl_3): δ 34.58, 40.99, 55.86, 75.53, 78.61, 115.20, 129.67, 131.16, 156.42, 159.70.



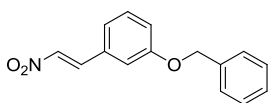
M7: To a stirred solution of diether **M7-2** (0.41 g, 0.99 mmol) in 150 mL of anhydrous methylene chloride (DCM) was added CuCl (0.733g, 7.3 mmol) and 1.6 mL (18.2 mmol) of tetramethylethylenediamine (TMEDA). O_2 was bubbled into this solution. The reaction was monitored by TLC. After 5 hours DCM was removed in *vacuo*. The crude product was purified by column chromatography (eluent: EtOAc/hexane = 3:1) to yield 0.11 g (25%) of the desired macrocycle **M7** as white solid. ^1H NMR (300 MHz, $\text{DMSO}-d_6$): δ 2.69 (t, $J = 7.2$ Hz, 8H),

3.26-3.33 (m, 8H), 4.90 (s, 8H), 6.84-6.88 (m, 8H), 7.07-7.12 (m, 8H), 8.68 (s, 4H). MS m/z $[M + NH_4]^+$ calculated for $[C_{48}H_{44}N_4O_8 + NH_4]^+$ 822.3, found: 822.3.



3-(benzyloxy)benzaldehyde (M8-2)⁸: 3-Hydroxybenzaldehyde **M8-1**

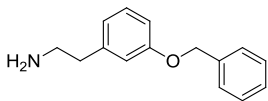
(5.00 g, 41.0 mol) was dissolved in absolute ethanol (100 mL) under N_2 atmosphere. Anhydrous potassium carbonate (8.61 g, 60.0 mmol) was added and the suspension was stirred for 5 min. Benzyl chloride (7.1 mL, 60.0 mmol) was then added and the solution was heated at reflux for 12 hours. The solution was concentrated on rotary evaporator, water was added and the mixture was extracted with EtOAc. The organic phase was washed twice with water, once with brine, dried over $MgSO_4$, filtered and concentrated. The crude product was purified by column chromatography (eluent: EtOAc/hexane = 1:4) to yield **M8-1** as a white solid (8.59 g, 98%). 1H NMR (400 MHz, $CDCl_3$): δ 5.13 (s, 2H), 7.35-7.50 (m, 9H), 10.00 (s, 1H). ^{13}C NMR (400 MHz, $CDCl_3$): δ 70.6, 113.6, 122.6, 124.1, 127.9, 128.6, 129.1, 130.5, 136.7, 138.2, 159.7, 192.5.



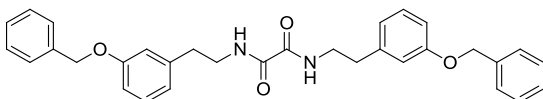
(E)-1-(benzyloxy)-3-(2-nitrovinyl)-benzene (M8-3): A mixture

of benzaldehyde **M8-2** (4.25g, 20.0 mmol), nitromethane (3.0 mL, 54.8 mmol) and $AcONH_4$ (3.4 g, 44.0 mmol) was refluxed for 1 hour. After cooling, the excess nitromethane was evaporated in *vacuo*, and reddish-brown solids were obtained. Recrystallization with EtOH gave **M8-3** as yellow needles, which were used in the following step without further purification. 1H NMR (400 MHz, $CDCl_3$): δ 5.10 (s, 2H), 7.10-7.16 (m, 3H), 7.33-7.45 (m, 6H), 7.55 (d, $J = 13.6$ Hz, 1H), 7.96 (d, $J = 13.6$ Hz,

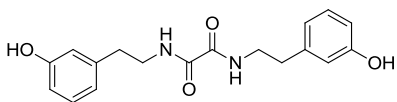
1H). ^{13}C NMR (400 MHz, CDCl_3): δ 70.25, 115.07, 118.79, 122.00, 127.47, 128.28, 128.75, 130.49, 131.39, 136.28, 137.38, 139.00, 159.30.



2-(3-(benzyloxy)phenyl)ethanamine (M8-4): The solution of **M8-3** was added dropwise to a well-stirred suspension of LiAlH_4 (3.0 g, 87.0 mmol) in anhydrous THF (200 mL) under N_2 . After refluxing for 4 hours, the mixture was cooled to 0 °C, and an aqueous solution of 30% KOH (100 mL) was added slowly. The aqueous phase was separated and extracted with diethyl ether (2×50 mL). The combined organic phase was dried over Na_2SO_4 and concentrated under reduced pressure to give 2-phenylethylamine **M8-4** (3.81g, 71%) as yellow oil. These amines were used for further reaction without purification.

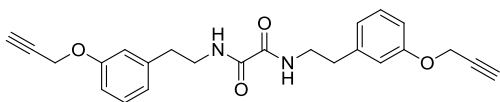


***N,N'*-bis(3-(benzyloxy)phenethyl)oxalamide (M8-5):** Compound **M8-4** (860 mg, 3.8 mmol), triethylamine (9.2 equiv, 92 mmol), and diethyl oxalate (280 mg, 1.9 mmol) were dissolved in anhydrous THF (30 mL) at 30 °C and stirred for 3 hours. Evaporation of the THF produced a colorless solid. Recrystallization from methanol afforded **M8-5** as a colorless solid in 85% yield. ^1H (400 MHz, CDCl_3): δ 2.89 (t, $J = 7.2$ Hz, 4H), 3.62 (q, $J = 6.6$ Hz, 4H), 6.85-6.93 (m, 6H), 7.27-7.32 (m, 2H), 7.39-7.51 (m, 10H). ^{13}C (400 MHz, CDCl_3): δ 35.46, 40.72, 69.99, 113.00, 115.35, 121.28, 127.53, 127.98, 128.59, 129.80, 136.96, 139.74, 159.15, 159.69.



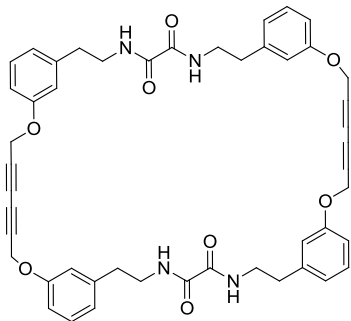
***N,N'*-bis(3-hydroxyphenethyl)oxalamide (M8-6):**

To a suspension of *N,N'*-bis(3-(benzyloxy)phenethyl)oxalamide **M8-5** (510 mg, 1.0 mmol) in 1,4-dioxane (5 mL) was added 10% Pd/C catalyst (610 mg). The reaction flask was evacuated and the atmosphere was replenished with hydrogen gas. This was repeated three times. The reaction was allowed to stirred at room temperature under an atmosphere of hydrogen for 1 day. The palladium catalyst was then removed by passing the reaction mixture through a bed of celite. The filtrate was evaporated to yield **M8-6** (43.6 mg, 53%) as a white solid. ¹H (400 MHz, CD₃OD): δ 2.76 (t, J = 7.2 Hz, 4H), 3.47 (t, J = 7.2 Hz, 4H), 6.63-6.71 (m, 6H), 7.10 (t, J = 7.8 Hz, 2H). ¹³C (400 MHz, CDCl₃): δ 34.83, 40.65, 113.01, 115.19, 119.54, 129.13, 140.15, 157.24, 160.18.



***N,N'*-bis(3-(prop-2-yn-1-yloxy)phenethyl)-oxalamide (M8-7):** Propargyl bromide (880 mg,

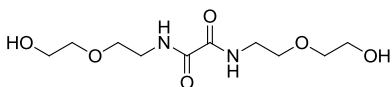
7.5 mmol) was added to a suspension of **M8-6** (1.2 g, 3.4 mmol) and potassium carbonate (2.4 g, 17.4 mmol) in ethanol (25 mL), and then the mixture was refluxed for 12 hours. The mixture was filtered and evaporated in *vacuo*, and the resulting residue was purified by column chromatography (eluent: EtOAc/hexane = 2:3) to afford **M8-7** as white solid (1.19 g, 86%). ¹H (400 MHz, CDCl₃): δ 2.52 (t, J = 2.4 Hz, 2H), 2.83 (t, J = 7.2 Hz, 4H), 3.56 (q, J = 7 Hz, 4H), 4.68 (d, J = 2.4 Hz, 4H), 6.81-6.87 (m, 6H), 7.22-7.26 (m, 2H), 7.49 (s, 2H). ¹³C (400 MHz, CDCl₃): δ 35.43, 40.71, 55.77, 75.64, 78.53, 113.09, 115.37, 121.91, 129.80, 139.81, 157.85, 159.69.



M8: To a stirred solution of diether **M8-7** (0.40 g, 0.99 mmol) in 150 mL of anhydrous methylene chloride (DCM) was added CuCl (0.733g, 7.3 mmol) and 1.6 mL (18.2 mmol) of tetramethylethylenediamine (TMEDA). O₂ was bubbled into this solution. The reaction was monitored by

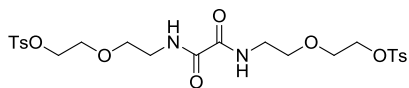
TLC. After 4 hours DCM was removed in *vacuo*. The crude product was purified by column chromatography (eluent: EtOAc/hexane = 3:1) to yield 0.11 g (28%) of the macrocycle **M8** as white solid. ¹H (300 MHz, DMSO-*d*₆): δ 2.73 (t, J = 6 Hz, 8H), 3.32 (s, 4H), 4.91 (s, 4H), 6.78-6.80 (m, 12H), 7.18 (t, J = 9 Hz, 4H), 8.73 (s, 4H). MS *m/z* [M + NH₄]⁺ calculated for [C₄₈H₄₄N₄O₈ + NH₄]⁺ 822.3, found: 822.3.

Monomer M8: ¹H (300 MHz, CDCl₃): δ 2.81 (t, J = 6.3 Hz, 4H), 3.60 (q, J = 6 Hz, 4H), 4.77 (s, 4H), 6.77-6.83 (m, 6H), 7.18-7.23 (m, 2H). MS *m/z* [M + NH₄]⁺ calculated for [C₂₄H₂₂N₂O₄ + NH₄]⁺ 411.2, found: 411.2.



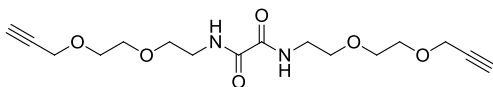
***N,N'*-bis(2-(2-hydroxyethoxy)ethyl)oxalamide (M9-2):**

2-(2-aminoethoxy)ethanol **M9-1** (420 mg, 3.8 mmol), triethylamine (9.2 equiv, 92 mmol), and diethyl oxalate (280 mg, 1.9 mmol) were dissolved in THF (30 mL) at 30 °C and stirred for 2 hours. Evaporation of the THF produced a colorless oil which was purified by column chromatography (eluent: EtOAc/hexane = 4:1) to yield 0.48g, (95%) of the desired compound **M9-2**. ¹H NMR (400 MHz, DMSO-*d*₆): δ 3.45-3.48 (m, 4H), 3.53-3.60 (m, 8H), 3.64-3.67 (m, 4H). ¹³C NMR (400 MHz, DMSO-*d*₆): δ 39.09, 60.81, 68.82, 72.07, 160.38.



**7,8-dioxo-3,12-dioxa-6,9-diazatetradecane-1,14-diyl
bis(4-methylbenzenesulfonate) (M9-3):** To a stirred

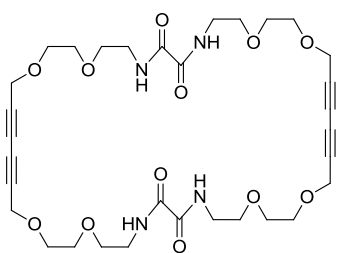
solution of *N,N'*-bis(2-(2-hydroxyethoxy)ethyl)oxalamide **M9-2** (2.64 g, 10 mmol) in 40 mL of dichloromethane was added 4-(Dimethylamino)-pyridine (DMAP) (1.22 g, 10 mmol), triethylamine (9.2 equiv, 92 mmol), and *p*-toluenesulfonyl chloride (4.75 g, 25 mmol). The mixture was stirred at room temperature. After 8 hours, the solution was washed three times with 0.1 N HCl. The organic layer was dried with MgSO₄ and concentrated in *vacuo*. The final products were obtained as white powder from column chromatography (eluent: EtOAc/hexane = 3:1). (5.10g, 89%). ¹H NMR (400 MHz, CDCl₃): δ 2.43 (s, 6H), 3.41-3.45 (m, 4H), 3.49-3.52 (m, 4H), 3.62-3.65 (m, 4H), 4.13-4.15 (m, 4H), 7.34 (d, J = 8.1 Hz, 4H), 7.61 (s, 2H), 7.79 (d, J = 8.3 Hz, 4H). ¹³C NMR (400 MHz, CDCl₃): δ 21.66, 39.53, 68.52, 69.00, 69.39, 128.00, 129.89, 132.91, 144.95, 159.69.



***N,N'*-bis(2-(2-(prop-2-yn-1-yloxy)ethoxy)
ethyl)oxalamide (M9-4):** A solution of

propargyl alcohol (1.29 g, 23 mmol) in 20 mL of freshly distilled THF was added slowly to a solution of sodium hydride (1.16 g, 48.3 mmol) in 25 mL of THF under nitrogen in ice bath. The mixture was stirred for an additional 30 min. Then, the solution of **M9-3** (5.7 g, 10 mmol) in 40 mL of THF was added dropwise, and the ice bath was removed. The reaction mixture was allowed to warm to room temperature and stirred for 6 hours before it was quenched by cold water. The THF was removed in *vacuo* and then the mixture was extracted with diethyl ether. The combined organic phases were dried with

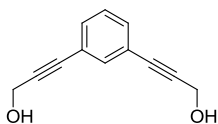
MgSO₄ and concentrated in *vacuo*. The pure white solid was obtained by column chromatography (eluent: EtOAc/hexane = 3:2). (2.2 g, 65%). ¹H NMR (400 MHz, CDCl₃): δ 2.43 (t, J = 1.6 Hz, 2H), 3.49-3.68 (m, 16H), 4.19 (d, J = 1.2 Hz, 4H), 7.76(s, 2H). ¹³C NMR (400 MHz, CDCl₃): δ 39.42, 58.39, 68.97, 69.29, 70.19, 74.63, 79.48, 159.73.



M9: To a stirred solution of diether **M9-4** (0.33 g, 0.98 mmol) in 100 ml of dry methylene chloride was added CuCl (0.733g, 7.3 mmol) and 1.6 mL (18.2 mmol) of TMEDA. O₂ was bubbled into this solution. The reaction was monitored by

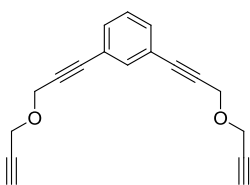
TLC. After 46 hours DCM was removed in *vacuo*. The crude product was purified by column chromatography (eluent: EtOAc/hexane 4:1) to yield 0.09 g (27%) of the desired macrocycle **M9**. ¹H NMR (400 MHz, CDCl₃): δ 3.51-3.70 (m, 32H), 4.28 (s, 8H), 7.78(s, 4H). ¹³C NMR (400 MHz, CDCl₃): δ 39.52, 59.03, 69.28, 70.23, 70.58, 75.39, 159.85. MS *m/z* [M + H]⁺ calculated for [C₃₂H₄₄N₄O₁₂ + H]⁺ 677.3, found: 677.3.

Monomer **M9**: ¹H NMR (400 MHz, CDCl₃): δ 3.51-3.72 (m, 16H), 4.27 (s, 4H), 7.76(s, 2H). MS *m/z* [M + H]⁺ calculated for [C₃₂H₄₄N₄O₁₂ + H]⁺ 338.7, found: 338.7.



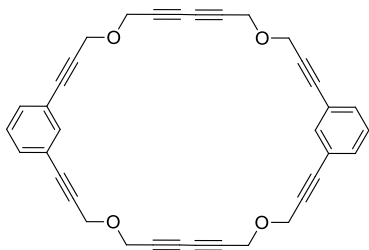
Bis-3,5-(3-hydroxy-prop-1-ynyl)benzene (M10-2)⁹ : To a stirred solution of 1,3-diiodobenzene **M10-1** (3.28 g, 10 mmol) in 75 mL of triethylamine (TEA) was added (Ph₃P)₂PdCl₂ (0.75 g, 1.1 mmol), CuI (0.06 g, 0.32 mmol)

and propargyl alcohol (4.0 mL, 68.4 mmol). This reaction mixture was stirred under room temperature. After 5 hours, TEA was removed in *vacuo*. The crude product was purified by column chromatography (eluent: EtOAc/hexane = 2:1) to give 1.63 g (88%) of diol as yellow oil. ¹H NMR (500 MHz, CDCl₃): δ 2.28 (s, 2H), 4.48 (s, 4H), 7.23 (t, J = 7.8 Hz, 1H), 7.36 (dd, J = 1.4 and 7.8 Hz, 2H), 7.48 (s, 1H); ¹³C NMR (500 MHz, CDCl₃): 51.44, 84.67, 87.88, 122.84, 128.37, 131.60, 134.64.

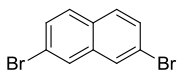


Bis-3,5-(3-prop-2-ynoxy-prop-1-ynyl)benzene (M10-3)⁹: A

solution of **M10-2** (0.94 g, 5 mmol) in 20 mL of freshly distilled THF was added slowly to a solution of sodium hydride (1.16 g, 48.3 mmol) in 30 mL of THF under nitrogen in ice bath. The mixture was stirred for an additional 20 min. Then, 18-crown-6 (2.8 g, 10.6 mmol) was added and stirred for another 20 min. 3.2 mL of propargyl bromide (30 mmol) was added dropwise, and the ice bath was removed. The reaction mixture was allowed to warm to room temperature and stirred for 3 hours before it was quenched by cold water. The THF was removed in *vacuo* and then the mixture was extracted with diethyl ether. The combined organic phases were dried with MgSO₄ and concentrated. The pure yellow oil was obtained by column chromatography (eluent: EtOAc/hexane = 1:4). (1.11 g, 85%). ¹H NMR (500 MHz, CDCl₃): δ 2.48 (t, J = 2.4 Hz, 2H), 4.32 (d, J = 2.3 Hz, 4H), 4.48 (s, 4H), 7.27 (t, J = 7.5 Hz, 1H), 7.40 (dd, J = 1.5 and 7.7 Hz, 2H), 7.54 (s, 1H); ¹³C NMR (500 MHz, CDCl₃): 56.56, 57.20, 75.07, 78.88, 84.81, 85.84, 122.75, 128.39, 131.77, 134.93.

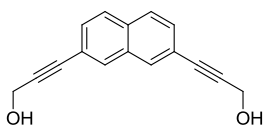


5,12,24,31-Tetraoxa-tricyclo[33.3.1.116,20]tetraconta-1(39),16,18,20(40),35,37-hexaene-2,7,9,14,21,26,28,33-octayne. (M10)⁹: To a stirred solution of diether **M10-3** (0.26 g, 0.99 mmol) in 250 mL of dry methylene chloride (DCM) was added CuCl (0.733g, 7.3 mmol) and 1.6 mL (18.2 mmol) of tetramethylethylenediamine (TMEDA). O₂ was bubbled into this solution. The reaction was monitored by TLC. After 4 hours DCM was removed in vacuo. The crude product was purified by column chromatography (5:1 DCM/hexanes) to yield 0.12 g (46%) of the desired macrocycle **M10** as white solid. Single crystals were grown by dissolving **M10** in DCM followed by the addition of an equal amount of hexanes slowly along the wall of the sample vial. The vial was covered by an aluminum foil, the cover punctured with 5-10 needle holes, and the solution was allowed to evaporate at room temperature yielding crystals of monoclinic polymorph of **M10**. In a separate experiment a similarly prepared solution in a similar vial was allowed to evaporate at 40 °C in a temperature controlled water bath yielding crystals of the triclinic polymorph of **M10**. ¹H NMR (500 MHz, CDCl₃): δ 4.41 (s, 8H), 4.49 (s, 8H), 7.27 (t, J = 8 Hz, 2H), 7.40 (dd, J = 1.4 and 7.7 Hz, 4H), 7.58 (s, 2H); ¹³C NMR (500 MHz, CDCl₃): 56.84, 57.29, 71.05, 74.77, 84.56, 86.30, 122.70, 128.44, 131.73, 135.46.

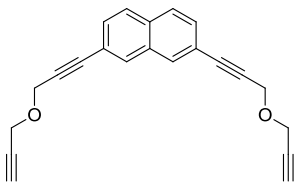


2,7-Dibromonaphthalene (M11-2)¹⁰: To a cooled suspension of triphenylphosphine (144 g, 0.55 mol) in 200 mL of dry acetonitrile was added bromine (88 g, 28.2 mL, 0.55 mol) dropwise below 5 °C. A heavy white precipitate was formed (an overhead stirrer was necessary at this point to ensure efficient

mixing). 2,7-dihydroxynaphthalene (40 g, 0.25 mol) in acetonitrile (200 mL) was added to this mixture. The precipitate became even thicker and stirring was maintained only with difficulty. The reaction mixture was heated to 70 °C for 45 min at which point the precipitate dissolved. The flask was fitted with an air-cooled distillation head and the acetonitrile was removed at atmospheric pressure. The temperature was then gradually raised to 250 °C. Evolution of HBr appeared to begin at about 190 °C and the HBr was trapped by means of a beaker filled with cold NaOH solution. The temperature was maintained at 250 °C for 55 min, and the dark oil was allowed to cool to approximately 100 °C. Then it was poured into a flask containing 500 mL of absolute ethanol. The flask was stoppered and allowed to sit overnight. A dark crystalline mass of crude 2,7-dibromonaphthalene was formed. The product was isolated by filtration and washed with small amounts of cold ethanol. Recrystallization from ethanol afforded **M11-2** as a white solid: yield 62%, mp 140-142 °C (lit.37 mp 140-141 °C).

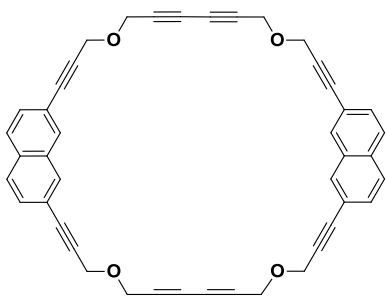


3,3'-(naphthalene-2,7-diyl)bis(prop-2-yn-1-ol) (M11-3): To a stirred solution of 2,7-dibromonaphthalene **M11-2** (2.86 g, 10 mmol) in 75 mL of triethylamine (TEA) was added $(\text{Ph}_3\text{P})_2\text{PdCl}_2$ (0.75 g, 1.1 mmol), CuI (0.06 g, 0.32 mmol) and propargyl alcohol (3.0 mL, 50.0 mmol). This reaction mixture was allowed stirred under room temperature. After 7 hours, TEA was removed in *vacuo*. The crude product was purified by column chromatography (eluent: EtOAc/hexane = 2:1) to give 1.86 g (79%) of diol as yellow oil. ^1H NMR (400 MHz, CD_3OD): δ 4.45 (s, 4H), 7.48 (d, $J = 8.5$ Hz, 2H), 7.80 (d, $J = 8.5$ Hz, 2H), 7.92 (s, 2H); ^{13}C NMR (500 MHz, CD_3OD): 49.85, 83.98, 88.37, 121.15, 127.59, 128.77, 130.62, 132.11, 132.58.



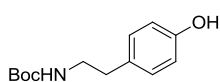
2,7-bis(3-(prop-2-yn-1-yloxy)prop-1-yn-1-yl)naphthalene

(M11-4): A solution of **M11-3** (1.19 g, 5 mmol) in 20 mL of freshly distilled THF was added slowly to a solution of sodium hydride (0.72 g, 30.0 mmol) in 30 mL of THF under nitrogen in ice bath. The mixture was stirred for an additional 20 min. Then, 18-crown-6 (2.8 g, 10.6 mmol) was added and stirred for another 20 min. 3.2 mL of propargyl bromide (20 mmol) was added dropwise, and the ice bath was removed. The reaction mixture was allowed to warm to room temperature and stirred for 3 hours before it was quenched by cold water. The THF was removed in *vacuo* and then the mixture was extracted with diethyl ether. The combined organic phases were dried with MgSO_4 and concentrated. The pure yellow oil was obtained by column chromatography (eluent: EtOAc/hexane = 2:3) (1.09 g, 70%). ^1H NMR (500 MHz, CDCl_3): δ 2.49 (t, $J = 2.4$ Hz, 2H), 4.36 (d, $J = 2.4$ Hz, 4H), 4.54 (s, 4H), 7.49 (dd, $J = 1.5$ and 8.5 Hz, 2H), 7.74 (s, 2H), 7.91 (s, 2H); ^{13}C NMR (500 MHz, CDCl_3): 56.68, 57.39, 75.11, 78.96, 85.00, 86.80, 120.60, 127.89, 129.34, 131.53, 132.35, 132.38.

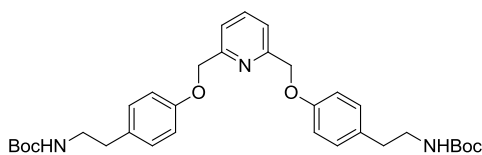


M11: To a stirred solution of diether **M11-4** (0.31 g, 0.99 mmol) in 200 mL of anhydrous methylene chloride (DCM) was added CuCl (0.733g, 7.3 mmol) and 1.6 mL (18.2 mmol) of tetramethylethylenediamine (TMEDA). O_2 was bubbled into this solution. The reaction was monitored by TLC. After 6 hours DCM was removed in *vacuo*. The crude product was purified by column chromatography (eluent: DCM/hexane = 3:1) to yield 0.09 g (31%) of

the desired macrocycle **M11** as white solid. $^1\text{H NMR}$ (300MHz, CDCl_3): δ 4.45 (s, 8H), 4.54 (s, 8H), 7.48 (d, $J = 8.7$ Hz, 4H), 7.74 (d, $J = 8.7$ Hz, 4H), 7.94 (s, 4H). MS m/z $[\text{M} + \text{H}]^+$ calculated for $[\text{C}_{44}\text{H}_{28}\text{O}_4 + \text{H}]^+$ 621.2, found: 621.2.



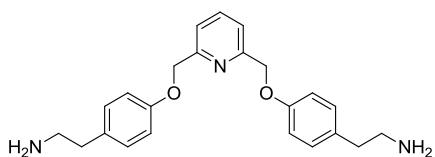
tert-butyl 4-hydroxyphenethylcarbamate (M12-1): To a solution of tyramine hydrochloride (1.08 g, 6.07 mmol) in a mixture of dioxane/water (9.0/3.0 mL, 0.5 M) was added triethylamine (0.85 mL, 6.07 mmol, 1.0 equiv). Di-tert-butyl carbonate (1.4008 g, 6.23 mmol, 1.0 equiv) was then added, and stirred at room temperature for 3 hours. The reaction mixture was concentrated in *vacuo*, and the residue was partitioned between CH_2Cl_2 and 5% hydrochloric acid. The aqueous phase was extracted with CH_2Cl_2 . The combined organic phases were dried over MgSO_4 and concentrated in *vacuo* to afford a pale yellow oil. The oil was purified by flash chromatography (eluent: EtOAc /DCM = 1:9) to yield the product as a clear oil (1.44 g, 98%). $^1\text{H NMR}$ (300 MHz, CDCl_3) δ 1.44 (s, 9H), 2.70 (t, $J = 6.9$ Hz, 2H), 3.38-3.28 (m, 2H), 6.29 (s, 1H), 4.63 (s, 1H), 6.78 (d, $J = 8.4$ Hz, 2H), 7.01 (d, $J = 8.4$ Hz, 2H).



di-tert-butyl((((pyridine-2,6-diylbis(methylene))bis(oxy))bis(4,1-phenylene))bis(ethane-2,1-diyl))dicarbamate (M12-2):

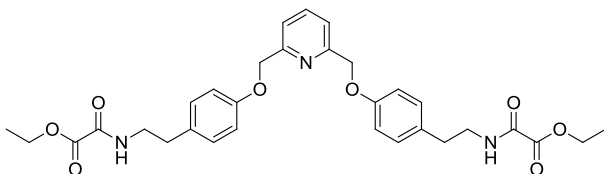
2,6-bis(bromomethyl) -pyridine (0.90 g, 3.4 mmol) was added to a suspension of tert-butyl-4-hydroxyphenethyl carbamate (1.93 g, 8.2 mmol) and potassium carbonate (2.4 g, 17.4 mmol) in acetone (25 mL), and then the mixture was stirred under room temperature. After 24 hours, the reaction mixture was filtered and evaporated, and the resulting residue

was extracted with EtOAc and H₂O. The combined organic layer was dried with MgSO₄ and evaporated in *vacuo*. The final products were obtained as white powder from silica column chromatography (eluent: EtOAc/hexane = 3:1). ¹H NMR (400 MHz, CDCl₃): δ 1.43 (s, 20H), 2.73 (t, J = 6.8 Hz, 4H), 3.33-3.34(m, 4H), 5.21 (s, 4H), 6.93 (q, J = 1.8 and 8.4Hz, 4H), 7.12 (d, J = 8.4 Hz, 4H), 7.48 (d, J = 8.1 Hz, 2H), 7.76 (t, J = 7.8 Hz, 1H).



2,2'-(((pyridine-2,6-diylbis(methylene))bis(oxy))bis(4,1-phenylene))diethanamine (M12-3): To a round flask was added **M12-2** (3.12 g, 5.4 mmol) and

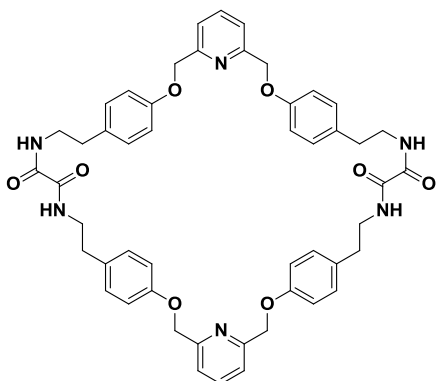
a mixture of dichloromethane/trifluoroacetic acid (1/2; 150 mL). The sample was stirred at room temperature for 8 hours. The solvent was removed under reduced pressure and the residue was partitioned between NaHCO₃ and dichloromethane (2 × 30 mL). The combined organic phases were dried with MgSO₄ and concentrated. The pure yellow solid was obtained in 75% yield (1.53 g). ¹H NMR (400 MHz, CDCl₃): δ 2.68 (t, J = 6.9 Hz, 4H), 2.94 (t, J = 6.6 Hz, 4H), 5.18 (s, 4H), 6.92 (dd, J = 2.4 and 8.7 Hz, 4H), 7.11 (d, J = 8.7 Hz, 4H), 7.45 (d, J = 7.5 Hz, 2H), 7.72 (t, J = 7.8 Hz, 1H).



diethyl-2,2'-((((pyridine-2,6-diylbis(methylene))bis(oxy))bis(4,1-phenylene))bis(ethane-2,1-diyl))bis(azanediy))bis(2-oxoacetate) (M12-4): To a cooled, magnetically stirred solution of

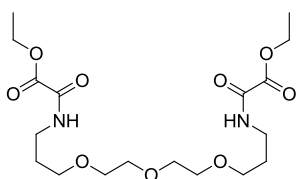
M12-3 (1.89 g, 5.0 mmol) and triethylamine (1.5 g, 15 mmol) in anhydrous THF (75 mL) under nitrogen was added ethyl 2-chloro-2-oxoacetate (1.64 g, 12.0 mmol) dropwise at

0 °C. The reaction mixture was allowed to warm to room temperature and was then stirred for 2 hours. The reaction mixture was cooled to 0 °C before quenching with water (25 mL). The mixture was extracted with CHCl₃ (3 × 25 mL). The combined organic extracts were dried over MgSO₄, filtered, and concentrated under reduced pressure. The residue was purified by column chromatography (eluent: EtOAc/hexane = 4:1) to afford **M12-4** (1.65 g, 57%). ¹H NMR (400 MHz, CDCl₃): δ 1.37 (t, J = 7.2 Hz, 6H), 2.81 (t, J = 6.9 Hz, 4H), 3.57 (q, J = 6.9 Hz, 4H), 4.33 (q, J = 6.9 Hz, 4H), 5.20 (s, 4H), 6.91-6.96 (m, 4H), 7.10-7.14 (m, 6H), 7.47 (d, J = 7.8 Hz, 2H), 7.76 (t, J = 7.5 Hz, 1H).



M12: A three-neck round-bottom flask was filled with 200 mL of DCM, and the mixture was stirred under N₂ atmosphere. Two separate addition funnels were charged with solutions of 2,2'-(((pyridine-2,6-diylbis(methylene))bis(oxy)) bis(4,1-phenylene)) diethanamine **M12-3** (377 mg, 1.0 mmol) in 25 mL of DCM and diethyl-2,2'-((((pyridine-2,6-diylbis (methylene))bis(oxy))bis(4,1-phenylene))bis(ethane-2,1-diyl))bis(azanediyl))bis(2-oxoacetate) **M12-4** (577 mg, 1.0 mmol) in 25 mL of DCM. These two solutions were added together dropwise over ~30 min and further stirred at room temperature for 72 hours. Evaporation of the DCM produced a colorless solid which was isolated by filtration. The residue was purified by column chromatography (eluent: EtOAc/hexane = 4:1) to afford **M12** (0.23 g, 27%) yield. ¹H NMR (400 MHz, CDCl₃): δ 2.81 (t, J = 6.9 Hz, 8H), 3.57 (q, J = 6.9 Hz, 8H), 5.22 (s,

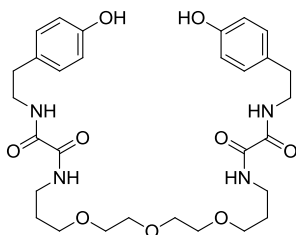
8H), 6.93-6.97 (m, 8H), 7.10-7.15 (m, 8H), 7.49 (d, J = 7.8 Hz, 4H), 7.78 (t, J = 7.5 Hz, 2H). MS m/z $[M + H]^+$ calculated for $[C_{50}H_{50}N_6O_8 + H]^+$ 863.4, found: 863.4.



diethyl 2,18-dioxo-7,10,13-trioxa-3,17-diazanonadecane-1,19

-dioate (19): 3,3'-((oxybis(ethane-2,1-diyl))bis(oxy))bis(propane-1-amine) **17** (840 mg, 3.8 mmol), triethylamine (6.5 equiv, 25

mmol), and diethyl oxalate (560 mg, 7.6 mmol) were stirred for 2 hours under room temperature. The reaction mixture was purified by column chromatography (eluent: DCM/CH₃CN = 3:2) to give **x** (1.51 g, 95%) as a colorless oil. ¹H NMR (400 MHz, CDCl₃): δ 1.34-1.39 (m, 6H), 1.79-1.87 (m, 4H), 3.46 (q, J = 7.6 Hz, 4H), 3.57-3.69 (m, 12H), 4.29-4.36 (m, 4H), 7.75 (s, 2H).

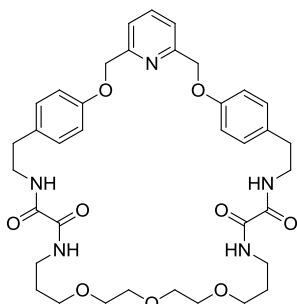


N,N'-(((oxybis(ethane-2,1-diyl))bis(oxy))bis(propane-3,1-

diyl))bis(N2-(4-hydroxyphenethyl)oxalamide) (20): To a solution of **19** (1.31 g, 3.1 mmol) and triethylamine (5.0 equiv, 15.5 mmol) in THF (75 mL) under nitrogen was added tyramine

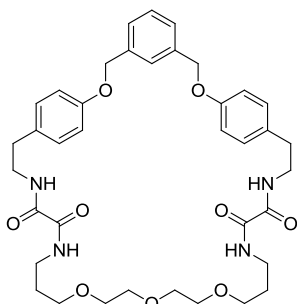
(850 mg, 6.2 mmol). The reaction mixture was allowed stirred at room temperature for 6 hours. Evaporation of the THF produced a colorless solid which was isolated by filtration. Recrystallization from methanol afforded **20** as a colorless solid in 86% yield. ¹H NMR (400 MHz, DMSO-*d*₆): δ 1.65-1.71 (m, 4H), 2.65 (t, J = 7.6 Hz, 4H), 3.18 (q, J = 6.6 Hz, 4H), 3.27-3.40 (m, 10H), 3.46-3.52 (m, 8H), 6.66 (d, J = 8.4 Hz, 4H), 6.98 (d, J = 8.4 Hz, 4H), 8.69 (s, 4 H), 9.17 (s, 2H). ¹³C NMR (400 MHz, DMSO-*d*₆): δ 29.39, 34.29, 37.01, 41.11, 68.72, 70.03, 70.21, 115.59, 129.55, 129.88, 156.13, 160.30, 160.40.

General Procedure for the Synthesis of Bis-oxalimides (M13-M17): Synthesis of Macrocycle **M13**: A three-neck round-bottom flask was filled with 200 mL of MeOH, and the mixture was stirred under N₂ atmosphere. Two separate addition funnels were charged with solutions of *N,N'*-(((oxybis(ethane-2,1-diyl))bis(oxy))bis(propane-3,1-diyl))bis(N₂-(4-hydroxyphenethyl)oxalamide) **20** (903 mg, 1.5 mmol) in 25 mL of MeOH and 2,6-bis(bromomethyl)pyridine (398 mg, 1.5 mmol) in 25 mL of MeOH. The diphenols and dibromo solutions were added together dropwise over ~30 min and further stirred at room temperature for 72 hours. Evaporation of the methanol produced a colorless solid which was isolated by filtration. Recrystallization from methanol afforded **M13** as a white solid in 67% yield.



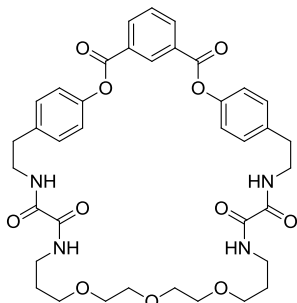
M13: ¹H NMR (300 MHz, DMSO-*d*₆): δ 1.65-1.69 (m, 4H), 2.71 (t, J = 6.3 Hz, 4H), 3.18 (q, J = 6.6 Hz, 4H), 3.27-3.40 (m, 10H), 3.44-3.49 (m, 8H), 5.18 (s, 4H), 6.82 (d, J = 8.7 Hz, 4H), 7.01 (d, J = 8.7 Hz, 4H), 7.37 (d, J = 7.5 Hz, 2H), 7.78 (t, J = 7.8 Hz, 1H). MS *m/z* [M + H]⁺ calculated for [C₃₇H₄₇N₅O₉ + H]⁺

706.3, found: 706.3.



M14: ¹H NMR (300 MHz, DMSO-*d*₆): δ 1.65-1.71 (m, 4H), 2.65 (t, J = 7.6 Hz, 4H), 3.18 (q, J = 6.6 Hz, 4H), 3.27-3.40 (m, 10H), 3.46-3.52 (m, 8H), 5.10 (s, 4H), 6.78 (d, J = 8.4 Hz, 4H), 7.00 (d, J = 8.4 Hz, 4H), 7.31-7.37 (m, 3H), 7.47 (s, 1H). MS

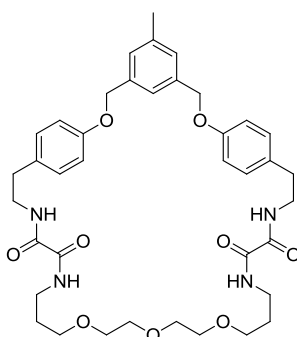
m/z $[M + H]^+$ calculated for $[C_{38}H_{48}N_4O_9 + H]^+$ 705.3, found: 703.3.



M15: 1H NMR (300 MHz, DMSO- d_6): δ 1.77-1.81 (m, 4H), 2.64 (t, $J = 8.1$ Hz, 4H), 3.18 (q, $J = 6.6$ Hz, 4H), 3.27-3.40 (m, 10H), 3.60-3.65 (m, 8H), 6.54 (d, $J = 8.7$ Hz, 4H), 6.84 (d, $J = 8.4$ Hz, 4H), 7.88 (t, $J = 7.5$ Hz, 1H), 8.05 (s, 2H), 8.07 (s, 1H).

MS m/z $[M + H]^+$ calculated for $[C_{38}H_{44}N_4O_{11} + H]^+$ 733.3,

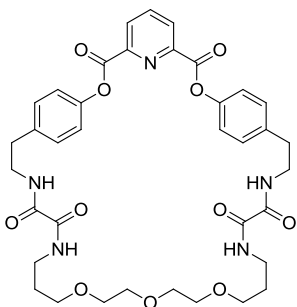
found: 733.3.



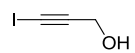
M16: 1H NMR (300 MHz, DMSO- d_6): δ 1.65-1.71 (m, 4H), 2.28 (s, 3H), 2.64 (t, $J = 8.1$ Hz, 4H), 3.18 (q, $J = 6.6$ Hz, 4H), 3.27-3.40 (m, 10H), 3.46-3.52 (m, 8H), 4.98 (s, 4H), 6.88 (t, $J = 7.5$ Hz, 4H), 7.06 (d, $J = 7.2$ Hz, 4H), 7.16 (s, 2H), 7.25 (s, 1H).

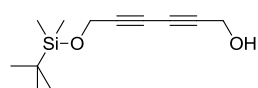
MS m/z $[M + H]^+$ calculated for $[C_{39}H_{50}N_4O_9 + H]^+$ 719.4,

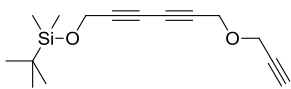
found: 719.4.



M17: 1H NMR (300 MHz, DMSO- d_6): δ 1.63-1.72 (m, 4H), 2.64 (t, $J = 8.1$ Hz, 4H), 3.18 (q, $J = 6.6$ Hz, 4H), 3.25-3.42 (m, 10H), 3.60-3.65 (m, 8H), 5.09 (s, 4H), 6.81 (d, $J = 8.7$ Hz, 4H), 7.01 (d, $J = 8.4$ Hz, 4H), 7.37 (s, 4H).

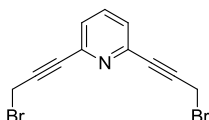

3-Iodoprop-2-yn-1-ol (5)¹¹: A solution of propargyl alcohol (5.8 mL, 100 mmol, 1 equiv) in 100 mL of methanol was added slowly to a solution of potassium hydroxide (14 g, 250 mmol, 2.5 equiv) in 25 mL of H₂O at 0 °C. The mixture was stirred for an additional 10 min. Then, iodine (27 g, 110 mmol, 1.1 equiv) was added in one portion. The reaction mixture was allowed to warm to room temperature and stirred for 3 hours before it was extracted with diethyl ether. The combined organic phases were washed with Na₂S₂O₃ and brine. Upon concentration of the solution in *vacuo*, 13.67 g (75%) of pure **5** was obtained in the form of yellow crystals. ¹H NMR (300 MHz, CDCl₃): δ 4.41 (s, 2H). ¹³C NMR (300 MHz, CDCl₃): δ 2.8, 52.1, 92.4.


6-(tert-Butyldimethylsilyloxy)hexa-2,4-diyne-1-ol (6)¹²: CuCl (1.23 g, 12.5 mmol) was dissolved in a mixture of 100 mL of H₂O and 50 mL of n-butylamine. Then, tert-butyldimethyl(prop-2-ynoxy)silane (10.20 g, 60 mmol) was added at 0 °C, followed by the dropwise addition of 3-iodoprop-2-yn-1-ol (7.59 g, 41.5 mmol). Whenever the reaction mixture turned to green, a few crystals of NH₂OH₃·HCl were added. After stirring for 20 min at 0 °C and for another 30 min at room temperature, the reaction mixture was filtered through a pad of silica gel. After aqueous workup, the crude product was purified by column chromatography (eluent; petroleum ether/EtOAc = 15:1) to give **6** (10.27 g, 55%) as a red liquid: ¹H NMR (400 MHz, CDCl₃) δ 0.12 (s, 6H), 0.90 (s, 9H), 1.75 (br, 1H), 4.34 (s, 2H), 4.38 (s, 2H).



tert-butyldimethyl((6-(prop-2-yn-1-yloxy)hexa-2,4-diyne-1-yl)oxy)silane (7): A solution of **6** (1.12 g, 5 mmol) in 25 mL of

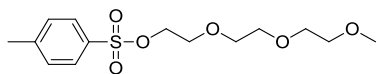
freshly distilled THF was added slowly to a solution of sodium hydride (0.72 g, 30.0 mmol) in 30 mL of THF under nitrogen in ice bath. The mixture was stirred for an additional 20 min. Then, 18-crown-6 (2.8 g, 10.6 mmol) was added and stirred for another 20 min. 3.2 mL of propargyl bromide (20 mmol) was added dropwise, and the ice bath was removed. The reaction mixture was allowed to warm to room temperature and stirred for 3 hours before it was quenched by cold water. The THF was removed in *vacuo* and then the mixture was extracted with diethyl ether. The combined organic phases were dried with MgSO₄ and concentrated. The pure yellow oil was obtained by column chromatography (eluent: EtOAc/hexane = 2:3) (0.92 g, 70%). ¹H NMR (300 MHz, CDCl₃): δ 0.17-0.20 (m, 6H), 0.95-0.98 (m, 9H), 2.53 (t, J = 2.4 Hz, 1H), 4.33 (d, J = 2.4 Hz, 2H), 4.42 (d, J = 10.5 Hz, 4H).



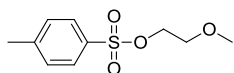
2,6-Bis(bromomethyl)pyridine (10)¹³: To a suspension of 3,3'-(pyridine-2,6-diyl)bis(prop-2-yn-1-ol) (1.87 g, 10.0 mmol) in

anhydrous tetrachloro-methane (20 mL) was slowly added of phosphorous tribromide (8.10 g, 30.0 mmol) at 210°C. The reaction mixture was heated under reflux for 2 hours, cooled to room temperature and treated with 20 mL of water. The organic layer was separated and the aqueous solution was extracted with tetrachloromethane (3 × 25 mL). The combined organic phases were dried with MgSO₄ and the solvent was removed in *vacuo*. The residual solid was recrystallized from hexane to afford 2.32 g (88%) of **10** as

colourless needles. M.p. 86-87°C. ^1H NMR (300 MHz, CDCl_3): δ 4.41 (s, 4 H), 7.75 (t, $J = 6.9$ Hz, 1 H), 7.89 (d, $J = 8.1$ Hz, 2 H).

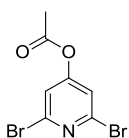


2-(2-(2-methoxyethoxy)ethoxy)ethyl-4-methylbenzenesulfonate (11): Triethylene glycol monomethyl ether (3.44 g, 21.0 mmol) and *p*-toluenesulfonyl chloride (4.37 g, 23.0 mmol) were dissolved in diethyl ether (10 mL). Freshly ground KOH (4.67 g, 83.0 mmol) was then added in several portions to the ice-cooled solution, keeping the temperature below 5 °C. After 4 hours of reaction, 7.5 mL of ice and water were added, the organic phase was extracted 3 times with diethyl ether. The combined organic fractions were dried with Na_2SO_4 , filtered, and the solvent was evaporated in *vacuo* to give **11** as a colorless oil (6.35 g, 96 %). ^1H NMR (400 MHz, CDCl_3 , δ): 2.45 (s, 3H), 3.38 (s, 3H), 3.53 (t, 2H), 3.61 (m, 6H), 3.70 (t, $J = 6$, 2H); 4.17 (t, $J = 6$, 2H), 7.35 (d, $J = 7.5$, 2H), 7.80 (d, $J = 7.5$, 2H); ^{13}C NMR (400 MHz, CDCl_3): δ 21.58, 58.95, 68.64, 69.23, 70.51, 70.71, 71.88, 127.93, 129.80, 133.06, 144.77.

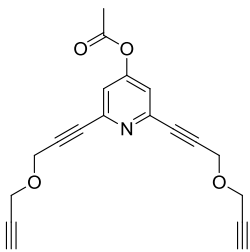


2-methoxyethyl-4-methylbenzenesulfonate (12): Ethylene glycol monomethyl ether (1.58 g, 20.8 mmol) and *p*-toluenesulfonyl chloride (4.38 g, 23.0 mmol) were dissolved in diethyl ether (10 mL). Freshly ground KOH (4.67 g, 83.0 mmol) was then added in several portions to the ice-cooled solution, keeping the temperature below 5 °C. After 4 hours of reaction, 7.5 mL of ice and water were added, the organic phase was extracted 3 times with diethyl ether. The combined organic fractions were dried on Na_2SO_4 , filtered, and the solvent was evaporated under reduced pressure to give **12** as a

colorless oil (4.63 g, 96 %). ^1H (400 MHz, CDCl_3): δ 2.42 (s, 3H), 3.27 (s, 3H), 3.55 (t, $J = 4.8$ Hz, 2H), 4.13 (t, $J = 4.7$ Hz, 2H); 7.34 (d, $J = 8.1$ Hz, 2H), 7.77 (d, $J = 8.2$ Hz, 2H), ^{13}C (300 MHz, CDCl_3): δ 21.4, 58.7, 69.0, 69.7, 127.7, 129.7, 132.7, 144.7.

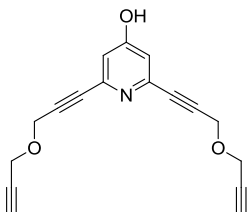


2,6-dibromopyridin-4-yl acetate: A mixture of 3,5-dibromophenol (0.85 g, 3.37 mmol) and acetic anhydride (1.03 g, 10.09 mmol) was heated at 70 °C for 2 hours. The mixture was poured onto ice, neutralized with K_2CO_3 , and extracted with diethyl ether (3×25 mL). The combined organic layers were washed with water (2×25 mL) and brine (30 mL) and dried with MgSO_4 . The solvent was removed with a rotary evaporator. The residue was purified by column chromatography (eluent: EtOAc/hexane = 2:3) to give **x** as a pale pink solid (0.89 g, 90%). ^1H NMR (400 MHz, CDCl_3): δ 2.28 (s, 3H) 7.30 (s, 2H). ^{13}C NMR (100 MHz, CDCl_3): δ 21.09, 120.38, 140.97, 158.87, 167.09.



2,6-bis(3-(prop-2-yn-1-yloxy)prop-1-yn-1-yl)pyridin-4-yl acetate: A mixture of dibromide **x** (4.41 g, 15.0 mmol), $i\text{-Pr}_2\text{NH}$ (40 mL), and THF (40 mL) was bubbled with nitrogen for 30 min, and then $\text{PdCl}_2(\text{PPh}_3)_2$ (488 mg, 0.65 mmol), propargyl ether (4.2 mL, 40 mmol), and CuI (25.77 mg, 0.135 mmol) were added to the mixture subsequently. The reaction mixture was stirred for 12 hours at room temperature. The insoluble materials were filtered off. The filtrate was concentrated with a rotary evaporator and the resulting residue was subjected to column chromatography (eluent: EtOAc/hexane = 2:1) to afford **x** (3.4 g, 71%) as a yellow oil. ^1H NMR (400 MHz, CDCl_3): δ 2.34 (s, 3H), 2.5 (t, $J = 3.2$

Hz, 2H), 4.33 (d, $J = 3.2$ Hz, 4H), 4.51 (s, 4H), 7.25 (s, 2H). ^{13}C NMR (400 MHz, CDCl_3): δ 21.12, 56.80, 56.84, 75.36, 78.67, 84.89, 85.64, 119.87, 144.28, 157.58, 167.50.



2,6-bis(3-(prop-2-yn-1-yloxy)prop-1-yn-1-yl)pyridin-4-ol: A

solution of potassium hydroxide (1.52 g) in water (10 ml) was added dropwise to a stirred solution of the acetate (1.51 g, 4.7 mmol) in methanol (75 ml) under an atmosphere of nitrogen. The reaction mixture was allowed stirred at room temperature for 50 min and then diluted with water and acidified. The crude phenol was isolated by extraction with dichloromethane. The pure yellow oil was obtained by column chromatography (eluent: EtOAc/hexane = 2:1) (1.05 g, 81%). ^1H NMR (400 MHz, CDCl_3): δ 2.46 (t, $J = 2.3$ Hz, 2H), 4.20 (d, $J = 2.3$ Hz, 4H), 4.38 (s, 4H), 6.87 (s, 2H). ^{13}C NMR (400 MHz, CDCl_3): δ 56.69, 56.78, 75.55, 78.54, 82.34, 87.67, 117.84, 139.05, 171.04.

4.3. References

- (1) Bankston, D.: Oxidative Cleavage of an Aromatic Ring: Cis,Cis-Monomethyl Muconate from 1,2-Dihydroxybenzene. In *Org. Synth.*; John Wiley & Sons, Inc., 2003.
- (2) Hunter, C. A.; Misuraca, M. C.; Turega, S. M.: Dissection of Complex Molecular Recognition Interfaces. *J. Am. Chem. Soc.* **2010**, *133*, 582-594.
- (3) Wang, T.: The Topochemical Polymerization of Diacetylenes Using Supramolecular Host-Guest Chemistry. Stony Brook University, 2005.
- (4) Chow, S. K.: Synthesis of 2,6-Pyridine-Based Diacetylene Macrocycle and Its Possible Formation to a Covalent Bonded Tubular Structure Via Topochemical Polymerization, Stony Brook University. Stony Brook University, 2008.
- (5) Waki, M.; Abe, H.; Inouye, M.: Helix Formation in Synthetic Polymers by Hydrogen Bonding with Native Saccharides in Protic Media. *Chemistry – A European Journal* **2006**, *12*, 7839-7847.
- (6) Brennan, D. J.; White, J. E.; Haag, A. P.; Kram, S. L.; Mang, M. N.; Pikulin, S.; Brown, C. N.: Poly(Hydroxy Amide Ethers): New High-Barrier Thermoplastics. *Macromolecules* **1996**, *29*, 3707-3716.
- (7) Luong Nguyen, T.; Scott, A.; Dinkelmeyer, B.; W. Fowler, F.; W. Lauher, J.: Design of Molecular Solids: Utility of the Hydroxyl Functionality as a Predictable Design Element. *New J. Chem.* **1998**, *22*, 129-135.
- (8) Xi, G.-L.; Liu, Z.-Q.: Antioxidant Effectiveness Generated by One or Two Phenolic Hydroxyl Groups in Coumarin-Substituted Dihydropyrazoles. *Eur. J. Med. Chem.* **2013**, *68*, 385-393.
- (9) Hsu, T.-J.; Fowler, F. W.; Lauher, J. W.: Preparation and Structure of a Tubular Addition Polymer: A True Synthetic Nanotube. *J. Am. Chem. Soc.* **2011**, *134*, 142-145.
- (10) Fu, T.-h.; Li, Y.; Thaker, H. D.; Scott, R. W.; Tew, G. N.: Expedient Synthesis of Smamps Via Click Chemistry. *ACS Medicinal Chemistry Letters* **2013**, *4*, 841-845.
- (11) Passiniemi, M.; Koskinen, A. M. P.: Stereoselective Total Synthesis of Pachastrissamine (Jaspine B). *Tetrahedron Lett.* **2008**, *49*, 980-983.
- (12) Trost, B. M.; Livingston, R. C.: An Atom-Economic and Selective Ruthenium-Catalyzed Redox Isomerization of Propargylic Alcohols. An Efficient Strategy for the Synthesis of Leukotrienes. *J. Am. Chem. Soc.* **2008**, *130*, 11970-11978.
- (13) Bergmann, E. D.; Pelchowicz, Z.: Syntheses of Macrocyclic Compounds. *J. Am. Chem. Soc.* **1953**, *75*, 4281-4286.

Bibliography

Chapter 1

- (1) Bong, D. T.; Clark, T. D.; Granja, J. R.; Ghadiri, M. R.: Self-Assembling Organic Nanotubes. *Angewandte Chemie-International Edition* **2001**, *40*, 988-1011.
- (2) Bradley, K.; Gabriel, J. C. P.; Gruner, G.: Flexible Nanotube Electronics. *Nano Lett.* **2003**, *3*, 1353-1355.
- (3) Dalton, A. B.; Collins, S.; Munoz, E.; Razal, J. M.; Ebron, V. H.; Ferraris, J. P.; Coleman, J. N.; Kim, B. G.; Baughman, R. H.: Super-Tough Carbon-Nanotube Fibres - These Extraordinary Composite Fibres Can Be Woven into Electronic Textiles. *Nature* **2003**, *423*, 703-703.
- (4) Gannon, C. J.; Cherukuri, P.; Yakobson, B. I.; Cognet, L.; Kanzius, J. S.; Kittrell, C.; Weisman, R. B.; Pasquali, M.; Schmidt, H. K.; Smalley, R. E.; Curley, S. A.: Carbon Nanotube-Enhanced Thermal Destruction of Cancer Cells in a Noninvasive Radiofrequency Field. *Cancer* **2007**, *110*, 2654-2665.
- (5) Moore, J. S.: Shape-Persistent Molecular Architectures of Nanoscale Dimension. *Acc. Chem. Res.* **1997**, *30*, 402-413.
- (6) Postma, H. W. C.; Teepen, T.; Yao, Z.; Grifoni, M.; Dekker, C.: Carbon Nanotube Single-Electron Transistors at Room Temperature. *Science* **2001**, *293*, 76-79.
- (7) Shu, L.; Mayor, M.: Shape-Persistent Macrocyclic with a Self-Complementary Recognition Pattern Based on Diacetylene-Linked Alternating Hexylbenzene and Perfluorobenzene Rings. *Chem. Commun.* **2006**, 4134-4136.
- (8) Simmons, T. J.; Hashim, D.; Vajtai, R.; Ajayan, P. M.: Large Area-Aligned Arrays from Direct Deposition of Single-Wall Carbon Nanotube Inks. *J. Am. Chem. Soc.* **2007**, *129*, 10088-10089.
- (9) Singh, R.; Pantarotto, D.; McCarthy, D.; Chaloin, O.; Hoebeke, J.; Partidos, C. D.; Briand, J. P.; Prato, M.; Bianco, A.; Kostarelos, K.: Binding and Condensation of Plasmid DNA onto Functionalized Carbon Nanotubes: Toward the Construction of Nanotube-Based Gene Delivery Vectors. *J. Am. Chem. Soc.* **2005**, *127*, 4388-4396.
- (10) Tseng, Y. C.; Xuan, P. Q.; Javey, A.; Malloy, R.; Wang, Q.; Bokor, J.; Dai, H. J.: Monolithic Integration of Carbon Nanotube Devices with Silicon Mos Technology. *Nano Lett.* **2004**, *4*, 123-127.
- (11) Zhang, M.; Fang, S. L.; Zakhidov, A. A.; Lee, S. B.; Aliev, A. E.; Williams, C. D.; Atkinson, K. R.; Baughman, R. H.: Strong, Transparent, Multifunctional, Carbon Nanotube Sheets. *Science* **2005**, *309*, 1215-1219.
- (12) Zhao, D. H.; Moore, J. S.: Shape-Persistent Arylene Ethynylene Macrocyclics: Syntheses and Supramolecular Chemistry. *Chem. Commun.* **2003**, 807-818.
- (13) Horwich, A. L.; Weber-Ban, E. U.; Finley, D.: Chaperone Rings in Protein Folding and Degradation. *Proc. Natl. Acad. Sci. U. S. A.* **1999**, *96*, 11033-11040.
- (14) Sigler, P. B.; Xu, Z. H.; Rye, H. S.; Burston, S. G.; Fenton, W. A.; Horwich, A. L.: Structure and Function in Groel-Mediated Protein Folding. *Annu. Rev. Biochem.* **1998**, *67*, 581-608.
- (15) Voges, D.; Zwickl, P.; Baumeister, W.: The 26s Proteasome: A Molecular Machine Designed for Controlled Proteolysis. *Annu. Rev. Biochem.* **1999**, *68*, 1015-1068.

- (16) Zwickl, P.; Voges, D.; Baumeister, W.: The Proteasome: A Macromolecular Assembly Designed for Controlled Proteolysis. *Philosophical Transactions of the Royal Society of London Series B-Biological Sciences* **1999**, 354, 1501-1511.
- (17) Eisenberg, B.: Ionic Channels in Biological Membranes: Natural Nanotubes. *Acc. Chem. Res.* **1998**, 31, 117-123.
- (18) Borgnia, M.; Nielsen, S.; Engel, A.; Agre, P.: Cellular and Molecular Biology of the Aquaporin Water Channels. *Annu. Rev. Biochem.* **1999**, 68, 425-458.
- (19) Ajayan, P. M.; Ebbesen, T. W.: Nanometre-Size Tubes of Carbon. *Reports on Progress in Physics* **1997**, 60, 1025-1062.
- (20) Iijima, S.: Helical Microtubules of Graphitic Carbon. *Nature* **1991**, 354, 56-58.
- (21) Song, L. Z.; Hobough, M. R.; Shustak, C.; Cheley, S.; Bayley, H.; Gouaux, J. E.: Structure of Staphylococcal Alpha-Hemolysin, a Heptameric Transmembrane Pore. *Science* **1996**, 274, 1859-1866.
- (22) Cowan, S. W.; Schirmer, T.; Rummel, G.; Steiert, M.; Ghosh, R.; Pauptit, R. A.; Jansonius, J. N.; Rosenbusch, J. P.: Crystal-Structures Explain Functional-Properties of 2 Escherichia-Coli Porins. *Nature* **1992**, 358, 727-733.
- (23) Schirmer, T.; Keller, T. A.; Wang, Y. F.; Rosenbusch, J. P.: Structural Basis for Sugar Translocation through Maltoporin Channels at 3.1-Angstrom Resolution. *Science* **1995**, 267, 512-514.
- (24) Weiss, M. S.; Schulz, G. E.: Structure of Porin Refined at 1.8 Angstrom Resolution. *J. Mol. Biol.* **1992**, 227, 493-509.
- (25) Merritt, E. A.; Sarfaty, S.; Vandenakker, F.; Lhoir, C.; Martial, J. A.; Hol, W. G. J.: Crystal-Structure of Cholera-Toxin B-Pentamer Bound to Receptor G(M1) Pentasaccharide. *Protein Sci.* **1994**, 3, 166-175.
- (26) Doyle, D. A.; Cabral, J. M.; Pfuetzner, R. A.; Kuo, A. L.; Gulbis, J. M.; Cohen, S. L.; Chait, B. T.; MacKinnon, R.: The Structure of the Potassium Channel: Molecular Basis of K⁺ Conduction and Selectivity. *Science* **1998**, 280, 69-77.
- (27) Ketchum, R. R.; Hu, W.; Cross, T. A.: High-Resolution Conformation of Gramicidin-a in a Lipid Bilayer by Solid-State Nmr. *Science* **1993**, 261, 1457-1460.
- (28) Caspar, D. L.; Namba, K.: Switching in the Self-Assembly of Tobacco Mosaic Virus. *Advances in biophysics* **1990**, 26, 157-185.
- (29) Klug, A.: From Macromolecules to Biological Assemblies (Nobel Lecture). *Angewandte Chemie-International Edition in English* **1983**, 22, 565-582.
- (30) Namba, K.; Stubbs, G.: Structure of Tobacco Mosaic-Virus at 3.6-a Resolution - Implications for Assembly. *Science* **1986**, 231, 1401-1406.
- (31) Bong, D. T.; Clark, T. D.; Granja, J. R.; Ghadiri, M. R.: Self-Assembling Organic Nanotubes. *Angew. Chem., Int. Ed.* **2001**, 40, 988-1011.
- (32) Parkin, I. P.: *Supramolecular Chemistry*. J.W. Steed and J.L. Atwood. John Wiley & Sons Ltd, Chichester, 2000. Xxvii + 745 Pages. £29.95 (Paperback). Isbn 0-471-98791-3. *Appl. Organomet. Chem.* **2001**, 15, 236-236.
- (33) Pedersen, C. J.: Cyclic Polyethers and Their Complexes with Metal Salts. *J. Am. Chem. Soc.* **1967**, 89, 7017.
- (34) Busch, D. H.; Stephenson, N. A.: Molecular-Organization, Portal to Supramolecular Chemistry - Structural-Analysis of the Factors Associated with Molecular-Organization in Coordination and Inclusion Chemistry, Including the Coordination Template Effect. *Coord. Chem. Rev.* **1990**, 100, 119-154.
- (35) Zhang, W.; Moore, J. S.: Shape-Persistent Macrocycles: Structures and Synthetic Approaches from Arylene and Ethynylene Building Blocks. *Angewandte Chemie-International Edition* **2006**, 45, 4416-4439.
- (36) Illuminati, G.; Mandolini, L.: Ring-Closure Reactions of Bifunctional Chain Molecules. *Acc. Chem. Res.* **1981**, 14, 95-102.

- (37) Hoger, S.; Meckenstock, A. D.; Pellen, H.: High-Yield Macrocyclization Via Glaser Coupling of Temporary Covalent Templated Bisacetylenes. *J. Org. Chem.* **1997**, *62*, 4556-4557.
- (38) Ishii, S. I.; Witkop, B.: Gramicidin A .1. Determination of Composition and Amino Acid Configuration by Enzymatic and Gas Chromatographic Methods. *J. Am. Chem. Soc.* **1963**, *85*, 1832.
- (39) Sarges, R.; Witkop, B.: Formyl Novel Nh₂-Terminal Blocking Group in Naturally Occurring Peptide - Identity of Seco-Gramicidin with Desformylgramicidin. *J. Am. Chem. Soc.* **1964**, *86*, 1861.
- (40) Sarges, R.; Witkop, B.: Gramicidin A .4. Primary Sequence of Valine + Isoleucine Gramicidin A. *J. Am. Chem. Soc.* **1964**, *86*, 1862.
- (41) Syngé, R. L. M.: Gramicidin-S - over-All Chemical Characteristics and Amino-Acid Composition. *Biochem. J.* **1945**, *39*, 363-367.
- (42) Wallace, B. A.: Recent Advances in the High Resolution Structures of Bacterial Channels: Gramicidin A. *Journal of Structural Biology* **1998**, *121*, 123-141.
- (43) Urry, D. W.: Gramicidin-a Transmembrane Channel - Proposed Pi(L,D) Helix. *Proc. Natl. Acad. Sci. U. S. A.* **1971**, *68*, 672.
- (44) Bishop, R.; Dance, I. G.: New Types of Helical Canal Inclusion Networks. *Top. Curr. Chem.* **1988**, *149*, 137-188.
- (45) Gin, M. S.; Yokozawa, T.; Prince, R. B.; Moore, J. S.: Helical Bias in Solvophobicity Folded Oligo(Phenylene Ethynylene)S. *J. Am. Chem. Soc.* **1999**, *121*, 2643-2644.
- (46) Nelson, J. C.; Saven, J. G.; Moore, J. S.; Wolynes, P. G.: Solvophobicity Driven Folding of Nonbiological Oligomers. *Science* **1997**, *277*, 1793-1796.
- (47) Prince, R. B.; Brunsveld, L.; Meijer, E. W.; Moore, J. S.: Twist Sense Bias Induced by Chiral Side Chains in Helically Folded Oligomers. *Angewandte Chemie-International Edition* **2000**, *39*, 228.
- (48) Prince, R. B.; Okada, T.; Moore, J. S.: Controlling the Secondary Structure of Nonbiological Oligomers with Solvophobic and Coordination Interactions. *Angewandte Chemie-International Edition* **1999**, *38*, 233-236.
- (49) Appella, D. H.; Christianson, L. A.; Klein, D. A.; Powell, D. R.; Huang, X. L.; Barchi, J. J.; Gellman, S. H.: Residue-Based Control of Helix Shape in Beta-Peptide Oligomers. *Nature* **1997**, *387*, 381-384.
- (50) Gellman, S. H.: Foldamers: A Manifesto. *Acc. Chem. Res.* **1998**, *31*, 173-180.
- (51) Stoncius, S.; Orentas, E.; Butkus, E.; Ohrstrom, L.; Wendt, O. F.; Warnmark, K.: An Approach to Helical Tubular Self-Aggregation Using C-2-Symmetric Self-Complementary Hydrogen-Bonding Cavity Molecules. *J. Am. Chem. Soc.* **2006**, *128*, 8272-8285.
- (52) Matsuda, K.; Stone, M. T.; Moore, J. S.: Helical Pitch of M-Phenylene Ethynylene Foldamers by Double Spin Labeling. *J. Am. Chem. Soc.* **2002**, *124*, 11836-11837.
- (53) Yashima, E.; Maeda, K.; Iida, H.; Furusho, Y.; Nagai, K.: Helical Polymers: Synthesis, Structures, and Functions. *Chem. Rev.* **2009**, *109*, 6102-6211.
- (54) Cornelissen, J. J. L. M.; Donners, J. J. J. M.; de Gelder, R.; Graswinckel, W. S.; Metselaar, G. A.; Rowan, A. E.; Sommerdijk, N. A. J. M.; Nolte, R. J. M.: B-Helical Polymers from Isocyanopeptides. *Science* **2001**, *293*, 676-680.
- (55) Amabilino, D. B.; Ramos, E.; Serrano, J.-L.; Sierra, T.; Veciana, J.: Chiral Teleinduction in the Polymerization of Isocyanides. *Polymer* **2005**, *46*, 1507-1521.
- (56) Amabilino, D. B.; Serrano, J.-L.; Veciana, J.: Reversible and Irreversible Conformational Changes in Poly(Isocyanide)S: A Remote Stereoelectronic Effect. *Chem. Commun.* **2005**, 322-324.
- (57) Takei, F.; Onitsuka, K.; Takahashi, S.: Thermally Induced Helical Conformational Change in Poly(Aryl Isocyanide)S with Optically Active Ester Groups. *Macromolecules* **2005**, *38*, 1513-1516.

- (58) Onitsuka, K.; Mori, T.; Yamamoto, M.; Takei, F.; Takahashi, S.: Helical Sense Selective Polymerization of Bulky Aryl Isocyanide Possessing Chiral Ester or Amide Groups Initiated by Arylrhodium Complexes. *Macromolecules* **2006**, *39*, 7224-7231.
- (59) Kajitani, T.; Okoshi, K.; Yashima, E.: Helix-Sense-Controlled Polymerization of Optically Active Phenyl Isocyanides. *Macromolecules* **2008**, *41*, 1601-1611.
- (60) Yashima, E.; Maeda, K.; Furusho, Y.: Single- and Double-Stranded Helical Polymers: Synthesis, Structures, and Functions. *Acc. Chem. Res.* **2008**, *41*, 1166-1180.
- (61) Schwartz, E.; Koepf, M.; Kitto, H. J.; Nolte, R. J. M.; Rowan, A. E.: Helical Poly(Isocyanides): Past, Present and Future. *Polymer Chemistry* **2011**, *2*, 33-47.
- (62) Hu, G.; Li, W.; Hu, Y.; Xu, A.; Yan, J.; Liu, L.; Zhang, X.; Liu, K.; Zhang, A.: Water-Soluble Chiral Polyisocyanides Showing Thermoresponsive Behavior. *Macromolecules* **2013**, *46*, 1124-1132.
- (63) Ashton, P. R.; Brown, C. L.; Menzer, S.; Nepogodiev, S. A.; Stoddart, J. F.; Williams, D. J.: Synthetic Cyclic Oligosaccharides - Syntheses and Structural Properties of a Cyclo (1->4)-Alpha-L-Rhamnopyranosyl-(1->4)-Alpha-D-Mannopyranosyl Trios Ide and -Tetraoside. *Chemistry-a European Journal* **1996**, *2*, 580-591.
- (64) Ashton, P. R.; Cantrill, S. J.; Gattuso, G.; Menzer, S.; Nepogodiev, S. A.; Shipway, A. N.; Stoddart, J. F.; Williams, D. J.: Achiral Cyclodextrin Analogues. *Chemistry-a European Journal* **1997**, *3*, 1299-1314.
- (65) Baldini, L.; Sansone, F.; Casnati, A.; Ugozzoli, F.; Ungaro, R.: Peptidocalix[4]Arene Self-Assembled Nanotubes. *J. Supramol. Chem.* **2002**, *2*, 219-226.
- (66) Casnati, A.; Liantonio, R.; Metrangolo, P.; Resnati, G.; Ungaro, R.; Ugozzoli, F.: Molecular and Supramolecular Homochirality: Enantiopure Perfluorocarbon Rotamers and Halogen-Bonded Fluorous Double Helices. *Angewandte Chemie-International Edition* **2006**, *45*, 1915-1918.
- (67) Dalgarno, S. J.; Cave, G. W. V.; Atwood, J. L.: Toward the Isolation of Functional Organic Nanotubes. *Angewandte Chemie-International Edition* **2006**, *45*, 570-574.
- (68) Dawson, C.; Horton, P. N.; Hursthouse, M. B.; James, S. L.: Channelled Crystals Formed by Tubular Stacking of a 4+4 Phenylene-Piperazine Macrocyclic. *CrystEngComm* **2010**, *12*, 1048-1050.
- (69) Fromm, K. M.; Bergougnant, R. D.: Transport Properties of Solid State Crown Ether Channel Systems. *Solid State Sci.* **2007**, *9*, 580-587.
- (70) Gattuso, G.; Menzer, S.; Nepogodiev, S. A.; Stoddart, J. F.; Williams, D. J.: Carbohydrate Nanotubes. *Angewandte Chemie-International Edition in English* **1997**, *36*, 1451-1454.
- (71) Gauthier, D.; Baillargeon, P.; Drouin, M.; Dory, Y. L.: Self-Assembly of Cyclic Peptides into Nanotubes and Then into Highly Anisotropic Crystalline Materials. *Angewandte Chemie-International Edition* **2001**, *40*, 4635.
- (72) Ghadiri, M. R.; Granja, J. R.; Buehler, L. K.: Artificial Transmembrane Ion Channels from Self-Assembling Peptide Nanotubes. *Nature* **1994**, *369*, 301-304.
- (73) Ghadiri, M. R.; Granja, J. R.; Milligan, R. A.; McRee, D. E.; Khazanovich, N.: Self-Assembling Organic Nanotubes Based on a Cyclic Peptide Architecture. *Nature* **1993**, *366*, 324-327.
- (74) Harada, A.; Li, J.; Kamachi, M.: The Molecular Necklace - a Rotaxane Containing Many Threaded Alpha-Cyclodextrins. *Nature* **1992**, *356*, 325-327.
- (75) Harada, A.; Li, J.; Kamachi, M.: Synthesis of a Tubular Polymer from Threaded Cyclodextrins. *Nature* **1993**, *364*, 516-518.
- (76) Kloo, L.; Svensson, P. H.; Taylor, M. J.: Investigations of the Polyiodides H₃O Center Dot I-X (X=3, 5 or 7) as Dibenzo-18-Crown-6 Complexes. *Journal of the Chemical Society-Dalton Transactions* **2000**, 1061-1065.

- (77) Lazar, A. N.; Dupont, N.; Navaza, A.; Coleman, A. W.: Helical Aquatubes of Calix 4 Arene Di-Methoxycarboxylic Acid. *Chem. Commun.* **2006**, 1076-1078.
- (78) Motesharei, K.; Ghadiri, M. R.: Diffusion-Limited Size-Selective Ion Sensing Based on Sam-Supported Peptide Nanotubes. *J. Am. Chem. Soc.* **1997**, *119*, 11306-11312.
- (79) Organo, V. G.; Leontiev, A. V.; Sgarlata, V.; Dias, H. V. R.; Rudkevich, D. M.: Supramolecular Features of Calixarene-Based Synthetic Nanotubes. *Angewandte Chemie-International Edition* **2005**, *44*, 3043-3047.
- (80) Semetey, V.; Didierjean, C.; Briand, J. P.; Aubry, A.; Guichard, G.: Self-Assembling Organic Nanotubes from Enantiopure Cyclo-N,N'-Linked Oligoureas: Design, Synthesis, and Crystal Structure. *Angewandte Chemie-International Edition* **2002**, *41*, 1895.
- (81) Shimizu, L. S.; Hughes, A. D.; Smith, M. D.; Davis, M. J.; Zhang, B. P.; zur Loye, H. C.; Shimizu, K. D.: Self-Assembled Nanotubes That Reversibly Bind Acetic Acid Guests. *J. Am. Chem. Soc.* **2003**, *125*, 14972-14973.
- (82) Shimizu, L. S.; Smith, M. D.; Hughes, A. D.; Shimizu, K. D.: Self-Assembly of a Bis-Urea Macrocyclic into a Columnar Nanotube. *Chem. Commun.* **2001**, 1592-1593.
- (83) Hisaki, I.; Shigemitsu, H.; Sakamoto, Y.; Hasegawa, Y.; Okajima, Y.; Nakano, K.; Tohnai, N.; Miyata, M.: Octadehydrodibenzo 12 Annulene-Based Organogels: Two Methyl Ester Groups Prevent Crystallization and Promote Gelation. *Angewandte Chemie-International Edition* **2009**, *48*, 5465-5469.
- (84) Cuccia, L. A.; Lehn, J. M.; Homo, J. C.; Schmutz, M.: Encoded Helical Self-Organization and Self-Assembly into Helical Fibers of an Oligoheterocyclic Pyridine-Pyridazine Molecular Strand. *Angewandte Chemie-International Edition* **2000**, *39*, 233.
- (85) Venkataraman, D.; Lee, S.; Zhang, J. S.; Moore, J. S.: An Organic-Solid with Wide Channels Based on Hydrogen-Bonding between Macrocycles. *Nature* **1994**, *371*, 591-593.
- (86) Höger, S.: Highly Efficient Methods for the Preparation of Shape-Persistent Macrocyclics. *Journal of Polymer Science Part A: Polymer Chemistry* **1999**, *37*, 2685-2698.
- (87) Zhou, X.; Liu, G.; Yamato, K.; Shen, Y.; Cheng, R.; Wei, X.; Bai, W.; Gao, Y.; Li, H.; Liu, Y.; Liu, F.; Czajkowsky, D. M.; Wang, J.; Dabney, M. J.; Cai, Z.; Hu, J.; Bright, F. V.; He, L.; Zeng, X. C.; Shao, Z.; Gong, B.: Self-Assembling Subnanometer Pores with Unusual Mass-Transport Properties. *Nature Communications* **2012**, *3*.
- (88) Gong, B.; Shao, Z.: Self-Assembling Organic Nanotubes with Precisely Defined, Sub-Nanometer Pores: Formation and Mass Transport Characteristics. *Acc. Chem. Res.* **2013**.
- (89) Gin, D. L.; Noble, R. D.: Designing the Next Generation of Chemical Separation Membranes. *Science* **2011**, *332*, 674-676.
- (90) Dawn, S.; Dewal, M. B.; Sobransingh, D.; Paderes, M. C.; Wibowo, A. C.; Smith, M. D.; Krause, J. A.; Pellechia, P. J.; Shimizu, L. S.: Self-Assembled Phenylethynylene Bis-Urea Macrocycles Facilitate the Selective Photodimerization of Coumarin. *J. Am. Chem. Soc.* **2011**, *133*, 7025-7032.
- (91) Desantis, P.; Morosett, S.; Rizzo, R.: Conformational-Analysis of Regular Enantiomeric Sequences. *Macromolecules* **1974**, *7*, 52-58.
- (92) Pasini, D.; Ricci, M.: Macrocycles as Precursors for Organic Nanotubes. *Curr. Org. Synth.* **2007**, *4*, 59-80.
- (93) Nagasawa, J. i.; Yoshida, M.; Tamaoki, N.: Synthesis, Gelation Properties and Photopolymerization of Macrocyclic Diacetylenedicarboxamides Derived from L-Glutamic Acid and Trans-1,4-Cyclohexanediol. *Eur. J. Org. Chem.* **2011**, *2011*, 2247-2255.
- (94) Gattuso, G.; Nepogodiev, S. A.; Stoddart, J. F.: Synthetic Cyclic Oligosaccharides. *Chem. Rev.* **1998**, *98*, 1919-1958.
- (95) Butler, P. J. G.: Self-Assembly of Tobacco Mosaic Virus: The Role of an Intermediate Aggregate in Generating Both Specificity and Speed. *Philosophical Transactions of the Royal Society of London Series B-Biological Sciences* **1999**, *354*, 537-550.

- (96) Lebeurier, G.; Nicolaieff, A.; Richards, K. E.: Inside-out Model for Self-Assembly of Tobacco Mosaic-Virus. *Proc. Natl. Acad. Sci. U. S. A.* **1977**, *74*, 149-153.
- (97) Soto, C. M.; Ratna, B. R.: Virus Hybrids as Nanomaterials for Biotechnology. *Curr. Opin. Biotechnol.* **2010**, *21*, 426-438.
- (98) Hudson, S. D.; Jung, H. T.; Percec, V.; Cho, W. D.; Johansson, G.; Ungar, G.; Balagurusamy, V. S. K.: Direct Visualization of Individual Cylindrical and Spherical Supramolecular Dendrimers. *Science* **1997**, *278*, 449-452.
- (99) Johansson, G.; Percec, V.; Ungar, G.; Zhou, J. P.: Fluorophobic Effect in the Self-Assembly of Polymers and Model Compounds Containing Tapered Groups into Supramolecular Columns. *Macromolecules* **1996**, *29*, 646-660.
- (100) Percec, V.; Bera, T. K.: Cell Membrane as a Model for the Design of Ion-Active Nanostructured Supramolecular Systems. *Biomacromolecules* **2002**, *3*, 167-181.
- (101) Percec, V.; Heck, J.; Tomazos, D.; Falkenberg, F.; Blackwell, H.; Ungar, G.: Self-Assembly of Taper-Shaped Monoesters of Oligo(Ethylene Oxide) with 3,4,5-Tris(P-Dodecyloxybenzyloxy)Benzoic Acid and of Their Polymethacrylates into Tubular Supramolecular Architectures Displaying a Columnar Mesophase. *Journal of the Chemical Society-Perkin Transactions 1* **1993**, 2799-2811.
- (102) Percec, V.; Heck, J. A.; Tomazos, D.; Ungar, G.: The Influence of the Complexation of Sodium and Lithium Triflate on the Self-Assembly of Tubular-Supramolecular Architectures Displaying a Columnar Mesophase Based on Taper-Shaped Monoesters of Oligoethylene Oxide with 3,4,5-Tris P-(N-Dodecan-1-Yloxy)Benzyloxy Benzoic Acid and of Their Polymethacrylates. *Journal of the Chemical Society-Perkin Transactions 2* **1993**, 2381-2388.
- (103) Percec, V.; Johansson, G.; Heck, J.; Ungar, G.; Batty, S. V.: Molecular Recognition Directed Self-Assembly of Supramolecular Cylindrical Channel-Like Architectures from 6,7,9,10,12,13,15,16-Octahydro-1,4,7,10,13-Pentaoxabenzocyclopentadecen- 2-Ylmethyl 3,4,5-Tris(P-Dodecyloxybenzyl-Oxy)Benzoate. *Journal of the Chemical Society-Perkin Transactions 1* **1993**, 1411-1420.
- (104) Percec, V.; Johansson, G.; Ungar, G.; Zhou, J. P.: Fluorophobic Effect Induces the Self-Assembly of Semifluorinated Tapered Monodendrons Containing Crown Ethers into Supramolecular Columnar Dendrimers Which Exhibit a Homeotropic Hexagonal Columnar Liquid Crystalline Phase. *J. Am. Chem. Soc.* **1996**, *118*, 9855-9866.
- (105) Percec, V.; Tomazos, D.; Heck, J.; Blackwell, H.; Ungar, G.: Self-Assembly of Taper-Shaped Monoesters of Oligo(Ethylene Oxide) with 3,4,5-Tris(N-Dodecan-1-Yloxy)Benzoic Acid and of Their Polymethacrylates into Tubular Supramolecular Architectures Displaying a Columnar Hexagonal Mesophase. *Journal of the Chemical Society-Perkin Transactions 2* **1994**, 31-44.
- (106) Ungar, G.; Abramic, D.; Percec, V.; Heck, J. A.: Self-Assembly of Twin Tapered Bisamides into Supramolecular Columns Exhibiting Hexagonal Columnar Mesophases. Structural Evidence for a Microsegregated Model of the Supramolecular Column. *Liq. Cryst.* **1996**, *21*, 73-86.
- (107) Kim, H.-J.; Liu, F.; Ryu, J.-H.; Kang, S.-K.; Zeng, X.; Ungar, G.; Lee, J.-K.; Zin, W.-C.; Lee, M.: Self-Organization of Bent Rod Molecules into Hexagonally Ordered Vesicular Columns. *J. Am. Chem. Soc.* **2012**, *134*, 13871-13880.
- (108) Kim, Y.; Li, W.; Shin, S.; Lee, M.: Development of Toroidal Nanostructures by Self-Assembly: Rational Designs and Applications. *Acc. Chem. Res.* **2013**.
- (109) Baumeister, B.; Matile, S.: Programmed Assembly of Expanded Rigid-Rod Beta-Barrels by Supramolecular Preorganization. *Chem. Commun.* **2000**, 913-914.
- (110) Baumeister, B.; Sakai, N.; Matile, S.: Giant Artificial Ion Channels Formed by Self-Assembled, Cationic Rigid-Rod Beta-Barrels. *Angewandte Chemie-International Edition* **2000**, *39*, 1955.

- (111) Das, G.; Matile, S.: Transmembrane Pores Formed by Synthetic P-Octiphenyl Beta-Barrels with Internal Carboxylate Clusters: Regulation of Ion Transport by Ph and Mg²⁺ Complexed 8-Aminonaphthalene-1,3,6-Trisulfonate. *Proc. Natl. Acad. Sci. U. S. A.* **2002**, *99*, 5183-5188.
- (112) Sakai, N.; Mareda, J.; Matile, S.: Rigid-Rod Molecules in Biomembrane Models: From Hydrogen-Bonded Chains to Synthetic Multifunctional Pores. *Acc. Chem. Res.* **2005**, *38*, 79-87.
- (113) Sakai, N.; Matile, S.: Synthetic Multifunctional Pores: Lessons from Rigid-Rod Beta-Barrels. *Chem. Commun.* **2003**, 2514-2523.
- (114) Sorde, N.; Das, G.; Matile, S.: Enzyme Screening with Synthetic Multifunctional Pores: Focus on Biopolymers. *Proc. Natl. Acad. Sci. U. S. A.* **2003**, *100*, 11964-11969.
- (115) Matile, S.: En Route to Supramolecular Functional Plasticity: Artificial Beta-Barrels, the Barrel-Stave Motif, and Related Approaches. *Chem. Soc. Rev.* **2001**, *30*, 158-167.
- (116) Sakai, N.; Majumdar, N.; Matile, S.: Self-Assembled Rigid-Rod Ionophores. *J. Am. Chem. Soc.* **1999**, *121*, 4294-4295.
- (117) Kim, Y.; Mayer, M. F.; Zimmerman, S. C.: A New Route to Organic Nanotubes from Porphyrin Dendrimers. *Angewandte Chemie-International Edition* **2003**, *42*, 1121-1126.
- (118) Takeuchi, T.; Mukawa, T.; Matsui, J.; Higashi, M.; Shimizu, K. D.: Molecularly Imprinted Polymers with Metalloporphyrin-Based Molecular Recognition Sites Coassembled with Methacrylic Acid. *Anal. Chem.* **2001**, *73*, 3869-3874.
- (119) Umpleby, R. J.; Baxter, S. C.; Rampey, A. M.; Rushton, G. T.; Chen, Y. Z.; Shimizu, K. D.: Characterization of the Heterogeneous Binding Site Affinity Distributions in Molecularly Imprinted Polymers. *Journal of Chromatography B-Analytical Technologies in the Biomedical and Life Sciences* **2004**, *804*, 141-149.
- (120) Zimmerman, S. C.; Wendland, M. S.; Rakow, N. A.; Zharov, I.; Suslick, K. S.: Synthetic Hosts by Monomolecular Imprinting inside Dendrimers. *Nature* **2002**, *418*, 399-403.
- (121) Hecht, S.; Khan, A.: Intramolecular Cross-Linking of Helical Folds: An Approach to Organic Nanotubes. *Angewandte Chemie-International Edition* **2003**, *42*, 6021-6024.
- (122) Scott, L. T.; Jackson, E. A.; Zhang, Q.; Steinberg, B. D.; Bancu, M.; Li, B.: A Short, Rigid, Structurally Pure Carbon Nanotube by Stepwise Chemical Synthesis. *J. Am. Chem. Soc.* **2011**, *134*, 107-110.
- (123) Colombo, G.; Soto, P.; Gazit, E.: Peptide Self-Assembly at the Nanoscale: A Challenging Target for Computational and Experimental Biotechnology. *Trends Biotechnol.* **2007**, *25*, 211-218.
- (124) Huang, K.; Tang, W.; Tang, R.; Xu, Z.; He, Z.; Li, Z.; Xu, Y.; Li, X.; He, G.; Feng, G.; He, L.; Shi, Y.: Positive Association between Olig2 and Schizophrenia in the Chinese Han Population. *Hum. Genet.* **2008**, *122*, 659-660.
- (125) Li, D.; Huang, J.; Kaner, R. B.: Polyaniline Nanofibers: A Unique Polymer Nanostructure for Versatile Applications. *Acc. Chem. Res.* **2009**, *42*, 135-145.
- (126) Brea, R. J.; Reiriz, C.; Granja, J. R.: Towards Functional Bionanomaterials Based on Self-Assembling Cyclic Peptide Nanotubes. *Chem. Soc. Rev.* **2010**, *39*, 1448-1456.
- (127) Feng, C.; Khulbe, K. C.; Matsuura, T.: Recent Progress in the Preparation, Characterization, and Applications of Nanofibers and Nanofiber Membranes Via Electrospinning/Interfacial Polymerization. *J. Appl. Polym. Sci.* **2010**, *115*, 756-776.
- (128) Anzini, P.; Xu, C.; Hughes, S.; Magnotti, E.; Jiang, T.; Hemmingsen, L.; Demeler, B.; Conticello, V. P.: Controlling Self-Assembly of a Peptide-Based Material Via Metal-Ion Induced Registry Shift. *J. Am. Chem. Soc.* **2013**, *135*, 10278-10281.
- (129) Tung, C.-H.; Wu, L.-Z.; Zhang, L.-P.; Chen, B.: Supramolecular Systems as Microreactors: Control of Product Selectivity in Organic Phototransformation. *Acc. Chem. Res.* **2002**, *36*, 39-47.
- (130) Yang, Q.; Han, D.; Yang, H.; Li, C.: Asymmetric Catalysis with Metal Complexes in Nanoreactors. *Chemistry – An Asian Journal* **2008**, *3*, 1214-1229.

- (131) Eddaoudi, M.; Moler, D. B.; Li, H. L.; Chen, B. L.; Reineke, T. M.; O'Keeffe, M.; Yaghi, O. M.: Modular Chemistry: Secondary Building Units as a Basis for the Design of Highly Porous and Robust Metal-Organic Carboxylate Frameworks. *Acc. Chem. Res.* **2001**, *34*, 319-330.
- (132) Rowsell, J. L. C.; Yaghi, O. M.: Metal-Organic Frameworks: A New Class of Porous Materials. *Microporous Mesoporous Mater.* **2004**, *73*, 3-14.
- (133) Malthete, J.; Levelut, A. M.; Lehn, J. M.: Tubular Mesophases - a Structural-Analysis. *Journal of the Chemical Society-Chemical Communications* **1992**, 1434-1436.
- (134) Zhang, J. S.; Moore, J. S.: Nanoarchitectures .6. Liquid-Crystals Based on Shape-Persistent Macrocyclic Mesogens. *J. Am. Chem. Soc.* **1994**, *116*, 2655-2656.
- (135) Cote, A. P.; Benin, A. I.; Ockwig, N. W.; O'Keeffe, M.; Matzger, A. J.; Yaghi, O. M.: Porous, Crystalline, Covalent Organic Frameworks. *Science* **2005**, *310*, 1166-1170.
- (136) Gorbitz, C. H.: Microporous Organic Materials from Hydrophobic Dipeptides. *Chemistry-a European Journal* **2007**, *13*, 1022-1031.
- (137) Shimizu, L. S.; Hughes, A. D.; Smith, M. D.; Samuel, S. A.; Ciurtin-Smith, D.: Assembled Columnar Structures from Bis-Urea Macrocycles. *Supramol. Chem.* **2005**, *17*, 27-30.
- (138) Geer, M. F.; Walla, M. D.; Solntsev, K. M.; Strassert, C. A.; Shimizu, L. S.: Self-Assembled Benzophenone Bis-Urea Macrocycles Facilitate Selective Oxidations by Singlet Oxygen. *The Journal of Organic Chemistry* **2013**, *78*, 5568-5578.
- (139) Eddaoudi, M.; Kim, J.; Rosi, N.; Vodak, D.; Wachter, J.; O'Keeffe, M.; Yaghi, O. M.: Systematic Design of Pore Size and Functionality in Isoreticular Mofs and Their Application in Methane Storage. *Science* **2002**, *295*, 469-472.
- (140) Rosi, N. L.; Eckert, J.; Eddaoudi, M.; Vodak, D. T.; Kim, J.; O'Keeffe, M.; Yaghi, O. M.: Hydrogen Storage in Microporous Metal-Organic Frameworks. *Science* **2003**, *300*, 1127-1129.
- (141) Sun, Y.; Wang, L.; Amer, W.; Yu, H.; Ji, J.; Huang, L.; Shan, J.; Tong, R.: Hydrogen Storage in Metal-Organic Frameworks. *J. Inorg. Organomet. Polym. Mater.* **2013**, *23*, 270-285.
- (142) Halder, G. J.; Kepert, C. J.; Moubaraki, B.; Murray, K. S.; Cashion, J. D.: Guest-Dependent Spin Crossover in a Nanoporous Molecular Framework Material. *Science* **2002**, *298*, 1762-1765.
- (143) Uemura, K.; Kitagawa, S.; Kondo, M.; Fukui, K.; Kitaura, R.; Chang, H. C.; Mizutani, T.: Novel Flexible Frameworks of Porous Cobalt(III) Coordination Polymers That Show Selective Guest Adsorption Based on the Switching of Hydrogen-Bond Pairs of Amide Groups. *Chemistry-a European Journal* **2002**, *8*, 3586-3600.
- (144) Lerner, M. B.; Kybert, N.; Mendoza, R.; Villechenon, R.; Bonilla Lopez, M. A.; Charlie Johnson, A. T.: Scalable, Non-Invasive Glucose Sensor Based on Boronic Acid Functionalized Carbon Nanotube Transistors. *Appl. Phys. Lett.* **2013**, *102*, -.
- (145) Kim, H. S.; Hartgerink, J. D.; Ghadiri, M. R.: Oriented Self-Assembly of Cyclic Peptide Nanotubes in Lipid Membranes. *J. Am. Chem. Soc.* **1998**, *120*, 4417-4424.
- (146) Helsel, A. J.; Brown, A. L.; Yamato, K.; Feng, W.; Yuan, L.; Clements, A. J.; Harding, S. V.; Szabo, G.; Shao, Z.; Gong, B.: Highly Conducting Transmembrane Pores Formed by Aromatic Oligoamide Macrocycles. *J. Am. Chem. Soc.* **2008**, *130*, 15784-15785.
- (147) Corma, A.; Garcia, H.: Zeolite-Based Photocatalysts. *Chem. Commun.* **2004**, 1443-1459.
- (148) Fiedler, D.; Leung, D. H.; Bergman, R. G.; Raymond, K. N.: Selective Molecular Recognition, C-H Bond Activation, and Catalysis in Nanoscale Reaction Vessels. *Acc. Chem. Res.* **2005**, *38*, 349-358.
- (149) Vriezema, D. M.; Aragonés, M. C.; Elemans, J.; Cornelissen, J.; Rowan, A. E.; Nolte, R. J. M.: Self-Assembled Nanoreactors. *Chem. Rev.* **2005**, *105*, 1445-1489.
- (150) Granja, J. R.; Ghadiri, M. R.: Channel-Mediated Transport of Glucose across Lipid Bilayers. *J. Am. Chem. Soc.* **1994**, *116*, 10785-10786.
- (151) Clark, T. D.; Buehler, L. K.; Ghadiri, M. R.: Self-Assembling Cyclic Beta(3)-Peptide Nanotubes as Artificial Transmembrane Ion Channels. *J. Am. Chem. Soc.* **1998**, *120*, 651-656.

- (152) Gokel, G. W.; Mukhopadhyay, A.: Synthetic Models of Cation-Conducting Channels. *Chem. Soc. Rev.* **2001**, *30*, 274-286.
- (153) Montenegro, J.; Ghadiri, M. R.; Granja, J. R.: Ion Channel Models Based on Self-Assembling Cyclic Peptide Nanotubes. *Acc. Chem. Res.* **2013**.
- (154) Otis, F.; Auger, M.; Voyer, N.: Exploiting Peptide Nanostructures to Construct Functional Artificial Ion Channels. *Acc. Chem. Res.* **2013**.
- (155) Langmi, H. W.; McGrady, G. S.: Non-Hydride Systems of the Main Group Elements as Hydrogen Storage Materials. *Coord. Chem. Rev.* **2007**, *251*, 925-935.
- (156) Ward, M. D.: Molecular Fuel Tanks. *Science* **2003**, *300*, 1104-1105.
- (157) Fraenkel, D.; Shabtai, J.: Encapsulation of Hydrogen in Molecular-Sieve Zeolites. *J. Am. Chem. Soc.* **1977**, *99*, 7074-7076.
- (158) Weitkamp, J.; Fritz, M.; Ernst, S.: Zeolites as Media for Hydrogen Storage. *Int. J. Hydrogen Energy* **1995**, *20*, 967-970.
- (159) Kessel, D.; Reiners, J.: Light-Activated Pharmaceuticals: Mechanisms and Detection. *Isr. J. Chem.* **2012**, *52*, 674-680.
- (160) Ogilby, P. R.: Singlet Oxygen: There Is Indeed Something New under the Sun. *Chem. Soc. Rev.* **2010**, *39*, 3181-3209.
- (161) Cuquerella, M. C.; Lhiaubet-Vallet, V.; Cadet, J.; Miranda, M. A.: Benzophenone Photosensitized DNA Damage. *Acc. Chem. Res.* **2012**, *45*, 1558-1570.
- (162) Arumugam, S.: Alkali Metal Cation Exchanged Nafion as an Efficient Micro-Environment for Oxidation of Olefins by Singlet Oxygen. *Journal of Photochemistry and Photobiology A: Chemistry* **2008**, *199*, 242-249.
- (163) Griesbeck, A. G.; Cho, M.: Singlet Oxygen Addition to Homoallylic Substrates in Solution and Microemulsion: Novel Secondary Reactions. *Tetrahedron Lett.* **2009**, *50*, 121-123.

Chapter 2

- (1) Shirakawa, H.; Ikeda, S.: Infrared Spectra of Poly(Acetylene). *Polymer Journal* **1971**, *2*, 231.
- (2) Burroughes, J. H.; Jones, C. A.; Friend, R. H.: New Semiconductor-Device Physics in Polymer Diodes and Transistors. *Nature* **1988**, *335*, 137-141.
- (3) Sirringhaus, H.; Tessler, N.; Friend, R. H.: Integrated Optoelectronic Devices Based on Conjugated Polymers. *Science* **1998**, *280*, 1741-1744.
- (4) Sauteret, C.; Hermann, J. P.; Frey, R.; Pradere, F.; Ducuing, J.; Baughman, R. H.; Chance, R. R.: Optical Nonlinearities in One-Dimensional-Conjugated Polymer Crystals. *Phys. Rev. Lett.* **1976**, *36*, 956-959.
- (5) Burroughes, J. H.; Bradley, D. D. C.; Brown, A. R.; Marks, R. N.; Mackay, K.; Friend, R. H.; Burns, P. L.; Holmes, A. B.: Light-Emitting-Diodes Based on Conjugated Polymers. *Nature* **1990**, *347*, 539-541.
- (6) Friend, R. H.; Gymer, R. W.; Holmes, A. B.; Burroughes, J. H.; Marks, R. N.; Taliani, C.; Bradley, D. D. C.; Dos Santos, D. A.; Bredas, J. L.; Logdlund, M.; Salaneck, W. R.: Electroluminescence in Conjugated Polymers. *Nature* **1999**, *397*, 121-128.
- (7) Wang, C. S.; Burkett, J.; Lee, C. Y. C.; Arnold, F. E.: Structure and Electrical-Conductivity of Ion-Implanted Rigid-Rod and Ladder Polymers. *Journal of Polymer Science Part B-Polymer Physics* **1993**, *31*, 1799-1807.
- (8) Wegner, G.: Topochemical Reactions of Monomers with Conjugated Triple Bonds .I. Polymerization of 2,4-Hexadiyn-1,6-Diols Derivatives in Crystalline State. *Zeitschrift Fur*

Naturforschung Part B-Chemie Biochemie Biophysik Biologie Und Verwandten Gebiete **1969**, B 24, 824.

(9) Cohen, M. D.; Schmidt, G. M. J.: Topochemistry .1. Survey. *Journal of the Chemical Society* **1964**, 1996.

(10) Enkelmann, V.: Solid-State Reactivity of Triacetylenes. *Chem. Mater.* **1994**, 6, 1337-1340.

(11) McGhie, A. R.; Kalyanaraman, P. S.; Garito, A. F.: Kinetics of Thermal Polymerization in Solid-State - 2,4-Hexadiyne-1,6 Diol Bis (Para-Toluenesulfonate). *Journal of Polymer Science Part C-Polymer Letters* **1978**, 16, 335-338.

(12) Bloor, D.; Koski, L.; Stevens, G. C.; Preston, F. H.; Ando, D. J.: Solid-State Polymerization of Bis-(Para-Toluene Sulfonate) of 2,4-Hexadiyne-1,6-Diol .1. X-Ray-Diffraction and Spectroscopic Observations. *J. Mater. Sci.* **1975**, 10, 1678-1688.

(13) Baughman, R. H.: Solid-State Reaction-Kinetics in Single-Phase Polymerizations. *J. Chem. Phys.* **1978**, 68, 3110-3121.

(14) Chance, R. R.; Eckhardt, H.; Swerdloff, M.; Federici, R. R.; Szobota, J. S.; Turi, E. A.; Boudreaux, D. S.; Schott, M.: Urethane-Substituted Polydiacetylenes - Solid-State Polymerization, Crystal Optics, and Conformational Transitions. *ACS Symp. Ser.* **1987**, 337, 140-151.

(15) Spagnoli, S.; Berrehar, J.; LapersonneMeyer, C.; Schott, M.; Rameau, A.; Rawiso, M.: Gamma-Ray Polymerization of Urethane-Substituted Diacetylenes: Reactivity and Chain Lengths. *Macromolecules* **1996**, 29, 5615-5620.

(16) Chang, Y. L.; West, M. A.; Fowler, F. W.; Lauher, J. W.: An Approach to the Design of Molecular-Solids - Strategies for Controlling the Assembly of Molecules into 2-Dimensional Layered Structures. *J. Am. Chem. Soc.* **1993**, 115, 5991-6000.

(17) Coe, S.; Kane, J. J.; Nguyen, T. L.; Toledo, L. M.; Wininger, E.; Fowler, F. W.; Lauher, J. W.: Molecular Symmetry and the Design of Molecular Solids: The Oxalamide Functionality as a Persistent Hydrogen Bonding Unit. *J. Am. Chem. Soc.* **1997**, 119, 86-93.

(18) Curtis, S. M.; Le, N.; Fowler, F. W.; Lauher, J. W.: A Rational Approach to the Preparation of Polydipyridyldiacetylenes: An Exercise in Crystal Design. *Cryst. Growth Des.* **2005**, 5, 2313-2321.

(19) Curtis, S. M.; Le, N.; Nguyen, T.; Xi, O. Y.; Tran, T.; Fowler, F. W.; Lauher, J. W.: What Have We Learned About Topochemical Diacetylene Polymerizations? *Supramol. Chem.* **2005**, 17, 31-36.

(20) Fowler, F. W.; Lauher, J. W.: A Rational Design of Molecular Materials. *J. Phys. Org. Chem.* **2000**, 13, 850-857.

(21) Kane, J. J.; Liao, R. F.; Lauher, J. W.; Fowler, F. W.: Preparation of Layered Diacetylenes as a Demonstration of Strategies for Supramolecular Synthesis. *J. Am. Chem. Soc.* **1995**, 117, 12003-12004.

(22) Kane, J. J.; Nguyen, T.; Xiao, J.; Fowler, F. W.; Lauher, J. W.: The Host Guest Co-Crystal Approach to Supramolecular Structure. *Mol. Cryst. Liq. Cryst.* **2001**, 356, 449-458.

(23) Liao, R. F.; Lauher, J. W.; Fowler, F. W.: The Application of the 2-Amino-4-Pyrimidones to Supramolecular Synthesis. *Tetrahedron* **1996**, 52, 3153-3162.

(24) Nguyen, T. L.; Fowler, F. W.; Lauher, J. W.: Commensurate and Incommensurate Hydrogen Bonds. An Exercise in Crystal Engineering. *J. Am. Chem. Soc.* **2001**, 123, 11057-11064.

(25) Nguyen, T. L.; Scott, A.; Dinkelmeyer, B.; Fowler, F. W.; Lauher, J. W.: Design of Molecular Solids: Utility of the Hydroxyl Functionality as a Predictable Design Element. *New J. Chem.* **1998**, 22, 129-135.

(26) Ouyang, X.; Fowler, F. W.; Lauher, J. W.: Single-Crystal-to-Single-Crystal Topochemical Polymerizations of a Terminal Diacetylene: Two Remarkable Transformations Give the Same Conjugated Polymer. *J. Am. Chem. Soc.* **2003**, 125, 12400-12401.

- (27) Toledo, L. M.; Lauher, J. W.; Fowler, F. W.: Design of Molecular-Solids - Application of 2-Amino-4(1h)-Pyridones to the Preparation of Hydrogen-Bonded Alpha-Networks and Beta-Networks. *Chem. Mater.* **1994**, *6*, 1222-1226.
- (28) Toledo, L. M.; Musa, K. M.; Lauher, J. W.; Fowler, F. W.: Development of Strategies for the Preparation of Designed Solids - an Investigation of the 2-Amino-4(1h)-Pyrimidone Ring-System for the Molecular Self-Assembly of Hydrogen-Bonded Alpha-Networks and Beta-Networks. *Chem. Mater.* **1995**, *7*, 1639-1647.
- (29) Zhao, X. Q.; Chang, Y. L.; Fowler, F. W.; Lauher, J. W.: An Approach to the Design of Molecular-Solids - the Ureylenedicarboxylic Acids. *J. Am. Chem. Soc.* **1990**, *112*, 6627-6634.
- (30) Okuno, T.; Izuoka, A.; Ito, T.; Kubo, S.; Sugawara, T.; Sato, N.; Sugawara, Y.: Reactivity of Mesogenic Diacetylenes Coupled with Phase Transitions between Crystal and Liquid Crystal Phases. *Journal of the Chemical Society-Perkin Transactions 2* **1998**, 889-895.
- (31) Xiao, J.; Yang, M.; Lauher, J. W.; Fowler, F. W.: A Supramolecular Solution to a Long-Standing Problem: The 1,6-Polymerization of a Triacetylene. *Angewandte Chemie-International Edition* **2000**, *39*, 2132.
- (32) Hoang, T.; Lauher, J. W.; Fowler, F. W.: The Topochemical 1,16-Polymerization of a Triene. *J. Am. Chem. Soc.* **2002**, *124*, 10656-10657.
- (33) Ajayan, P. M.: Nanotubes from Carbon. *Chem. Rev.* **1999**, *99*, 1787-1799.
- (34) Baughman, R. H.; Zakhidov, A. A.; de Heer, W. A.: Carbon Nanotubes - the Route toward Applications. *Science* **2002**, *297*, 787-792.
- (35) Bong, D. T.; Clark, T. D.; Granja, J. R.; Ghadiri, M. R.: Self-Assembling Organic Nanotubes. *Angewandte Chemie-International Edition* **2001**, *40*, 988-1011.
- (36) Gattuso, G.; Menzer, S.; Nepogodiev, S. A.; Stoddart, J. F.; Williams, D. J.: Carbohydrate Nanotubes. *Angewandte Chemie-International Edition in English* **1997**, *36*, 1451-1454.
- (37) Pasini, D.; Ricci, M.: Macrocycles as Precursors for Organic Nanotubes. *Curr. Org. Synth.* **2007**, *4*, 59-80.
- (38) Hecht, S.; Khan, A.: Intramolecular Cross-Linking of Helical Folds: An Approach to Organic Nanotubes. *Angewandte Chemie-International Edition* **2003**, *42*, 6021-6024.
- (39) Yashima, E.; Maeda, K.; Furusho, Y.: Single- and Double-Stranded Helical Polymers: Synthesis, Structures, and Functions. *Acc. Chem. Res.* **2008**, *41*, 1166-1180.
- (40) Hill, J. P.; Jin, W. S.; Kosaka, A.; Fukushima, T.; Ichihara, H.; Shimomura, T.; Ito, K.; Hashizume, T.; Ishii, N.; Aida, T.: Self-Assembled Hexa-Peri-Hexabenzocoronene Graphitic Nanotube. *Science* **2004**, *304*, 1481-1483.
- (41) Moore, J. S.: Shape-Persistent Molecular Architectures of Nanoscale Dimension. *Acc. Chem. Res.* **1997**, *30*, 402-413.
- (42) Harada, A.; Hashizume, A.; Yamaguchi, H.; Takashima, Y.: Polymeric Rotaxanes. *Chem. Rev.* **2009**, *109*, 5974-6023.
- (43) Hartgerink, J. D.; Clark, T. D.; Ghadiri, M. R.: Peptide Nanotubes and Beyond. *Chemistry-a European Journal* **1998**, *4*, 1367-1372.
- (44) Xu, Y.; Smith, M. D.; Geer, M. F.; Pellechia, P. J.; Brown, J. C.; Wibowo, A. C.; Shimizu, L. S.: Thermal Reaction of a Columnar Assembled Diacetylene Macrocyclic. *J. Am. Chem. Soc.* **2010**, *132*, 5334.
- (45) Lauher, J. W.; Fowler, F. W.; Goroff, N. S.: Single-Crystal-to-Single-Crystal Topochemical Polymerizations by Design. *Acc. Chem. Res.* **2008**, *41*, 1215-1229.
- (46) Baughman, R. H.: Solid-State Synthesis of Large Polymer Single-Crystals. *Journal of Polymer Science Part B-Polymer Physics* **1974**, *12*, 1511-1535.
- (47) Li, Z.; Fowler, F. W.; Lauher, J. W.: Weak Interactions Dominating the Supramolecular Self-Assembly in a Salt: A Designed Single-Crystal-to-Single-Crystal Topochemical Polymerization of a Terminal Aryldiacetylene. *J. Am. Chem. Soc.* **2009**, *131*, 634-643.

- (48) Sun, A. W.; Lauher, J. W.; Goroff, N. S.: Preparation of Poly(Diiododiacetylene), an Ordered Conjugated Polymer of Carbon and Iodine. *Science* **2006**, *312*, 1030-1034.
- (49) Baldwin, K. P.; Matzger, A. J.; Scheiman, D. A.; Tessier, C. A.; Vollhardt, K. P. C.; Youngs, W. J.: Synthesis, Crystal-Structure, and Polymerization of 1,2/5,6/9,10-Tribenzo-3,7,11,13-Tetrahydro 14 Annulene. *Synlett* **1995**, 1215.
- (50) Haley, M. M.; Brand, S. C.; Pak, J. J.: Carbon Networks Based on Dehydrobenzoannulenes: Synthesis of Graphdiyne Substructures. *Angewandte Chemie-International Edition in English* **1997**, *36*, 836-838.
- (51) Suzuki, M.; Comito, A.; Khan, S. I.; Rubin, Y.: Nanochannel Array within a Multilayered Network of a Planarized Dehydro 24 Annulene. *Org. Lett.* **2010**, *12*, 2346-2349.
- (52) Nagasawa, J. i.; Yoshida, M.; Tamaoki, N.: Synthesis, Gelation Properties and Photopolymerization of Macrocyclic Diacetylenedicarboxamides Derived from L-Glutamic Acid and Trans-1,4-Cyclohexanediol. *Eur. J. Org. Chem.* **2011**, 2247-2255.
- (53) Dalgarno, S. J.; Thallapally, P. K.; Barbour, L. J.; Atwood, J. L.: Engineering Void Space in Organic Van Der Waals Crystals: Calixarenes Lead the Way. *Chem. Soc. Rev.* **2007**, *36*, 236-245.

Chapter 3

- (1) Chui, J. K. W.; Fyles, T. M.: Ionic Conductance of Synthetic Channels: Analysis, Lessons, and Recommendations. *Chem. Soc. Rev.* **2012**, *41*, 148-175.
- (2) Matile, S.; Vargas Jentsch, A.; Montenegro, J.; Fin, A.: Recent Synthetic Transport Systems. *Chem. Soc. Rev.* **2011**, *40*, 2453-2474.
- (3) Carlson, L. J.; Krauss, T. D.: Photophysics of Individual Single-Walled Carbon Nanotubes. *Acc. Chem. Res.* **2008**, *41*, 235-243.
- (4) Xu, Y.; Smith, M. D.; Krause, J. A.; Shimizu, L. S.: Control of the Intramolecular [2+2] Photocycloaddition in a Bis-Stilbene Macrocyclic. *The Journal of Organic Chemistry* **2009**, *74*, 4874-4877.
- (5) Roy, K.; Wibowo, A. C.; Pellechia, P. J.; Ma, S.; Geer, M. F.; Shimizu, L. S.: Absorption of Hydrogen Bond Donors by Pyridyl Bis-Urea Crystals. *Chem. Mater.* **2012**, *24*, 4773-4781.
- (6) Lim, Y.-b.; Moon, K.-S.; Lee, M.: Stabilization of an A Helix by B-Sheet-Mediated Self-Assembly of a Macrocyclic Peptide. *Angew. Chem., Int. Ed.* **2009**, *48*, 1601-1605.
- (7) Roy, K.; Wang, C.; Smith, M. D.; Pellechia, P. J.; Shimizu, L. S.: Alkali Metal Ions as Probes of Structure and Recognition Properties of Macrocyclic Pyridyl Urea Hosts. *The Journal of Organic Chemistry* **2010**, *75*, 5453-5460.
- (8) Yang, J.; Dewal, M. B.; Profeta, S.; Smith, M. D.; Li, Y.; Shimizu, L. S.: Origins of Selectivity for the [2+2] Cycloaddition of A,B-Unsaturated Ketones within a Porous Self-Assembled Organic Framework. *J. Am. Chem. Soc.* **2007**, *130*, 612-621.
- (9) Abe, H.; Chida, Y.; Kurokawa, H.; Inouye, M.: Selective Binding of D_{2h}-Symmetrical, Acetylene-Linked Pyridine/Pyridone Macrocycles to Maltoside. *The Journal of Organic Chemistry* **2011**, *76*, 3366-3371.
- (10) Shimizu, L. S.; Hughes, A. D.; Smith, M. D.; Samuel, S. A.; Ciurtin-Smith, D.: Assembled Columnar Structures from Bis-Urea Macrocycles. *Supramol. Chem.* **2005**, *17*, 27-30.
- (11) Shimizu, L. S.; Hughes, A. D.; Smith, M. D.; Davis, M. J.; Zhang, B. P.; zur Loye, H.-C.; Shimizu, K. D.: Self-Assembled Nanotubes That Reversibly Bind Acetic Acid Guests. *J. Am. Chem. Soc.* **2003**, *125*, 14972-14973.

- (12) Ouyang, X.; Fowler, F. W.; Lauher, J. W.: Single-Crystal-to-Single-Crystal Topochemical Polymerizations of a Terminal Diacetylene: Two Remarkable Transformations Give the Same Conjugated Polymer. *J. Am. Chem. Soc.* **2003**, *125*, 12400-12401.
- (13) Kim, W. H.; Kodali, N. B.; Kumar, J.; Tripathy, S. K.: A Novel, Soluble Poly(Diacetylene) Containing an Aromatic Substituent. *Macromolecules* **1994**, *27*, 1819-1824.
- (14) Semetey, V.; Didierjean, C.; Briand, J.-P.; Aubry, A.; Guichard, G.: Self-Assembling Organic Nanotubes from Enantiopure Cyclo-N,N'-Linked Oligoureas: Design, Synthesis, and Crystal Structure. *Angew. Chem., Int. Ed.* **2002**, *41*, 1895-1898.
- (15) Ranganathan, D.; Lakshmi, C.; Karle, I. L.: Hydrogen-Bonded Self-Assembled Peptide Nanotubes from Cystine-Based Macrocyclic Bisureas. *J. Am. Chem. Soc.* **1999**, *121*, 6103-6107.
- (16) Hemmerlin, C.; Marraud, M.; Rognan, D.; Graff, R.; Semetey, V.; Briand, J.-P.; Guichard, G.: Helix-Forming Oligoureas: Temperature-Dependent Nmr, Structure Determination, and Circular Dichroism of a Nonamer with Functionalized Side Chains. *Helv. Chim. Acta* **2002**, *85*, 3692-3711.
- (17) Harris, K. D. M.: Fundamental and Applied Aspects of Urea and Thiourea Inclusion Compounds. *Supramol. Chem.* **2007**, *19*, 47-53.
- (18) Harris, K. D. M.: Meldola Lecture: Understanding the Properties of Urea and Thiourea Inclusion Compounds. *Chem. Soc. Rev.* **1997**, *26*, 279-289.
- (19) Yang, J.; Dewal, M. B.; Sobransingh, D.; Smith, M. D.; Xu, Y.; Shimizu, L. S.: Examination of the Structural Features That Favor the Columnar Self-Assembly of Bis-Urea Macrocycles. *The Journal of Organic Chemistry* **2008**, *74*, 102-110.

Chapter 4

- (1) Bankston, D.: Oxidative Cleavage of an Aromatic Ring: Cis,Cis-Monomethyl Muconate from 1,2-Dihydroxybenzene. In *Org. Synth.*; John Wiley & Sons, Inc., 2003.
- (2) Hunter, C. A.; Misuraca, M. C.; Turega, S. M.: Dissection of Complex Molecular Recognition Interfaces. *J. Am. Chem. Soc.* **2010**, *133*, 582-594.
- (3) Wang, T.: The Topochemical Polymerization of Diacetylenes Using Supramolecular Host-Guest Chemistry. Stony Brook University, 2005.
- (4) Chow, S. K.: Synthesis of 2,6-Pyridine-Based Diacetylene Macrocycle and Its Possible Formation to a Covalent Bonded Tubular Structure Via Topochemical Polymerization, Stony Brook University. Stony Brook University, 2008.
- (5) Waki, M.; Abe, H.; Inouye, M.: Helix Formation in Synthetic Polymers by Hydrogen Bonding with Native Saccharides in Protic Media. *Chemistry – A European Journal* **2006**, *12*, 7839-7847.
- (6) Brennan, D. J.; White, J. E.; Haag, A. P.; Kram, S. L.; Mang, M. N.; Pikulin, S.; Brown, C. N.: Poly(Hydroxy Amide Ethers): New High-Barrier Thermoplastics. *Macromolecules* **1996**, *29*, 3707-3716.
- (7) Luong Nguyen, T.; Scott, A.; Dinkelmeyer, B.; W. Fowler, F.; W. Lauher, J.: Design of Molecular Solids: Utility of the Hydroxyl Functionality as a Predictable Design Element. *New J. Chem.* **1998**, *22*, 129-135.
- (8) Xi, G.-L.; Liu, Z.-Q.: Antioxidant Effectiveness Generated by One or Two Phenolic Hydroxyl Groups in Coumarin-Substituted Dihydropyrazoles. *Eur. J. Med. Chem.* **2013**, *68*, 385-393.
- (9) Hsu, T.-J.; Fowler, F. W.; Lauher, J. W.: Preparation and Structure of a Tubular Addition Polymer: A True Synthetic Nanotube. *J. Am. Chem. Soc.* **2011**, *134*, 142-145.

- (10) Fu, T.-h.; Li, Y.; Thaker, H. D.; Scott, R. W.; Tew, G. N.: Expedient Synthesis of Smamps Via Click Chemistry. *ACS Medicinal Chemistry Letters* **2013**, *4*, 841-845.
- (11) Passiniemi, M.; Koskinen, A. M. P.: Stereoselective Total Synthesis of Pachastrissamine (Jaspine B). *Tetrahedron Lett.* **2008**, *49*, 980-983.
- (12) Trost, B. M.; Livingston, R. C.: An Atom-Economic and Selective Ruthenium-Catalyzed Redox Isomerization of Propargylic Alcohols. An Efficient Strategy for the Synthesis of Leukotrienes. *J. Am. Chem. Soc.* **2008**, *130*, 11970-11978.
- (13) Bergmann, E. D.; Pelchowicz, Z.: Syntheses of Macrocyclic Compounds. *J. Am. Chem. Soc.* **1953**, *75*, 4281-4286.

Appendix

Molecular Structure and Crystallography Data

Molecular Structure and Crystallography Data for Compound ct3t

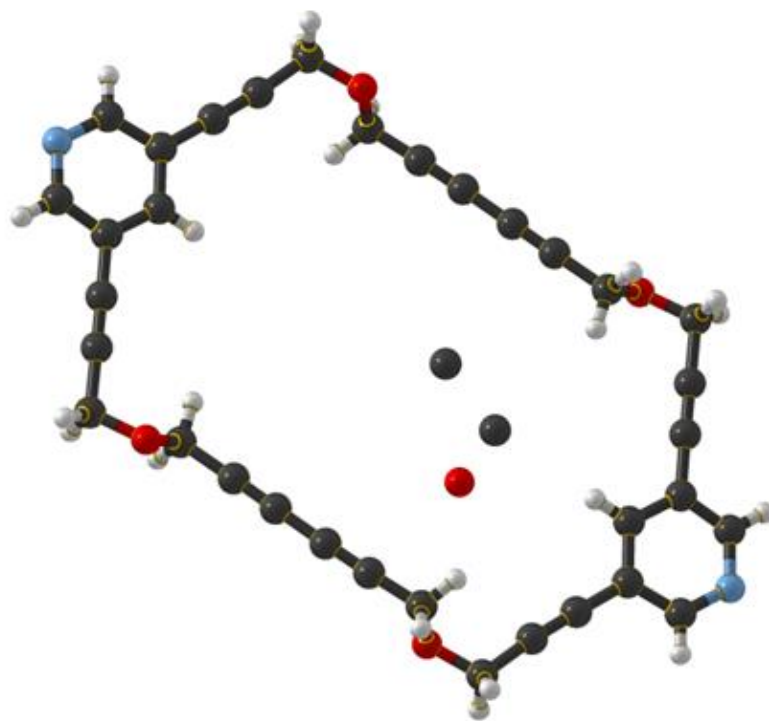


Table 1. Crystal data and structure refinement for ct3t.

Identification code	ct3t	
Empirical formula	C ₃₄ H ₂₂ N ₂ O ₄	
Formula weight	522.54	
Temperature	273(2) K	
Wavelength	0.71073 nm	
Crystal system	monoclinic	
Space group	P2 ₁ /n	
Unit cell dimensions	a = 4.113(4) Å	α = 90°
	b = 16.795(17) Å	β = 92.482(15)°
	c = 23.25(2) Å	γ = 90°
Volume	1604(3) Å ³	
Z	2	
Density (calculated)	1.082 Mg/m ³	
Absorption coefficient	0.072 mm ⁻¹	
F(000)	544	
Theta range for data collection	1.50 to 28.86°	
Index ranges	-5 ≤ h ≤ 5, -21 ≤ k ≤ 18, -28 ≤ l ≤ 29	
Reflections collected	10022	
Independent reflections	3792 [R(int) = 0.1921]	
Completeness to theta = 28.86°	89.7 %	
Refinement method	Full-matrix least-squares on F ²	
Data / restraints / parameters	3792 / 0 / 223	
Goodness-of-fit on F ²	0.716	
Final R indices [I > 2σ(I)]	R1 = 0.1054, wR2 = 0.2572	
R indices (all data)	R1 = 0.3721, wR2 = 0.3976	
Largest diff. peak and hole	0.624 and -0.281 e.Å ⁻³	

Table 2. Atomic coordinates ($\times 10^4$) and equivalent isotropic displacement parameters ($\text{\AA}^2 \times 10^3$) for ct3t. $U(\text{eq})$ is defined as one third of the trace of the orthogonalized U_{ij} tensor.

	x	y	z	$U(\text{eq})$
N(1)	5514(18)	9940(4)	8661(3)	72(4)
C(9)	3730(20)	9446(5)	8332(4)	62(5)
C(5)	2770(20)	8709(5)	8520(4)	45(4)
C(6)	3790(20)	8457(5)	9067(4)	66(5)
C(8)	6450(20)	9696(5)	9185(4)	76(5)
C(10)	6840(20)	8745(5)	9965(6)	77(6)
C(11)	7830(20)	8582(5)	10430(7)	66(6)
C(12)	9040(30)	8378(6)	11029(4)	79(5)
O(2)	7335(14)	7724(3)	11250(2)	73(3)
C(7)	5650(20)	8962(5)	9404(4)	65(5)
C(3)	-770(20)	7801(5)	7808(4)	76(3)
C(4)	860(20)	8209(5)	8141(4)	73(3)
O(1)	-4000(14)	6640(3)	7607(2)	83(2)
C(14)	6590(20)	6350(6)	11292(4)	89(3)
C(2)	-2690(20)	7361(5)	7386(3)	77(2)
C(13)	8070(20)	7006(5)	10975(4)	89(3)
C(15)	5460(20)	5814(6)	11537(4)	84(3)
C(1)	-1680(20)	6040(5)	7669(4)	92(3)
C(17)	-3040(30)	5376(5)	7933(4)	89(3)
C(16)	-4140(20)	4812(5)	8167(4)	83(3)
O(101)	-1350(40)	6562(6)	9278(5)	226(7)
C(101)	3100(200)	6087(15)	9381(10)	740(80)
C(102)	1780(50)	5622(17)	10037(9)	366(19)

Table 3. Bond lengths Å and angles ° for ct3t.

N(1)-C(8)	1.326(10)
N(1)-C(9)	1.327(11)
C(9)-C(5)	1.376(12)
C(5)-C(6)	1.387(11)
C(5)-C(4)	1.428(13)
C(6)-C(7)	1.365(11)
C(8)-C(7)	1.379(11)
C(10)-C(11)	1.170(11)
C(10)-C(7)	1.421(19)
C(11)-C(12)	1.50(2)
C(12)-O(2)	1.412(9)
O(2)-C(13)	1.403(9)
C(3)-C(4)	1.214(11)
C(3)-C(2)	1.437(12)
O(1)-C(1)	1.391(9)
O(1)-C(2)	1.430(9)
C(14)-C(15)	1.173(12)
C(14)-C(13)	1.470(12)
C(15)-C(16)#1	1.382(13)
C(1)-C(17)	1.402(12)
C(17)-C(16)	1.190(12)
C(16)-C(15)#1	1.382(13)
O(101)-C(101)	1.99(8)
C(101)-C(102)	1.81(5)
C(8)-N(1)-C(9)	117.9(8)
N(1)-C(9)-C(5)	122.5(9)
C(6)-C(5)-C(9)	119.1(8)
C(6)-C(5)-C(4)	121.5(8)
C(9)-C(5)-C(4)	119.4(9)
C(7)-C(6)-C(5)	118.4(8)
N(1)-C(8)-C(7)	123.4(9)
C(11)-C(10)-C(7)	178.7(9)
C(10)-C(11)-C(12)	178.9(10)

O(2)-C(12)-C(11)	111.5(8)
C(13)-O(2)-C(12)	112.5(7)
C(6)-C(7)-C(8)	118.7(9)
C(6)-C(7)-C(10)	122.0(8)
C(8)-C(7)-C(10)	119.3(9)
C(4)-C(3)-C(2)	176.1(9)
C(3)-C(4)-C(5)	178.2(9)
C(1)-O(1)-C(2)	112.5(7)
C(15)-C(14)-C(13)	178.3(11)
O(1)-C(2)-C(3)	113.2(7)
O(2)-C(13)-C(14)	108.2(8)
C(14)-C(15)-C(16)#1	179.3(11)
C(17)-C(1)-O(1)	109.6(8)
C(16)-C(17)-C(1)	178.4(11)
C(17)-C(16)-C(15)#1	176.8(11)
O(101)-C(101)-C(102)	89(4)

Symmetry transformations used to generate equivalent atoms:

#1 -x,-y+1,-z+2

Table 4. Anisotropic displacement parameters ($\times 10^3$) for ct3t. The anisotropic displacement factor exponent takes the form: $-2\pi^2 [h^2 a^{*2} U^{11} + \dots + 2 h k a^* b^* U^{12}]$

	U ¹¹	U ²²	U ³³	U ²³	U ¹³	U ¹²
N(1)	103(7)	52(5)	59(7)	4(4)	-4(5)	-6(4)
C(9)	86(9)	48(7)	54(8)	2(5)	9(5)	-2(5)
C(5)	47(6)	45(7)	42(7)	-13(4)	-8(4)	1(4)
C(6)	89(8)	54(7)	55(7)	5(4)	10(5)	0(5)
C(8)	118(9)	54(7)	55(8)	-3(5)	-7(5)	-14(5)
C(10)	95(8)	76(6)	60(13)	4(6)	-4(7)	-6(5)
C(11)	76(8)	61(6)	62(13)	3(5)	3(6)	-5(5)
C(12)	98(10)	71(7)	67(8)	11(5)	-4(5)	-11(5)
O(2)	106(5)	53(4)	59(4)	5(3)	10(3)	0(3)
C(7)	68(7)	71(8)	58(8)	2(5)	4(5)	4(5)
C(3)	86(7)	76(6)	68(6)	1(5)	5(5)	5(5)
C(4)	77(7)	71(6)	74(7)	18(5)	30(5)	17(5)
O(1)	101(5)	57(4)	93(4)	1(3)	20(3)	-6(3)
C(14)	111(8)	74(7)	80(7)	6(5)	-2(6)	13(6)
C(2)	93(7)	63(6)	76(6)	-2(4)	7(5)	-9(5)
C(13)	114(8)	72(7)	79(6)	18(5)	0(5)	-5(6)
C(15)	104(8)	72(7)	76(7)	6(5)	3(5)	3(6)
C(1)	106(8)	59(6)	112(8)	5(5)	27(6)	13(6)
C(17)	122(9)	55(6)	90(7)	1(5)	1(6)	-7(6)
C(16)	97(8)	69(6)	82(7)	0(5)	-13(5)	-1(5)
O(101)	402(19)	91(8)	195(10)	-8(6)	128(11)	-15(10)
C(101)	1900(200)	210(30)	138(18)	-18(17)	10(50)	450(80)
C(102)	280(20)	580(40)	218(19)	-270(20)	-122(18)	220(30)

Table 5. Hydrogen coordinates ($\times 10^4$) and isotropic displacement parameters ($\text{\AA}^2 \times 10^3$) for ct3t.

	x	y	z	U(eq)
H(9)	3104	9604	7960	75
H(6)	3218	7957	9201	79
H(8)	7705	10039	9418	91
H(12A)	11341	8252	11028	94
H(12B)	8777	8836	11278	94
H(2A)	-4461	7695	7240	93
H(2B)	-1342	7232	7066	93
H(13A)	10409	6934	10972	106
H(13B)	7208	7014	10580	106
H(1A)	-928	5891	7294	110
H(1B)	175	6231	7902	110

Molecular Structure and Crystallography Data for Compound m1ea.

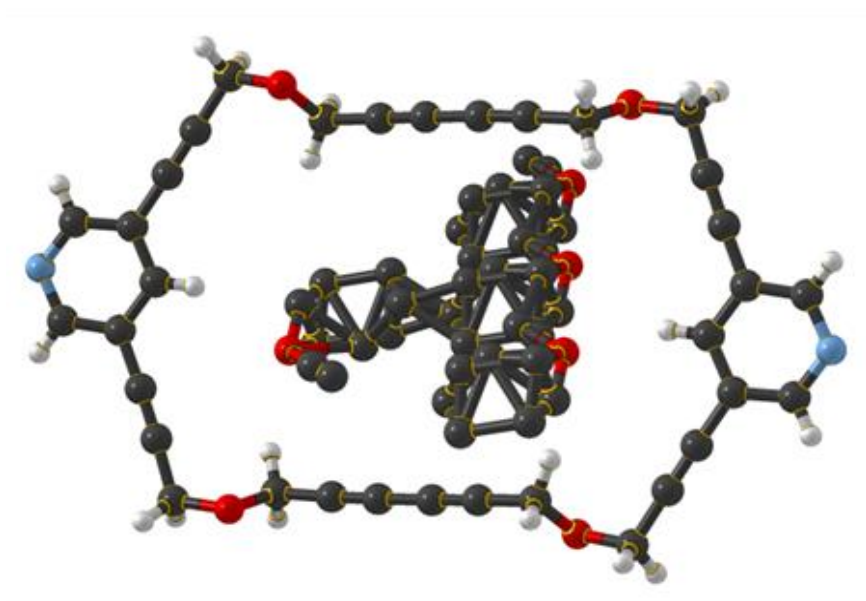


Table 1. Crystal data and structure refinement for m1ea.

Identification code	m1ea	
Empirical formula	C ₃₈ H ₃₀ N ₂ O ₆	
Formula weight	610.64	
Temperature	293(2) K	
Wavelength	1.54178 nm	
Crystal system	Monoclinic	
Space group	P2(1)/n	
Unit cell dimensions	a = 4.06810(10) Å	α = 90°
	b = 16.8512(5) Å	β = 91.601(3)°
	c = 23.1848(7) Å	γ = 90°
Volume	1588.75(8) Å ³	
Z	2	
Density (calculated)	1.276 Mg/m ³	
Absorption coefficient	0.706 mm ⁻¹	
F(000)	640	
Theta range for data collection	3.81 to 69.52°	
Index ranges	-4 ≤ h ≤ 4, -19 ≤ k ≤ 20, -27 ≤ l ≤ 28	
Reflections collected	11391	
Independent reflections	2938 [R(int) = 0.0219]	
Completeness to theta = 69.52°	99.2 %	
Absorption correction	None	
Refinement method	Full-matrix least-squares on F ²	
Data / restraints / parameters	2938 / 0 / 275	
Goodness-of-fit on F ²	1.140	
Final R indices [I > 2σ(I)]	R1 = 0.0571, wR2 = 0.1498	
R indices (all data)	R1 = 0.0636, wR2 = 0.1540	
Largest diff. peak and hole	0.675 and -0.216 e.Å ⁻³	

Table 2. Atomic coordinates ($\times 10^4$) and equivalent isotropic displacement parameters ($\text{\AA}^2 \times 10^3$) for m1ea. U(eq) is defined as one third of the trace of the orthogonalized U_{ij} tensor.

	x	y	z	U(eq)
O(1)	12421(4)	7312(1)	11229(1)	26(1)
O(3)	838(4)	8301(1)	7578(1)	27(1)
N(4)	10469(5)	5003(1)	8649(1)	29(1)
C(5)	10678(5)	6007(1)	9388(1)	23(1)
C(6)	7715(5)	6254(1)	8497(1)	24(1)
C(7)	12932(5)	6427(1)	10420(1)	25(1)
C(8)	9293(6)	9864(1)	11809(1)	31(1)
C(9)	2194(5)	7589(1)	7351(1)	25(1)
C(10)	8155(6)	10424(1)	12053(1)	32(1)
C(11)	14130(6)	6644(1)	11002(1)	27(1)
C(12)	11744(6)	8691(2)	11251(1)	31(1)
C(13)	10594(6)	9229(1)	11514(1)	31(1)
C(14)	8643(6)	5495(1)	8322(1)	26(1)
C(15)	13159(6)	8026(1)	10935(1)	30(1)
C(16)	5762(5)	6743(1)	8113(1)	24(1)
C(17)	8744(5)	6512(1)	9042(1)	23(1)
C(18)	4144(5)	7136(1)	7779(1)	24(1)
C(19)	11884(5)	6246(1)	9951(1)	24(1)
C(20)	11452(6)	5261(1)	9172(1)	25(1)
C(22)	3302(6)	8892(1)	7663(1)	34(1)
O(101)	3363(6)	8399(1)	9252(1)	36(1)
C(103)	6961(9)	9417(2)	10072(1)	39(1)
C(101)	4960(30)	9344(7)	9390(5)	76(5)
C(102)	7650(50)	8653(8)	9677(5)	60(4)
C(105)	410(90)	8677(10)	9451(13)	190(19)
C(104)	5840(90)	8783(12)	9180(12)	145(12)
C(108)	5070(100)	9650(30)	9970(30)	100(20)
C(106)	5100(400)	9640(40)	9590(90)	700(300)
C(110)	6070(50)	8398(16)	9522(12)	104(8)

C(109)	140(60)	8962(13)	9423(11)	96(9)
--------	---------	----------	----------	-------

Table 3. Bond lengths Å and angles ° for m1ea.

O(1)-C(15)	1.420(3)
O(1)-C(11)	1.432(3)
O(3)-C(22)	1.423(3)
O(3)-C(9)	1.428(3)
N(4)-C(14)	1.335(3)
N(4)-C(20)	1.339(3)
C(5)-C(20)	1.393(3)
C(5)-C(17)	1.397(3)
C(5)-C(19)	1.439(3)
C(6)-C(17)	1.389(3)
C(6)-C(14)	1.397(3)
C(6)-C(16)	1.437(3)
C(7)-C(19)	1.197(3)
C(7)-C(11)	1.467(3)
C(8)-C(10)	1.200(4)
C(8)-C(13)	1.383(3)
C(9)-C(18)	1.468(3)
C(10)-C(22)#1	1.461(3)
C(12)-C(13)	1.196(4)
C(12)-C(15)	1.465(3)
C(16)-C(18)	1.201(3)
C(22)-C(10)#1	1.461(3)
O(101)-C(104)	1.21(4)
O(101)-C(110)	1.25(3)
O(101)-C(105)	1.38(5)
C(103)-C(102)	1.608(11)
C(103)-C(108)#1	1.78(5)

C(103)-C(106)#1	1.97(19)
C(101)-C(106)	0.68(16)
C(101)-C(104)	1.13(2)
C(102)-C(110)	0.85(3)
C(102)-C(105)#2	1.25(4)
C(102)-C(109)#2	1.30(3)
C(105)-C(102)#3	1.25(4)
C(105)-C(110)#3	1.84(4)
C(105)-C(104)#3	1.95(4)
C(104)-C(109)#2	1.85(4)
C(104)-C(105)#2	1.95(4)
C(108)-C(106)	0.9(2)
C(108)-C(108)#1	1.20(10)
C(108)-C(106)#1	1.58(19)
C(108)-C(103)#1	1.78(5)
C(106)-C(108)#1	1.58(19)
C(106)-C(103)#1	1.97(19)
C(110)-C(105)#2	1.84(4)
C(110)-C(109)#2	1.93(3)
C(109)-C(102)#3	1.30(3)
C(109)-C(104)#3	1.85(4)
C(109)-C(110)#3	1.93(3)
C(15)-O(1)-C(11)	112.22(17)
C(22)-O(3)-C(9)	111.22(17)
C(14)-N(4)-C(20)	117.4(2)
C(20)-C(5)-C(17)	118.2(2)
C(20)-C(5)-C(19)	120.3(2)
C(17)-C(5)-C(19)	121.5(2)
C(17)-C(6)-C(14)	118.3(2)
C(17)-C(6)-C(16)	122.0(2)
C(14)-C(6)-C(16)	119.6(2)
C(19)-C(7)-C(11)	178.4(3)
C(10)-C(8)-C(13)	178.4(3)
O(3)-C(9)-C(18)	113.21(18)
C(8)-C(10)-C(22)#1	178.4(3)

O(1)-C(11)-C(7)	112.47(18)
C(13)-C(12)-C(15)	179.4(3)
C(12)-C(13)-C(8)	178.7(3)
N(4)-C(14)-C(6)	123.6(2)
O(1)-C(15)-C(12)	108.42(19)
C(18)-C(16)-C(6)	177.9(2)
C(6)-C(17)-C(5)	118.8(2)
C(16)-C(18)-C(9)	177.4(2)
C(7)-C(19)-C(5)	178.3(2)
N(4)-C(20)-C(5)	123.7(2)
O(3)-C(22)-C(10)#1	108.77(19)
C(104)-O(101)-C(110)	49.2(13)
C(104)-O(101)-C(105)	126.9(12)
C(110)-O(101)-C(105)	126.6(14)
C(102)-C(103)-C(108)#1	140(2)
C(102)-C(103)-C(106)#1	162.8(18)
C(108)#1-C(103)-C(106)#1	126(5)
C(106)-C(101)-C(104)	152(8)
C(110)-C(102)-C(105)#2	121(2)
C(110)-C(102)-C(109)#2	127(3)
C(105)#2-C(102)-C(109)#2	222.4(10)
C(110)-C(102)-C(103)	120(2)
C(105)#2-C(102)-C(103)	112.7(17)
C(109)#2-C(102)-C(103)	95.1(16)
C(102)#3-C(105)-O(101)	158.0(12)
C(102)#3-C(105)-C(110)#3	323.2(10)
O(101)-C(105)-C(110)#3	142.2(17)
C(102)#3-C(105)-C(104)#3	344.2(13)
O(101)-C(105)-C(104)#3	139(2)
C(110)#3-C(105)-C(104)#3	331.2(12)
C(101)-C(104)-O(101)	96(3)
C(101)-C(104)-C(109)#2	92(2)
O(101)-C(104)-C(109)#2	145.9(18)
C(101)-C(104)-C(105)#2	104(2)
O(101)-C(104)-C(105)#2	133.9(17)
C(109)#2-C(104)-C(105)#2	214.7(6)

C(106)-C(108)-C(108)#1 98(7)
 C(106)-C(108)-C(106)#1 131(9)
 C(108)#1-C(108)-C(106)#133(6)
 C(106)-C(108)-C(103)#1 89(8)
 C(108)#1-C(108)-C(103)#127(3)
 C(106)#1-C(108)-C(103)#148(3)
 C(101)-C(106)-C(108) 134(10)
 C(101)-C(106)-C(108)#1 172(10)
 C(108)-C(106)-C(108)#1 49(9)
 C(101)-C(106)-C(103)#1 146(9)
 C(108)-C(106)-C(103)#1 65(10)
 C(108)#1-C(106)-C(103)#126(3)
 C(102)-C(110)-O(101) 149(3)
 C(102)-C(110)-C(105)#2 35.7(17)
 O(101)-C(110)-C(105)#2 142.1(18)
 C(102)-C(110)-C(109)#2 32.3(17)
 O(101)-C(110)-C(109)#2 133.4(17)
 C(105)#2-C(110)-C(109)#214.9(7)
 C(102)#3-C(109)-C(104)#347.7(13)
 C(102)#3-C(109)-C(110)#320.5(11)
 C(104)#3-C(109)-C(110)#331.4(10)

Symmetry transformations used to generate equivalent atoms:

#1 -x+1,-y+2,-z+2 #2 x+1,y,z #3 x-1,y,z

Table 4. Anisotropic displacement parameters ($\text{Å}^2 \times 10^3$) for m1ea. The anisotropic displacement factor exponent takes the form: $-2\pi^2 [h^2 a^{*2} U_{11} + \dots + 2 h k a^* b^* U_{12}]$

	U ₁₁	U ₂₂	U ₃₃	U ₂₃	U ₁₃	U ₁₂
O(1)	24(1)	25(1)	29(1)	-3(1)	2(1)	0(1)
O(3)	19(1)	23(1)	40(1)	-1(1)	4(1)	3(1)
N(4)	31(1)	22(1)	32(1)	-1(1)	-2(1)	3(1)

C(5)	17(1)	25(1)	27(1)	1(1)	2(1)	-3(1)
C(6)	18(1)	25(1)	31(1)	4(1)	3(1)	-2(1)
C(7)	20(1)	22(1)	34(1)	-2(1)	1(1)	2(1)
C(8)	24(1)	26(1)	41(1)	-1(1)	-3(1)	0(1)
C(9)	22(1)	24(1)	29(1)	0(1)	1(1)	4(1)
C(10)	24(1)	27(1)	44(1)	1(1)	-2(1)	0(1)
C(11)	23(1)	25(1)	32(1)	-5(1)	-4(1)	3(1)
C(12)	28(1)	27(1)	40(1)	-1(1)	-2(1)	-3(1)
C(13)	26(1)	27(1)	40(1)	0(1)	-1(1)	-1(1)
C(14)	26(1)	26(1)	26(1)	-1(1)	-2(1)	-1(1)
C(15)	29(1)	27(1)	36(1)	-3(1)	4(1)	-4(1)
C(16)	22(1)	22(1)	28(1)	-1(1)	3(1)	-1(1)
C(17)	21(1)	19(1)	31(1)	-1(1)	3(1)	0(1)
C(18)	21(1)	22(1)	29(1)	-2(1)	4(1)	-2(1)
C(19)	19(1)	21(1)	31(1)	0(1)	2(1)	1(1)
C(20)	23(1)	24(1)	29(1)	3(1)	-1(1)	1(1)
C(22)	23(1)	24(1)	54(2)	-1(1)	8(1)	2(1)
O(101)	60(2)	18(1)	30(1)	3(1)	9(1)	3(1)
C(103)	46(2)	33(2)	38(2)	1(1)	-12(1)	-9(1)
C(101)	93(9)	54(8)	79(8)	17(5)	-22(6)	-27(6)
C(102)	81(11)	51(8)	48(6)	-27(6)	5(7)	15(7)
C(105)	270(30)	48(9)	230(30)	109(13)	-230(30)	-92(15)
C(104)	240(40)	36(9)	150(20)	1(12)	-50(20)	28(16)
C(108)	34(18)	80(30)	170(60)	100(40)	-80(30)	-50(20)
C(106)	700(300)	70(50)	1200(500)	270(130)	-900(400)	-220(100)
C(110)	57(13)	119(19)	140(20)	61(16)	27(13)	25(11)
C(109)	95(14)	59(13)	134(17)	91(13)	15(13)	35(11)

Table 5. Hydrogen coordinates ($\times 10^4$) and isotropic displacement parameters ($\text{\AA}^2 \times 10^3$) for mlea.

	x	y	z	U(eq)
H(9A)	3577	7723	7031	30
H(9B)	416	7256	7202	30
H(11A)	13867	6194	11257	32
H(11B)	16457	6766	10991	32
H(14)	7951	5322	7957	31
H(15A)	12237	8009	10545	36
H(15B)	15522	8091	10914	36
H(17)	8156	7012	9174	28
H(20)	12722	4923	9404	30
H(22A)	4162	9051	7294	40
H(22B)	5101	8683	7900	40

Molecular Structure and Crystallography Data for Compound NMFM10506

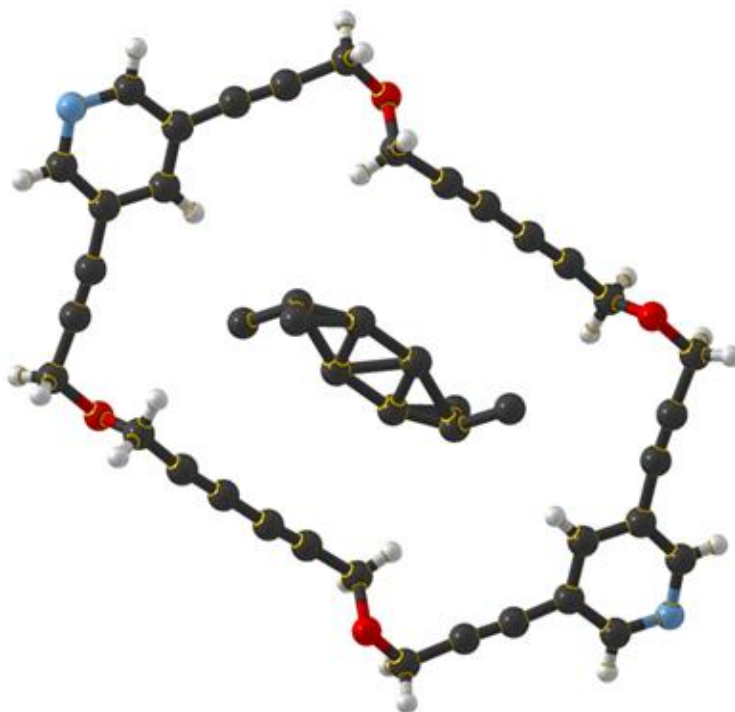


Table 1. Crystal data and structure refinement for NMFm10506.

Identification code	nmfm10506	
Empirical formula	C ₃₄ H ₂₂ N ₂ O ₄	
Formula weight	522.54	
Temperature	293(2) K	
Wavelength	1.54178 nm	
Crystal system	Monoclinic	
Space group	P2(1)/n	
Unit cell dimensions	a = 4.1315(8) Å	α = 90°
	b = 16.913(2) Å	β = 92.540(17)°
	c = 23.436(4) Å	γ = 90°
Volume	1636.1(5) Å ³	
Z	2	
Density (calculated)	1.061 Mg/m ³	
Absorption coefficient	0.566 mm ⁻¹	
F(000)	544	
Theta range for data collection	3.78 to 75.76°	
Index ranges	-4 ≤ h ≤ 4, -21 ≤ k ≤ 20, -28 ≤ l ≤ 28	
Reflections collected	17582	
Independent reflections	3231 [R(int) = 0.0815]	
Completeness to theta = 75.76°	94.9 %	
Absorption correction	None	
Refinement method	Full-matrix least-squares on F ²	
Data / restraints / parameters	3231 / 0 / 200	
Goodness-of-fit on F ²	1.193	
Final R indices [I > 2σ(I)]	R1 = 0.1312, wR2 = 0.3393	
R indices (all data)	R1 = 0.2103, wR2 = 0.4014	
Extinction coefficient	0.014(3)	
Largest diff. peak and hole	1.391 and -0.365 e.Å ⁻³	

Table 2. Atomic coordinates ($\times 10^4$) and equivalent isotropic displacement parameters ($\times 10^3$) for NMF10506. $U(\text{eq})$ is defined as one third of the trace of the orthogonalized U^{ij} tensor.

	x	y	z	$U(\text{eq})$
O(1)	-2361(10)	2283(2)	-1246(2)	71(1)
O(2)	8977(10)	3342(2)	2394(2)	79(1)
N(3)	-485(13)	53(3)	1338(2)	80(2)
C(4)	-655(14)	1034(3)	593(2)	61(1)
C(5)	4162(15)	1786(3)	1863(2)	66(2)
C(6)	2239(14)	1295(3)	1485(2)	63(1)
C(7)	5768(15)	2181(3)	2192(2)	67(2)
C(8)	-3018(19)	3005(3)	-970(3)	83(2)
C(9)	1307(16)	545(3)	1663(2)	72(2)
C(10)	7715(16)	2643(3)	2611(2)	74(2)
C(11)	1237(14)	1539(3)	943(2)	66(2)
C(12)	-4033(17)	1631(4)	-1018(2)	81(2)
C(13)	-2807(14)	1428(3)	-425(3)	70(2)
C(14)	-1826(14)	1258(3)	35(2)	68(2)
C(15)	-1602(17)	3655(4)	-1285(3)	85(2)
C(16)	1970(17)	5371(4)	-2071(3)	83(2)
C(17)	-1438(15)	299(3)	817(2)	72(2)
C(18)	848(16)	4805(4)	-1833(3)	81(2)
C(19)	-461(16)	4185(4)	-1551(3)	79(2)
C(20)	6590(17)	3953(3)	2337(3)	88(2)
C(1)	6540(40)	3400(5)	746(6)	174(6)
C(3)	-1130(190)	3766(9)	644(10)	780(70)

Table 3. Bond lengths Å and angles ° for NMFM10506.

O(1)-C(8)	1.414(7)
O(1)-C(12)	1.418(7)
O(2)-C(10)	1.398(6)
O(2)-C(20)	1.431(7)
N(3)-C(9)	1.331(7)
N(3)-C(17)	1.333(7)
C(4)-C(17)	1.392(7)
C(4)-C(11)	1.398(7)
C(4)-C(14)	1.427(8)
C(5)-C(7)	1.198(7)
C(5)-C(6)	1.430(8)
C(6)-C(11)	1.382(7)
C(6)-C(9)	1.394(8)
C(7)-C(10)	1.467(8)
C(8)-C(15)	1.461(9)
C(12)-C(13)	1.498(8)
C(13)-C(14)	1.170(7)
C(15)-C(19)	1.201(9)
C(16)-C(18)	1.210(9)
C(16)-C(20)#1	1.442(9)
C(18)-C(19)	1.364(9)
C(20)-C(16)#1	1.442(9)
C(1)-C(3)#2	1.18(6)
C(3)-C(1)#3	1.18(6)
C(8)-O(1)-C(12)	113.1(5)
C(10)-O(2)-C(20)	112.3(5)
C(9)-N(3)-C(17)	117.6(5)
C(17)-C(4)-C(11)	117.3(5)
C(17)-C(4)-C(14)	120.5(5)
C(11)-C(4)-C(14)	122.2(5)
C(7)-C(5)-C(6)	178.1(6)
C(11)-C(6)-C(9)	118.1(5)
C(11)-C(6)-C(5)	122.1(5)

C(9)-C(6)-C(5)	119.8(5)
C(5)-C(7)-C(10)	177.9(6)
O(1)-C(8)-C(15)	109.3(5)
N(3)-C(9)-C(6)	123.5(5)
O(2)-C(10)-C(7)	114.1(5)
C(6)-C(11)-C(4)	119.5(5)
O(1)-C(12)-C(13)	112.2(5)
C(14)-C(13)-C(12)	179.0(7)
C(13)-C(14)-C(4)	178.7(6)
C(19)-C(15)-C(8)	179.0(7)
C(18)-C(16)-C(20)#1	177.6(7)
N(3)-C(17)-C(4)	124.0(5)
C(16)-C(18)-C(19)	178.0(7)
C(15)-C(19)-C(18)	177.6(7)
O(2)-C(20)-C(16)#1	108.5(5)

Symmetry transformations used to generate equivalent atoms:

#1 -x+1,-y+1,-z #2 x+1,y,z #3 x-1,y,z

Table 4. Anisotropic displacement parameters ($\times 10^3$) for NMFM10506. The anisotropic displacement factor exponent takes the form: $-2\pi^2 [h^2 a^{*2} U^{11} + \dots + 2 h k a^* b^* U^{12}]$

	U ¹¹	U ²²	U ³³	U ²³	U ¹³	U ¹²
O(1)	81(3)	69(2)	62(2)	12(2)	6(2)	-1(2)
O(2)	72(3)	67(2)	99(3)	3(2)	11(2)	-8(2)
N(3)	105(4)	66(3)	68(3)	9(2)	-11(3)	-14(3)
C(4)	66(4)	59(3)	58(3)	4(2)	4(3)	4(3)
C(5)	70(4)	66(3)	63(3)	-1(3)	6(3)	2(3)
C(6)	72(4)	60(3)	58(3)	-6(2)	6(3)	-1(3)
C(7)	76(4)	64(3)	62(3)	0(3)	9(3)	-1(3)
C(8)	92(5)	75(4)	83(4)	14(3)	12(4)	7(3)
C(9)	90(4)	68(3)	57(3)	9(3)	-3(3)	5(3)
C(10)	82(4)	71(3)	68(3)	2(3)	4(3)	-13(3)
C(11)	71(4)	58(3)	69(3)	4(2)	3(3)	-4(3)
C(12)	89(5)	79(4)	73(4)	15(3)	-17(3)	-15(3)
C(13)	69(4)	71(3)	70(3)	5(3)	1(3)	-5(3)
C(14)	69(4)	69(3)	66(3)	8(3)	-1(3)	-2(3)
C(15)	89(5)	72(4)	92(4)	6(3)	-11(4)	9(4)
C(16)	82(4)	69(4)	98(4)	-4(3)	-1(4)	2(3)
C(17)	89(4)	62(3)	64(3)	-2(3)	-6(3)	-6(3)
C(18)	79(4)	69(3)	93(4)	2(3)	-6(3)	-4(3)
C(19)	88(5)	65(3)	83(4)	9(3)	-6(3)	-6(3)
C(20)	84(5)	68(3)	114(5)	6(3)	18(4)	-2(3)
C(1)	286(16)	66(5)	180(11)	3(6)	122(12)	-2(7)
C(3)	2000(200)	114(11)	194(17)	-16(11)	-360(50)	-170(40)

Table 5. Hydrogen coordinates ($\times 10^4$) and isotropic displacement parameters ($\text{\AA}^2 \times 10^{-3}$) for NMFM10506.

	x	y	z	U(eq)
H(8A)	-2103	2995	-582	100
H(8B)	-5340	3080	-955	100
H(9)	1973	380	2028	86
H(10A)	6382	2772	2928	88
H(10B)	9495	2317	2758	88
H(11)	1817	2036	811	79
H(12A)	-3787	1175	-1264	97
H(12B)	-6323	1755	-1013	97
H(17)	-2703	-41	589	86
H(20A)	5846	4098	2709	106
H(20B)	4743	3768	2104	106

Molecular Structure and Crystallography Data for Compound m1mono1

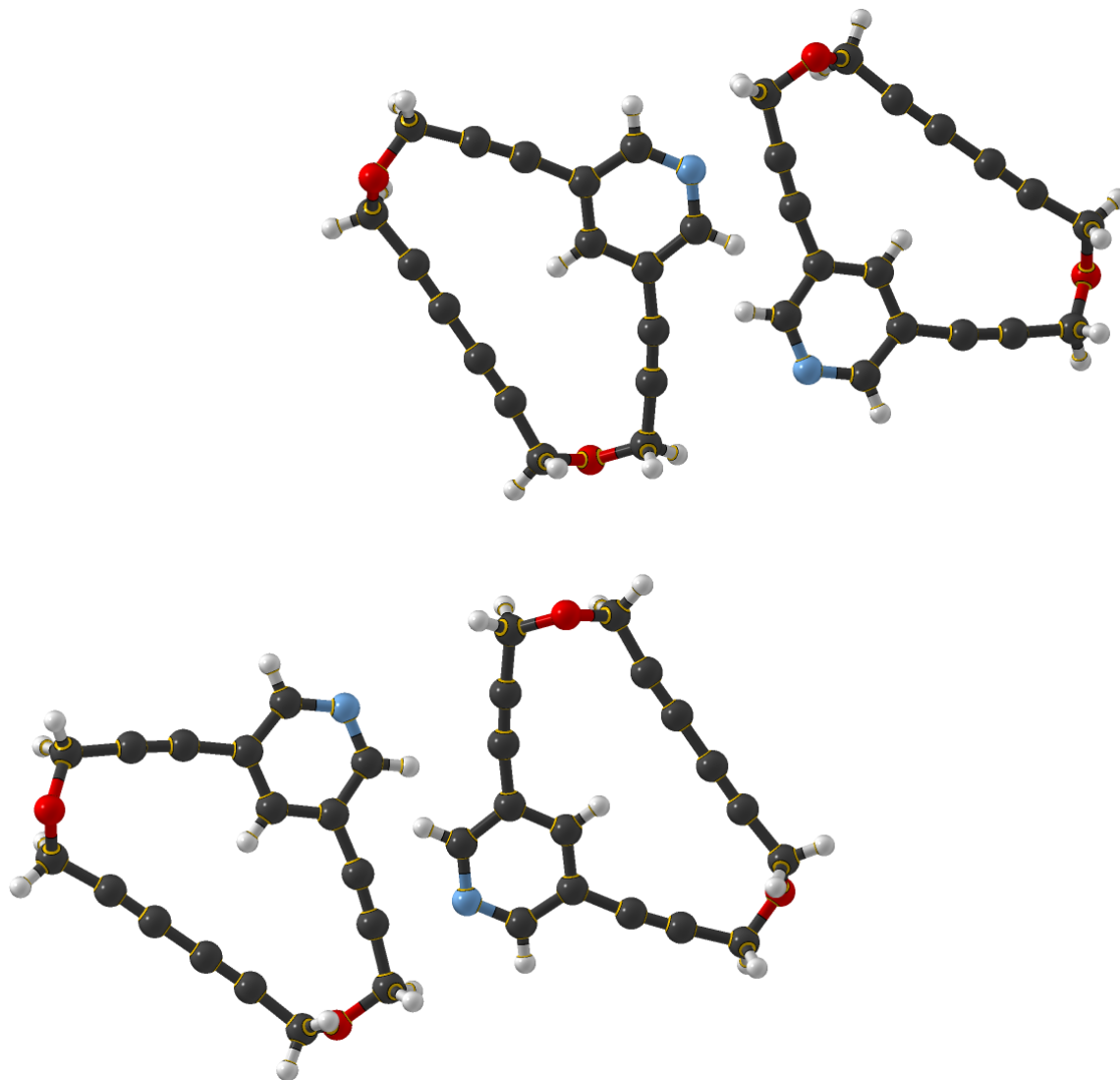


Table 1. Crystal data and structure refinement for m1mono1.

Identification code	m1mono1	
Empirical formula	C17 H11 N O2	
Formula weight	261.27	
Temperature	293(2) K	
Wavelength	1.54178 nm	
Crystal system	Monoclinic	
Space group	P2(1)/c	
Unit cell dimensions	a = 4.1031(2) Å	$\alpha = 90^\circ$
	b = 27.9007(10) Å	$\beta = 90.216(3)^\circ$
	c = 11.6679(3) Å	$\gamma = 90^\circ$
Volume	1335.72(9) Å ³	
Z	4	
Density (calculated)	1.299 Mg/m ³	
Absorption coefficient	0.694 mm ⁻¹	
F(000)	544	
Theta range for data collection	4.11 to 73.34°	
Index ranges	-3 ≤ h ≤ 4, -34 ≤ k ≤ 33, -14 ≤ l ≤ 14	
Reflections collected	5461	
Independent reflections	2469 [R(int) = 0.0278]	
Completeness to theta = 73.34°	92.3 %	
Absorption correction	None	
Refinement method	Full-matrix least-squares on F ²	
Data / restraints / parameters	2469 / 0 / 182	
Goodness-of-fit on F ²	1.017	
Final R indices [I > 2σ(I)]	R1 = 0.0453, wR2 = 0.1192	
R indices (all data)	R1 = 0.0712, wR2 = 0.1394	
Extinction coefficient	0.0047(8)	
Largest diff. peak and hole	0.132 and -0.122 e.Å ⁻³	

Table 2. Atomic coordinates ($\times 10^4$) and equivalent isotropic displacement parameters ($\text{\AA}^2 \times 10^3$) for m1mono1. U(eq) is defined as one third of the trace of the orthogonalized U_{ij} tensor.

	x	y	z	U(eq)
O(1)	12896(3)	5874(1)	-2206(1)	57(1)
O(2)	8265(4)	5515(1)	4650(1)	77(1)
C(3)	11750(5)	5544(1)	676(2)	57(1)
C(4)	13063(5)	5619(1)	-219(2)	57(1)
C(5)	8930(6)	5384(1)	2604(2)	63(1)
C(6)	12113(6)	6649(1)	-1352(2)	62(1)
C(7)	10221(5)	5457(1)	1712(2)	58(1)
C(8)	14812(6)	5674(1)	-1308(2)	63(1)
C(9)	7642(6)	6923(1)	2384(2)	66(1)
N(10)	7845(7)	7713(1)	1587(2)	91(1)
C(11)	8979(6)	6743(1)	1390(2)	69(1)
C(12)	11100(6)	6850(1)	-537(2)	63(1)
C(13)	9757(6)	7047(1)	497(2)	62(1)
C(14)	13321(6)	6376(1)	-2339(2)	63(1)
C(15)	7098(7)	7415(1)	2429(2)	81(1)
C(16)	7335(6)	5242(1)	3680(2)	74(1)
C(17)	9168(7)	7532(1)	648(2)	77(1)
C(18)	6592(7)	6304(1)	4027(2)	79(1)
C(19)	6938(6)	6604(1)	3321(2)	75(1)
C(20)	6244(8)	5917(1)	4866(2)	94(1)

Table 3. Bond lengths Å and angles ° for m1mono1.

O(1)-C(14)	1.420(2)
O(1)-C(8)	1.422(2)
O(2)-C(16)	1.415(3)
O(2)-C(20)	1.417(3)
C(3)-C(4)	1.196(3)
C(3)-C(7)	1.385(3)
C(4)-C(8)	1.469(3)
C(5)-C(7)	1.187(3)
C(5)-C(16)	1.473(3)
C(6)-C(12)	1.181(3)
C(6)-C(14)	1.470(3)
C(9)-C(11)	1.380(3)
C(9)-C(15)	1.391(3)
C(9)-C(19)	1.439(3)
N(10)-C(17)	1.326(3)
N(10)-C(15)	1.325(3)
C(11)-C(13)	1.382(3)
C(12)-C(13)	1.437(3)
C(13)-C(17)	1.385(3)
C(18)-C(19)	1.184(4)
C(18)-C(20)	1.465(4)
C(14)-O(1)-C(8)	113.55(16)
C(16)-O(2)-C(20)	114.3(2)
C(4)-C(3)-C(7)	179.8(3)
C(3)-C(4)-C(8)	175.4(2)
C(7)-C(5)-C(16)	174.1(3)
C(12)-C(6)-C(14)	177.1(2)
C(5)-C(7)-C(3)	179.4(3)
O(1)-C(8)-C(4)	114.06(18)
C(11)-C(9)-C(15)	117.1(2)
C(11)-C(9)-C(19)	119.7(2)
C(15)-C(9)-C(19)	123.2(2)
C(17)-N(10)-C(15)	117.9(2)

C(9)-C(11)-C(13)	120.2(2)
C(6)-C(12)-C(13)	174.0(2)
C(11)-C(13)-C(17)	117.6(2)
C(11)-C(13)-C(12)	119.22(19)
C(17)-C(13)-C(12)	123.2(2)
O(1)-C(14)-C(6)	112.60(16)
N(10)-C(15)-C(9)	123.7(2)
O(2)-C(16)-C(5)	114.7(2)
N(10)-C(17)-C(13)	123.4(2)
C(19)-C(18)-C(20)	177.4(3)
C(18)-C(19)-C(9)	172.1(3)
O(2)-C(20)-C(18)	113.9(2)

Symmetry transformations used to generate equivalent atoms:

Table 4. Anisotropic displacement parameters ($\times 10^3$) for m1mono1. The anisotropic displacement factor exponent takes the form: $-2\pi^2 [h^2 a^{*2} U^{11} + \dots + 2 h k a^* b^* U^{12}]$

	U ¹¹	U ²²	U ³³	U ²³	U ¹³	U ¹²
O(1)	68(1)	54(1)	50(1)	-3(1)	6(1)	-4(1)
O(2)	72(1)	106(1)	53(1)	6(1)	0(1)	-5(1)
C(3)	65(1)	50(1)	55(1)	4(1)	-2(1)	6(1)
C(4)	60(1)	52(1)	58(1)	1(1)	-1(1)	6(1)
C(5)	63(1)	71(1)	54(1)	9(1)	-5(1)	1(1)
C(6)	74(1)	51(1)	61(1)	2(1)	10(1)	-3(1)
C(7)	66(1)	55(1)	53(1)	5(1)	-3(1)	7(1)
C(8)	63(1)	64(1)	63(1)	6(1)	11(1)	10(1)
C(9)	68(1)	62(1)	69(1)	-15(1)	6(1)	0(1)
N(10)	139(2)	59(1)	74(1)	-16(1)	-9(1)	26(1)
C(11)	87(2)	48(1)	73(1)	-13(1)	16(1)	4(1)
C(12)	77(2)	47(1)	63(1)	2(1)	5(1)	1(1)
C(13)	71(1)	51(1)	63(1)	-8(1)	-1(1)	5(1)
C(14)	74(1)	57(1)	57(1)	2(1)	17(1)	-2(1)
C(15)	100(2)	74(2)	69(1)	-26(1)	1(1)	22(1)
C(16)	75(2)	90(2)	56(1)	11(1)	1(1)	-13(1)
C(17)	113(2)	51(1)	65(1)	-9(1)	-9(1)	11(1)
C(18)	78(2)	87(2)	72(1)	-12(1)	25(1)	-8(1)
C(19)	77(2)	75(2)	73(1)	-20(1)	19(1)	-3(1)
C(20)	97(2)	116(2)	68(1)	1(2)	31(1)	-14(2)

Table 5. Hydrogen coordinates ($\times 10^4$) and isotropic displacement parameters ($\text{\AA}^2 \times 10^{-3}$) for m1monol.

	x	y	z	U(eq)
H(8A)	16697	5877	-1181	76
H(8B)	15597	5362	-1549	76
H(11)	9357	6415	1320	83
H(14A)	12178	6480	-3024	75
H(14B)	15620	6444	-2442	75
H(15)	6157	7541	3087	97
H(16A)	4995	5269	3580	89
H(16B)	7828	4908	3829	89
H(17)	9729	7740	59	92
H(20A)	6750	6041	5622	112
H(20B)	3990	5812	4871	112

Molecular Structure and Crystallography Data for Compound m2mono1

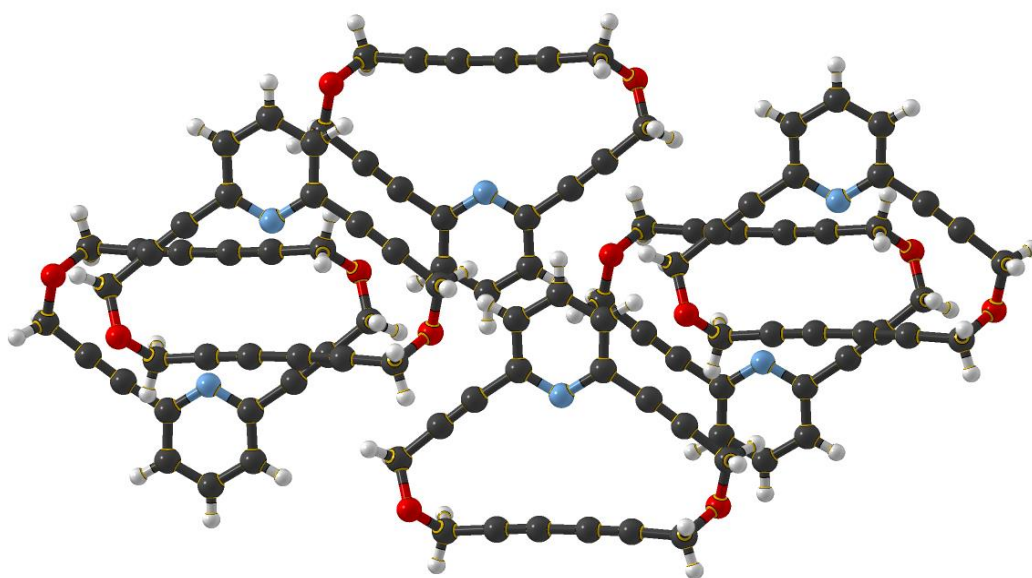


Table 1. Crystal data and structure refinement for m2mono1.

Identification code	m2mono1	
Empirical formula	C ₁₇ H ₁₁ N O ₂	
Formula weight	261.27	
Temperature	293(2) K	
Wavelength	1.54178 nm	
Crystal system	Monoclinic	
Space group	C2/c	
Unit cell dimensions	a = 15.5258(8) Å	α = 90°
	b = 10.0376(6) Å	β = 102.165(7)°
	c = 8.8061(8) Å	γ = 90°
Volume	1341.54(16) Å ³	
Z	4	
Density (calculated)	1.294 Mg/m ³	
Absorption coefficient	0.691 mm ⁻¹	
F(000)	544	
Theta range for data collection	5.28 to 77.29°	
Index ranges	-19 ≤ h ≤ 15, -11 ≤ k ≤ 11, -7 ≤ l ≤ 9	
Reflections collected	1662	
Independent reflections	1004 [R(int) = 0.0098]	
Completeness to theta = 77.29°	70.1 %	
Absorption correction	None	
Refinement method	Full-matrix least-squares on F ²	
Data / restraints / parameters	1004 / 0 / 93	
Goodness-of-fit on F ²	1.044	
Final R indices [I > 2σ(I)]	R1 = 0.0431, wR2 = 0.1241	
R indices (all data)	R1 = 0.0522, wR2 = 0.1344	
Extinction coefficient	0.0022(5)	
Largest diff. peak and hole	0.140 and -0.129 e.Å ⁻³	

Table 2. Atomic coordinates ($\times 10^4$) and equivalent isotropic displacement parameters ($\text{\AA}^2 \times 10^3$) for m2mono1. $U(\text{eq})$ is defined as one third of the trace of the orthogonalized U_{ij} tensor.

	x	y	z	$U(\text{eq})$
N(1)	5000	2375(2)	2500	53(1)
O(2)	7357(1)	-673(1)	1036(2)	62(1)
C(3)	5329(1)	-1259(2)	2077(3)	55(1)
C(4)	5602(1)	3065(2)	1932(2)	50(1)
C(5)	5620(1)	4438(2)	1905(3)	63(1)
C(6)	6757(1)	1551(2)	959(3)	58(1)
C(7)	5900(1)	-1287(2)	1367(3)	59(1)
C(8)	6245(1)	2267(2)	1371(3)	55(1)
C(9)	5000	5125(3)	2500	76(1)
C(10)	7377(1)	639(2)	444(3)	65(1)
C(11)	6569(1)	-1374(2)	419(3)	73(1)

Table 3. Bond lengths Å and angles ° for m2mono1.

N(1)-C(4)#1	1.341(2)
N(1)-C(4)	1.341(2)
O(2)-C(11)	1.415(2)
O(2)-C(10)	1.419(2)
C(3)-C(7)	1.188(2)
C(3)-C(3)#1	1.385(3)
C(4)-C(5)	1.379(3)
C(4)-C(8)	1.446(2)
C(5)-C(9)	1.375(2)
C(6)-C(8)	1.185(3)
C(6)-C(10)	1.466(3)
C(7)-C(11)	1.466(2)
C(9)-C(5)#1	1.375(2)
C(4)#1-N(1)-C(4)	117.8(2)
C(11)-O(2)-C(10)	113.85(18)
C(7)-C(3)-C(3)#1	178.46(19)
N(1)-C(4)-C(5)	122.79(17)
N(1)-C(4)-C(8)	115.26(18)
C(5)-C(4)-C(8)	121.95(16)
C(9)-C(5)-C(4)	118.41(19)
C(8)-C(6)-C(10)	178.7(2)
C(3)-C(7)-C(11)	176.5(2)
C(6)-C(8)-C(4)	176.1(2)
C(5)-C(9)-C(5)#1	119.8(3)
O(2)-C(10)-C(6)	113.52(15)
O(2)-C(11)-C(7)	114.24(19)

Symmetry transformations used to generate equivalent atoms:

#1 -x+1,y,-z+1/2

Table 4. Anisotropic displacement parameters ($\text{Å}^2 \times 10^3$) for m2mono1. The anisotropic displacement factor exponent takes the form: $-2\pi^2 [h^2 a^{*2} U^{11} + \dots + 2 h k a^* b^* U^{12}]$

	U11	U22	U33	U23	U13	U12
N(1)	56(1)	44(1)	66(2)	0	25(1)	0
O(2)	51(1)	58(1)	82(1)	8(1)	25(1)	2(1)
C(3)	52(1)	46(1)	72(2)	-2(1)	24(1)	-2(1)
C(4)	50(1)	47(1)	54(2)	2(1)	14(1)	-1(1)
C(5)	60(1)	49(1)	83(2)	6(1)	22(1)	-6(1)
C(6)	58(1)	57(1)	67(2)	7(1)	28(1)	-2(1)
C(7)	55(1)	52(1)	75(2)	-7(1)	27(1)	-4(1)
C(8)	55(1)	51(1)	65(2)	6(1)	24(1)	-4(1)
C(9)	76(2)	38(2)	119(3)	0	30(2)	0
C(10)	60(1)	65(1)	80(2)	10(1)	37(1)	3(1)
C(11)	65(1)	73(2)	91(2)	-22(1)	41(1)	-13(1)

Table 5. Hydrogen coordinates ($\times 10^4$) and isotropic displacement parameters ($\text{\AA}^2 \times 10^3$) for m2mono1.

	x	y	z	U(eq)
H(5)	6042	4889	1494	76
H(9)	5000	6052	2500	92
H(10A)	7240	602	-682	78
H(10B)	7968	991	769	78
H(11A)	6712	-2305	306	87
H(11B)	6322	-1028	-609	87

Molecular Structure and Crystallography Data for Compound n2ring

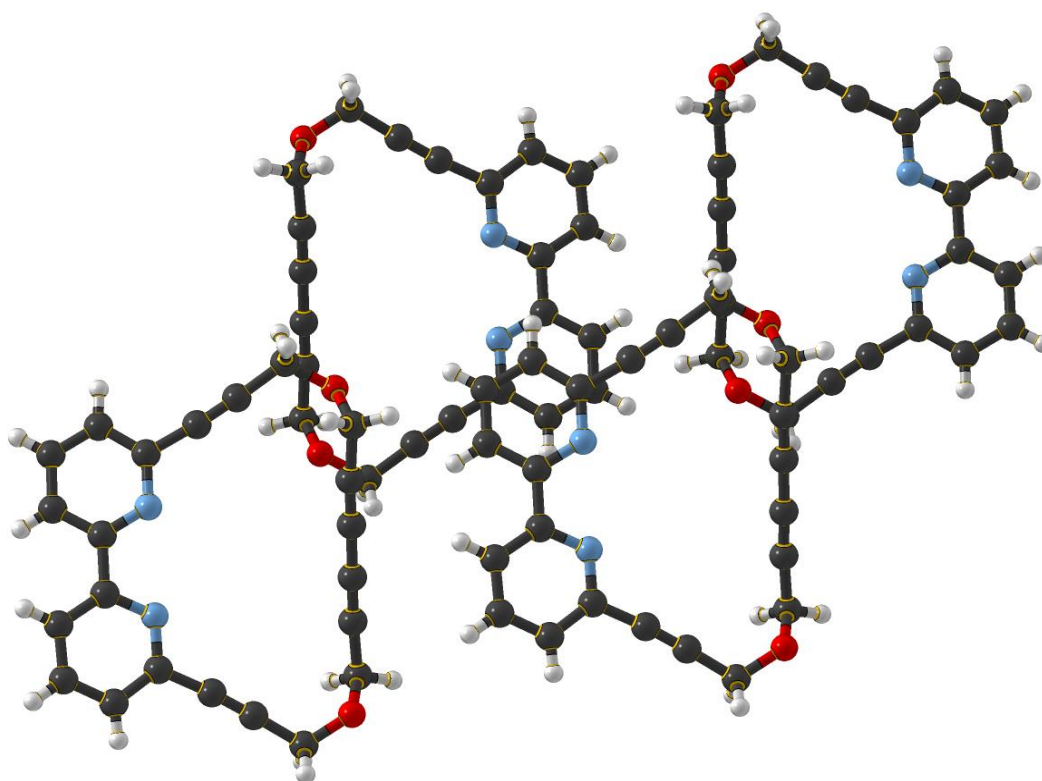


Table 1. Crystal data and structure refinement for n2ring.

Identification code	n2ring	
Empirical formula	C ₄₄ H ₂₈ N ₄ O ₄	
Formula weight	676.70	
Temperature	293(2) K	
Wavelength	0.71073 nm	
Crystal system	Triclinic	
Space group	P-1	
Unit cell dimensions	a = 8.6450(11) Å	α = 70.964(10)°
	b = 10.1422(10) Å	β = 84.874(10)°
	c = 10.8603(12) Å	γ = 70.511(10)°
Volume	848.37(17) Å ³	
Z	1	
Density (calculated)	1.325 Mg/m ³	
Absorption coefficient	0.086 mm ⁻¹	
F(000)	352	
Theta range for data collection	3.43 to 29.70°	
Index ranges	-11 ≤ h ≤ 11, -12 ≤ k ≤ 13, -14 ≤ l ≤ 14	
Reflections collected	9749	
Independent reflections	4064 [R(int) = 0.1007]	
Completeness to theta = 29.70°	84.6 %	
Absorption correction	None	
Refinement method	Full-matrix least-squares on F ²	
Data / restraints / parameters	4064 / 0 / 236	
Goodness-of-fit on F ²	0.958	
Final R indices [I > 2σ(I)]	R1 = 0.0658, wR2 = 0.0940	
R indices (all data)	R1 = 0.2678, wR2 = 0.1606	
Extinction coefficient	0.0073(11)	
Largest diff. peak and hole	0.190 and -0.188 e.Å ⁻³	

Table 2. Atomic coordinates ($\times 10^4$) and equivalent isotropic displacement parameters ($\times 10^3$) for n2ring. $U(\text{eq})$ is defined as one third of the trace of the orthogonalized U_{ij} tensor.

	x	y	z	$U(\text{eq})$
N(1)	2951(4)	10779(3)	8147(3)	47(1)
O(2)	812(3)	6575(3)	4757(3)	64(1)
N(3)	1727(4)	8506(3)	8689(3)	47(1)
C(4)	2554(4)	10209(4)	9385(3)	45(1)
O(5)	4220(3)	13541(3)	3131(2)	65(1)
C(6)	2118(4)	8848(4)	9687(3)	46(1)
C(7)	3082(5)	10471(5)	3649(4)	55(1)
C(8)	3786(5)	12627(4)	6512(4)	51(1)
C(9)	3421(5)	12699(4)	8748(4)	58(1)
C(10)	3373(4)	12000(4)	7852(3)	47(1)
C(11)	1400(5)	7242(4)	8956(4)	53(1)
C(12)	2572(5)	10844(5)	10336(4)	60(1)
C(13)	2042(5)	9640(5)	3847(3)	54(1)
C(14)	1007(5)	6884(4)	7863(4)	56(1)
C(15)	1419(5)	6288(5)	10205(4)	66(1)
C(16)	3015(5)	12093(5)	10005(4)	67(1)
C(17)	2148(5)	7930(5)	10970(4)	62(1)
C(18)	4142(5)	13209(4)	5451(4)	54(1)
C(19)	1142(5)	8936(5)	4018(4)	57(1)
C(20)	682(5)	6516(4)	7021(4)	55(1)
C(21)	4645(5)	13941(4)	4155(4)	63(1)
C(22)	3968(5)	11174(5)	3485(4)	56(1)
C(23)	224(5)	6011(4)	6014(4)	60(1)
C(24)	5078(5)	12050(5)	3192(4)	67(1)
C(25)	1780(6)	6656(5)	11232(4)	73(1)
C(26)	23(5)	8110(5)	4144(4)	64(1)

Table 3. Bond lengths Å and angles ° for n2ring.

N(1)-C(10)	1.339(4)
N(1)-C(4)	1.343(4)
O(2)-C(23)	1.417(4)
O(2)-C(26)	1.424(4)
N(3)-C(11)	1.339(4)
N(3)-C(6)	1.342(4)
C(4)-C(12)	1.388(5)
C(4)-C(6)	1.477(5)
O(5)-C(21)	1.415(4)
O(5)-C(24)	1.427(4)
C(6)-C(17)	1.398(5)
C(7)-C(22)	1.177(5)
C(7)-C(13)	1.385(6)
C(8)-C(18)	1.177(5)
C(8)-C(10)	1.450(5)
C(9)-C(16)	1.369(5)
C(9)-C(10)	1.388(5)
C(11)-C(15)	1.383(5)
C(11)-C(14)	1.447(5)
C(12)-C(16)	1.372(5)
C(13)-C(19)	1.186(5)
C(14)-C(20)	1.180(5)
C(15)-C(25)	1.375(5)
C(17)-C(25)	1.367(5)
C(18)-C(21)	1.465(5)
C(19)-C(26)	1.449(5)
C(20)-C(23)	1.482(5)
C(22)-C(24)	1.463(5)
C(10)-N(1)-C(4)	117.4(3)
C(23)-O(2)-C(26)	114.0(3)
C(11)-N(3)-C(6)	118.0(3)
N(1)-C(4)-C(12)	122.2(4)
N(1)-C(4)-C(6)	116.2(3)

C(12)-C(4)-C(6)	121.6(3)
C(21)-O(5)-C(24)	113.9(3)
N(3)-C(6)-C(17)	121.0(4)
N(3)-C(6)-C(4)	117.9(3)
C(17)-C(6)-C(4)	121.0(3)
C(22)-C(7)-C(13)	179.8(5)
C(18)-C(8)-C(10)	175.4(4)
C(16)-C(9)-C(10)	117.6(4)
N(1)-C(10)-C(9)	123.8(3)
N(1)-C(10)-C(8)	117.5(3)
C(9)-C(10)-C(8)	118.7(4)
N(3)-C(11)-C(15)	123.5(4)
N(3)-C(11)-C(14)	117.0(3)
C(15)-C(11)-C(14)	119.5(4)
C(16)-C(12)-C(4)	119.1(4)
C(19)-C(13)-C(7)	179.6(5)
C(20)-C(14)-C(11)	176.2(4)
C(25)-C(15)-C(11)	118.6(4)
C(9)-C(16)-C(12)	119.9(4)
C(25)-C(17)-C(6)	120.4(4)
C(8)-C(18)-C(21)	177.5(4)
C(13)-C(19)-C(26)	176.6(4)
C(14)-C(20)-C(23)	177.0(4)
O(5)-C(21)-C(18)	115.0(3)
C(7)-C(22)-C(24)	176.3(4)
O(2)-C(23)-C(20)	114.2(3)
O(5)-C(24)-C(22)	111.3(3)
C(17)-C(25)-C(15)	118.5(4)
O(2)-C(26)-C(19)	111.2(3)

Symmetry transformations used to generate equivalent atoms:

Table 4. Anisotropic displacement parameters ($\times 10^3$) for n2ring. The anisotropic displacement factor exponent takes the form: $-2\pi^2 [h^2 a^{*2} U_{11} + \dots + 2 h k a^* b^* U_{12}]$

	U ₁₁	U ₂₂	U ₃₃	U ₂₃	U ₁₃	U ₁₂
N(1)	48(2)	48(2)	46(2)	-17(2)	3(2)	-18(2)
O(2)	74(2)	61(2)	67(2)	-31(2)	19(2)	-28(2)
N(3)	51(2)	52(2)	45(2)	-19(2)	4(2)	-22(2)
C(4)	45(2)	51(3)	40(2)	-13(2)	0(2)	-18(2)
O(5)	85(2)	57(2)	56(2)	-14(2)	-6(2)	-28(2)
C(6)	42(2)	52(3)	41(2)	-12(2)	5(2)	-16(2)
C(7)	63(3)	56(3)	50(3)	-22(2)	2(2)	-18(2)
C(8)	52(3)	43(3)	64(3)	-18(2)	2(2)	-20(2)
C(9)	71(3)	52(3)	60(3)	-19(2)	0(2)	-28(2)
C(10)	49(3)	47(2)	43(2)	-11(2)	-1(2)	-16(2)
C(11)	55(3)	52(3)	57(3)	-17(2)	3(2)	-24(2)
C(12)	78(3)	63(3)	41(2)	-19(2)	4(2)	-24(3)
C(13)	54(3)	57(3)	49(3)	-19(2)	0(2)	-15(2)
C(14)	58(3)	51(3)	63(3)	-17(2)	2(2)	-24(2)
C(15)	83(3)	57(3)	60(3)	-8(2)	1(2)	-35(2)
C(16)	93(4)	65(3)	52(3)	-26(2)	-2(2)	-30(3)
C(17)	76(3)	66(3)	48(3)	-10(2)	-1(2)	-33(3)
C(18)	58(3)	48(3)	58(3)	-16(2)	5(2)	-23(2)
C(19)	60(3)	59(3)	53(3)	-20(2)	-3(2)	-18(2)
C(20)	60(3)	48(3)	60(3)	-17(2)	3(2)	-22(2)
C(21)	78(3)	60(3)	62(3)	-17(2)	3(2)	-38(3)
C(22)	61(3)	58(3)	56(3)	-24(2)	11(2)	-23(2)
C(23)	68(3)	50(3)	72(3)	-25(2)	5(2)	-27(2)
C(24)	72(3)	69(3)	73(3)	-34(3)	15(2)	-31(3)
C(25)	99(4)	71(3)	49(3)	-2(2)	-3(2)	-42(3)
C(26)	62(3)	70(3)	61(3)	-19(2)	-2(2)	-23(3)

Table 5. Hydrogen coordinates ($\times 10^4$) and isotropic displacement parameters ($\text{\AA}^2 \times 10^3$) for n2ring.

	x	y	z	U(eq)
H(9)	3717	13548	8503	70
H(12)	2287	10430	11186	72
H(15)	1193	5416	10348	79
H(16)	3040	12527	10633	80
H(17)	2421	8186	11650	74
H(21A)	4149	14998	3966	76
H(21B)	5826	13719	4171	76
H(23A)	649	4943	6283	72
H(23B)	-963	6300	5962	72
H(24A)	5936	11621	3860	81
H(24B)	5593	12029	2364	81
H(25)	1774	6052	12085	88
H(26A)	-907	8465	4654	77
H(26B)	-385	8266	3287	77